The Geochemistry and Sedimentology of Quaternary Shelf Sediments off the Tugela River, Natal, South Africa.

by

Taryl A. Felhaber

Department of Geochemistry,
University of Cape Town.

April 1984

Thesis submitted in fulfilment of the requirements for the degree of Master of Science at the University of Cape Town.

"nGi zu Zama"

Zulu phrase

(Nico Snyman, 25 March 1982)

This thesis is dedicated to my parents,

Thomas and Shirley Felhaber

and to my husband,

Theunis Stander.

ABSTRACT

This thesis is comprised of geochemical, mineralogical and sedimentological studies of 101 sediment samples recovered from the continental shelf off the Tugela River Mouth, Natal, South Africa, and nine samples taken from the Lower Tugela River. The purpose of the research was to examine the geochemical nature of the sediments in relation to their particle size distributions and the hydrological conditions present in the area in order to elucidate the relationship between an inner shelf mud belt and an outer shelf mud belt located in the area. The river samples were analysed to help in understanding the changes undergone by the continental shelf sediments during their residence on the shelf.

All samples were analysed for 10 major and 23 trace elements by X-ray fluorescence spectrometry, particle size distribution, carbonate and organic matter content. X-ray diffractograms were run on all samples to obtain qualitative mineralogy. Multivariate statistical tests were used to aid the interpretation of the data, and to statistically distinguish between the two mud belts.

A detailed sedimentological model of the hydraulic populations of sediment in the area has been formulated. The information from this model, taken in conjunction with the mineralogy, provided a framework within which the geochemical data could be interpreted. A geochemical model of sedimentation was developed, based upon the information from the

results of the statistical tests and the known geochemical associations of elements in sediments.

A geochemical distinction was found between the inner and outer shelf mud belts. An age of 40 650 yr BP was previously reported for a sample on the mid-shelf in the study area, supporting the reconstruction of a paleoenvironment showing the outer shelf mud belt to be the paleodepocentre for the Tugela River with the inner shelf mud belt representing the present-day depocentre of the Tugela River.

CONTENTS

LIST OF FIGURES

(in the text)

LIST OF TABLES

(in the text)

page

(in the appendices)

CHAPTER I INTRODUCTION

The geochemistry of sediments has only recently begun to be accepted as a means by which to classify and define sediment behaviour in the marine environment (Holmes, 1982). It appears as though the majority of studies concerning marine sediments has in the past been done to substantiate the concept of uniformitarianism, otherwise known as 'the present is the key to the past', and/or to quantify the anthropogenic effects of man's activities on the marine environment. It is important to study the geochemistry of marine sediments in a more specific sense, however, in order to build up the presently small volume of knowledge that exists on the behaviour of elements in the sediments of different oceanic regions. Although the textural, structural, mineralogical and biological aspects of continental shelf sediments have been studied to a reasonable extent, the geochemistry of near-shore sediments has not attracted the same amount of attention (Calvert, 1976).

This thesis is comprised of detailed geochemical, sedimentological and mineralogical data obtained from surficial sediment samples recovered from the continental shelf off the Tugela River, on the east coast of South Africa. The continental shelf off the east coast is classified as a high energy environment where little present-day mud deposition is occurring (Flemming, pers.comm.). Nevertheless, there are two separate belts of mud on the shelf in the study area, the full extent of which were determined during the course of sampling. The subsequent analyses and interpretation were performed in

order to explain the relationship between these two areas of mud and the surrounding, predominantly sandy, sediments. The primary objective of the research was to see if a geochemical distinction exists between the inner and outer shelf mud samples, i.e. whether the muds found on both the inner and outer shelf are part of the same Recent depositional event or whether they represent different periods of deposition with possibly different geochemical compositions. As most of the outer shelf sediments found off the east coast of South Africa have been classified as relict (Flemming, 1978), it seemed logical to assume that the outer shelf mud belt is also a relict deposit that represents the depocentre of the Tugela River during lower sea-level stands in the Pleistocene, the inner shelf mud belt would then be the modern depocentre for sediments from the Tugela River. Multivariate statistical tests were used on the geochemical and textural data from the sediment samples in the hope of distinguishing between the sedimentary groups, particularly the two mud groups, and to aid in the determination of the environments of deposition. Samples were also taken from the lower Tugela River and its estuary to help ascertain the changes undergone by the sediments during deposition and residence on the continental shelf.

A geochemical model of sedimentation in the study area was derived from the results of the statistical tests together with information from the elemental distributions in the area and known chemical relationships of the elements examined. The model was set within the framework of the determined sedi-

mentology and mineralogy of the sediment samples. It became evident in the formulation of this model that the classification of the sediments into defined groups could not have been achieved from either the chemical or textural data alone. The geochemical model facilitates understanding of the relationships between the geochemistry of these sediments and their particle-size and mineralogical characteristics, and provides a basis on which further research in this field may be established.

CHAPTER II THE TUGELA RIVER

1. The Tugela River System

The Tugela River System lies in a basin which covers 29 100 km^2 (almost a third of the province of Natal), and is comprised of the eight major catchments of, in order downstream, the Upper Tugela (above Bergville), the Little Tugela, the Klip, the Bushmans, the Sundays, the Mooi, the Buffalo, and the Lower Tugela Rivers (fig. 2-1). The Tugela Basin lies in a typically subtropical, temperate summer rainfall area, with the mean annual rainfall for the whole catchment being 843 mm (Oliff, 1960). Oliff (1960) calculated the average annual percent run-off of this precipitation as 23%, but Orme (1974) states that the run-off in all the Natal rivers, of which the Tugela is the largest and most important, accounts for only 16.5% of Natal's total precipitation, with most of the water being lost via evapotranspiration. The average annual flow of the Tugela ranges from 184-226 m^3/s (5.8 - 7.1 x 10^9 m^3/yr), with the average winter (April - September) flow being 73.6 m^3/s and the average summer (October - March) flow reaching 481 m^3/s. Oliff (1960) measured current speeds at several stations along the river system and found that although the speeds varied considerably at different places, there were no consistent differences between his delineated zones. The average speeds for these zones are as follows: in unimpeded flows through rapids, 79 cm/s (2.8 km/h) in summer, 61 cm/s in winter; amongst rocks in rapids, 39 cm/s in summer, 25 cm/s (0.9 km/h) in winter; in slow runs, 8 - 30 cm/s at most times; in unimpeded river runs, 3 - 30 cm/s

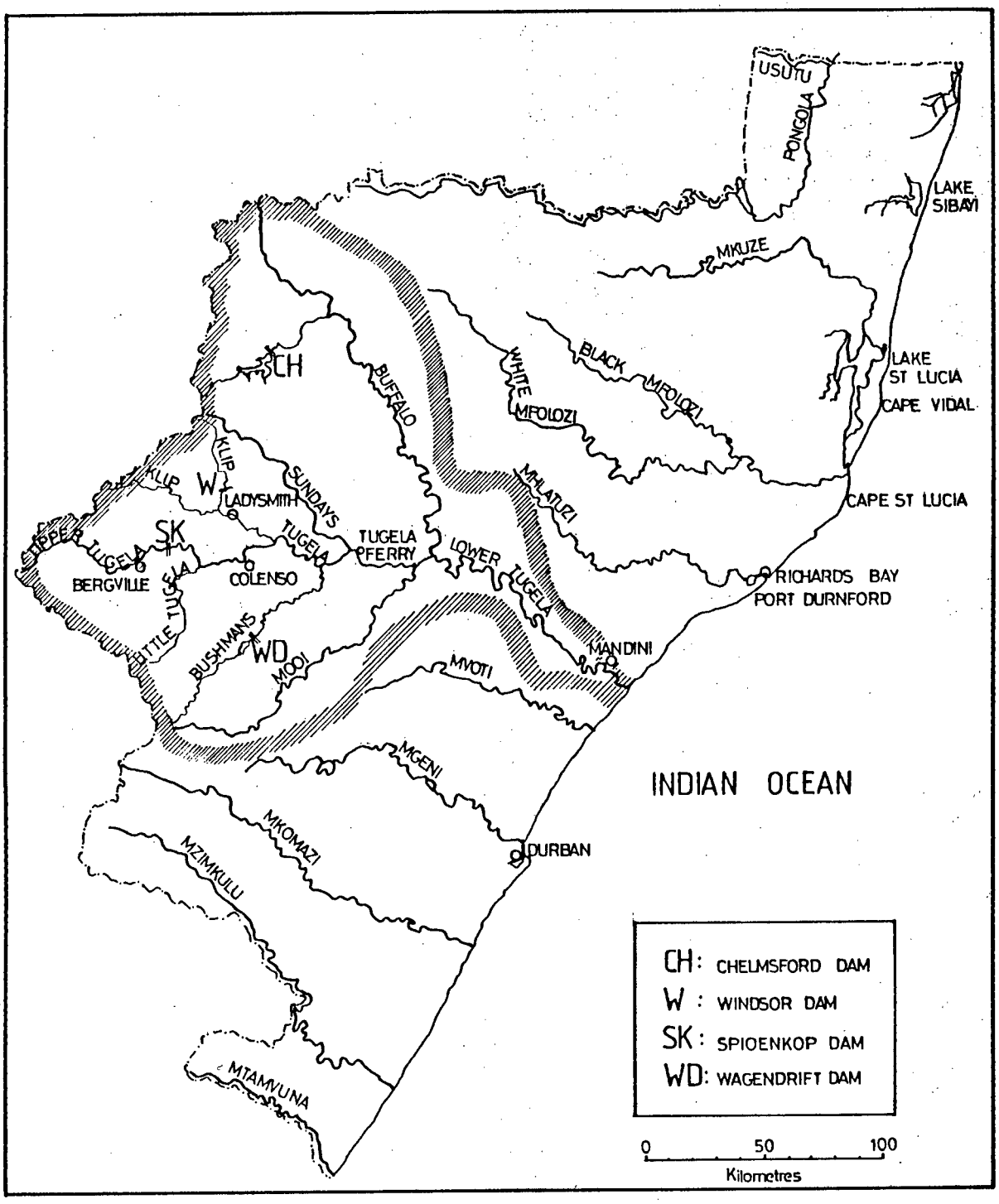

Figure 2-1. Map of Natal showing the Tugela River Basin (outlined).

in winter and over 152 cm/s (5.5 km/h) recorded during summer floods; and in the marginal vegetation areas the flow speed was only 3.5 cm/s in summer with little detectable movement in winter. Noting the high speeds recorded during summer floods, it is not surprising to learn that the name Tugela means 'the fearsome one' or 'the one that acts with frightening suddenness' in Zulu (Begg, 1978).

2. The Estuary

The poorly defined Tugela River flood plain is roughly 1 500 m wide at the mouth, 700 m of which are occupied by a stable sand spit covered with coastal dune forest that extends northeastwards into the estuary from the south bank. The spit is formed by the predominant littoral drift to the north, and is often extended by foredune vegetation for an additional 70 m from which sand periodically builds outwards to confine the river discharge to a channel less than 50 m wide (Orme, 1974). The Coastal Plain is virtually absent at the Tugela River Mouth and a series of Holocene beach ridges form a prograding shore at the margins of the low, rolling hills that are covered with indigenous coastal forest. Most of the land on the flood plain is presently occupied by heavily cultivated sugar cane fields. The bed level of the estuary shelves upwards towards the coast due to the amount of silt transported to the coast and thus permits minimal sea water penetration (Begg, 1978), causing the length of the estuary always to be short, with variation dependent only upon the rate of flow of the river. Thus, during floods, there is no estuary in the true sense, whereas during low volume flows the estuary ex-

tends approximately 0.8 km upstream from the mouth (Oliff, 1960).

3. Silt Loads and Erosion

Middleton and Oliff (1961) studied the suspended silt loads in the Tugela for the period between 1955 and 1956, calculating the mean annual discharge of the river as 226.4 m^3/s (7.1×10^9 m^3/yr), and mean annual silt load as 10.5×10^6 tons/yr and the mean annual concentration of suspended sediment by weight as 0.23%. The mean annual suspended load (terrigenous material) has since been recalculated by Flemming and Hay (1984) as 7.0×10^6 m^3/yr. The silt load estimate by Middleton and Oliff represents a mechanical denudation of the basin of 375 tons/km^2 per year, with an estimated 700 tons/km^3 of sediment being eroded annually from large portions of the Upper Tugela watershed (Orme, 1974). A more recent report by Murgatroyd (1979) stated that the present day observed rate of suspended sediment transport is 453 tons/km^2 per year, which is more than 28 times greater than the calculated geologically normal rate, showing severe erosion problems in large segments of the catchment. This was indicated in Oliff's 1960 study of the Tugela, where he found that more than 3/4 of the silt load was contributed by the section between Colenso and Mandini (viz. the more-eroded dry thornveld areas). He also noted that the suspended load between Bergville and Colenso was more than twice that of the whole catchment, indicating large amounts of silt were contributed by the easily eroded subsoils of the tall grassveld and farmlands in that section. Erosion is undoubtedly enhanced by poor grazing and

tillage practices, especially in areas of traditional African farming which comprise a minimum of 30% of the catchment (Orme, 1974). It is interesting to note that the mechanical denudation figure cited by Orme (1974) of 375 tons/km^2 per year is much higher than that for such major sediment transporting rivers as the Zambesi (75 tons/km^2 per year), the Mississippi (154 - 230 tons/km^2 per year) and the Colorado (271 tons/km^2 per year).

Presently there are four small dams on the Tugela River (fig. 2-1) at Chelmsford, Spioenkop, Windsor and Wagen Drift (Begg, 1978). It has long been thought that the construction of large dams on the Lower Tugela would result in the interception of the sediment supply to the beaches of northern Natal, consequently exposing them to severe erosion by the very strong wave-driven currents in the region. Nicholson (1983) has recently proposed a counter argument to such thinking in stating that although the elimination of the river-borne sediment, and the resulting removal of the offshore bar opposite the estuary mouth by wave action, will initially induce a period of erosion, it will eventually lead to greater stability of the adjacent coastline by no longer subjecting it to the large annual fluctuations caused by flood discharges.

4. Pollution

By world standards, the Tugela River is almost pollution-free. There do exist, however, potential sources for pollution, as the river ultimately collects most of the drainage from the Natal Coalfields via the Sundays and Buffalo Rivers,

the latter contributing 25% of the flow after Tugela Ferry. Coalfield drainage has been shown to produce excess acidity in rivers close to mines as a result of the presence of iron sulphides in the coal measures. Increased acidity is known to enhance the mobility of many toxic heavy metal species. These iron sulphides, existing mainly as crystalline pyrite (FeS_2) and its polymorph marcasite, are oxidised in air and water to ferric and ferrous sulphates, with or without the accompaniment of free sulphuric acid (Kemp, 1967). It should be noted that pH values for the Tugela in 1960 were 7.3 - 7.8 in summer and 7.5 - 8.3 in winter, unusually basic values for river water (world average 7.0 (Mason, 1966)). Such basic pH values might be attributed to the composition of dissolved material in the river being comprised mainly of calcium and magnesium bicarbonates contributed by the Beaufort and Ecca beds (cf. chap. III) which underlie the majority of the middle basin. The concentration of all dissolved solids (bicarbonates, sulphates, chlorides, etc.) was never found to exceed 202 mg/l in 1960, with approximately 160 mg/l being bicarbonate. The composition of the dissolved material in the river, coupled with the dilution of the Buffalo and Sundays Rivers upon entering the main Tugela System, is what keeps the acidity at manageable, non-threatening levels (Oliff, 1960).

Another possible contribution to pollution in the Tugela comes from sewage disposal of settlements and fertilization and pesticide runoff from farmlands adjacent to the rivers. 'Domestic' effluents constitute the largest single source of elevated metal values in rivers, being enriched in heavy

metals such as chromium, mercury, lead, copper, zinc, cadmium and arsenic, among others (Förstner and Wittman, 1981). In addition, sewage contains many organic and inorganic compounds that can cause havoc in the aquatic environment, particularly in the form of eutrophication caused by elevated nitrate and phosphate concentrations. Pesticides used in agriculture are transported into the rivers by runoff and are known to be hazardous to aquatic life.

The large paper processing plant at Mandini (fig. 2-1) could be another primary source of polluting effluent. The most potentially toxic compounds from pulp and paper mill effluents are organic compounds, but as these are fairly easily oxidised in the aquatic and marine environments they do not usually pose a serious threat, except in stagnant waters. However, the fungicides used to retard mould growth at several stages in the paper manufacturing process are a problem, especially the mercuric compounds used in the past. Polychlorinated phenolics (PCPs) are now used as fungicides, and although these are toxic to fish and invertebrates, the concentrations found in effluents are usually too low to cause adverse effects. Heavy metals other than mercury found in paper mill effluents are chromium, copper, lead, nickel and zinc (Pearson, 1980; Förstner and Wittman, 1981).

CHAPTER III GEOLOGIC SETTING OF THE TUGELA RIVER BASIN

1. Topography and Geomorphology

The topography of the Tugela River Basin is shown in figure 3-1 (after Oliff, 1960). Altitudes in the Basin range from greater than 2 400 m in the Drakensburg Escarpment, which lies along Natal's western boundary, to sea-level in the coastal lowlands bordering the Indian Ocean towards the east. Geomorphic regions are shown in figure 3-2 (after Orme, 1974); the Tugela River Basin, shown outlined, encompasses virtually all the types of geomorphology found in the area. Many faults lie in and around the basin, with two major transverse faults intersecting the river valley itself (fig. 3-3). The most noteable of these faults is the one closest to Mandini, as this is the location of the most prominent exposures of the Tugela Formation of the Archaen Basement Complex.

2. Geology

Orme (1974) divides the underlying geology of Natal into four principal rock groups. The Archaen granitic migmatites and gneisses of the basement complex are the oldest rocks, with an average age of 1 000 million years. Of this metamorphic complex, the group of major concern in the Tugela Basin is the Tugela Group which consists mainly of migmatitic hornblende gneisses and amphibolites, with minor constituents of pelitic and semi-pelitic schists and gneisses with a few discontinuous units of magnetite quartzite and lithographic limestone (SACS, 1980). Lying unconformably on the Archaen rocks, in a 50 - 100 km wide belt parallel to and inland from the coast, are

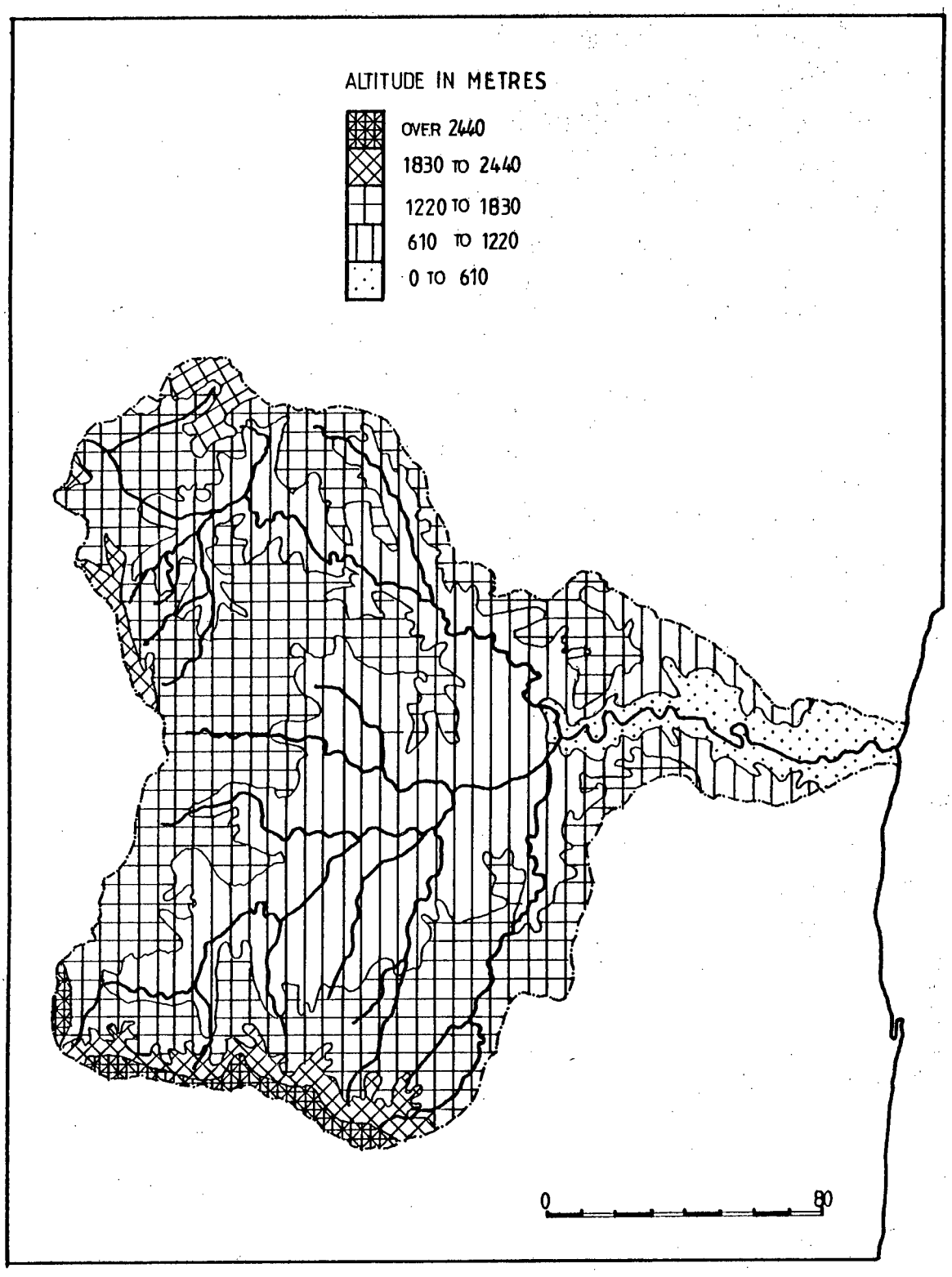

Figure 3-1. The topography of the Tugela River Basin (after Oliff, 1960).

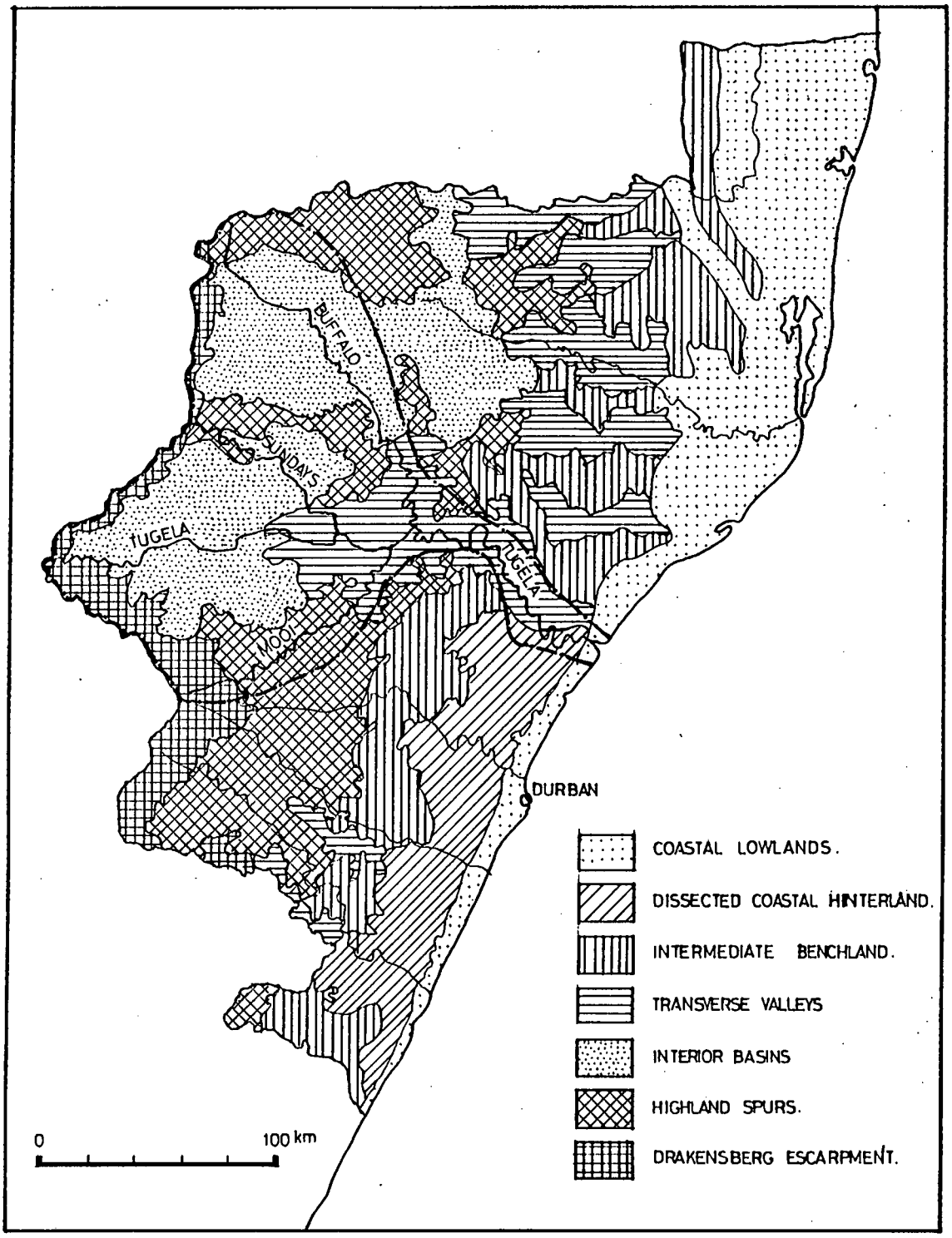

Figure 3-2. Geomorphic regions of Natal (after Orme, 1974). The Tugela River Basin is outlined.

the sandstones and shales of the Table Mountain Group (Upper Silurian to Middle Carboniferous). This, in turn, is overlain by the stratigraphic sequence of the Karoo System, consisting of the Dwyka tillites, the Ecca and Beaufort sandstones and shales, in which the coal seams are located, and the Stormberg volcanics (Upper Carboniferous to Lower Jurassic). The Karoo System covers most of interior Natal. The upper part of the Stormberg Series is characterised by extrusive basalts and andesitic rhyolites called the Drakensberg Volcanic Beds, to which are related the intrusive dolerites in the older rocks (Maud, 1968). The last group is that of relatively undeformed Cretaceous and Cenozoic sediments of marine, aeolian and fluvial origin that underlie the Zululand coastal plain (Orme, 1974).

The downstream order of the surficial geology in the Tugela River Basin (figs. 3-3 and 3-4) is:

1) the Drakensberg Volcanic Beds,
2) the mudstones, sandstones and shales of the lower Stormberg Series,
3) the mudstones and shales of the Beaufort Series in the flatter upper half of the basin,
4) the Ecca Series sandstones and shales in the middle portion,
5) the Archaen granites and gneisses of the Natal Metamorphic Complex, which is exposed by faulting in the lower portion, and
6) beds of Table Mountain Sandstone towards the coast.

Figure 3-3. The geology of the Tugela River Basin.

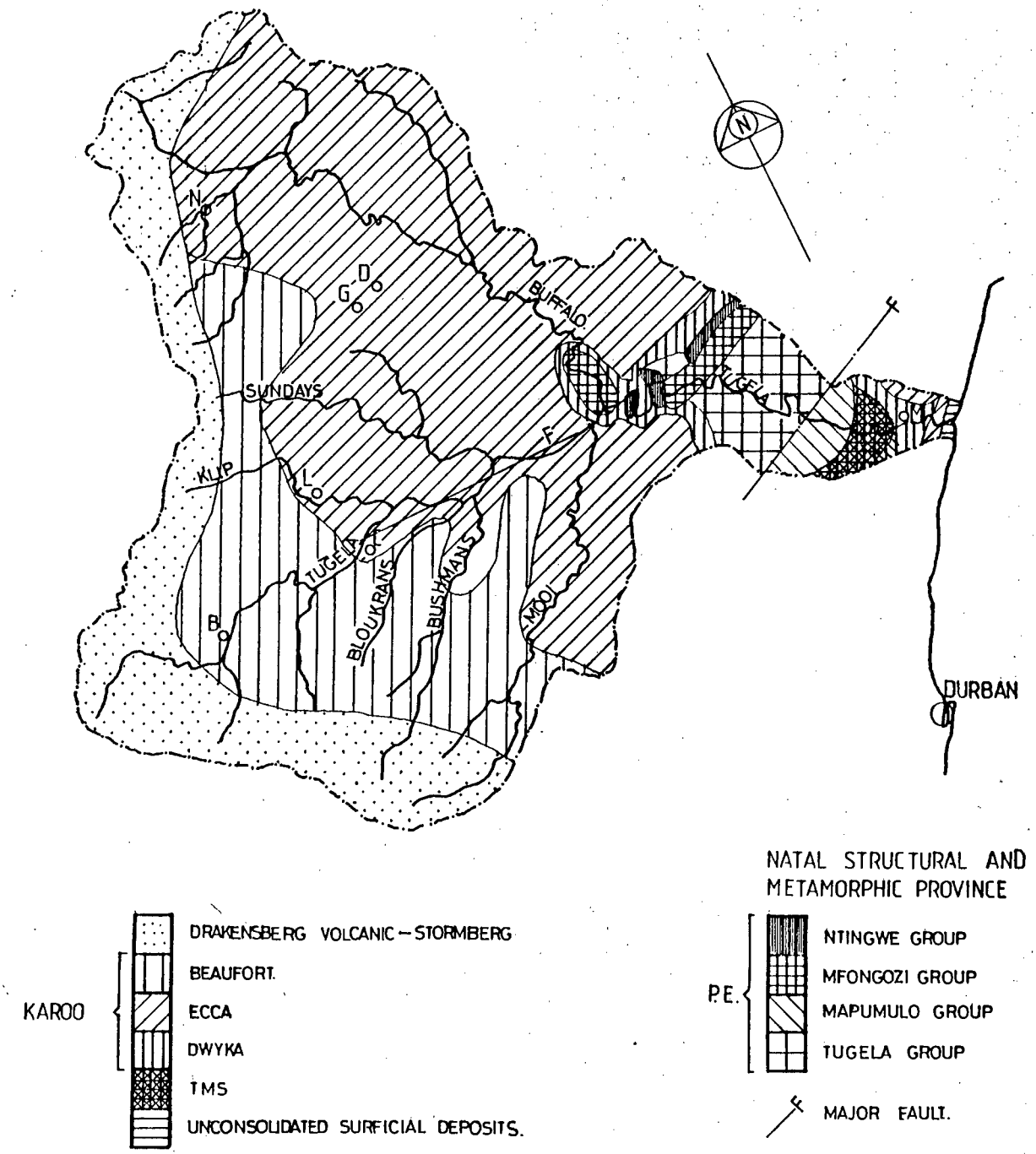

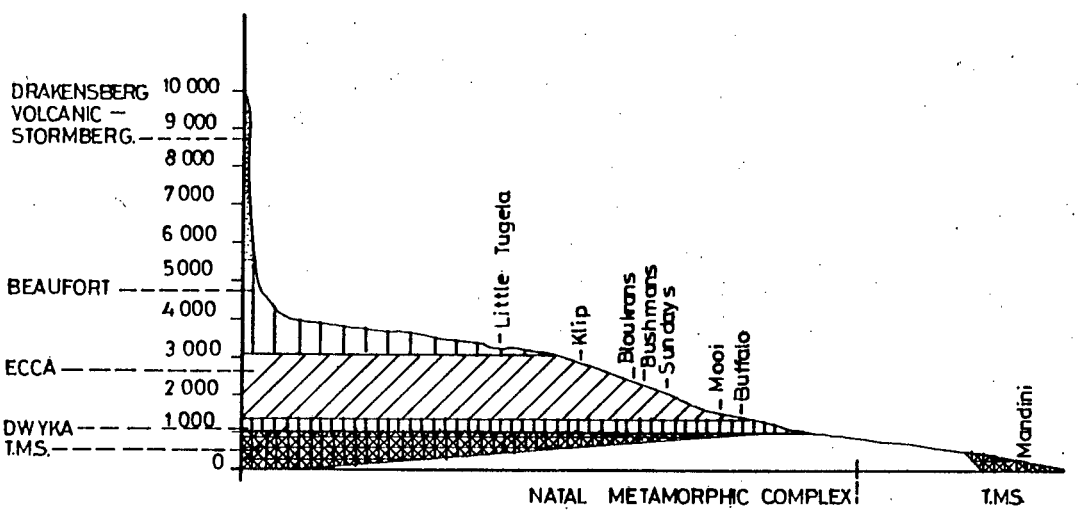

Figure 3-4. Cross-section of the Tugela River Basin showing the geology. The points of entrance of the tributaries into the main river system are indicated.

The Upper Tugela, the Buffalo, the Bushmans and the Mooi Rivers have their sources high on the face of the Drakensberg lavas. The other catchments commence in beds of the Stormberg Series. The majority of the middle and upper basin lies on the Beaufort and Ecca beds of the Karoo System, as seen in figure 3-3, with the lower, eastern part of the basin lying upon Dwyka tillite and the Archaen granites and gneisses of the Tugela and Mfongosi Systems (Oliff, 1960). The mechanical weakness of the shales and tillites underlying much of the basin, coupled with the relatively steep gradients of most of the rivers in the Tugela catchment, favours the unusually high erosion rate discussed in chapter II, section 3.

The Tugela estuary is cut into Dwyka tillites and Ecca shales of the Karoo System, which appear at depth in bore-holes drilled into bottom sediments of the river. Data from a borehole drilled near the Ultimatum Tree (6 km above the mouth) show Dwyka tillite at 61.8 cm below the present floodplain, which lies just above mean sea level (Orme, 1974). This till-ite is overlain by 6.8 m of dark grey silt and fine sand, which, in turn, is overlain by 43 m of grey to brown silty fine to medium sand and topped by 2 m of brown clayey sand. The thick grey to brown silty sand is typical of what the Tugela presently discharges into the ocean, and the top layer of brown clayey sand is a weathering product of the material underlying the flood plain. Twelve km above the mouth the bed-rock channel is 10.7 m below mean sea level and is overlain by 17 m of alluvium beneath the present channel bed (Orme, 1974).

3. Coastal Barrier-Lagoon Systems

The depth to basement rock in the Tugela and other Natal rivers was not caused by subsidence, and is thus an indication that sea-level was once much lower than at present. Exposure of the Tugela Bank, which presently lies just offshore opposite the mouth during periods of low sea-level, is thought to have furnished the source of supply of the sand in the Port Durnford Beds and the high coastal dunes of Zululand (Maud, 1968). Hobday and Orme (1974) performed a detailed study of the Pleistocene Port Durnford Formation, exposed north of the Tugela River Mouth (cf. fig. 2-1), and interpreted their findings as follows. The Port Durnford Formation gives clear evidence of a major Pleistocene marine transgression from a previously considerably lower sea-level to an elevation approximately 8 m above present, followed by a regression to still lower sea levels. The first regression mentioned above left residual marine and nearshore sediments, as well as aeolian sands, orientated north-south along the coastal plain. Several transgressions were superimposed on this regressive sequence, with the Port Durnford transgression initiating a major barrier-lagoon complex along the present-day coastline. This complex is now preserved as the Port Durnford Formation. During the last glaciation (Wisconsin) in late Pleistocene times, the sea-level fell at least 100 m and possibly 130 m below present sea-level and rivers passed through the earlier deposits to lay a cover of marine, aeolian and fluvial sands on the continental shelf. Onshore, the sands were transformed into clayey sands by weathering and eluviation, while aeolianite and beachrock formed at lower levels. The Port Durnford Formation was eroded

into blocks that were subsequently invaded by the sea during the Flandrian Transgression (15 000 yr BP to 5 000 yr BP). This transgression brought many barrier-lagoon complexes into existence along the Natal coast. Thus, the remnants of the Pleistocene barrier-lagoon complex provided the framework around which Holocene barrier and lagoon development has taken place. As the Port Durnford Formation was formed by a transgressive sequence similar to what exists today, its preserved sedimentary sequence is what is expected to form in the barrier-lagoon complexes across modern Natal estuaries (Hobday and Orme, 1974).

CHAPTER IV GEOLOGIC/OCEANOGRAPHIC SETTING OF THE SOUTHEAST AFRICAN CONTINENTAL SHELF

1. Shelf Morphology

The continental shelf of southeast Africa was initially formed during the Mesozoic break-up of Gondwanaland. The fragmentation occurred in two phases with the first, approximately 180 my BP, breaking Gondwanaland into western and eastern halves along the eastern African coastline of Mocambique, northern Natal and the Mocambique ridge. The second phase, occurring approximately 125 - 130 my BP, broke western Gondwanaland apart separating Africa from South America (Flemming in Heydorn, 1976). This early Cretaceous rifting stage which preceded the continental drifting, during which marine conditions were established in the southern part of Africa, was established by offshore drilling on the Agulhas Bank by SOEKOR (Southern Oil Exploration Corporation) (Hobday, 1980). The Natal coast has been found to have closely coinciding Cretaceous, Tertiary, Pleistocene and Recent shorelines south of the Zululand coastal plain. During the late Tertiary, the shoreline became oscillatory and during Pleistocene time it migrated eastward until attaining its present position by the Upper Pleistocene (Maud, 1968).

The modern shelf morphology is predominantly a result of Pleistocene sea-level fluctuations, as discussed in chapter III, section 3., modified by more recent sedimentation. The entire shelf between Durban and Cape St. Lucia (fig. 4-1), is dominated by a large structural offset superimposed on which lies

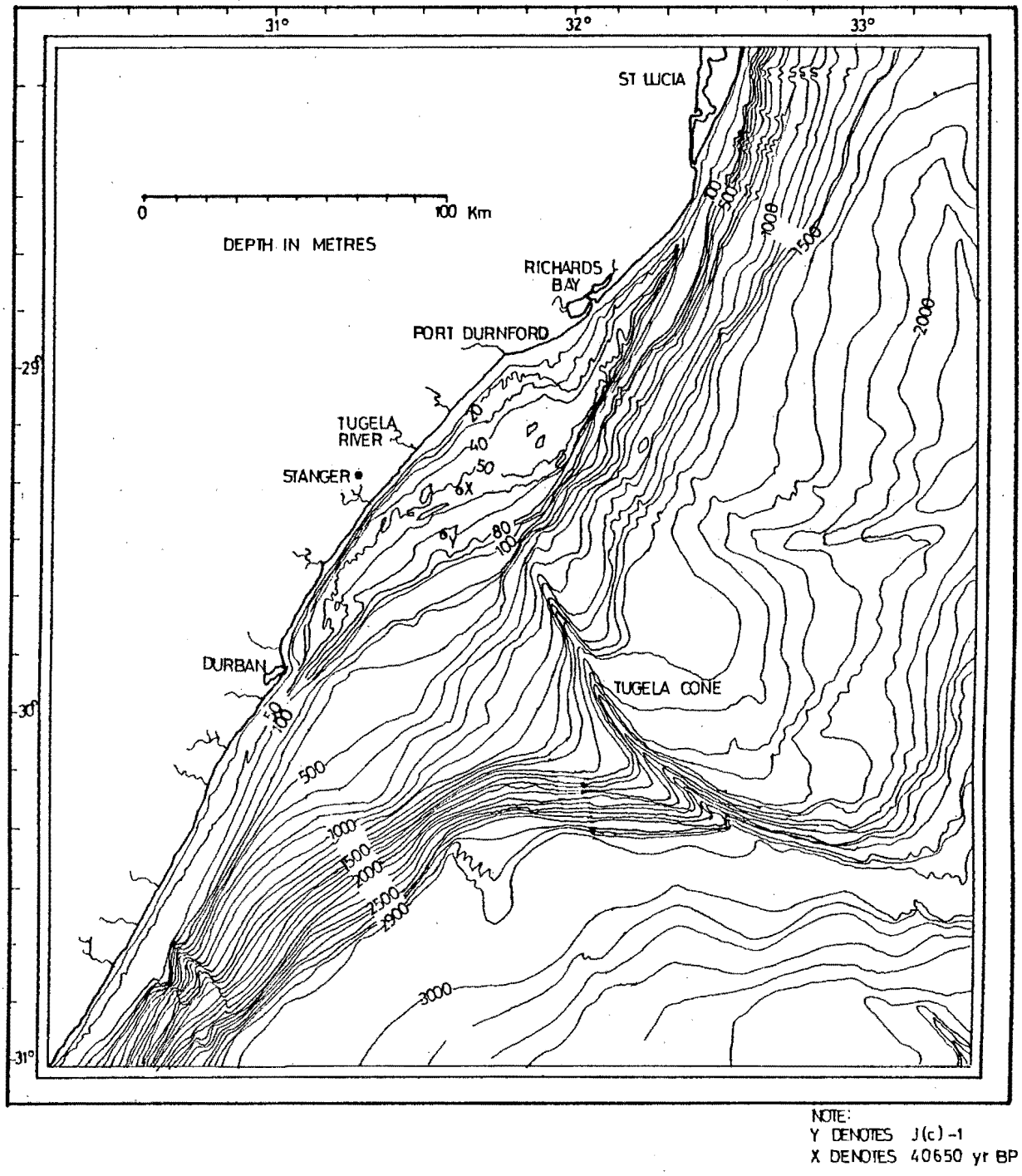

Figure 4-1. The continental shelf off Natal and Zululand. (Modified from Goodlad, 1978).

the Tugela River sediment cone, or delta (Flemming 1978; Goodlad 1978). Moving in a northerly direction from the southern border of Natal, the shelf is narrow, 5 - 6 km (world average 43 km (Shepard, 1963)), and parallels the coast until north of Durban where the shelf break trends northeast away from the coast and broadens to a maximum width of 45 km southeast of the Tugela River Mouth. North of this, the shelf break reverts to the orientation found south of Durban, with the shelf narrowing gradually to 4.5 km off Cape St. Lucia. The coastline also swings out, but northward from where the shelf widens, at Port Durnford (Moir, 1975; Goodlad, 1978). The shelf break occurs for the most part around the 100 m isobath (world average 130 m), but is poorly defined south of latitude $29^{o}30'$, where the shelf begins to widen north of Durban. At this latitude, a gradual change in slope occurs at the 100 m mark, going from $0^{o}17'$ on the shelf to 1^{o} on the slope. North of latitude $29^{o}30'$, the slope of the shelf is $0^{o}07'$, changing to $2^{o}10'$ on the continental slope opposite the Tugela River Mouth. The slope of the continental slope off the St. Lucia estuary mouth steepens to $4^{o}09'$. The poor definition of the slope break at latitude $29^{o}30'$ is due to the pointing of the Tugela Canyon's cleft at the flexure of the shelf break in the vicinity, with the upper regions of the 2 800 m deep canyon thus not clearly defined at the 100 m isobath (Moir, 1975). There is an inshore discontinuous shelf break apparent 2 km offshore between Durban and Tugela Mouth (Goodlad, 1978).

Flemming (1981) divides the shelf platform, morphologically, into a nearshore zone and an offshore zone that are sepa-

rated by a drowned, partly reworked Pleistocene sediment ridge that stretches subparallel to the coastline at water depths of 40 - 60 m. This ridge is not continuous, but remnants are found along most parts of the shelf. The ridge peaks of 5 - 20 m relief are more common north of latitude 29°30', northwest of the Tugela River Mouth, suggesting that it forms the remains of a southward extension of the Zululand coastal plain barrier-lagoon system which formed during the Pleistocene regression (Moir, 1975).

Echograms generally show a smooth bottom profile, though local isobaths indicate an undulating topography of broad shallow troughs separated by north-south trending low, wide ridges. Seismics show a 2 km wide belt of sediment lying on the seaward edge of the nearshore rise between the Tugela and Matigulu Rivers, with a maximum thickness of 14 m. The base of the deposit is clearly defined by a strong acoustical reflector and several internal reflectors in the underlying sub-bottom, although the upper surface is irregular in places. South of the Tugela River Mouth, up to 11 m of sediment occurs. Although seismic penetration is often poor, there is no evidence of a modern delta existing seaward of the Tugela. Just north of the Tugela River Mouth, extensive areas of rocky seafloor are exposed (Moir, 1975; Flemming, 1978 and 1981).

2. Stratigraphy

The only borehole data available on the continental shelf off the Tugela River is that of the J(c) - 1 borehole drilled by SOEKOR while exploring for oil. The following information

is from a study performed on this borehole by Du Toit and Leith (1974). The position of the borehole was 29°27'41.30" South, 31°35'39.70" East (fig. 4-1), and it was taken from a water depth of 71.6 m, 24 km east of the Natal coast at Stanger. The borehole intersected 1 390 m of Pliocene-Paleocene sediments, 733 m of marine Upper Cretaceous sediments and 49 m of Dwyka tillite before being abandoned in basement quartzitic sandstones of the Cape Supergroup. From the stratigraphy of the core, the authors calculated the overall sedimentation rate for the Cretaceous and Tertiary sediments at 30.5 m/my. A relatively slow rate (15 m/my) during the Paleocene, along with paleontological indications of deposition in shallow water, suggested the presence of a lower Paleocene pro-delta clay rich in organic matter. A high sedimentation rate of 61 m/my in the overlying Upper Paleocene-Eocene succession, along with other factors, showed existence of a sub-aqueous prograding delta in the Eocene. The Oligocene succession, showing a subdued rate of sedimentation (23 m/my) and a complete sequence that is thin compared to the Eocene, indicates that the Lower Oligocene was a time of delta-destructive marine transgression. A shelly limestone of Miocene age was deposited over the Oligocene succession in the vicinity of J(c) - 1 (Du Toit and Leith, 1974).

3. Currents and Waves

The dominant hydrologic feature off the southeast African coast is the Agulhas Current. Bang and Pearce (1976) state that the Agulhas Current was initially established in mid-Tertiary times, but Hutson (1980), using micropaleontological

evidence obtained from a core taken in the Southwest Indian Ocean, has shown that the current was a seasonal phenomenon that only reached its present-day effectiveness in the Late Pleistocene. The Mocambique-Agulhas Current is part of the Western Boundary Current System of the southwestern Indian Ocean and flows above and parallel to the shelf break at velocities up to 4 knots (2.0 m/s). The mean width of the Current is 100 km and its depth has been traced to 2 500 m (Bang and Pearce in Heydorn, 1976). It gains its identity between 25^{o} and 30^{o} south (Goodlad, 1979). The distance offshore of the current has been significantly correlated with local atmospheric pressure gradients (Orme, 1973). The surface water of the Agulhas Current is a mixture of tropical surface water and subtropical surface water with a resultant core temperature two degrees warmer than the continental shelf waters and salinites in the 35.2×10^{-3} to 35.4×10^{-3} range. Beneath the surface, the temperature and salinity of the current's water decrease with depth (Heydorn, 1976). It should be noted that the inshore continental shelf waters are derived locally from the Agulhas Current and are cooler than the core of the Agulhas due to wind-induced upwelling and not to advection of cold water from the south-west (Pearce, 1976).

The nearshore current regime between Durban and Port Durnford is somewhat less well understood than the Agulhas Current. In general, the area is classified as a high-energy environment dominated by south-southeasterly swells. No consistent seasonal pattern has been established for shelf flow along the Natal coast (Pearce et al., 1978). The prevailing

northeasterly and southwesterly winds in the region blow with relatively equal frequency and velocity (Orme, 1974). Wind stress is the primary forcing mechanism in the wider shelf region off the Tugela River Mouth, effecting the migration of shallow local low-pressure atmospheric cells in a northeasterly direction up the coast. When these periodic coastal lows pass over the sea, the wind changes rapidly from northeast to southwest, with a period of between two and three days existing between the peaks of these lows in both summer and winter (Pearce et al., 1978). The southwest winds associated with the atmospheric lows reinforce the deep water waves that approach virtually normal to the coast near the Tugela Mouth from the south-southeast. Further north, the waves refract because of the narrowing of the shelf and thus approach the shore at a 5 - 20^{o} angle. This pronounced wave obliquity to the north and south of the widest part of the continental shelf promotes a strong unidirectional longshore current that flows northeastwards within the surf zone (Orme, 1973).

Wave motion along the western edge of the Agulhas Current generates a cyclonic eddy circulation between the current and the coast in the lee of the structural offset mentioned in section 1. of this chapter. This appears offshore as a system of reversing coastal currents (Orme, 1973). These currents are predominantly north-flowing, with maximum surface velocities of 1 m/s, as seen in measurements taken between Durban and Port Durnford where the current is north-flowing 53% of the time, south-flowing 44% (Harris, 1964). There is, however, a steady decrease in the frequency of northerly flow seen in

travelling across the shelf towards the slope, accompanied by an equivalent increase in southerly flow. The eddy is not a permanent feature and it has been postulated that at any one time a succession of eddies of a variety of scales exists in this region (Pearce et al., 1978). These eddies, which encompass the entire water column, are generated by the interaction between atmospheric pressure changes, the driving energy of the Agulhas Current and the local coastal and bottom topography (Pearce, 1976). A map of the currents is shown in figure 4-2.

4. Surficial Sediments

4.1 Texture

The textural character of the sediments on the southeast African continental shelf is dominated by sand-size and coarser materials, with the coarsest sediments found near the shelf break. This distribution is considered to be a function of the high-energy conditions prevailing over the mostly narrow shelf, complemented by the winnowing action of the Agulhas Current along the shelf break. The highest concentration of gravel in the region lies 10 nautical miles offshore between Durban and the Tugela River Mouth, and is thought to be related to the eddy circulation existing in the area (Moir, 1976). Moir (1976) further suggested that the accumulation of gravelly residue in this area is the net result of the combined effects of a meagre input of fine-grained sediment that is initially carried northeastwards by the longshore current and northward winnowing by the local coastal currents. Side-scan sonar records and dredge hauls taken offshore between Durban

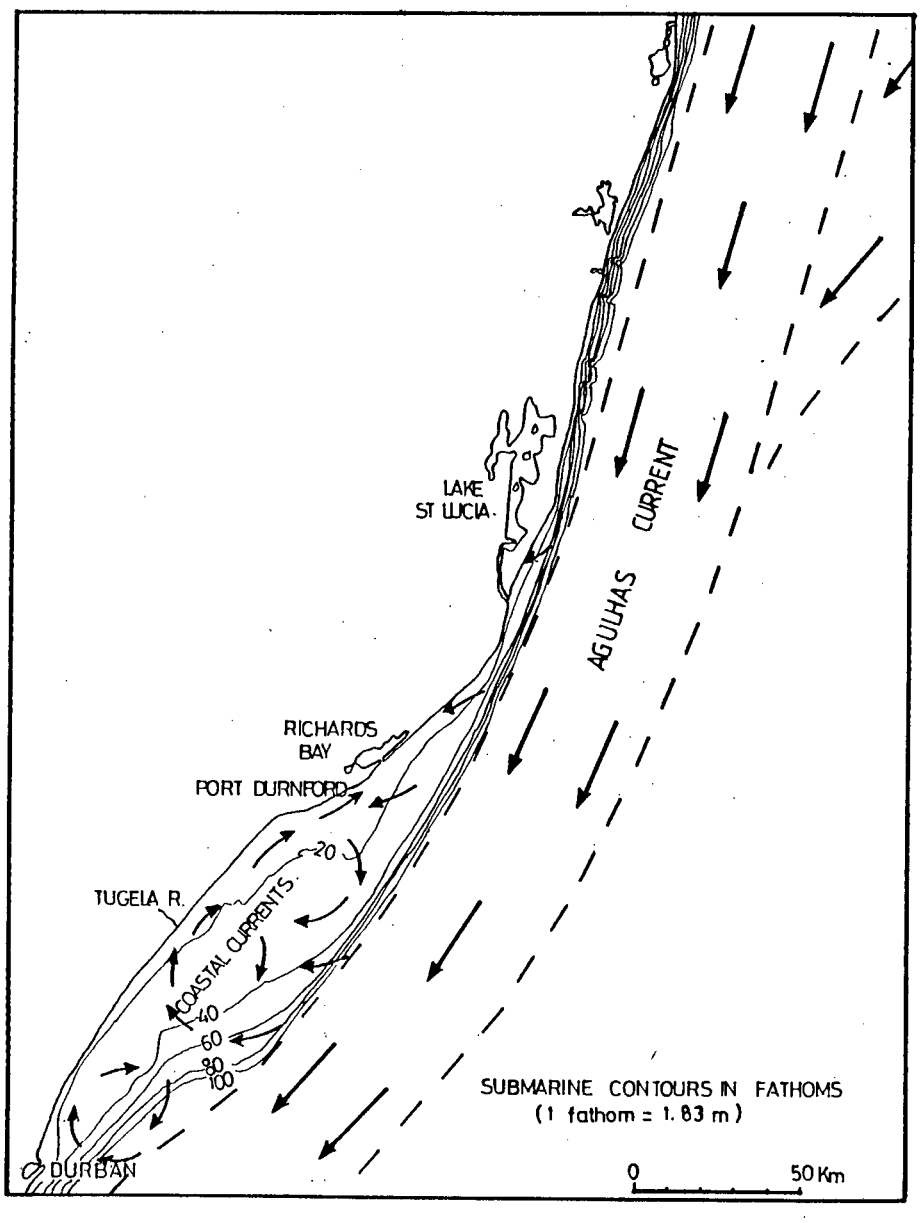

Figure 4-2. Currents off the coast of Natal (after Orme, 1973).

and Richards Bay confirmed the existence of extensive areas of rippled gravel deposits and have shown that they lie on muddy carbonaceous material dated at more than 40 650 yr BP (Flemming, 1978). It appears that relict estuarine deposits were truncated and covered by a transgressive sheet of terrigeneous gravels which, at depths greater than 60 m, periodically form rippled surfaces as a result of the present swell regime. Toward the south, the gravel is covered by a thin layer of sand in which scouring by the Agulhas Current has produced features resembling low amplitude dunes of long wavelength. The dredge haul results also show algal reef bioherms covering exposed bedrock, the reefs being relict features of Late Pleistocene age (Flemming, 1978).

Superimposed on the generally sandy character of the shelf are zones of muddy-sand, sandy-mud and mud which are attributable to the influence of fluvial input on the local sedimentation system. The existence of two well-defined, roughly coast-parallel belts of mud on the continental shelf off the Tugela River Mouth was established in the course of sampling for this study (cf. chapter VIII). A textural analysis of the sediments in the study area done by Moir (1976) showed high (>50%) concentrations of clay in the nearshore muds as opposed to only $\pm$25% in the outer shelf muds. Moir found that the silt content of the outer shelf muddy sediments was also less than that of the nearshore muds. Moir's study further showed that two areas are present on the continental slope east of Durban where terrigenous sandy mud escapes over the shelf break, permitting postulation that these could be

the remains of older sedimentation related to Pleistocene low sea-level stands when the Tugela and other rivers extended across the shelf.

4.2 Composition

Flemming (1978) has identified two predominant facies along most of the southeast African continental shelf. These are described as an inner shelf modern terrigenous facies that forms an inshore sand prism characterised by a high quartz content, and an outer shelf relict carbonate facies that is dominated by gravels composed of relict algal nodules and shell fragments. The former is considered to be wave dominated, the latter, current dominated, with the transition occurring along the 50 - 60 m isobath. The inshore terrigenous belt accumulated over approximately the last 6 000 years after the sea-level attained its present position following the last glaciation. In the counter-current region off Durban, however, a more complex transitional facies was observed where the carbonate contents deviate from the established distinct trend. This transitional facies results from lateral mixing of the two major facies, and is complicated further by the relatively large amount of terrigenous input of fines that comes mostly from the Tugela River. Continental slope sediments are composed primarily of muddy foraminiferal sands (Flemming in Heydorn, 1976; Flemming, 1978).

4.3 Sediment Dispersal

Sediment dispersal along the southeast African continental margin is controlled by four major factors. These are:

1) the morphology of the upper continental margin;
2) the wave regime and wind-driven circulation system;
3) the influence of the Agulhas Current; and
4) sediment supply (Flemming, 1981).

The amount of sediment supplied by the Tugela River was discussed in chapter II, section 3.; the following is a summary of how the first three factors affect this supply, as has been described in the preceding sections of this chapter.

The sediment discharge from the Tugela River produces an asymmetrical T-shaped plume that extends 3 to 5 km offshore and 15 km alongshore during the summer rainy season (Orme, 1974). The dominating northeast coastal current, in conjunction with the nearshore circulation system in the area off the Tugela River Mouth (cf. fig. 4-2), is a significant factor in the transport of sediments up the coast beyond the surf zone, as well as in the redistribution of materials across the inner parts of the shelf. One aspect of such redistribution is the movement of sediments by the onshore components of the coastal current regime back towards the nearshore circulation system (Orme, 1973). The northeast disposition of the nearshore mud belt off the Tugela reflects the role played by the local and nearshore current systems; the southward trend of the outer mud belt indicates the more direct influence of the Agulhas Current. The demarcation of the boundary between southerly flow of the Agulhas Current and the northerly flow of the eddy system is seen on the seabed as bedload partings (Flemming, 1980).

The sedimentation picture presented becomes more complex when considering features of the water column and of the sediments themselves. Pearce and co-workers (1978) found that, in calculating the mean cross-shelf velocity components, there was a suggestion of an onshore tendency in the lower half of the water column and an offshore flow in the near-surface layer. This observation corresponds to the concept of a frictionally-driven Eckman 'upwelling' (southerly alongshore flow near the bottom being deflected to the right in the southern hemisphere) along the surfaces near the seabed and a compensating flow away from the coast in surface waters, making the observed flow pattern consistent with the idea that the nearshore water is drawn up by frictional processes from depths of 50 to 100 m in the Agulhas Current. They concluded that the 'upwelling' was most likely an intermittent pulsing of water onto the shelf, rather than a steady process, accomodating previous data on current reversals in the area (Pearce et al., 1978). This work coordinates well with the textural distribution of sediment in the region, viz. mostly sand and exposed bedrock close to shore just north and south of the Tugela River Mouth with the mud belt further offshore. Consideration of all the components affecting sedimentation along the East coast of southern Africa, and their ultimate relation to the Agulhas Current, it is easy to understand the statement made by Flemming (1981) that the Agulhas Current is the most important factor controlling sedimentation in this area.

CHAPTER V METHODS

1. Sampling

1.1 River and Estuary Samples

The river and estuary samples were collected on 25 March, 1982. At that time, the river had not flooded for 3 years. However, the Tugela has been known to flood as late as April, and the summer rains from December, 1981 to the time of sampling had been heavier than in the preceding two years.

The two estuary samples were collected with a hand corer composed of a plastic barrel with a stainless steel T-shaped handle. Both were taken from a 1 m depth, approximately 3 m from the shore at the positions shown in figure 6-1 (in chap. VI). The seven river samples (fig. 6-1 in chap. VI) were taken from a small boat using a stainless steel corer, barrel length 19.5 cm, attached to a nylon rope. Some difficulties were experienced with the boat sampling in retaining the less consolidated samples due to the lack of a core 'catcher' on the corer. In addition, especially in the deeper channels, strong currents reduced the velocity with which the corer could enter the sediment. At those locations where problems were encountered, the taking of several small samples yielded sufficient material to provide a geochemically representative sample. Depths and visual descriptions of the samples may be found in Appendix A, table A-1.

1.2 Continental Shelf Samples

Continental shelf samples were taken with a Shipek grab

during cruise number 82-05 (29 March - 2 April, 1982) of the CSIR's Research Vessel Meiring Naude. As the samples were taken, they were visually categorized into textural divisions. This information, in conjunction with seismic profiles previously made in the area (Flemming, cruise report MN81-08), permitted preliminary delineation of the two mud belts in which subsequent sampling was concentrated. Sample sites are shown in figure 6-2 (chap. VI), with accurate positions and visual descriptions given in Appendix A, table A-2.

The shipek grab is one of the best methods for surficial sediment collection, as it can collect samples with almost equal success on all types of bottom material with little or no disturbance of the surface and virtually no washout from the bucket upon ascent (Golterman et al., 1983). To avoid possible contamination from the paint on the sides of the grab, approximately 500 ml samples were taken from the centre of the bucket. Samples were stored in acid-rinsed plastic containers which were placed into a freezer on-board the ship. Samples were frozen to inhibit oxidation, with the risk accepted of altering the structures of the existing clay minerals.

2. Sample Preparation

A complete flow chart for sample preparation and analysis is shown in figure 5-1.

Samples were initially removed from the freezer and thawed to allow as thorough a mixing by shaking as possible, permitting the taking of a random homogeneous subsample. After

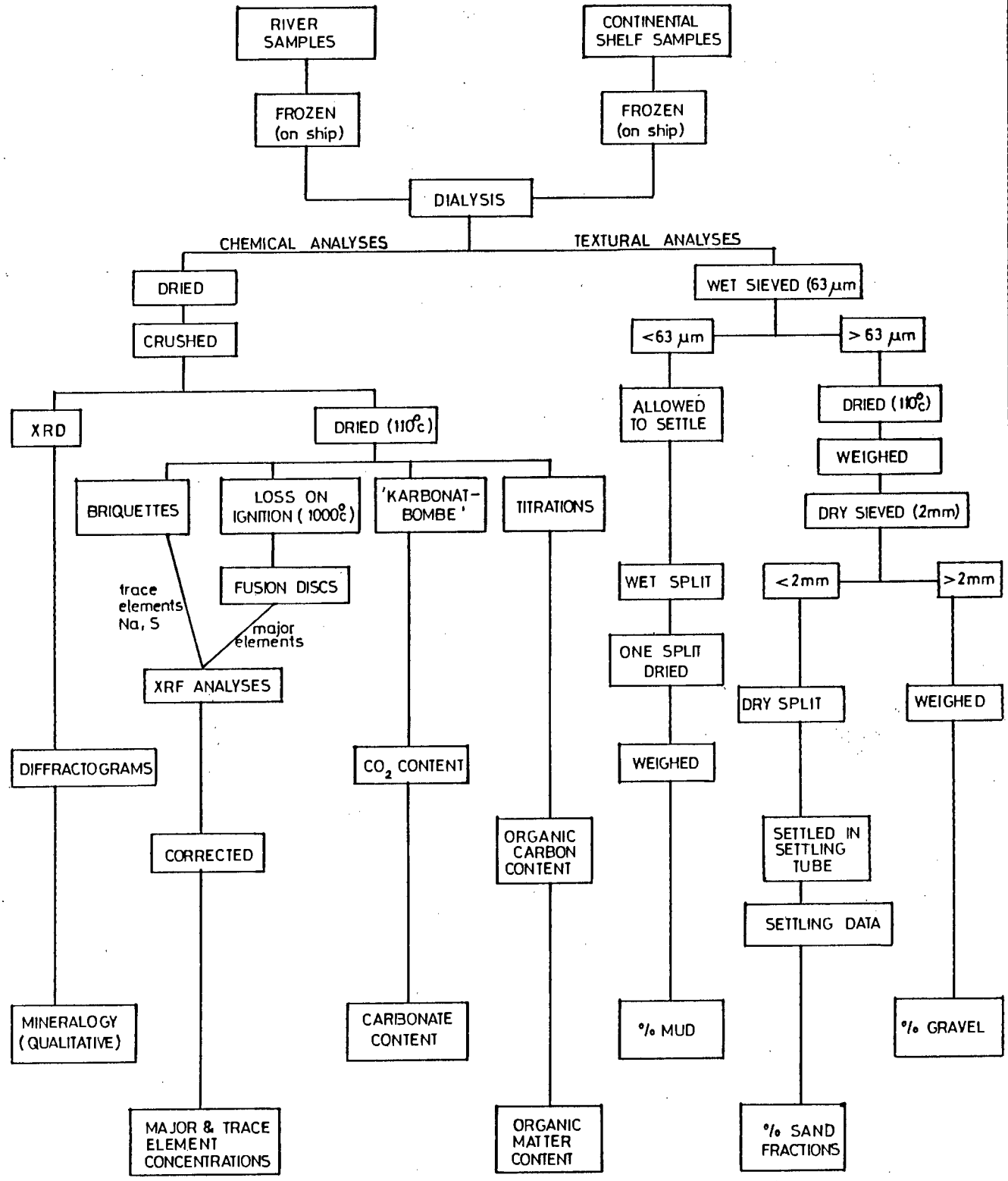

Figure 5-1. Flow chart for sample preparation and analyses.

mixing, roughly 100 - 150 g subsamples were taken from each sample by removing a 'core' through the centre of the container. It was necessary to sample all levels of the container to prevent bias from differential particle settling after shaking. The subsamples were placed directly into 400 mm lengths of dialysis tubing and hung, 20 at a time, in plastic buckets rigged with cord across their tops. All samples were dialysed in distilled water for three sequential periods of 6, 12 and 24 hr. Detailed experiments described by Birch (1975) have shown that dialysis performed in this fashion will extract the interstitial water and salt from samples without stripping the sediment of exchangeable cations.

Following dialysis, the samples were removed from the tubing and placed into clean petri dishes. After mixing by stirring, a small subsample ($\pm$5 g) was taken from each, stored in small glass vials and refrozen. These subsamples were later used for particle size analysis. Samples were then dried in an oven, initially at 50^{o}C, then, after breaking up partially dried samples, at 110^{o}C.

After complete drying, the samples were crushed using a 100 cc agate vessel on a Siebtechnik swing mill. Samples varied in the amount of time necessary to crush them, but all were ground until a fineness of approximately -300 mesh was attained. The vessel was thoroughly cleaned after crushing each sample by, first, blowing out excess sample remaining in the vessel with compressed air, followed by sequential rinsing of the vessel with tap water, distilled water and acetone,

and, finally, being dried by blowing out again with compressed air. The samples were crushed in the order of

1) sand,
2) muddy sand,
3) sandy mud, and
4) mud,

based on visual assessments, to help prevent inter-sample contamination. The vessel was cleaned by grinding pure quartz in it at the beginning and end of each crushing session.

3. Analytical Techniques

3.1 X-ray Fluorescence Spectrometry

All samples were analysed for 10 major and 23 trace elements by X-ray fluorescence spectrometry (XRFS). Analyses were performed on three different instruments, a Siemens SRS-1, a Philips 1220 and a Philips 1400 XRF spectrometer. The standards and instrumental conditions used were those routinely set up in the Geochemistry Department at the University of Cape Town; some of the parameters may be found in Appendix B, table B-1. Data reduction was done on a Hewlett Packard HP1000 computer using inhouse software MAJOR and TRACE. The lower limits of detection and errors (standard deviations) for all elements determined are given in Appendix B, table B-2.

Major element analyses for SiO_2, TiO_2, Al_2O_3, Fe_2O_3(total Fe), MnO, MgO, CaO, K_2O, and P_2O_5 were performed on lithium tetraborate fusion discs (with heavy absorber) prepared following the method of Norrish and Hutton (1969) using sample material roasted at 1000°C. Loss on ignition was determined

from the mass lost by the roasted sample relative to the sample dried at 110°C. Sodium and sulfur were determined on 6 g boric acid-backed briquettes. The trace elements Rb, Sr, Y, Zr, Nb, U, Th, Pb, Zn, Cu, Ni, Co, Cr, V, Ba, Sc, Br, Ga, La, Ce, Nd, and As were determined on briquettes composed of 18 g dried sample (110°C) mixed with 2 g Hoechst wax. These 10% wax briquettes were made by mixing the sample with the wax in a Turbular mixer for 1 - 2 hr, then forming the briquette in a steel die in a hydraulic press using 10 tons pressure. All samples were re-dried at 110°C for a minimum of 4 hr before preparation.

3.2 X-ray Diffraction

X-ray diffractograms were run on all samples to determine the bulk mineralogy. Each crushed sample was hand pressed into a standard Philips aluminum cavity mount with the top of the sample polished flush with the surface of the mount by rubbing with a glass slide. The polishing was done to induce preferred orientation in the sample to enhance any clay mineral peaks present in the resulting diffractograms. The samples were run on a Philips X-ray diffractometer using CuK_{α} radiation with monochromator and a scintillation counter with pulse height selection. The instrumental conditions were 40 kV, 20 mA, with a time constant of 2, a scanning speed of $2^{\circ}2\theta$/min and a chart speed of 2 cm/min. The divergence and receiving slits were $\frac{1}{4}^{\circ}2\theta$ and the antiscatter slit, $\frac{1}{2}^{\circ}2\theta$. The small slit settings were used to reduce the background noise as well as to enhance the low angle peaks.

3.3 Carbonate Determinations

The carbonate content of all samples was determined gasometrically using a 'karbonat-bombe' after the method described by Müller and Gastner (1971). This method involves the measurement of the CO_2 gas evolved when a known amount of sample is reacted with a fixed amount of hydrochloric acid. The amount of sample needed for each analysis was calculated from the CaO value obtained from XRFS analyses, assuming all CaO as $CaCO_3$, in order to achieve readings as close as possible to that of the standard. The percentages of $CaCO_3$ were calculated by simple proportionality to results obtained from running a standard of 0.5 g 100% $CaCO_3$. A standard was run after every five determinations. The absolute error of a single determination is given as $\pm$ 1% by Müller and Gastner (1971). Birch (1979), however, gives the precision of the method as better than 3% for values >5% $CaCO_3$ and <4% for smaller concentrations, with absolute accuracy as $\pm$2% for samples with >5% $CaCO_3$.

3.4 Organic Carbon Determinations

Organic carbon content was determined for all samples using the standard wet oxidation technique developed by Morgans (1956). This method involves the oxidation of all non-oxidized carbon in the sediment by hot chromic acid followed by titration of the excess acid against ferrous sulphate. All analyses were made in duplicate, with a standard run with each group of twenty analyses. The method assumes that all the organic carbon in the sediment is in the same state of oxidation, thus it yields only approximate results.

Birch (1975) states that organic carbon levels of >1% have precisions of 15% and levels <1% have precisions of 30% at the 95% confidence level. A study by Summerhayes (1972a) showed the method to be accurate within roughly 3% at the 95% confidence level for samples containing more than 1% organic carbon.

Organic matter values were obtained by multiplying the organic carbon percentages by 1.8 (Willis, pers. comm.).

3.5 Particle Size Analysis

The textural compositions of all the sediments sampled were determined using the standard techniques of the Marine Geoscience Unit at the University of Cape Town. The sub-samples that had been refrozen following dialysis (section 2.) were allowed to thaw and disperse in beakers of distilled water. The mud and sand fractions were separated by wet sieving through a 63 μm sieve. The mud fractions were stored in plastic tubs and left to settle. The sand fractions were dried at 110^{o}C and weighed.

The sand fractions were dry-sieved (2 mm) to separate out gravel, which was weighed, and then split into 2 - 3 g subsamples using a microsplitter. The subsamples were settled in a settling tube designed and built as described by Flemming and Thum (1978). The resultant analogue curves were digitized and the data were statistically analyzed for various textural parameters using the program SETTLEPROG/TOTALSTATS on a UNIVAC 1108 computer. Nineteen of the samples had either too

little sand remaining after the mud was removed or contained too much organic material to be settled. The sand fractions of these samples were classified by dry sieving through a series of sieves (1 mm, 500 μm, 250 μm, 125 μm).

The percentages of mud in the samples were determined volumetrically. Initially, the excess water was decanted from the tubs of settled mud. The mud was then resuspended in a known volume of water and split with a wet splitter. Noting the volumes of both splits, one split was dried and weighed, the other stored for future analysis. By calculating the percentage of mud in the dried split back to 100% volume, the figure for the total amount of mud present was derived.

CHAPTER VI DATA

Positions of the river and estuary samples are shown in figure 6-1. Figure 6-2 indicates the sample positions on the continental shelf.

The data for all analyses are presented in Table 6-1. All data for trace element analyses done on the 10% wax briquettes have been corrected for dilution.

Data which are used for interpretation in any sediment sampling program are subject to numerous sources of error. The major source of error in all of the analyses performed is from the sampling. Sampling error becomes greater as the concentrations of minerals and their constituent elements become smaller. An attempt was made to reduce this error at each stage of analysis by taking subsamples in proper proportion to the size of the particles in the samples (Kleeman, 1967). Thus, to facilitate random subsampling, initially large subsamples were taken ($\pm$150 g) from the original samples, and smaller subsamples taken (18 g, 5 g and 0.28 g for wax-mixed briquettes, boric acid-backed briquettes and fusion discs respectively) from the -300 mesh ground samples.

Another possible source of error results from improper storage of the samples causing a change in composition. Such error was prevented in this study by freezing the samples as they were taken and only thawing them immediately before pre-

paration for analysis. Other errors may result from the analytical procedures used, either from operator or instrumental sources. The possible effects on the resultant data may be inferred from the precision and/or accuracy discussed for each of the techniques used in this study (cf. chap. V, section 3.). It is believed that the quality of all the data used in the following interpretation is more than acceptable for the needs of this project.

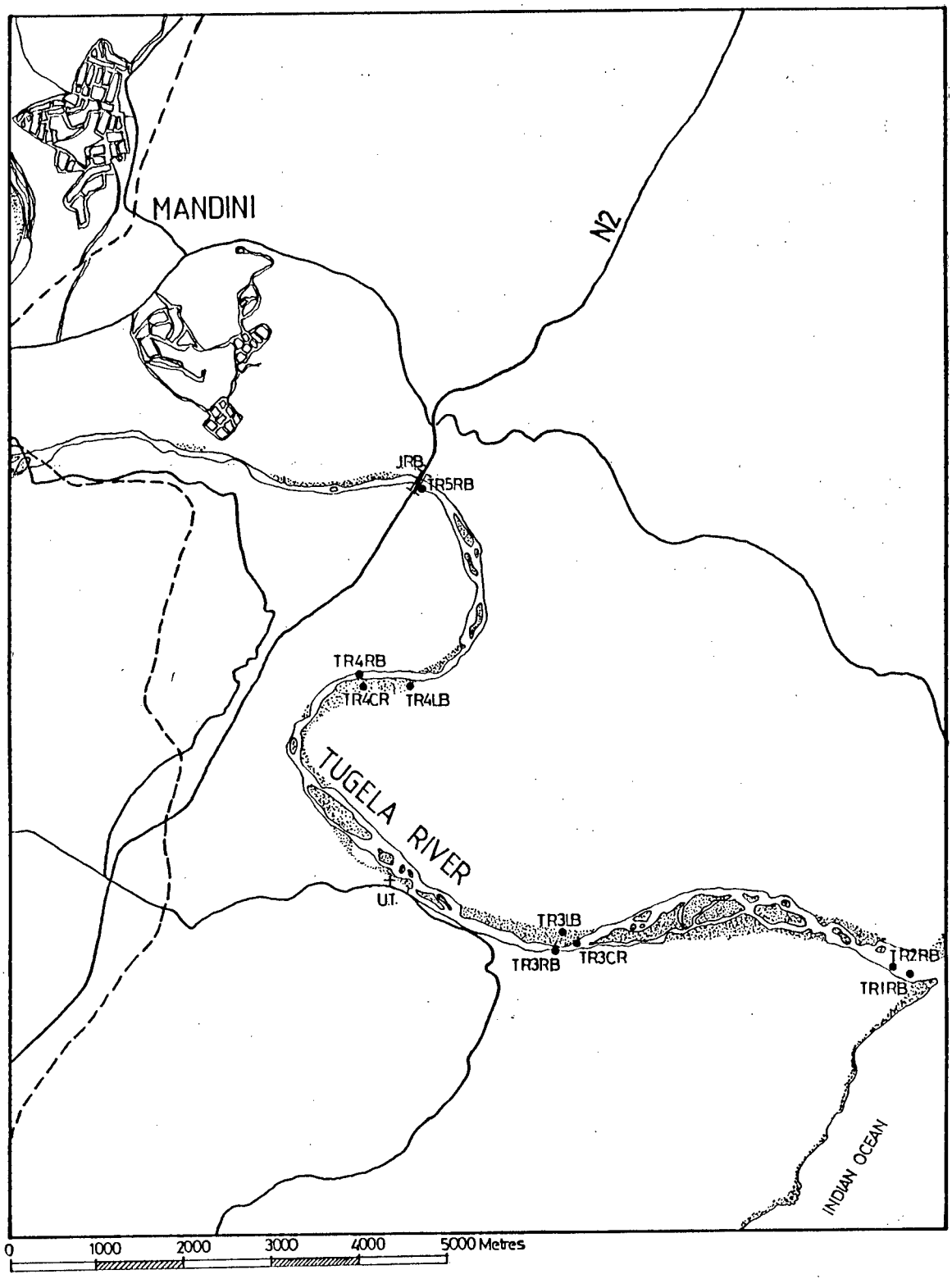

Figure 6-1. Sample positions in the Tugela River and its estuary.

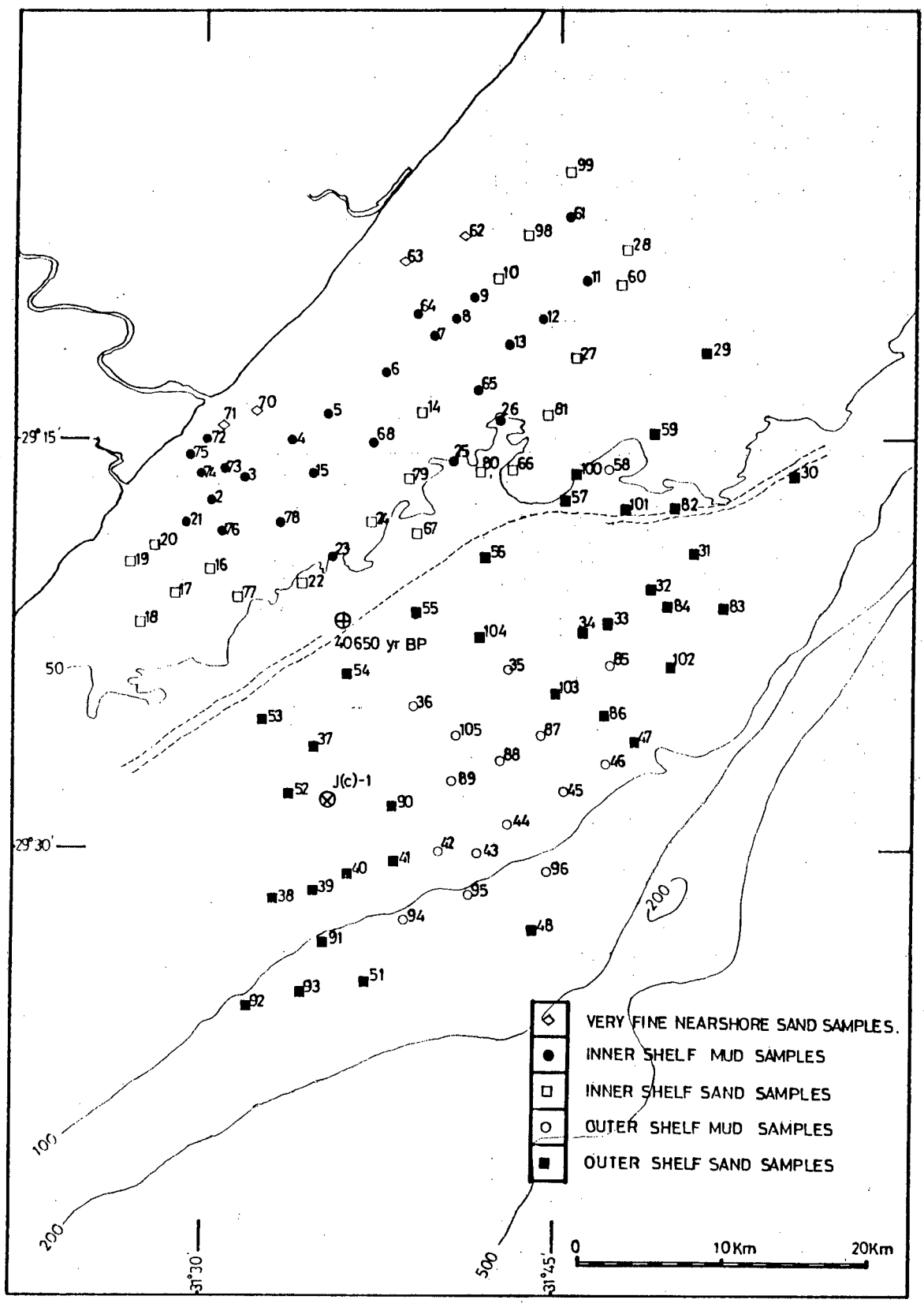

Figure 6-2. Sample positions on the continental shelf off the Tugela River.

Table 6-1. Geochemical and Sedimentological Data for Tugela Sediments. All data for trace element analyses done on 10% wax briquettes have been corrected for dilution.

Trace element concentrations less than the detection limits are given as half the detection limit of that element for the sample involved.

TABLE 6.1. GEOCHEMICAL AND SEDIMENTOLOGICAL DATA FOR TUGELA SEDIMENTS.

	TR1RB	TR2RB	TR3RB	TR3CR	TR3LB	TR4RB	TR4CR	TR4LB	TR5RB	TM002
WT%										
SIO2	60.82	54.81	79.03	79.77	69.80	75.30	83.26	80.31	76.71	53.97
TIO2	.95	1.00	.54	.53	.92	.71	.43	.53	.78	.94
AL2O3	15.44	18.36	8.00	7.52	12.66	10.08	6.53	6.52	7.69	20.07
FE2O3	8.07	8.87	3.77	3.72	5.39	4.47	3.48	5.09	5.95	8.36
MNO	.12	.15	.06	.07	.08	.06	.06	.09	.10	.10
MGO	1.42	1.59	1.15	1.17	1.36	1.20	1.11	1.56	1.84	1.72
CAO	1.54	1.29	1.67	1.68	1.84	1.64	1.62	2.26	2.49	.96
NA2O	.55	.54	1.23	1.21	1.20	1.33	1.23	1.26	1.20	.75
K2O	1.62	1.84	1.54	1.50	1.88	1.83	1.40	1.15	1.36	2.62
P2O5	.13	.15	.08	.08	.11	.09	.06	.07	.07	.14
LOI	8.89	11.14	2.67	2.65	4.44	3.17	1.22	1.11	1.73	10.27
TOTAL	99.55	99.74	99.74	99.90	99.68	99.88	100.40	99.95	99.92	99.90
LOI										
CO2	1.06	.74	.77	.75	.71	.55	.53	.47	.45	.88
H2O+	5.31	6.17	.46	.50	2.62	1.36	.44	.31	.78	6.63
ORG M	2.52	4.23	1.44	1.40	1.11	1.26	.25	.33	.50	2.76
ppm										
S	516	606	217	223	244	189	59	56	89	3975
RB	79	94	54	53	75	65	48	38	47	141
SR	113	117	160	155	178	162	143	154	152	100
Y	31	36	16	15	28	24	13	13	19	36
ZR	248	222	270	224	363	372	207	180	258	192
NB	16	16	6.9	7.7	15	11	5.7	5.3	9.3	16
U	2.5	2.3	1.7	1.2	2.5	1.7	1.1	1.7	1.1	3.7
TH	14	14	7.5	6.6	11	8.6	5.3	5.5	6.8	16
PB	22	22	20	15	19	16	14	12	13	28
ZN	72	85	33	33	55	42	28	30	41	99
CU	54	59	14	14	29	20	10	12	16	46
NI	82	95	32	31	51	38	25	31	38	69
CO	35	38	16	17	24	20	14	18	21	30
CR	208	214	115	114	154	120	102	215	242	164
V	156	161	72	72	108	88	65	93	118	148
BA	580	643	572	546	665	655	522	451	496	521
SC	28	27	11	11	17	14	9.5	11	14	25
BR	12	14	1.3	.4	2.6	1.3	.4	.4	.4	14
GA	18	21	7.6	8.3	14	10	6.3	6.9	8.9	24
LA	36	41	17	17	25	24	12	13	15	46
CE	77	84	38	37	58	46	26	25	36	93
ND	41	50	20	23	33	23	15	14	19	49
AS	6.5	8.2	2.4	2.7	4.0	3.3	2.9	2.8	3.6	11
WT%										
GRAVEL								.80		
VCS		.40	.90					2.30		.10
CS	2.10	1.40	23.50	5.70	.20		12.70	54.40	11.20	.10
MS	24.40	2.60	36.80	49.50	2.30	3.60	66.20	35.70	36.20	.30
FS	1.50	2.50	18.50	26.90	19.80	48.20	17.40	4.10	36.60	.70
VFS		7.80	5.20	7.00	14.40	19.70	1.30	.20	7.40	3.20
MUD	72.00	85.30	15.10	10.90	63.30	28.50	2.40	2.50	8.60	95.60
Stats										
MEAN	1.48		1.51	1.84	2.97	2.81	1.54	.90	1.92	
RELSRT	1.08		2.88	3.04	3.29	2.78	1.93	1.18	3.58	
SKEWNS	-.02		.28	.39	.14	.21	.23	.08		
DEPTH	1.00	1.00	1.00	1.25	1.00	.75	.50	1.00	1.00	34.00
XCOORD	31.495	31.495	31.463	31.463	31.463	31.440	31.440	31.440	31.444	31.503
YCOORD	29.224	29.224	29.218	29.218	29.218	29.190	29.190	29.190	29.173	29.287

*** ALL ZERO VALUES PRINTED AS BLANKS. ***

TABLE 6.1. GEOCHEMICAL AND SEDIMENTOLOGICAL DATA FOR TUGELA SEDIMENTS.

	TM003	TM004	TM005	TM006	TM007	TM008	TM009	TM010	TM011	TM012
WT%										
SIO2	52.77	53.33	63.51	59.66	64.42	64.89	65.24	76.73	58.24	58.23
TIO2	.90	.95	.94	.96	.77	.83	.81	.15	.96	.95
AL2O3	20.19	20.40	15.45	17.08	13.62	13.41	13.29	4.13	17.41	17.63
FE2O3	8.79	8.71	6.48	7.41	6.27	6.28	6.02	1.69	7.70	7.72
MNO	.12	.12	.08	.09	.08	.08	.07	.07	.08	.09
MGO	1.79	1.66	1.38	1.55	1.63	1.66	1.53	1.01	1.64	1.69
CAO	.89	.64	1.24	1.11	2.54	2.51	2.54	7.71	1.56	1.70
NA2O	.70	.72	1.08	.91	.88	.95	.95	.94	.84	.83
K2O	2.51	2.55	2.30	2.33	1.94	1.92	1.94	1.28	2.35	2.38
P2O5	.15	.14	.12	.14	.12	.12	.12	.07	.16	.16
LOI	11.12	10.78	6.94	8.36	7.48	7.20	7.08	6.51	8.80	8.73
TOTAL	99.93	100.00	99.52	99.60	99.75	99.85	99.59	100.29	99.74	100.11
LOI										
CO2	.78	.66	.75	.73	1.60	1.53	1.60	5.78	1.29	1.32
H2O+	7.32	6.70	4.32	5.49	3.78	4.02	3.80	.73	5.31	5.47
ORG M	3.02	3.42	1.87	2.14	2.10	1.65	1.68		2.20	1.94
ppm										
S	1980	1120	1840	1770	1365	1375	1765	556	1555	1400
RB	130	134	110	120	93	95	92	34	125	126
SR	101	91	132	112	152	159	161	307	130	133
Y	36	37	31	31	25	26	26	8.0	30	29
ZR	181	149	307	232	202	241	246	72	222	216
NB	16	16	16	17	13	13	14	1.3	18	18
U	2.7	3.1	2.6	2.9	2.6	1.9	3.0	.5	4.1	4.4
TH	15	16	14	15	11	13	12	2.4	13	12
PB	27	27	24	24	20	20	20	8.7	25	26
ZN	100	99	72	82	65	66	63	11	84	85
CU	51	51	31	37	27	27	27	4.0	34	36
NI	76	72	53	58	47	48	46	9.2	62	61
CO	32	31	26	27	25	25	23	8.8	27	26
CR	178	170	137	150	137	146	148	42	160	157
V	159	157	120	130	112	112	109	30	132	133
BA	510	524	526	487	426	431	434	346	458	458
SC	27	26	19	21	19	20	19	5.8	24	25
BR	17	13	13	18	16	17	14	.3	29	28
GA	24	24	18	20	15	16	16	3.7	21	21
LA	46	47	32	37	32	35	33	9.5	37	39
CE	97	95	77	84	74	75	68	21	91	86
ND	49	53	41	42	39	41	33	11	43	40
AS	12	9.7	12	15	14	13	13	9.3	18	17
WT%										
GRAVEL								.40		
VCS		.10		.40			.10	4.20		.10
CS	.10		.10	.10	1.30	3.00	3.00	35.40	.10	.10
MS	.70	.40	.40	.80	21.40	21.70	20.00	54.50	1.10	1.00
FS	1.30	.40	1.10	.90	10.50	7.30	7.90	5.50	1.50	.80
VFS	4.70	1.20	9.00	2.30	1.10	1.20	1.10		1.50	1.60
MUD	93.20	97.90	89.40	95.50	65.70	66.80	67.90		95.80	96.40
Stats										
MEAN					1.84	1.69	1.71	1.10		
RELSRT					1.89	2.12	2.31	1.63		
SKEWNS					.03	.05	.05	-.13		
DEPTH	32.00	28.00	31.00	35.00	35.00	34.00	32.00	30.00	44.00	44.00
XCOORD	31.527	31.558	31.583	31.623	31.660	31.673	31.688	31.707	31.768	31.737
YCOORD	29.272	29.248	29.232	29.207	29.183	29.173	29.160	29.150	29.150	29.173

*** ALL ZERO VALUES PRINTED AS BLANKS. ***

TABLE 6.1. GEOCHEMICAL AND SEDIMENTOLOGICAL DATA FOR TUGELA SEDIMENTS.

	TM013	TM014	TM015	TM016	TM017	TM018	TM019	TM020	TM021	TM022-1
WT%										
SIO2	56.92	73.98	54.06	70.90	73.79	75.10	75.11	66.37	62.55	73.98
TIO2	.94	.45	.94	.43	.33	.23	.43	.15	.64	.20
AL2O3	18.08	7.75	20.33	4.16	3.73	3.83	3.79	3.84	12.48	4.51
FE2O3	8.01	4.19	8.62	2.81	1.32	1.18	1.95	1.20	5.72	2.04
MNO	.08	.07	.09	.09	.06	.06	.08	.06	.08	.06
MGO	1.71	1.44	1.75	1.74	.80	.73	.81	.84	1.39	1.00
CAO	1.53	4.88	.60	9.62	9.50	8.91	8.46	13.50	4.91	8.86
NA2O	.81	1.09	.72	.90	.77	.80	.81	.80	.71	.98
K2O	2.41	1.38	2.55	.98	1.43	1.72	1.37	1.55	1.87	1.27
P2O5	.15	.09	.14	.12	.09	.06	.09	.07	.12	.10
LOI	9.34	5.63	10.33	8.09	8.46	7.84	7.50	11.82	9.41	7.89
TOTAL	99.98	100.95	100.13	99.84	100.28	100.46	100.40	100.20	99.88	100.89
LOI										
CO2	1.28	3.27	.60	6.92	7.52	7.17	6.48	10.98	3.57	6.69
H2O+	5.88	1.56	7.13	1.06	.81	.63	.76	.45	3.99	1.06
ORG M	2.18	.80	2.60	.11	.13	.04	.26	.39	1.85	.14
ppm										
S	1610	1105	477	740	845	533	954	1710	2460	848
RB	131	53	142	29	40	46	40	42	88	37
SR	125	261	89	410	416	396	434	719	242	412
Y	31	16	36	14	12	8.8	13	7.5	23	11
ZR	210	169	182	313	351	203	367	128	193	95
NB	17	6.7	18	5.3	6.7	4.0	5.8	1.4	9.9	2.8
U	3.3	2.4	2.2	.9	.9	.9	.5	.5	2.4	.9
TH	13	5.6	15	4.9	4.1	1.1	6.4	4.0	12	1.1
PB	26	14	26	11	9.6	11	12	11	20	10
ZN	88	37	100	20	8.2	6.5	10	6.8	56	14
CU	38	9.9	52	2.8	.5	.5	1.7	1.7	25	1.2
NI	63	27	77	14	5.0	3.4	5.9	4.2	41	9.2
CO	26	19	31	10	4.1	3.3	7.7	6.0	20	7.8
CR	162	98	178	88	30	21	37	25	122	44
V	135	70	156	48	20	18	32	21	104	29
BA	452	346	477	240	389	506	383	367	390	320
SC	25	13	28	8.8	5.1	4.9	5.2	4.5	19	7.5
BR	30	6.1	16	2.2	.6	1.9	3.5	2.3	21	3.4
GA	23	8.9	25	4.2	3.6	3.7	3.2	3.5	15	4.2
LA	40	19	44	17	11	9.0	14	10	27	9.4
CE	91	46	97	32	27	12	35	26	67	22
ND	42	21	48	15	14	7.9	20	14	32	11
AS	18	11	16	7.1	7.7	9.0	15	10	15	8.9
WT%										
GRAVEL		1.50		.50	.90	2.50	.10	6.00		
VCS	.10	1.90			.70	10.80				
CS	.10	16.90		6.20	24.30	45.70	5.20	36.20	2.40	4.70
MS	.90	41.00	1.00	70.30	63.70	38.20	49.00	47.80	31.90	70.00
FS	1.30	19.40	.70	22.20	8.80	2.50	44.10	8.40	10.60	23.80
VFS	1.80		1.80				1.00	.70	.20	.20
MUD	95.80	19.30	96.50	.80	1.60	.30	.60	.90	54.90	1.30
Stats										
MEAN		1.49		1.66	1.33	.78	1.92	1.26	1.67	1.73
RELSRT		2.27		1.70	1.56	1.34	2.08	1.55	1.76	1.65
SKEWNS		-.01		.01	.02	-.10	-.17	.26	.08	-.01
DEPTH	43.00	40.00	37.00	42.00	41.00	41.00	36.00	36.00	36.00	51.00
XCOORD	31.713	31.652	31.573	31.507	31.480	31.457	31.448	31.463	31.487	31.568
YCOORD	29.190	29.232	29.268	29.328	29.343	29.360	29.325	29.313	29.298	29.337

*** ALL ZERO VALUES PRINTED AS BLANKS. ***

TABLE 6.1. GEOCHEMICAL AND SEDIMENTOLOGICAL DATA FOR TUGELA SEDIMENTS.

	TM022-2	TM023	TM024	TM025	TM026	TM027	TM028	TM029	TM030	TM031
WT%										
SIO2	71.38	59.31	74.99	54.41	55.64	77.13	68.64	69.17	51.08	61.26
TIO2	.28	.70	.26	.83	.93	.53	.68	.30	.16	.68
AL2O3	5.74	13.89	5.21	15.29	18.28	6.07	10.53	5.06	3.15	9.25
FE2O3	2.59	6.19	2.89	7.20	8.05	4.46	4.99	2.90	1.60	4.31
MNO	.06	.06	.08	.07	.07	.20	.06	.11	.12	.06
MGO	1.11	1.49	1.40	1.70	1.68	2.15	1.62	1.86	1.51	1.54
CAO	8.66	5.18	7.35	5.72	1.78	4.78	4.20	10.32	21.48	9.33
NA2O	.92	.75	1.14	.74	.76	1.27	.99	1.16	.74	1.03
K2O	1.30	1.90	1.25	2.04	2.37	1.18	1.64	1.08	.88	1.54
P2O5	.10	.13	.09	.14	.18	.12	.10	.08	.09	.11
LOI	8.55	10.32	5.99	11.44	10.01	3.14	6.68	8.39	19.19	10.81
TOTAL	100.69	99.92	100.65	99.58	99.75	101.03	100.13	100.43	100.00	99.92
LOI										
CO2	6.46	3.70	5.01	4.09	1.39	2.29	2.78	6.92	17.50	6.91
H2O+	1.55	4.47	.63	4.86	5.79	.20	2.61	.97	1.12	2.66
ORG M	.54	2.15	.35	2.49	2.83	.65	1.29	.50	.57	1.24
ppm										
S	1110	3630	458	2695	2235	312	1130	709	2070	2245
RB	45	100	34	109	132	33	74	31	26	66
SR	398	259	315	274	132	217	207	419	1020	496
Y	12	24	11	26	30	16	21	12	12	20
ZR	121	198	106	238	198	212	222	111	86	332
NB	3.7	12	3.1	14	18	5.4	10	2.6	.8	10
U	.9	3.3	.9	4.5	3.6	.9	.9	.9	1.0	2.1
TH	2.4	12	1.1	15	13	3.0	8.3	1.2	3.7	7.3
PB	12	21	9.8	23	28	31	15	12	10	15
ZN	21	66	18	77	89	28	50	19	10	41
CU	5.5	25	4.2	30	37	5.4	17	3.5	2.4	14
NI	16	46	17	53	65	29	37	18	9.1	33
CO	8.6	20	11	25	26	16	19	11	5.7	16
CR	61	135	79	153	165	176	125	97	37	110
V	41	103	53	119	135	95	89	55	29	74
BA	315	355	340	378	437	343	376	279	191	348
SC	9.0	21	9.6	24	26	14	17	10	10	18
BR	13	45	2.0	38	40	.7	14	.7	5.5	20
GA	5.7	17	5.5	19	22	7.3	12	4.9	3.4	10
LA	13	31	9.6	37	39	13	24	9.4	9.2	22
CE	31	75	21	92	91	28	54	22	24	58
ND	16	36	9.6	40	42	14	27	12	11	28
AS	8.5	14	16	16	18	24	11	15	21	9.1
WT%										
GRAVEL	1.20	.60	1.10	1.10	.50			.20	.20	
VCS			7.40	.10		.60		.30		
CS	5.10	.20	53.50	2.70		38.00	4.30	55.20	8.20	
MS	56.70	4.40	35.80	6.70	.50	56.70	36.40	18.90	71.80	2.10
FS	26.70	28.60	1.30	12.90	2.90	2.10	10.40	21.50	17.80	47.40
VFS	.70	5.10		4.40	1.70		.70	3.40	1.20	12.60
MUD	9.60	61.10	.90	72.10	94.40	2.60	48.20	.50	.80	37.90
Stats										
MEAN	1.76	2.52	.81	2.25	2.85	1.08	1.66	1.23	1.66	2.75
RELSRT	1.95	2.84	1.21	5.00	3.51	1.13	1.77	2.39	1.65	2.14
SKEWNS		.14	-.05	-.10	.17	-.07	-.04	.52	-.13	.25
DEPTH	51.00	51.00	47.00	50.00	48.00	44.00	42.00	45.00	60.00	60.00
XCOORD	31.568	31.588	31.615	31.673	31.707	31.763	31.797	31.857	31.917	31.848
YCOORD	29.337	29.322	29.298	29.260	29.237	29.197	29.132	29.195	29.272	29.318

*** ALL ZERO VALUES PRINTED AS BLANKS. ***

TABLE 6.1. GEOCHEMICAL AND SEDIMENTOLOGICAL DATA FOR TUGELA SEDIMENTS.

	TM032	TM033	TM034	TM035	TM036	TM037	TM038	TM039	TM040	TM041
WT%										
SIO2	62.79	63.96	65.29	60.85	58.21	56.73	25.86	33.57	36.94	36.51
TIO2	.69	.74	.74	.86	.78	.56	.13	.12	.25	.44
AL2O3	9.43	10.15	10.05	13.16	12.66	9.48	3.12	3.37	4.99	6.41
FE2O3	4.26	4.47	4.48	5.98	5.89	4.68	2.00	1.84	3.20	3.79
MNO	.06	.06	.06	.07	.06	.05	.02	.06	.04	.04
MGO	1.51	1.47	1.51	1.63	1.57	1.40	2.41	2.33	2.22	2.04
CAO	8.49	7.56	6.96	5.28	7.10	11.62	34.08	29.88	25.48	24.91
NA2O	1.12	1.18	1.20	.99	.88	.82	.52	.58	.70	.70
K2O	1.65	1.78	1.80	2.01	1.93	1.78	1.04	1.44	1.39	1.22
P2O5	.10	.10	.10	.12	.14	.12	.11	.11	.14	.13
LOI	9.76	8.81	7.99	8.92	10.64	13.03	30.45	26.78	24.02	23.78
TOTAL	99.86	100.28	100.18	99.87	99.86	100.27	99.74	100.08	99.37	99.97
LOI										
CO2	6.22	5.30	4.91	3.55	5.14	8.63	28.17	25.00	22.13	15.86
H2O+	2.08	2.32	2.16	3.71	3.72	3.11	1.51	1.17	1.06	7.05
ORG M	1.46	1.19	.92	1.66	1.78	1.29	.77	.61	.83	.87
ppm										
S	1845	1585	1575	1685	1475	1385	2315	2020	1960	1945
RB	67	82	79	93	102	81	35	44	51	54
SR	465	430	395	270	330	491	1490	1245	1065	1085
Y	20	21	22	24	22	18	9.6	8.9	13	16
ZR	356	387	372	324	277	206	60	69	104	186
NB	10	11	11	13	13	8.2	.8	.8	2.6	5.8
U	.9	2.8	3.0	3.1	2.2	1.0	1.1	1.0	1.0	2.4
TH	7.7	12	11	12	13	9.6	5.3	6.6	6.8	8.8
PB	15	19	19	21	22	20	14	15	19	17
ZN	42	45	44	61	61	44	11	8.7	21	32
CU	13	14	12	21	20	13	.7	.6	4.2	8.4
NI	32	33	34	46	44	29	7.2	6.7	15	22
CO	16	16	16	20	18	13	5.2	4.3	6.9	11
CR	112	119	120	148	135	96	45	42	68	86
V	72	78	77	100	92	66	28	26	45	55
BA	380	409	418	396	386	359	163	253	228	188
SC	17	18	17	19	21	17	4.6	5.1	8.4	10
BR	22	27	27	39	59	39	16	11	22	30
GA	9.7	12	12	15	16	11	3.0	4.3	6.0	8.0
LA	23	24	22	29	26	22	7.7	6.2	11	15
CE	59	57	53	66	62	56	22	16	34	46
ND	28	28	26	36	29	24	12	9.4	18	23
AS	9.1	9.2	8.7	11	13	12	15	20	21	12
WT%										
GRAVEL	.10		.10	.40	3.50	13.00	11.40	8.50	3.80	9.50
VCS						1.40	11.00	17.80	1.90	2.00
CS		.10		.50	2.20	5.40	59.10	65.80	46.10	29.20
MS	2.60	1.70	2.00	3.30	7.80	14.60	11.30	5.80	31.80	19.50
FS	37.10	32.30	36.30	14.50	12.90	19.50	2.10	.70	3.90	10.70
VFS	18.80	22.90	21.80	12.60	4.80	5.90	1.70		.50	4.60
MUD	41.40	43.00	39.80	68.70	68.80	40.20	3.40	1.40	12.00	24.50
Stats										
MEAN	2.90	3.02	2.94	2.87	2.27	2.06	.55	.33	.94	1.30
RELSRT	2.38	1.87	1.94	3.36	4.76	4.69	1.05	.70	1.30	2.85
SKEWNS	.18	.29	.22	-.18	-.05	-.15	.11	.08	.12	.40
DEPTH	61.00	62.00	62.00	66.00	70.00	67.00	71.00	75.00	78.00	77.00
XCOORD	31.817	31.787	31.768	31.715	31.647	31.577	31.548	31.578	31.602	31.635
YCOORD	29.340	29.360	29.367	29.388	29.410	29.435	29.530	29.525	29.515	29.508

*** ALL ZERO VALUES PRINTED AS BLANKS. ***

TABLE 6.1. GEOCHEMICAL AND SEDIMENTOLOGICAL DATA FOR TUGELA SEDIMENTS.

	TM042	TM043	TM044	TM045	TM046	TM047	TM048	TM051	TM052	TM053
WT%										
SIO2	61.82	62.62	62.68	58.96	50.08	32.65	36.92	60.35	61.95	60.63
TIO2	.81	.85	.84	.90	.65	.46	.53	.60	.38	.36
AL2O3	11.36	13.55	12.93	15.42	10.58	6.80	8.51	8.16	6.94	6.13
FE2O3	4.89	5.66	5.34	6.90	4.63	3.45	4.50	4.51	2.93	2.95
MNO	.06	.06	.06	.06	.05	.05	.05	.05	.03	.04
MGO	1.46	1.48	1.43	1.63	1.87	2.33	2.61	1.62	1.19	1.30
CAO	7.30	4.42	4.73	3.20	13.90	26.75	21.79	11.22	12.04	13.44
NA2O	1.08	1.04	1.10	.90	.85	.66	.72	1.12	.90	.83
K2O	1.87	2.08	2.05	2.19	1.57	.98	1.25	1.49	1.78	1.33
P2O5	.11	.12	.12	.15	.12	.11	.13	.12	.09	.09
LOI	9.23	8.13	8.04	9.33	15.80	25.83	22.80	11.24	12.24	13.15
TOTAL	99.99	100.01	99.32	99.64	100.10	100.07	99.81	100.48	100.47	100.25
LOI										
CO2	5.18	3.06	3.17	2.25	11.23	22.00	17.55	7.89	9.86	10.81
H2O+	3.19	3.35	3.63	4.98	3.29	2.48	3.65	2.49	1.54	1.54
ORG M	.86	1.72	1.24	2.10	1.28	1.35	1.60	.86	.84	.80
ppm										
S	1410	1355	1215	1810	1980	2705	2220	1175	1455	2020
RB	89	107	103	108	83	51	58	63	67	53
SR	384	267	285	194	696	1400	1060	527	512	609
Y	22	23	25	26	20	17	18	17	14	14
ZR	373	292	309	230	234	179	201	281	173	174
NB	13	14	14	16	10	5.2	7.5	9.1	6.3	5.2
U	2.6	2.2	3.0	2.8	3.2	2.2	.6	.9	.9	.9
TH	12	11	13	14	12	10	9.3	7.4	6.9	7.6
PB	21	23	23	22	19	13	14	16	15	16
ZN	50	60	58	72	47	33	42	43	27	26
CU	15	20	20	26	18	12	16	8.4	6.8	6.6
NI	37	46	44	55	38	27	32	25	17	16
CO	16	19	20	21	16	12	15	14	7.6	8.7
CR	123	138	134	159	116	85	106	95	66	60
V	83	97	93	113	81	60	73	55	44	37
BA	384	429	430	416	279	138	188	284	369	272
SC	18	19	19	20	17	12	15	12	10	9.1
BR	37	49	44	55	36	27	31	29	26	22
GA	13	16	15	18	12	7.4	10	10	8.0	7.5
LA	22	26	25	28	24	19	22	17	13	17
CE	56	59	62	74	55	45	57	45	34	46
ND	26	29	30	33	28	24	30	23	18	21
AS	8.2	11	11	15	11	12	11	8.8	9.9	8.1
WT%										
GRAVEL	.40				1.40	19.20	10.60		.70	4.00
VCS		.10			.40	2.10	3.20		.60	1.20
CS	.40	.10			13.40	21.70	19.60	.90	20.40	5.30
MS	1.80	.50	.30	.20	22.20	23.90	18.30	3.60	31.40	23.70
FS	17.80	7.40	7.30	1.20	6.00	5.40	3.60	42.90	21.70	45.20
VFS	24.00	14.30	17.30	4.10	3.80	1.00	2.50	26.40	5.70	6.00
MUD	55.60	77.60	75.10	94.50	52.80	26.70	42.20	26.20	19.50	14.60
Stats										
MEAN	3.10	3.18	3.22	3.36	1.49	1.14	1.06	2.93	1.65	2.09
RELSRT	2.13	1.72	1.64	2.18	3.03	1.94	2.25	2.43	3.45	3.44
SKEWNS	.03	.21	.23	.06	.24	.07	.16	.07	.14	-.20
DEPTH	79.00	85.00	82.00	90.00	90.00	90.00	133.00	124.00	70.00	67.00
XCOORD	31.665	31.693	31.717	31.753	31.783	31.807	31.733	31.617	31.562	31.542
YCOORD	29.500	29.503	29.485	29.463	29.447	29.433	29.550	29.582	29.465	29.422

*** ALL ZERO VALUES PRINTED AS BLANKS. ***

TABLE 6.1. GEOCHEMICAL AND SEDIMENTOLOGICAL DATA FOR TUGELA SEDIMENTS.

	TM054	TM055	TM056	TM057	TM058	TM059	TM060	TM061	TM062	TM063
WT%										
SIO2	70.06	75.89	78.88	80.11	60.07	66.01	72.89	64.57	77.16	73.28
TIO2	.34	.47	.42	.40	.88	.53	.61	.72	1.44	1.02
AL2O3	7.10	6.08	5.54	5.21	15.27	4.79	5.08	12.09	8.97	11.25
FE2O3	3.78	4.14	3.46	3.22	6.64	3.29	4.30	5.37	3.98	4.35
MNO	.11	.06	.11	.11	.07	.11	.15	.08	.07	.07
MGO	1.54	2.12	1.71	1.62	1.51	1.67	1.82	1.43	1.10	1.16
CAO	7.98	5.12	4.45	4.68	3.21	11.24	7.24	4.49	1.66	1.61
NA2O	1.43	1.18	1.12	1.16	.91	1.11	.98	.90	1.72	1.53
K2O	1.56	1.06	1.09	1.08	2.19	1.10	1.24	1.78	1.92	2.06
P2O5	.11	.10	.09	.07	.14	.08	.09	.12	.11	.09
LOI	6.57	4.24	4.07	3.89	8.55	9.11	5.45	8.34	1.82	3.11
TOTAL	100.58	100.46	100.94	101.55	99.44	99.04	99.85	99.89	99.95	99.53
LOI										
CO2	5.21	2.86	2.67	2.91	2.20	7.75	4.40	3.15	.79	.77
H2O+	1.32	.93	.99	.56	4.59	1.36	.90	3.47	.77	1.56
ORG M	.04	.45	.41	.42	1.76		.15	1.72	.26	.78
ppm										
S	505	504	429	354	2680	651	399	1520	293	418
RB	49	32	38	35	121	33	36	85	67	80
SR	403	250	249	240	205	427	270	228	147	160
Y	12	13	13	12	25	16	15	24	41	30
ZR	87	172	166	186	251	259	353	235	1445	692
NB	3.5	5.2	4.8	5.0	15	6.4	6.4	12	18	15
U	.9	1.4	.9	.9	2.7	.9	.9	2.6	4.6	2.1
TH	3.5	5.9	6.2	2.9	14	6.8	5.0	12	24	13
PB	16	12	15	13	24	11	15	19	16	17
ZN	24	31	27	24	72	18	22	57	36	47
CU	6.5	8.3	6.1	3.8	26	4.3	4.1	22	7.1	15
NI	20	27	24	19	54	16	21	40	24	32
CO	13	17	14	13	22	10	14	21	15	19
CR	90	117	98	90	149	148	182	122	193	124
V	66	74	60	57	115	63	84	95	92	91
BA	446	293	302	307	437	290	334	380	555	571
SC	11	12	10	10	22	10	14	18	12	14
BR	6.7	6.5	9.5	5.6	48	4.5	4.4	16	.4	3.3
GA	7.6	6.5	6.2	5.4	19	5.2	5.9	14	9.0	12
LA	12	12	11	11	31	10	9.9	28	42	28
CE	22	26	28	24	76	29	24	68	85	60
ND	10	17	14	12	36	15	13	36	44	31
AS	18	9.8	12	11	15	11	15	13	5.6	7.6
WT%										
GRAVEL	16.40	.30	.20	.10		2.20	1.20	.40		
VCS	14.40					7.00	2.30			
CS	55.10	5.90	1.80	2.20		69.80	58.10	.20		
MS	11.30	66.00	67.00	58.60	1.20	18.80	34.90	3.70		
FS	1.20	23.90	27.80	37.70	2.90	1.60	2.30	38.10	10.80	2.20
VFS		.60	.70		11.10			2.10	65.30	50.00
MUD	1.60	3.30	2.50	1.40	84.80	.60	1.20	55.50	23.90	47.80
Stats										
MEAN	.49	1.73	1.81	1.88		.66	.91	2.41	3.27	3.37
RELSRT	.93	1.73	1.55	1.68		.93	1.11	1.75	1.07	.97
SKEWNS	-.02	-.11	-.01	-.10		.01	.20		.23	.22
DEPTH	60.00	54.00	51.00	49.00	51.00	45.00	42.00	35.00	23.00	20.00
XCOORD	31.598	31.650	31.698	31.753	31.785	31.818	31.793	31.757	31.682	31.640
YCOORD	29.390	29.355	29.318	29.285	29.267	29.243	29.153	29.113	29.123	29.138

*** ALL ZERO VALUES PRINTED AS BLANKS. ***

TABLE 6.1. GEOCHEMICAL AND SEDIMENTOLOGICAL DATA FOR TUGELA SEDIMENTS.

	TM064	TM065	TM066	TM067	TM068	TM070	TM071	TM072	TM073	TM074
WT%										
SIO2	60.42	56.78	72.04	78.55	56.15	80.26	75.37	64.73	55.62	61.39
TIO2	.95	.93	.49	.28	.92	1.39	1.26	.91	.96	1.01
AL2O3	16.89	17.49	6.80	5.26	18.22	6.76	10.00	12.97	20.08	16.67
FE2O3	7.32	7.98	3.98	3.24	8.18	3.88	4.26	5.31	8.00	7.01
MNO	.07	.08	.09	.08	.09	.09	.07	.08	.06	.09
MGO	1.55	1.74	1.58	1.48	1.63	1.33	1.12	1.28	1.58	1.42
CAO	1.28	1.77	5.83	4.78	1.33	1.90	1.68	1.31	.53	1.10
NA2O	.93	.86	1.02	1.08	.80	1.48	1.75	1.34	.78	.99
K2O	2.31	2.30	1.20	1.22	2.33	1.63	1.91	2.09	2.46	2.39
P2O5	.12	.14	.09	.07	.14	.09	.10	.10	.12	.13
LOI	8.03	9.77	6.53	4.38	10.21	1.21	2.32	9.26	9.80	7.27
TOTAL	99.87	99.84	99.65	100.42	100.00	100.02	99.84	99.38	99.99	99.47
LOI										
CO2	.88	1.44	3.97	3.24	1.09	.77	.80	.90	.58	.65
H2O+	4.67	5.93	1.87	.74	6.69	.23	1.03	4.03	6.98	4.96
ORG M	2.48	2.40	.69	.40	2.43	.21	.49	4.33	2.24	1.66
ppm										
S	2090	1990	973	407	2440	183	192	4375	1925	1475
RB	117	135	51	48	125	54	69	90	133	114
SR	116	129	283	325	116	124	155	145	84	116
Y	31	29	17	13	31	36	35	32	35	34
ZR	249	206	202	116	196	1460	972	398	216	321
NB	16	16	6.7	4.5	16	16	16	16	16	17
U	4.0	3.9	2.5	.7	2.5	4.2	4.1	2.5	2.8	2.3
TH	15	15	7.9	5.1	15	24	17	13	16	14
PB	25	27	18	16	28	14	18	21	25	22
ZN	79	82	32	28	90	31	41	61	93	78
CU	36	34	10	7.4	41	5.8	14	30	47	36
NI	57	59	23	25	65	22	30	45	72	54
CO	30	27	16	14	29	14	18	27	29	29
CR	152	157	105	82	162	193	153	117	183	144
V	130	130	69	49	136	94	92	100	152	129
BA	482	453	292	346	459	502	571	537	503	548
SC	22	25	13	8.1	23	12	13	16	27	20
BR	14	38	17	2.4	31	.4	.4	6.1	11	7.0
GA	19	21	8.1	7.1	22	7.0	10	14	23	20
LA	40	37	17	9.4	41	41	28	38	41	39
CE	86	89	41	20	97	93	64	75	86	87
ND	46	41	19	12	48	47	37	39	46	47
AS	14	18	11	19	18	3.9	4.4	6.8	11	12
WT%										
GRAVEL	.50		.90	.40						
VCS	.50	.10						.80		
CS	.10	.10	1.50	9.10	.30			1.90	.10	.10
MS	1.60	.80	19.70	71.70	2.80			2.60	.70	.40
FS	1.70	1.70	57.20	16.50	4.20	71.50	15.20	2.00	.50	.50
VFS	2.90	2.50	4.00	1.50	3.00	24.70	43.50	16.30	3.40	4.60
MUD	92.70	94.80	16.70	.80	89.70	3.80	41.30	76.40	95.30	94.40
Stats										
MEAN			2.21	1.60		2.83	3.21			
RELSRT			2.28	1.68		1.47	1.30			
SKEWNS			-.02	.02		.10	.18			
DEPTH	32.00	45.00	48.00	49.00	42.00	15.00	13.00	17.00	24.00	24.00
XCOORD	31.647	31.688	31.717	31.650	31.617	31.535	31.512	31.502	31.512	31.495
YCOORD	29.170	29.218	29.266	29.307	29.250	29.230	29.237	29.248	29.267	29.270

*** ALL ZERO VALUES PRINTED AS BLANKS. ***

TABLE 6.1. GEOCHEMICAL AND SEDIMENTOLOGICAL DATA FOR TUGELA SEDIMENTS.

	TM075	TM076	TM077	TM078	TM079	TM080	TM081	TM082	TM083	TM084
WT%										
SIO2	56.05	62.10	71.92	54.09	69.62	75.88	75.57	66.43	36.93	53.28
TIO2	.96	.63	.25	.89	.50	.51	.50	.57	.26	.68
AL2O3	19.06	12.42	5.44	18.79	7.62	6.38	5.87	8.49	2.82	8.89
FE2O3	8.05	5.72	4.31	8.54	4.66	5.30	4.13	3.85	2.21	4.56
MNO	.11	.06	.12	.09	.06	.09	.17	.06	.07	.06
MGO	1.67	1.46	1.19	1.73	1.78	2.08	1.85	1.41	2.30	1.81
CAO	1.09	4.66	7.58	1.14	6.11	3.74	5.44	7.36	27.89	13.18
NA2O	.76	.81	.99	.78	1.02	1.07	1.21	1.20	.64	.95
K2O	2.61	1.77	1.46	2.36	1.37	1.27	1.22	1.58	.57	1.49
P2O5	.13	.12	.11	.15	.09	.10	.10	.10	.04	.10
LOI	9.58	9.36	6.59	11.07	7.16	4.14	4.19	8.66	25.06	14.57
TOTAL	100.07	99.11	99.96	99.63	99.99	100.56	100.25	99.71	98.79	99.57
LOI										
CO2	.70	3.35	5.40	.84	4.02	2.13	2.97	5.37	23.76	10.75
H2O+	6.92	4.41	1.05	6.78	2.48	1.62	1.01	2.37	.78	2.43
ORG M	1.96	1.60	.14	3.45	.66	.39	.21	.92	.52	1.39
ppm										
S	1305	2415	373	3835	1135	429	389	1555	2425	2220
RB	130	96	40	143	54	43	38	67	22	69
SR	111	234	246	107	271	187	238	405	1245	661
Y	36	24	11	32	15	14	15	18	12	21
ZR	286	165	94	186	161	197	212	243	145	330
NB	17	11	3.1	16	6.9	5.7	4.7	8.7	.8	11
U	3.1	2.0	.9	3.4	.9	.9	.9	2.3	2.1	2.4
TH	15	13	3.5	17	7.6	6.7	3.4	9.2	6.8	9.0
PB	25	21	16	31	16	16	13	17	11	16
ZN	93	58	15	90	36	33	23	35	12	42
CU	43	26	5.6	45	11	7.7	6.4	10	2.6	13
NI	65	43	14	67	27	30	23	26	10	31
CO	28	24	12	30	18	19	15	14	7.9	16
CR	166	122	77	170	114	145	144	97	59	114
V	141	103	64	147	73	82	80	66	39	77
BA	553	371	372	458	318	311	356	351	105	272
SC	24	20	8.9	26	13	13	12	13	5.0	14
BR	12	20	6.1	37	15	11	6.8	20	11	29
GA	23	16	5.2	24	8.7	6.6	6.1	9.0	2.6	10
LA	40	33	6.9	41	16	12	8.3	18	8.2	22
CE	86	72	20	90	40	31	27	45	26	54
ND	49	34	9.8	43	20	16	14	23	15	26
AS	11	11	25	16	12	19	20	9.5	15	10
WT%										
GRAVEL		.20	26.10		1.80	1.10	.60	.30	6.00	.40
VCS			5.20		.40		.40		2.40	
CS		.50	59.50	.30	13.40	20.00	55.80	.70	20.30	1.20
MS	.40	8.50	7.50	1.90	52.00	67.00	35.90	7.00	59.50	16.80
FS	.50	34.30	.40	3.40	12.00	3.50	2.70	47.40	9.60	34.60
VFS	6.00	2.30		3.00	1.30	.80	1.40	14.60	1.00	8.20
MUD	93.10	54.20	1.30	91.40	19.10	7.60	3.20	30.00	1.20	38.80
Stats										
MEAN		2.28	.53		1.49	1.24	.91	2.64	1.38	2.32
RELSRT		2.15	.72		1.90	1.05	1.07	2.86	1.90	3.46
SKEWNS		-.05	.06		.10	.06	.05	.02	-.24	.14
DEPTH	19.00	40.00	50.00	43.00	48.00	50.00	44.00	51.00	71.00	69.00
XCOORD	31.488	31.510	31.523	31.550	31.643	31.695	31.742	31.833	31.867	31.827
YCOORD	29.258	29.305	29.345	29.300	29.272	29.268	29.232	29.290	29.352	29.350

*** ALL ZERO VALUES PRINTED AS BLANKS. ***

TABLE 6.1. GEOCHEMICAL AND SEDIMENTOLOGICAL DATA FOR TUGELA SEDIMENTS.

	TM085	TM086	TM087	TM088	TM089	TM090	TM091	TM092	TM093	TM094
WT%										
SIO2	60.10	54.89	61.38	61.83	60.69	41.50	51.64	53.90	50.98	63.01
TIO2	.81	.60	.81	.79	.85	.36	.61	.53	.54	.74
AL2O3	12.21	7.92	12.29	12.79	12.07	5.76	6.82	6.80	6.55	11.35
FE2O3	5.59	3.91	5.35	5.60	5.55	4.35	4.25	3.86	4.00	4.86
MNO	.06	.05	.05	.06	.06	.05	.04	.04	.04	.05
MGO	1.63	1.82	1.56	1.56	1.64	1.89	1.91	1.63	1.98	1.40
CAO	5.96	13.74	5.80	5.12	6.38	21.88	16.18	15.58	17.19	6.36
NA2O	1.01	.97	1.07	1.07	1.06	.73	.85	.84	.82	1.24
K2O	1.91	1.38	1.97	2.01	1.89	1.35	1.15	1.18	1.13	1.93
P2O5	.12	.10	.11	.11	.11	.13	.10	.12	.11	.10
LOI	9.72	14.57	9.05	8.58	9.27	21.15	16.04	15.37	16.76	8.38
TOTAL	99.12	99.95	99.44	99.52	99.57	99.15	99.59	99.85	100.10	99.42
LOI										
CO2	5.66	11.00	3.96	3.48	4.53	17.68	12.72	12.34	13.25	4.40
H2O+	2.44	2.39	3.77	3.50	3.19	2.28	2.16	1.91	2.62	2.61
ORG M	1.62	1.18	1.32	1.60	1.55	1.19	1.16	1.12	.89	1.37
ppm										
S	1615	1760	1595	1430	1440	1780	1995	1755	1795	1020
RB	96	60	85	99	92	50	51	51	48	88
SR	333	620	313	290	323	965	724	689	727	340
Y	23	19	23	21	22	12	17	16	15	20
ZR	301	308	301	266	367	150	335	231	262	282
NB	12	7.8	13	13	13	4.3	9.6	7.1	6.8	12
U	2.7	.9	2.5	3.8	4.2	1.0	1.0	2.4	2.3	2.2
TH	12	8.3	12	13	12	6.1	8.5	7.2	6.6	11
PB	23	14	18	22	21	17	14	14	13	18
ZN	54	35	54	54	55	24	39	37	36	47
CU	19	11	18	20	18	7.0	8.7	7.9	8.1	15
NI	44	26	41	42	39	17	23	21	20	34
CO	19	14	20	18	18	10	13	11	11	17
CR	139	101	136	135	131	71	92	82	87	112
V	98	68	94	93	90	54	55	50	50	77
BA	386	271	394	415	387	222	198	204	188	418
SC	19	13	18	19	17	8.2	11	11	11	16
BR	45	26	29	45	44	26	31	32	30	43
GA	15	9.4	14	14	14	6.1	8.4	7.5	7.8	13
LA	24	20	27	24	24	14	16	15	14	21
CE	63	49	61	59	60	37	45	40	41	56
ND	29	23	34	27	27	19	22	22	21	26
AS	11	12	9.2	10	9.4	29	7.0	6.1	6.8	8.8
WT%										
GRAVEL		1.20	2.00			10.10	1.70	.70	1.90	
VCS						1.30	.30	.60	.10	
CS	.20	7.40		.10	.60	31.60	3.40	4.20	7.20	.20
MS	2.50	36.30	1.10	.70	2.10	32.90	10.90	8.30	10.90	.20
FS	20.10	15.20	17.00	12.70	16.90	6.40	45.30	51.60	47.00	9.80
VFS	9.80	4.40	15.40	15.20	16.00	1.40	10.40	9.60	8.80	27.50
MUD	67.40	35.50	64.50	71.30	64.40	16.30	28.00	25.00	24.10	62.30
Stats										
MEAN	2.78	1.73	3.05	3.11	3.01	1.11	2.46	2.49	2.30	3.24
RELSRT	3.29	2.78	2.15	1.99	2.68	1.81	3.91	3.78	4.21	1.54
SKEWNS	.15	.14	.20	.21		.10	-.29	-.33	-.46	.24
DEPTH	70.00	73.00	72.00	74.00	74.00	70.00	97.00	103.00	108.00	100.00
XCOORD	31.787	31.783	31.737	31.707	31.673	31.633	31.585	31.550	31.570	31.642
YCOORD	29.387	29.417	29.430	29.445	29.457	29.473	29.557	29.595	29.587	29.543

*** ALL ZERO VALUES PRINTED AS BLANKS. ***

TABLE 6.1. GEOCHEMICAL AND SEDIMENTOLOGICAL DATA FOR TUGELA SEDIMENTS.

	TM095	TM096	TM098	TM099	TM100	TM101	TM102	TM103	TM104	TM105
WT%										
SIO2	62.49	53.76	75.35	76.59	71.76	68.69	34.04	63.58	61.96	61.12
TIO2	.78	.80	.21	.14	.59	.20	.12	.72	.58	.77
AL2O3	12.07	12.66	3.54	2.77	8.14	4.69	2.33	10.32	9.55	11.14
FE2O3	5.27	5.88	1.75	1.04	4.54	2.05	1.52	4.66	4.72	5.13
MNO	.06	.07	.06	.04	.06	.08	.10	.06	.05	.06
MGO	1.48	1.78	1.06	.79	1.70	1.31	2.53	1.54	1.64	1.57
CAO	5.57	8.90	8.91	9.40	5.18	11.45	30.99	7.04	8.95	7.15
NA2O	1.17	.90	.79	.68	1.16	1.05	.63	1.23	1.02	1.01
K2O	1.96	1.82	.99	.76	1.44	1.28	.55	1.79	1.66	1.84
P2O5	.11	.13	.05	.05	.09	.06	.05	.10	.12	.10
LOI	8.50	12.64	7.49	8.00	5.79	9.63	27.18	8.70	10.21	9.92
TOTAL	99.46	99.34	100.20	100.26	100.45	100.49	100.04	99.74	100.46	99.81
LOI										
CO2	3.67	6.36	6.68	7.22	3.12	8.31	24.81	4.93	6.27	5.27
H2O+	3.22	4.21	.81	.38	1.84	.95	2.00	2.51	2.72	3.34
ORG M	1.61	2.07		.40	.83	.37	.37	1.26	1.22	1.31
ppm										
S	1100	1345	681	800	960	665	2355	1525	1225	1485
RB	94	96	27	23	57	37	19	78	72	86
SR	309	451	348	390	254	446	1190	385	391	336
Y	21	22	9.6	9.7	16	9.3	13	22	16	21
ZR	282	268	96	68	233	94	55	321	208	319
NB	13	13	.6	1.7	7.5	.7	.7	12	7.9	12
U	3.2	3.7	.5	.5	.9	.9	1.0	2.0	2.5	4.0
TH	11	13	3.5	3.5	6.6	2.3	6.3	10	10	12
PB	21	21	8.2	6.2	16	11	22	18	17	20
ZN	51	56	12	8.4	33	10	7.2	43	39	48
CU	17	21	3.3	1.7	12	3.9	3.0	13	13	17
NI	37	44	9.7	6.3	29	10	7.6	32	30	37
CO	17	19	9.1	4.8	14	7.8	6.9	17	14	18
CR	123	144	47	31	129	50	35	113	121	129
V	85	95	31	19	80	35	30	77	75	84
BA	415	340	256	194	375	329	108	384	353	375
SC	16	19	5.8	4.5	14	8.1	4.0	15	14	17
BR	50	61	.4	.4	18	5.7	10	26	32	40
GA	13	15	3.4	2.5	8.8	4.6	2.0	11	11	13
LA	20	22	8.4	9.1	14	6.4	7.8	18	16	22
CE	54	65	19	15	35	16	25	59	45	58
ND	26	31	10	9.5	18	8.0	14	28	21	27
AS	9.8	12	9.0	6.4	14	12	18	8.8	10	11
WT%										
GRAVEL		1.40	.40	.10	2.80	5.70	2.70		5.80	.30
VCS		.30			3.60	6.00	1.10		6.60	
CS		3.40	16.40	.60	31.10	77.50	32.70	.20	21.20	2.60
MS	.30	6.20	76.10	46.30	38.20	8.70	61.00	1.40	18.00	11.20
FS	6.80	7.30	5.50	51.60	3.20	1.40	2.50	31.30	10.10	19.10
VFS	20.60	5.60	1.60	1.40	.10	.20		21.50	4.00	10.60
MUD	72.30	75.80			21.00	.50		45.60	34.30	56.20
Stats										
MEAN	3.24	2.21	1.42	2.00	1.02	.51	1.15	2.95	1.18	2.43
RELSRT	1.52	5.84	1.38	1.48	1.53	.72	1.26	1.86	2.92	4.81
SKEWNS	.22	-.05	-.06	-.10	-.12	.16	-.20	.09	.17	-.18
DEPTH	99.00	114.00	27.00	24.00	51.00	49.00	68.00	66.00	63.00	70.00
XCOORD	31.687	31.742	31.727	31.758	31.763	31.797	31.830	31.750	31.697	31.678
YCOORD	29.527	29.513	29.123	29.083	29.268	29.292	29.387	29.405	29.370	29.428

*** ALL ZERO VALUES PRINTED AS BLANKS. ***

CHAPTER VII INTRODUCTION TO THE DISCUSSION

Bathymetry of the study area is shown in figure 7-1. The bathymetry was taken from Goodlad (1978), in combination with the depth readings taken for the samples of this study.

The interpretation of the data is approached from basically three directions in order to arrive at a more comprehensive picture of the continental shelf sediments. The river and estuary samples will be dealt with subsequently.

The first aspect discussed is the sedimentology of the area as revealed through interpretation of the particle size data. In determining the hydraulic populations of the sediments and their implications, however, only the sand fractions were used. Although this approach may be somewhat inadequate for an environment where there is as much mud present as off the Tugela River, it nonetheless is helpful in elucidating the complex relationship between the hydrodynamic regime, both past and present, and the present-day situation of the sediments.

The second part of the discussion presents a brief overview of the mineralogic trends in the area. As the X-ray diffractograms represent the bulk sample mineralogy, only qualitative results were arrived at. The dilution of the samples by quartz and calcite is the major factor obscuring the trends of the minor, and possibly more interpretatively important, minerals. Only the obviously evident mineralogy

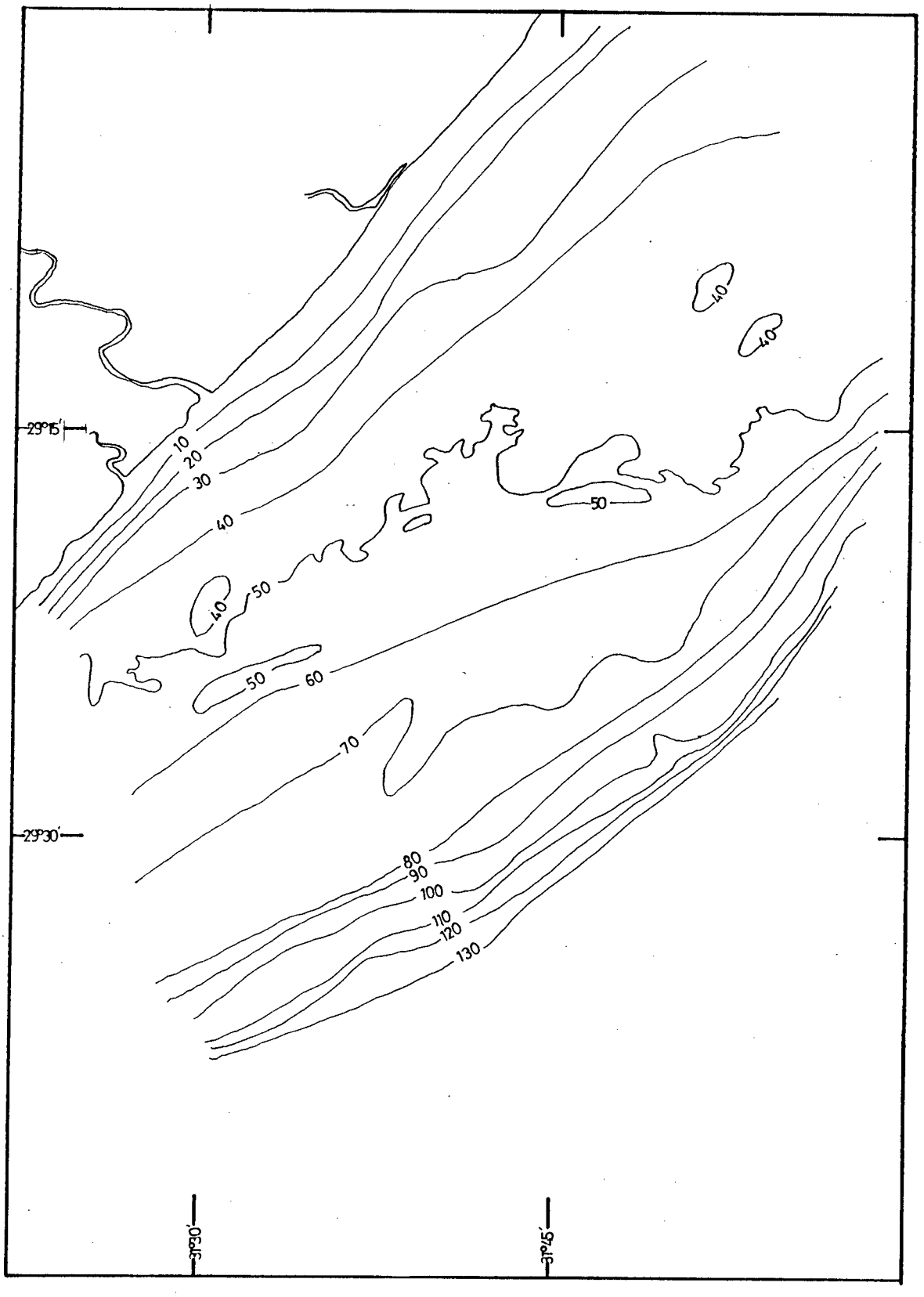

Figure 7-1. Bathymetry of the study area.

is reported.

The third approach to the data is through the geochemistry. Although the geochemistry would undoubtedly have been more definitive had individual size fractions been analysed, elemental trends in the sediments are readily distinguishable from the bulk sample data. The geochemical data allow a more subtle means of discriminating between the inner and outer shelf muds than do the sedimentological and mineralogical data. It also establishes a framework for the speculation of provenance of the sediments.

It is shown that the usage of these three approaches to a sedimentologically complex area, although at times contradictory, presents a reasonably well-defined picture in which the major question of the study may be answered, i.e. are the muds found on both the inner and outer shelf part of the same Recent depositional events, or do they represent different times of deposition with possibly different geochemical compositions.

CHAPTER VIII SEDIMENTOLOGY

1. Introduction

The sedimentology of the study area is complex. The region just to the south was described by Flemming (1978) as containing a 'transitional facies where lateral mixing is occurring'. An attempt is made in this chapter to better define the sedimentology of the area through a close examination of the textural composition of the total samples and the hydraulic populations of the sand-size fractions of the sediments. Interpretation of the grain size data is done using the methods described by Nota (1958), Cook and Mayo (1977) and Flemming (1977). The chemical composition of the sediments is dealt with in chapter X, and is thus excluded from the following discussion.

2. Textural Composition

The textural composition of the sediments is shown in figures 8-1 and 8-2. Figure 8-1 uses Shepard's 1954 classification, figure 8-2 uses that of Folk (1954). Folk's classification scheme is more sensitive to showing the content of smaller amounts of contributing size group constituents in the sediments. In the study area, this is important in regard to the gravel-size fraction (>2 mm).

2.1 Gravel

Gravel is sparsely distributed in the area (fig. 8-3), with few samples showing concentrations greater than 5%. Patches of higher gravel concentration (>10%) are found on

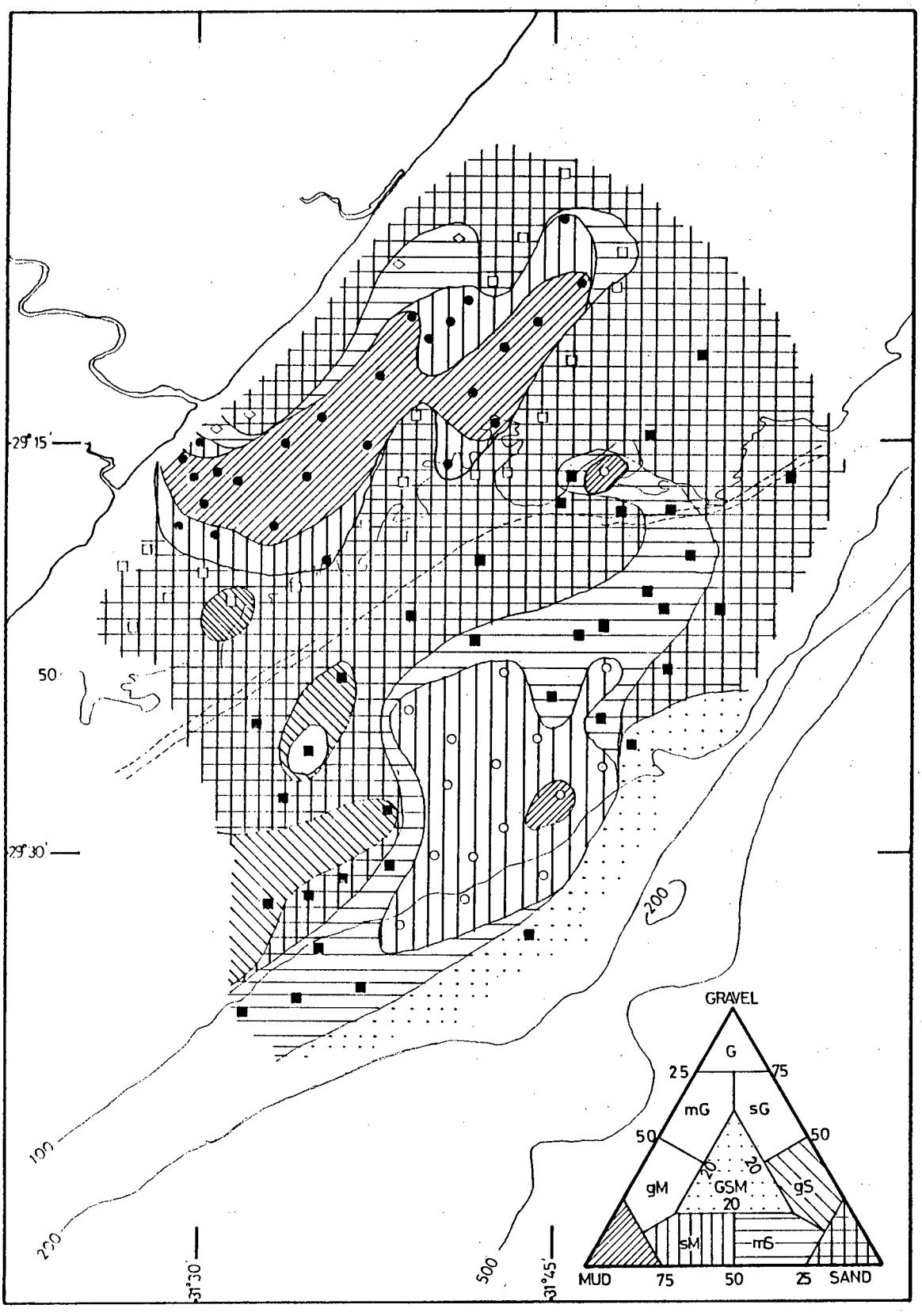

Figure 8-1. Textural composition (after Shepard, 1954).

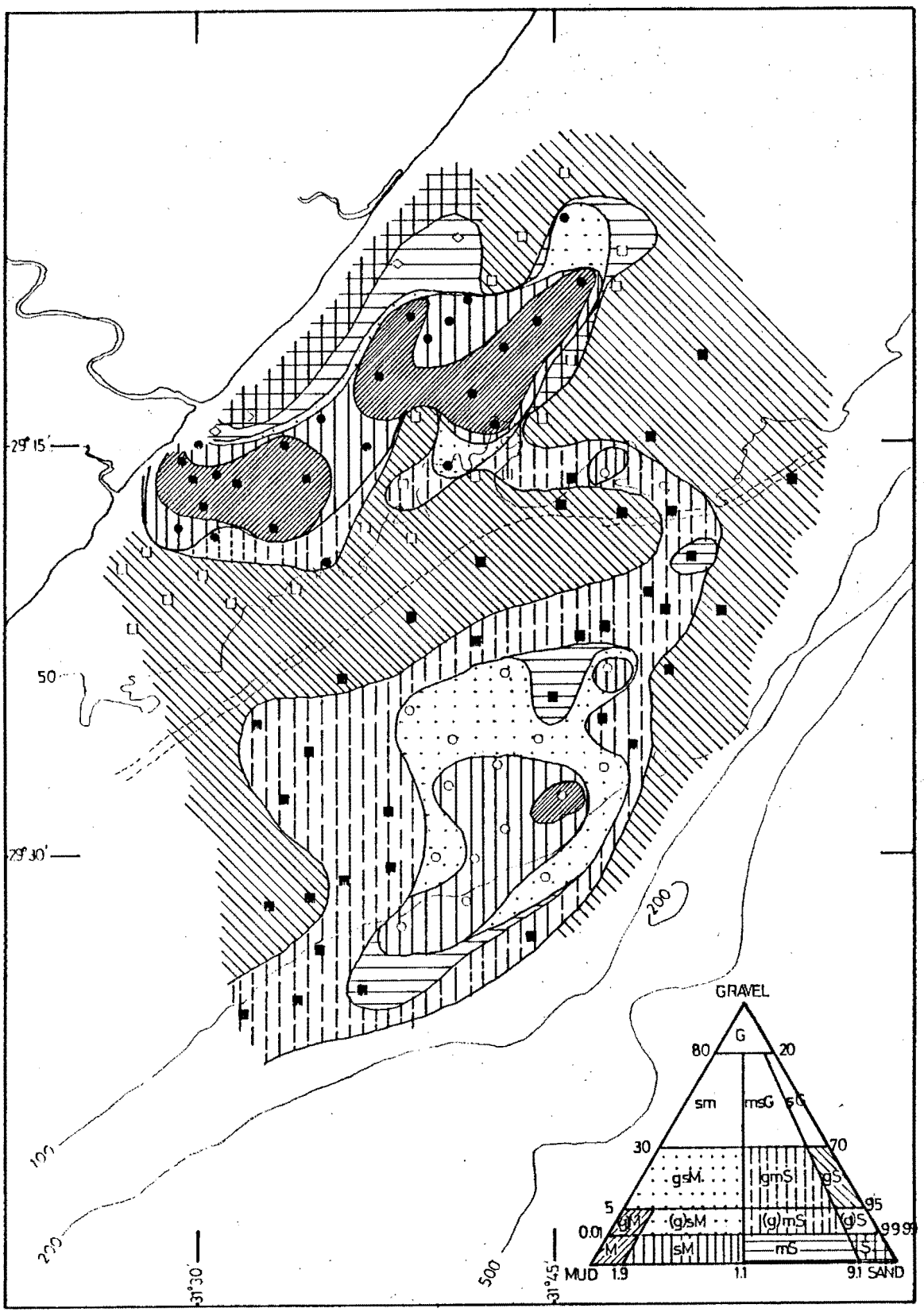

Figure 8-2. Textural composition (after Folk, 1954).

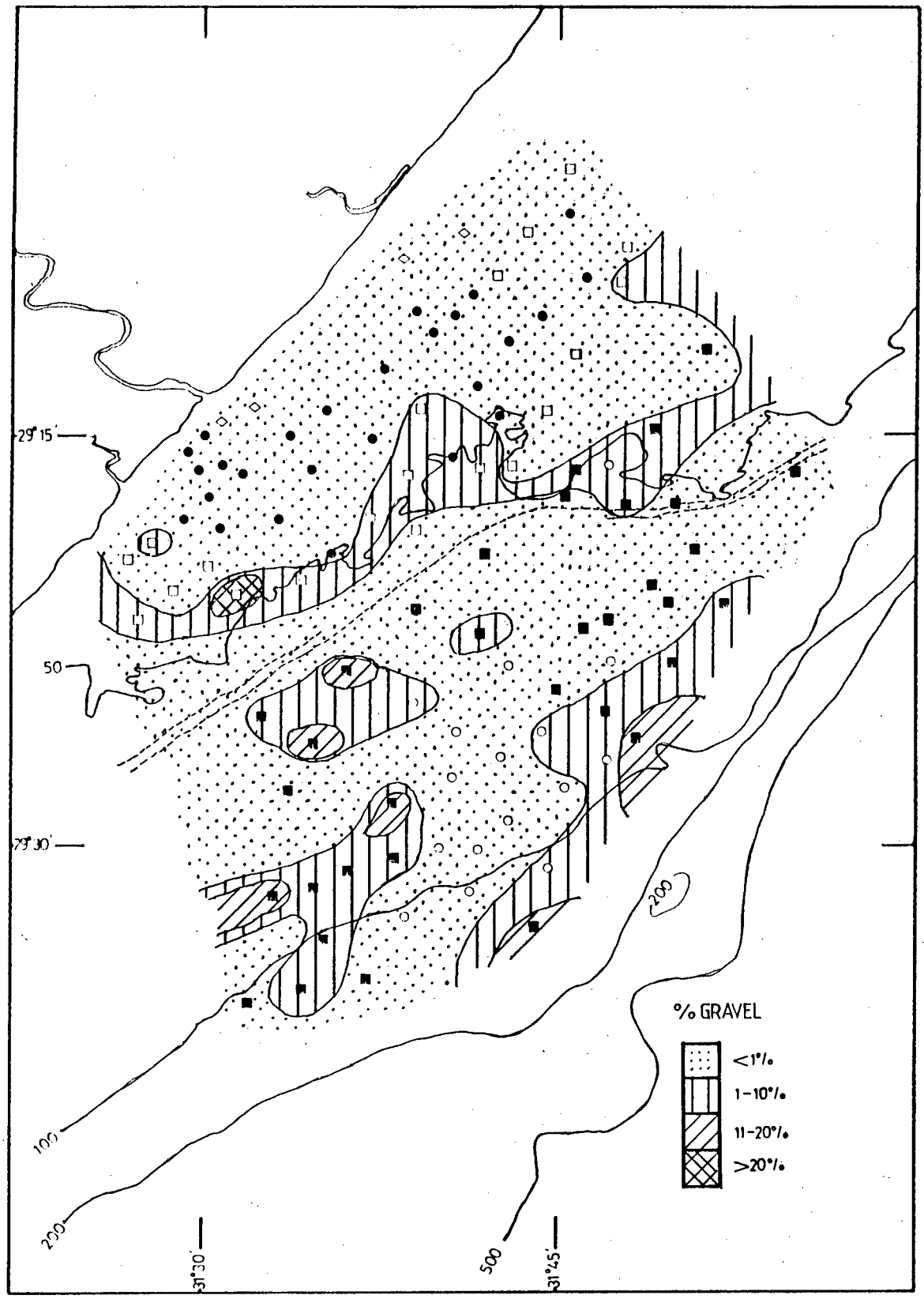

Figure 8-3. Distribution of gravel.

the mid-shelf (defined as the region between the inner and outer mud belts), and on the outer shelf along the shelf break. These findings are consistent with those of Flemming (1978) which show that the transition from biogenic gravels to finer terrigenous sands consistently occurs along the 50 - 60 m isobath on the continental shelf off the east Coast.

2.2 Very Coarse Sand

The very coarse sand distribution (fig. 8-4) is patchy in the study area except for a belt of 5 - 20% concentration occurring on the mid-shelf, seaward of the relict dune cordon. The very coarse sand follows essentially the same distribution pattern as does the gravel, suggesting that these two components are hydraulically related.

2.3 Coarse Sand

The concentration of coarse sand in the area is higher than that of very coarse sand or gravel. The coarse sand distribution (fig. 8-5) closely follows that of the coarser fractions, but extending considerably the total areal coverage of the coarser size fractions. Large (>50%) proportions of coarse sand are found in the sediments on the mid-shelf, seaward of the relict dune cordon to the southwest, and shoreward of this ridge to the northeast. The latter area lies between the 40 and 50 m isobaths, covering the plateau-like feature indicated on the bathymetric map (cf. fig. 7-1).

The gravel, very coarse sand and coarse sand concentra-

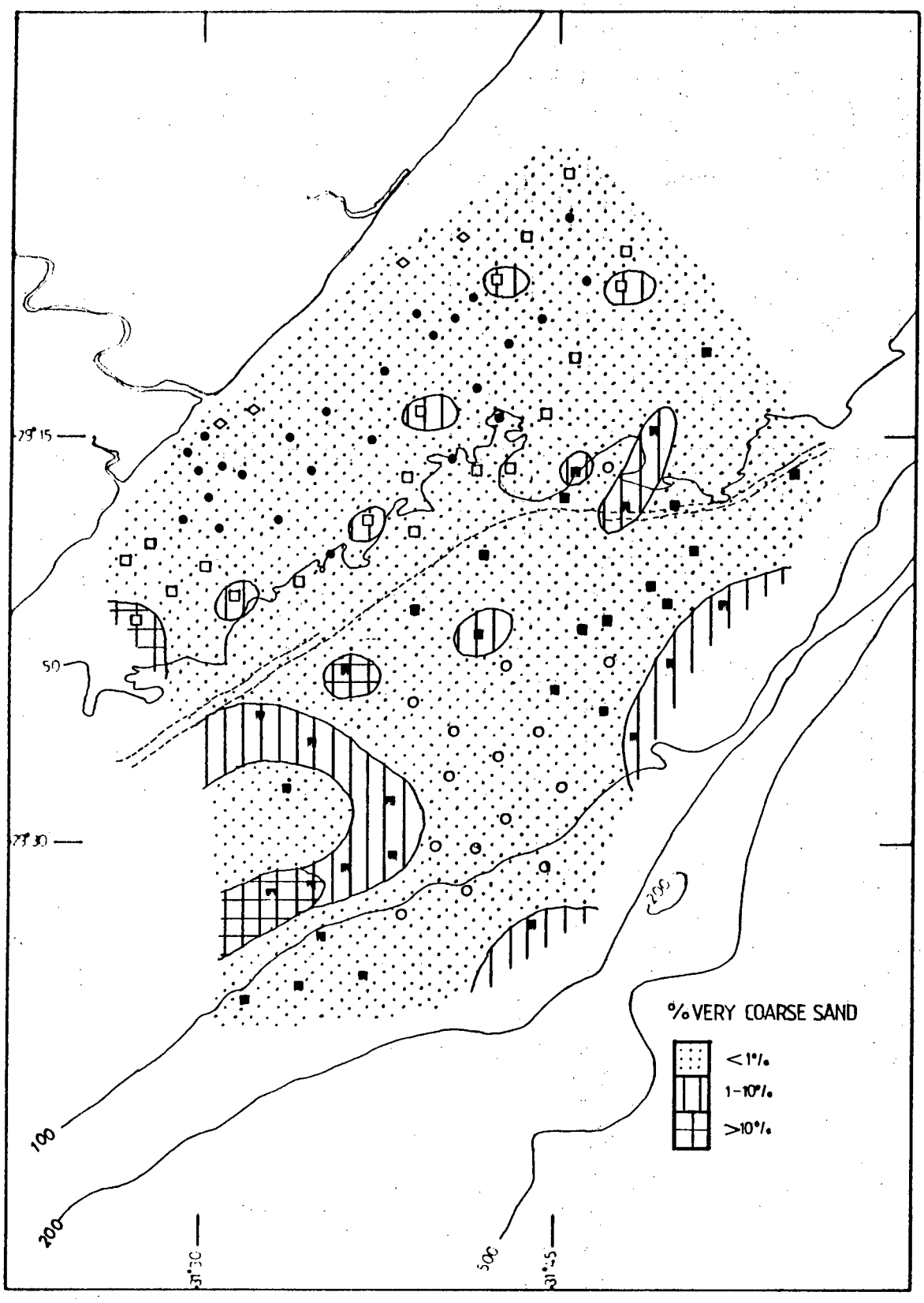

Figure 8-4. Distribution of very coarse sand.

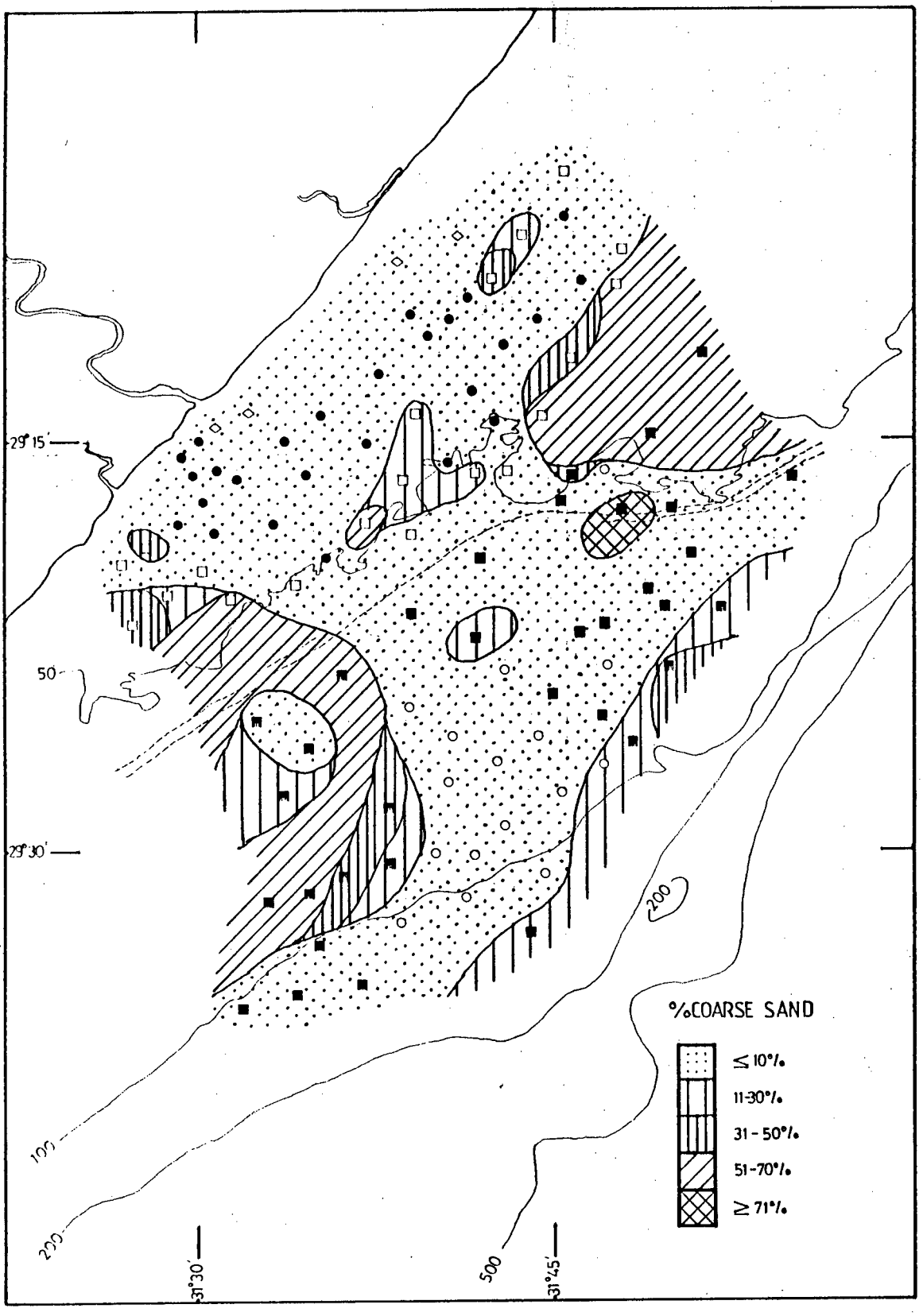

Figure 8-5. Distribution of coarse sand.

tions together show a distinct distribution that is concentrated on the mid-shelf in a fairly wide belt that flares out at both the northeast and southwest ends corresponding to the boundaries of the mud belts (fig. 8-6). Lower concentrations are found on the outer shelf along the shelf break. It is interesting to note the dearth of coarse sediments in the centre of the mid-shelf, immediately surrounding the relict dune ridge. Since a correlation between this cordon and coarse sediment is often observed elsewhere along the East Coast (Flemming, 1980; Moir, 1976), it may be suggested that the eddy dynamics are indeed intimately involved in sediment dispersal in this area.

2.4 Medium Sand

Most of the sand-sized sediments in the study area have a mean size in the 1 - 2 phi (ø) range, and are thus classified as medium sand. The highest concentration of medium sand (60 - 80%) is found on the mid-shelf, covering areas where the proportion of coarser sediments is very low or absent (fig. 8-7). The northeast portion of the study area also has high concentrations of medium sand, perhaps indicating the source of these sands to be the southward-moving northern shelf sand stream described by Flemming (1978). As the medium sand distribution seems to complement the pattern established by the coarser sediments, it might be useful to consider the medium sands hydraulically as part of the coarser sand fractions.

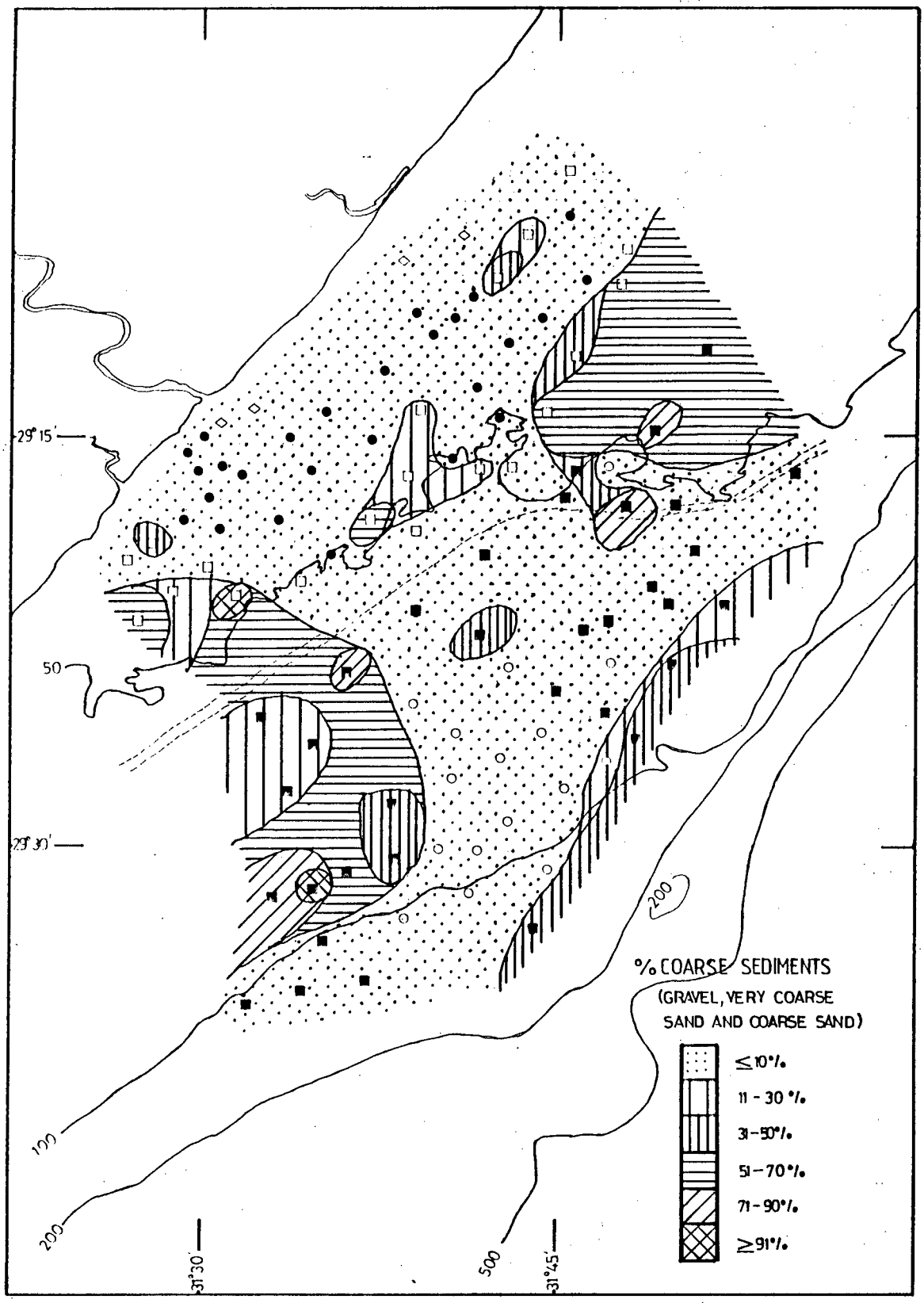

Figure 8-6. Distribution of the combined coarse fractions (gravel and very coarse sand and coarse sand).

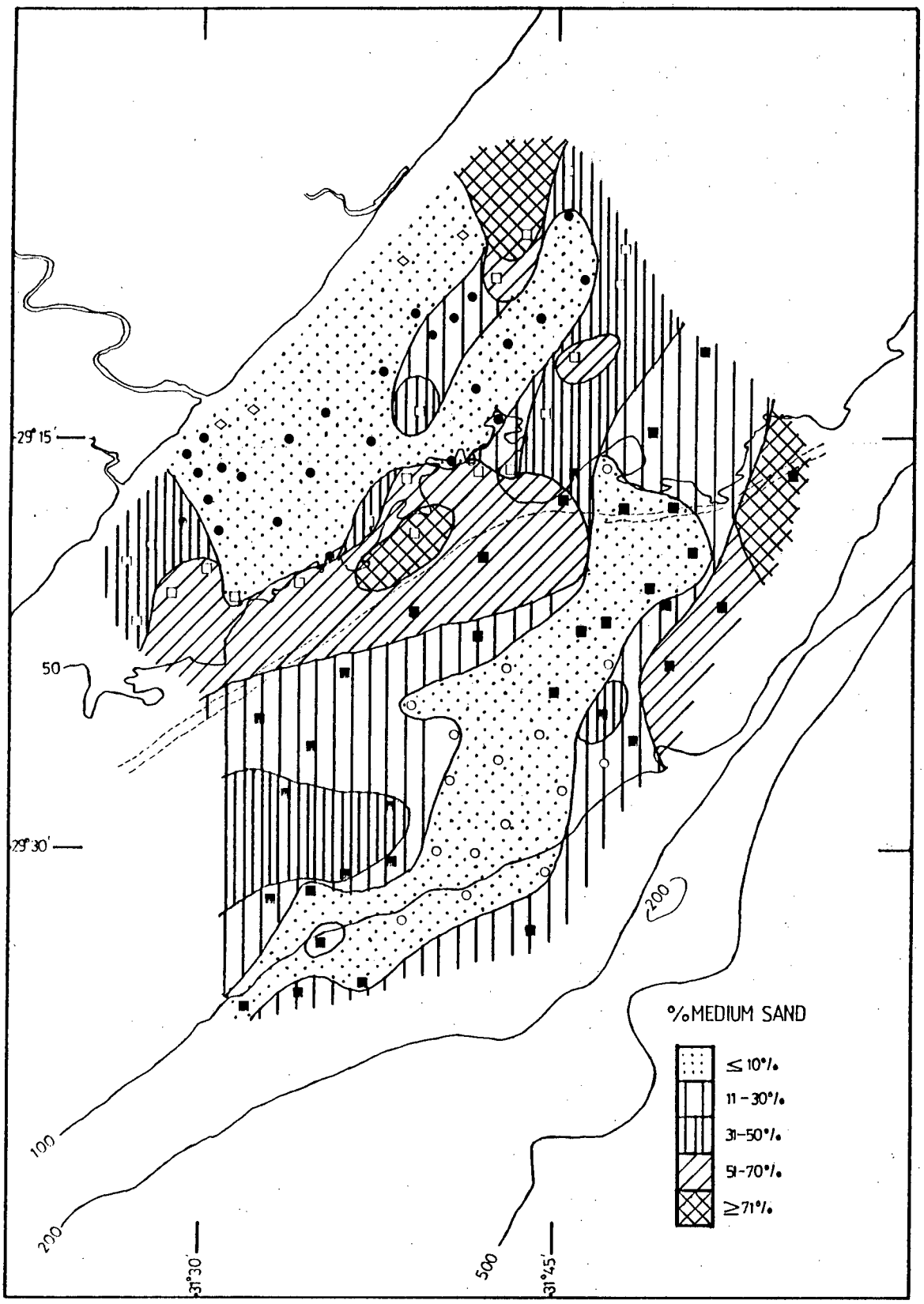

Figure 8-7. Distribution of medium sand.

2.5 Fine Sand

The distribution of fine sand (fig. 8-8) shows almost all the sandy samples to have some proportion of fine sand, with few areas of high concentration. The highest concentration of fine sand is found nearshore, north of the Tugela River Mouth. Two other areas of high concentration are found on the mid-shelf and southwest of the outer mud belt on the outer shelf.

2.6 Very Fine Sand

Very fine sand is concentrated in only two areas in the region (fig. 8-9). The belt of highest concentration is nearshore, inshore of the northeast portion of the inner shelf mud belt. The other area, containing 11 - 30% very fine sand, coincides with the outer shelf mud belt. Thus, while in the nearshore area mud and very fine sand are hydraulically separated, they appear to belong to the same suspended population in the offshore case.

2.7 Mud

The two major areas of mud deposition found in the study area are the primary focus of this thesis (fig. 8-10). The nearshore belt trends northeast-southwest, parallel to the shoreline. It is separated from the coast by a belt of very fine to fine sand that is very well sorted. Some exposures of rock outcrops are found in the nearshore area as well. The outer shelf mud belt has an oval configuration with a generally northeast-southwest trend similar to that of the inner belt. The outer area contains a smaller proportion

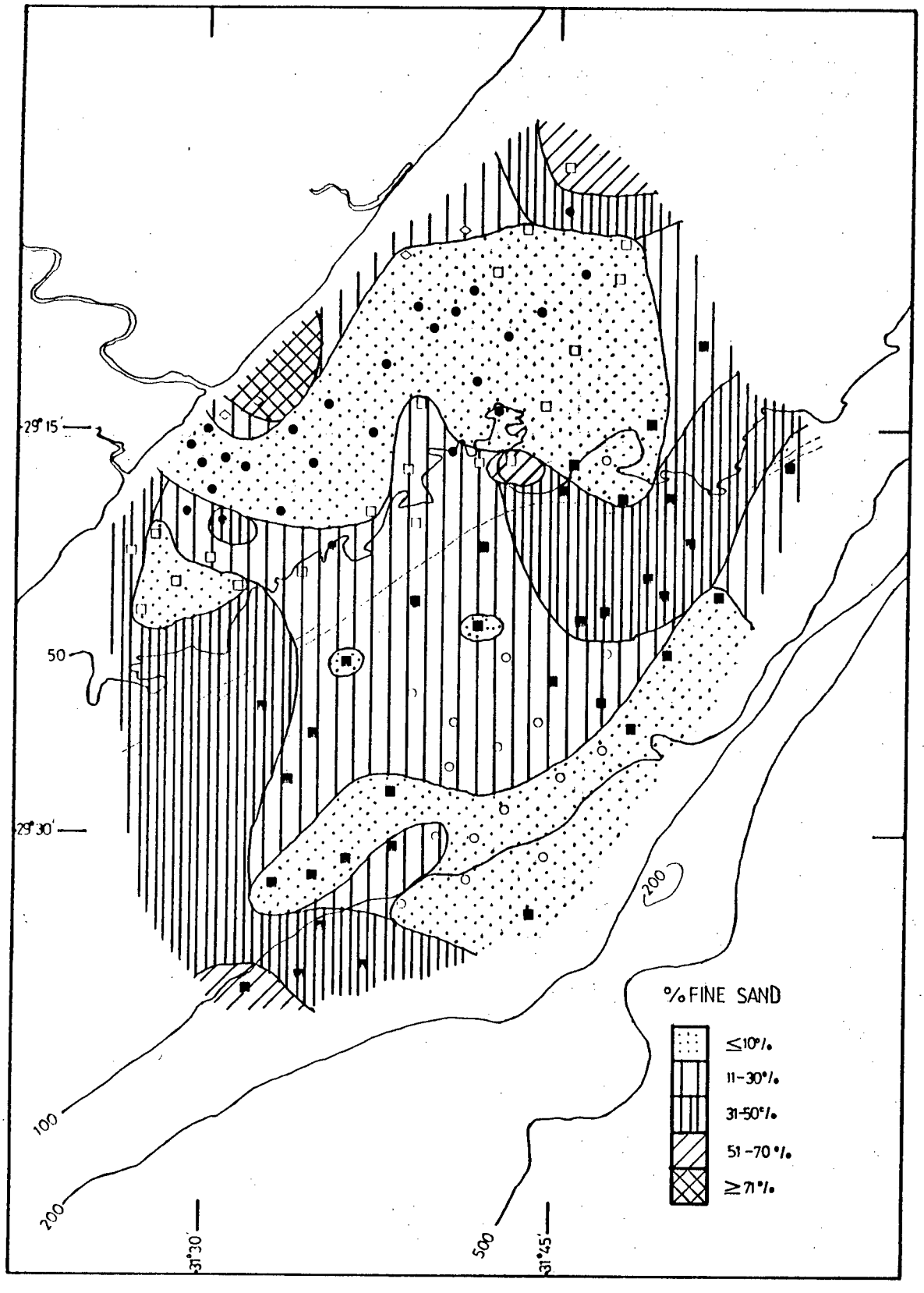

Figure 8-8. Distribution of fine sand.

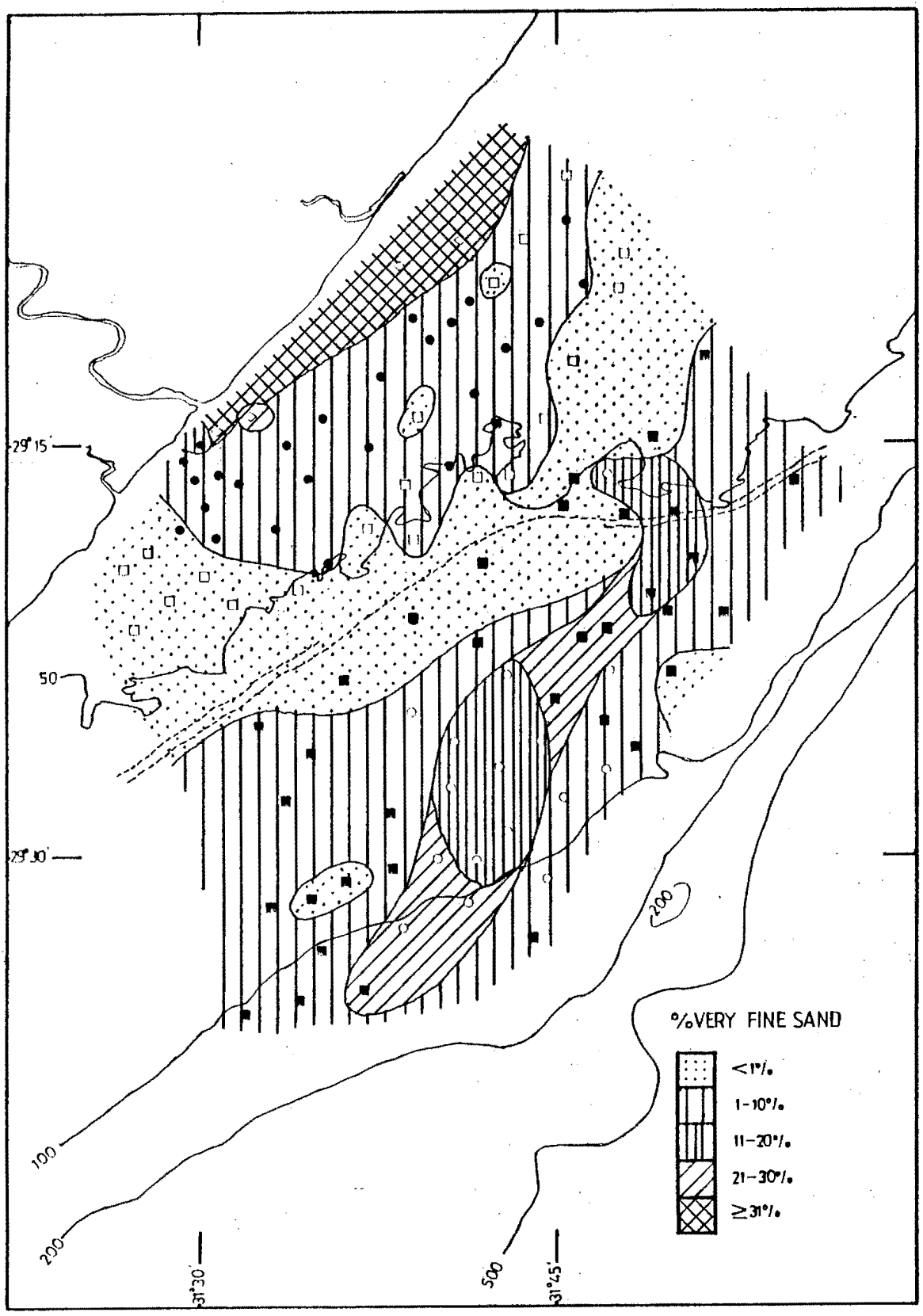

Figure 8-9. Distribution of very fine sand.

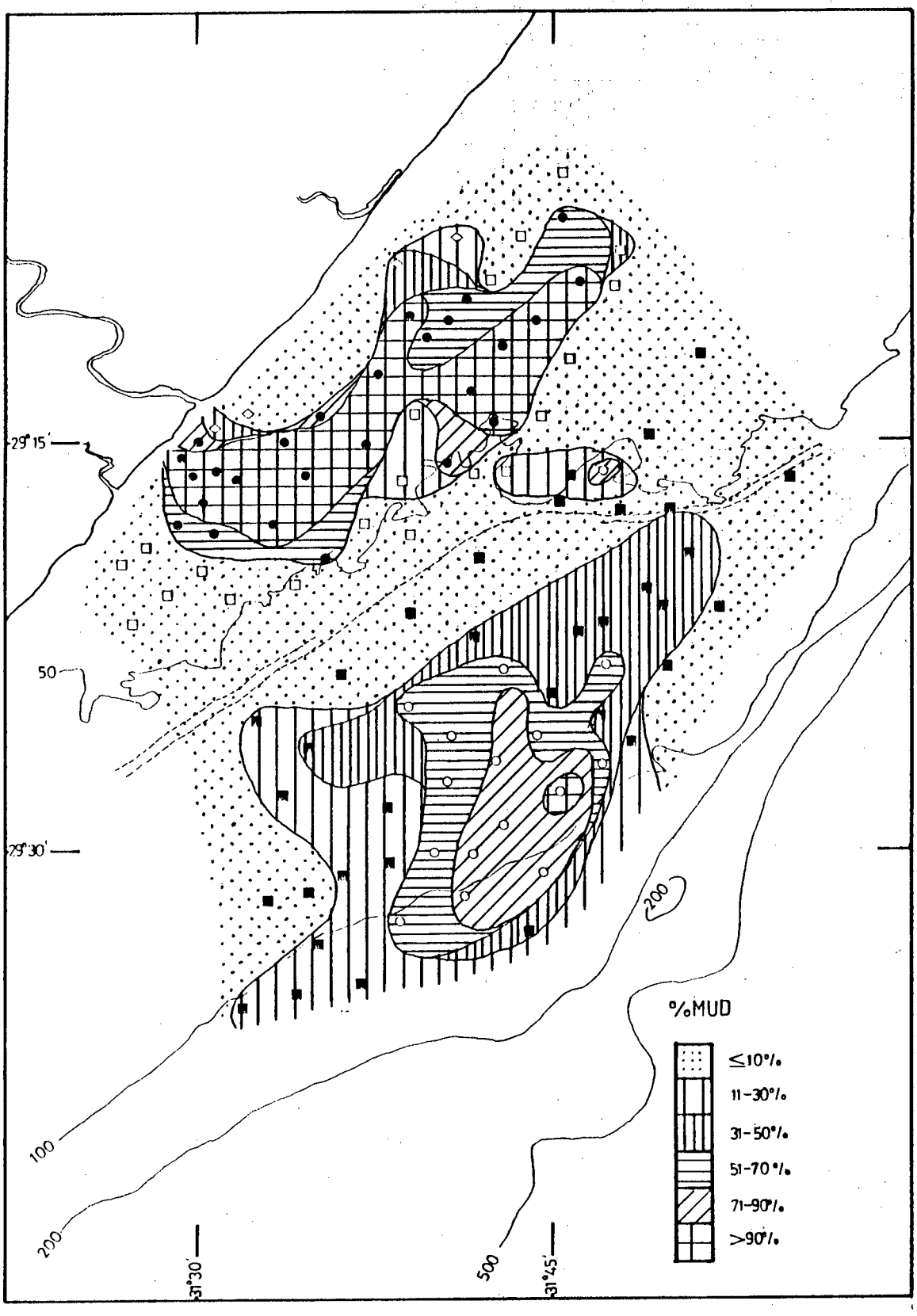

Figure 8-10. Distribution of mud.

(60 - 80%) of mud (<63 μm) than the nearshore belt (>90%). One muddy sample (TM058) was found on the middle shelf that appears to be unrelated to the two main belts. As discussed in chapter X, section 2.1.2, this sample was classified statistically with the outer shelf mud group.

The separation of the very fine and fine sands from the mud on the inner shelf, as opposed to the overlap of the fine fractions with mud on the outer shelf, is significant in demonstrating the existence of different energy regimes. It appears as though the outer shelf mud and overlapping sand were deposited simultaneously in a relatively high energy environment that treated the very fine sand fraction in the same way as mud in the processes of transport and deposition. The present hydrodynamic regime on the inner shelf appears to be subtle enough to allow a sharp hydraulic separation of the finer sand fractions from the mud.

3. Interpretation of Size Parameters for the Sand Fractions.

3.1 Mean Diameter (ø), Relative Sorting and Skewness (Mixing Model)

Hydraulic grain size determinations were made on all samples with a sufficiently large sand-sized fraction (roughly >10% sand, depending upon the nature of the sand-sized material). This excluded eighteen continental shelf samples that contained large percentages of mud and one of the estuarine samples. The parameters of mean diameter (ø), relative sorting (standard deviation), skewness and kurtosis were obtained from these analyses. These parameters were studied

in some detail in the hope of elucidating the relationship between the inner and outer shelf sediments, and to ascertain whether the area may be described more definitively in terms of sediment transport and mixing. Kurtosis values were not found to be of use in determining sedimentary groups, as virtually all the samples have highly positive kurtosis values, and are not included in the following discussion. Distribution maps of mean diameter (ø), relative sorting, and skewness are shown in figures 8-11, 8-12 and 8-13 respectively.

In plotting the mean diameter (ø) against the relative sorting (fig. 8-14) a trend emerges that shows two dynamically distinct hydraulic end-members, with a region that defines mixing around the most poorly sorted samples. One end-member consists of the fine, very well sorted nearshore sands and the fine and very fine, less well sorted sands found in and surrounding the outer shelf mud belt. The other end-member, possibly two separate populations, is composed of the medium and coarse sands of the mid-shelf region. This end-member progresses through a mixture of inner and outer shelf sands before reaching the area of the plot defining mixing. The inner shelf sands tend to be coarser and better sorted than the sands found outside of the relict dune cordon, with the exception of the four nearest shore sand samples.

The plot of skewness v. mean diameter (ø) (fig. 8-15) shows a poorly defined sine curve with a large amount of scatter. The majority of samples are positively skewed, i.e. have a tendency towards fineness.

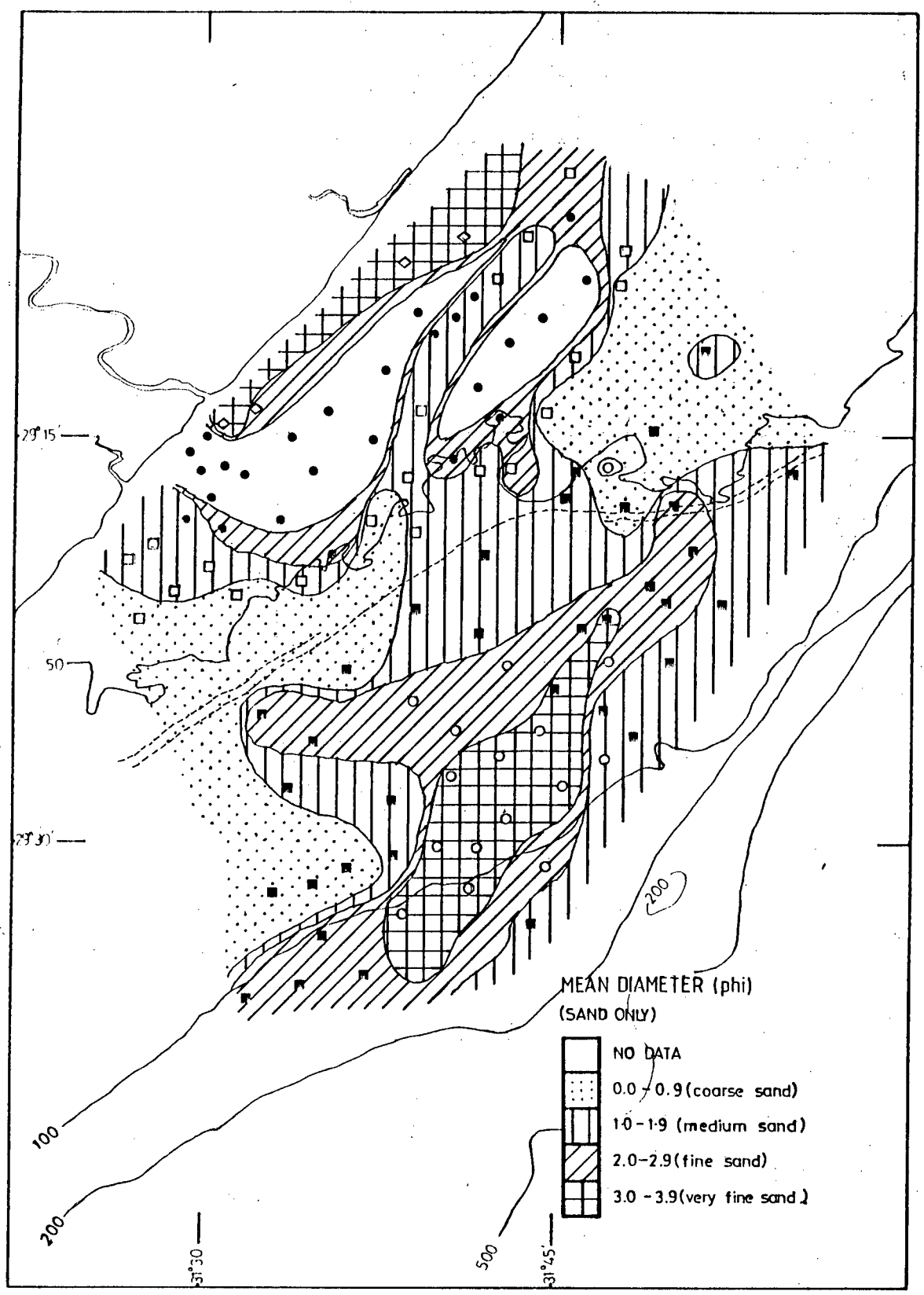

Figure 8-11. Mean diameter (ø) of the sand fractions.

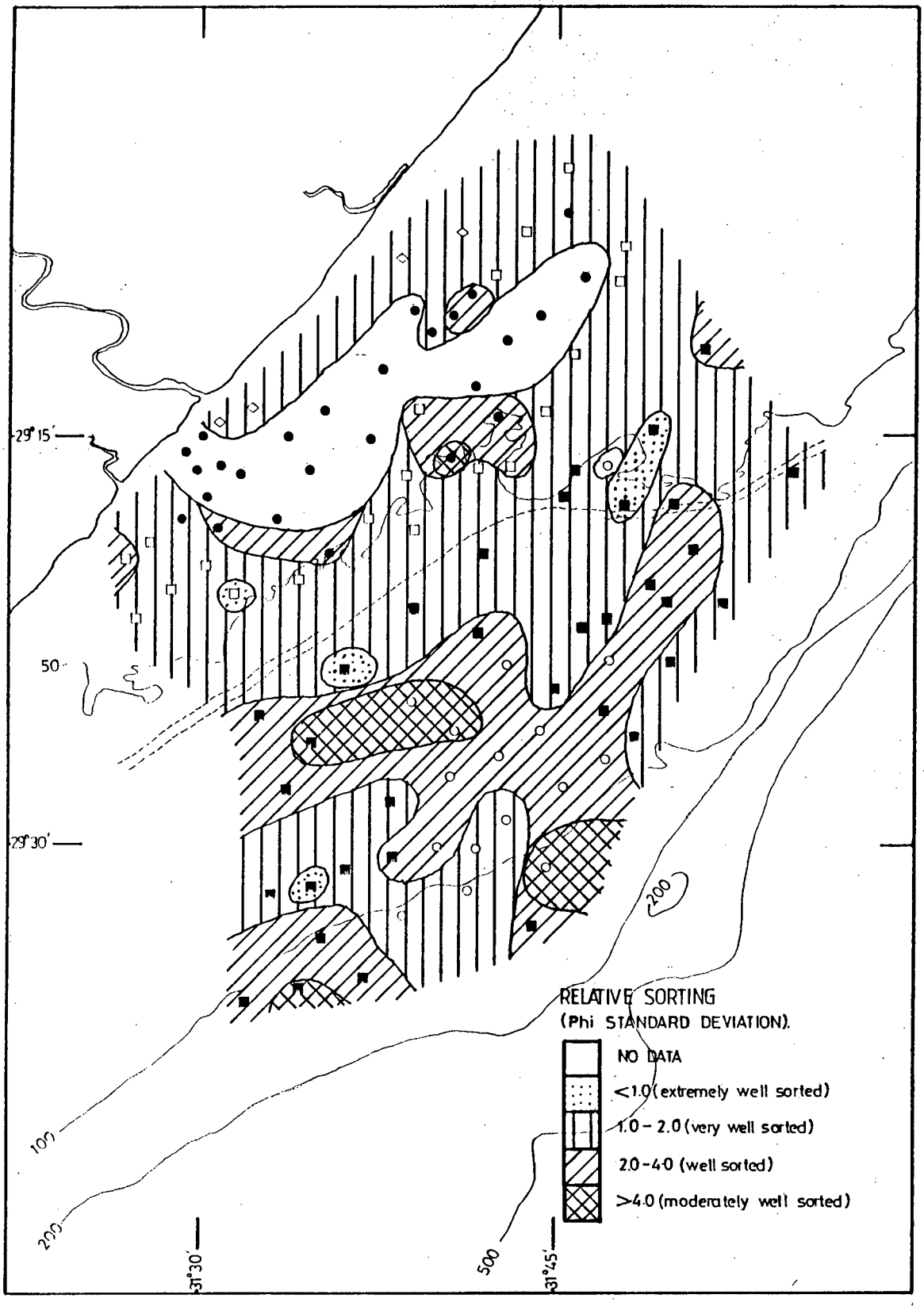

Figure 8-12. Relative sorting (ø standard deviation) of the sand fractions.

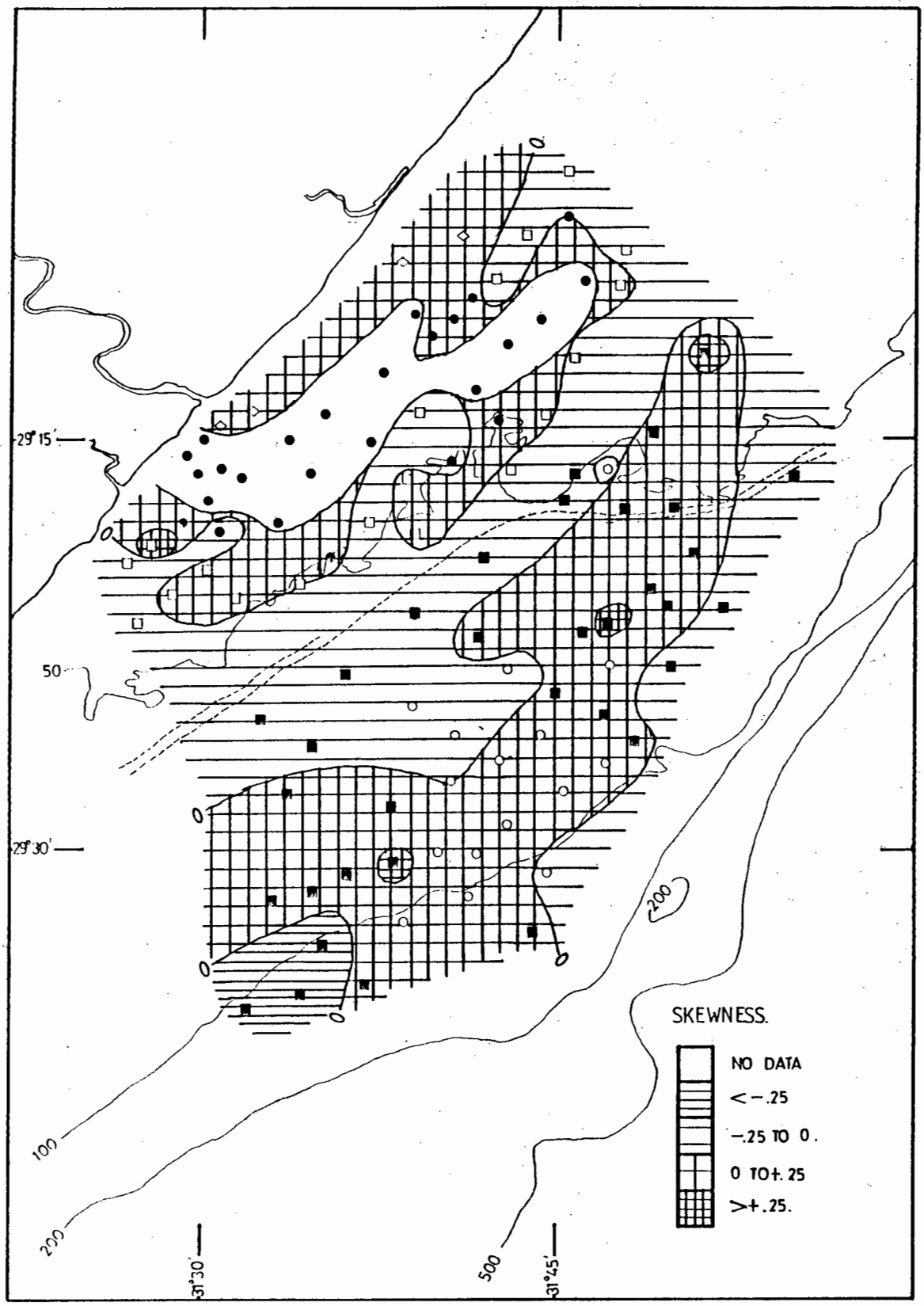

Figure 8-13. Skewness of the sand fractions.

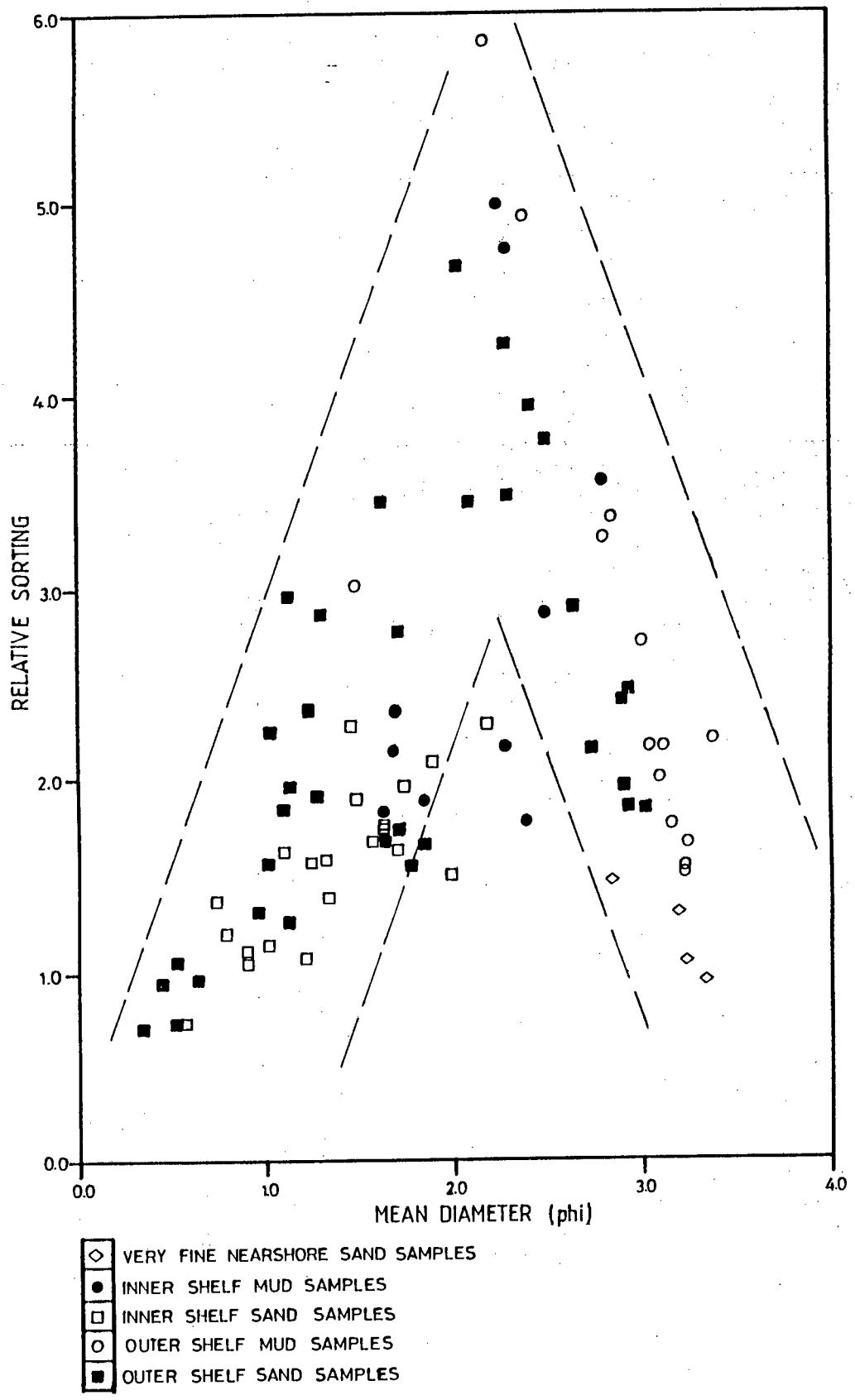

Figure 8-14. The relationship between mean diameter and relative sorting of the sand fractions.

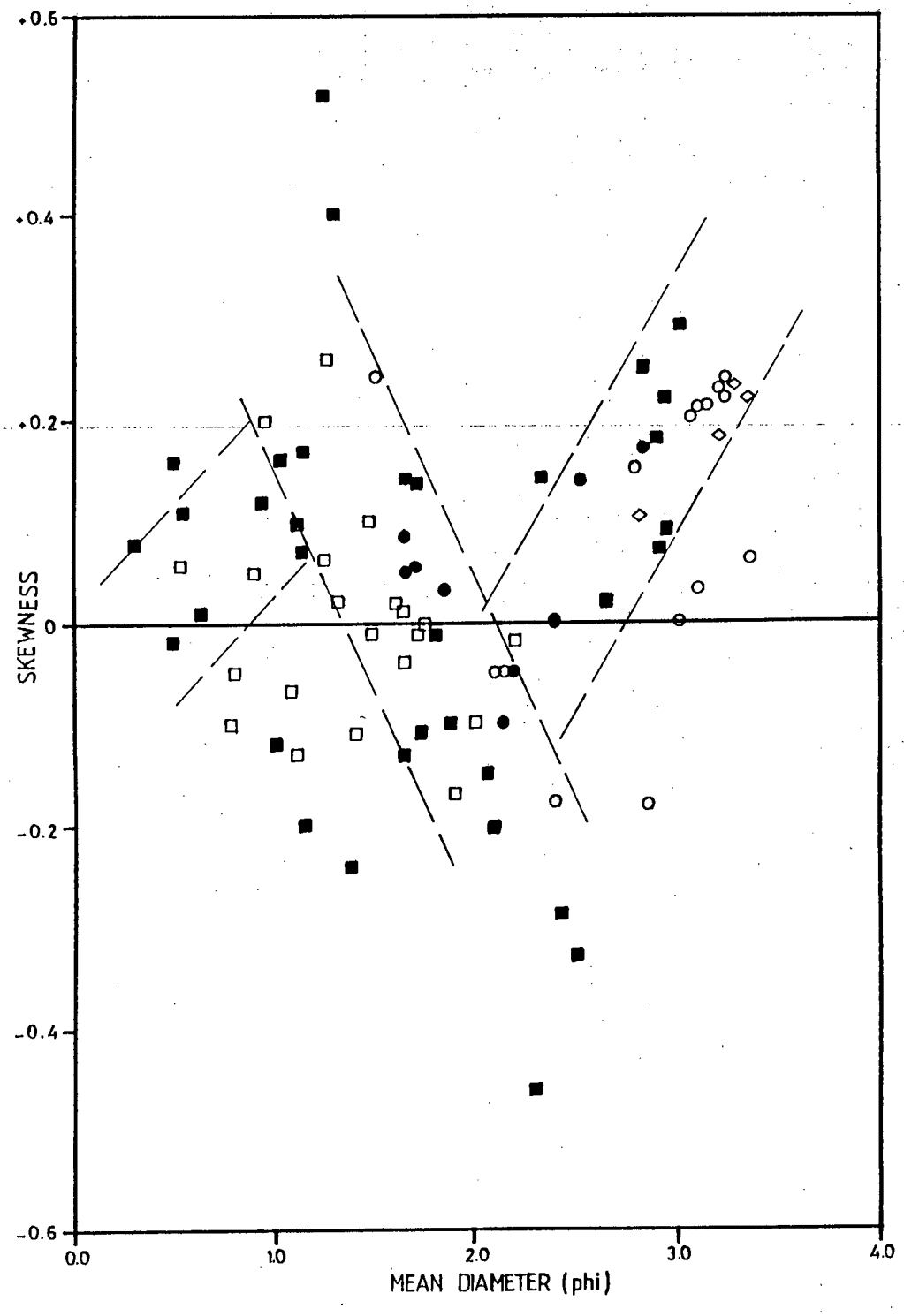

Figure 8-15. The relationship between mean diameter and skewness of the sand fractions. (for key, see figure 8-14).

A comparison of the two plots mentioned above shows that the two end-members defined in fig. 8-14 are not lognormally distributed. If they were, the skewness should be zero at the same mean size where the poorest sorting occurs, i.e. were equal mixing taking place. This is shown in figure 8-16. The parent populations of all mixing end-members themselves are therefore already composed of mixed sediments. Whether this is an inherent source related phenomenon or whether a reflection of a more complex depositional history is not entirely clear. Nevertheless, considering the known facts regarding the Pleistocene transgressive sequence and the present-day hydrodynamics of the shelf area already discussed in chapter IV, such mixing would not be unexpected.

The plot of skewness v. relative sorting (fig. 8-17) shows a degree of separation between the inner shelf samples and those from the outer shelf, but as a considerable degree of overlap is present the usefulness of the plot as a diagnostic tool is diminished (cf. Leeder, 1982).

The distribution of the hydraulic populations as found by the above methods is shown in figure 8-18, and is a visual representation of the mixing model defined above. This map varies considerably from the textural composition maps because it deals strictly with the sand-sized fractions of the sediments, not the bulk sediments. In order to test the applicability of the mixing model in the study area, four small areas shown to contain components of all three defined end-members were selected (fig. 8-19) and subjected to the

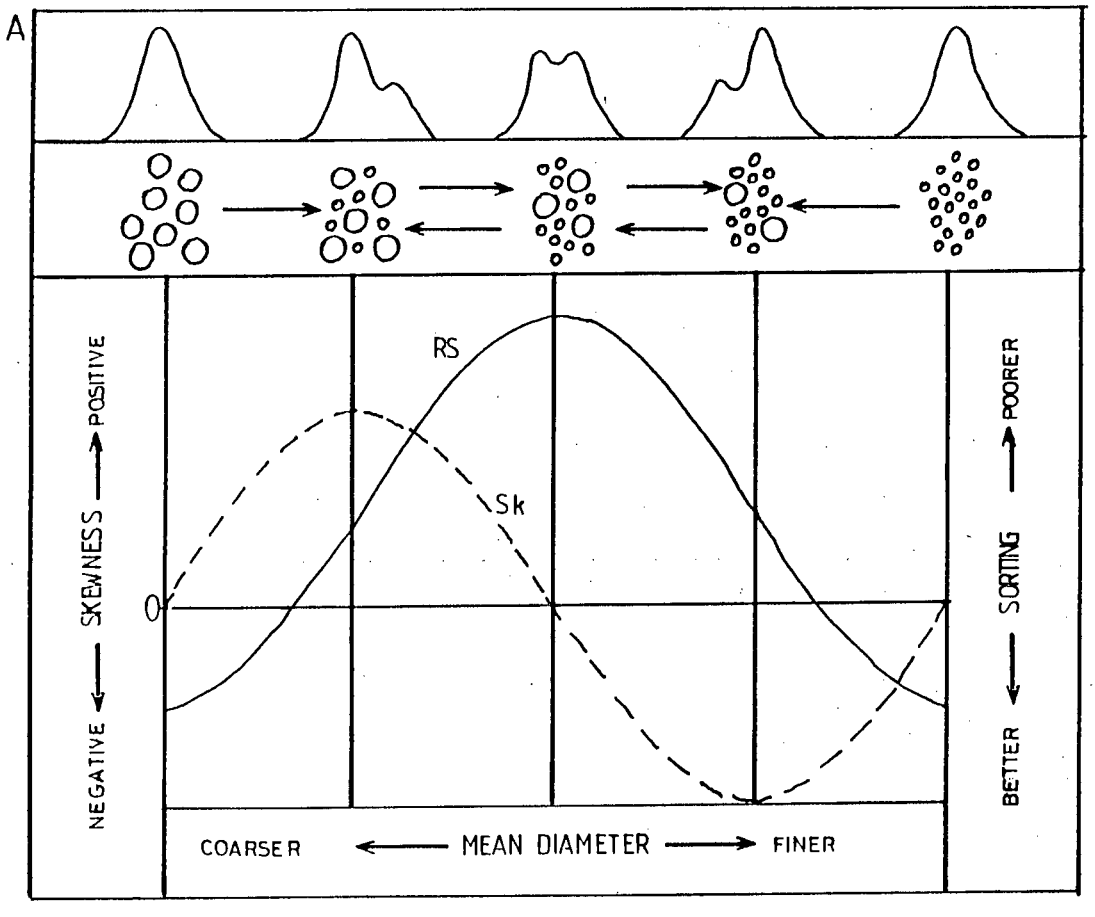

Figure 8-16. Size distribution characteristics of sediments consisting of two progressively mixing hydraulic populations (A-idealized model from Flemming (1977) after Folk and Ward (1957)).

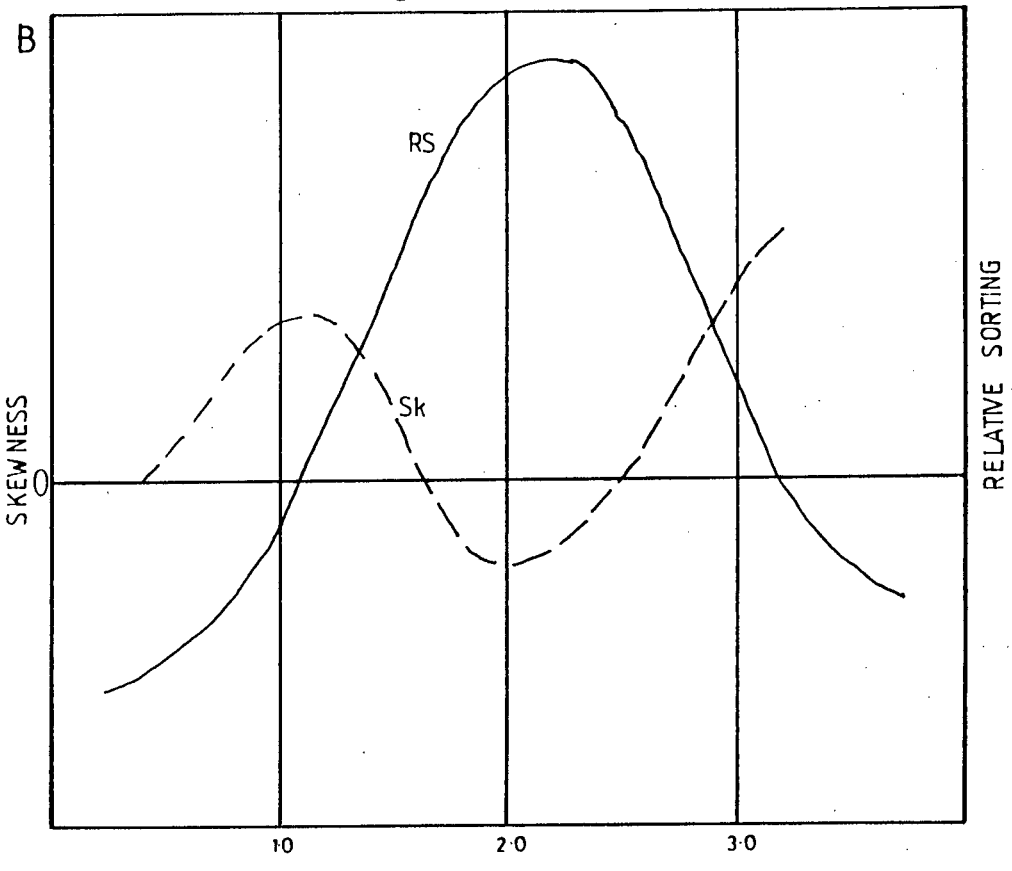

(B-mixing model for the sand fractions of the sediments of this study).

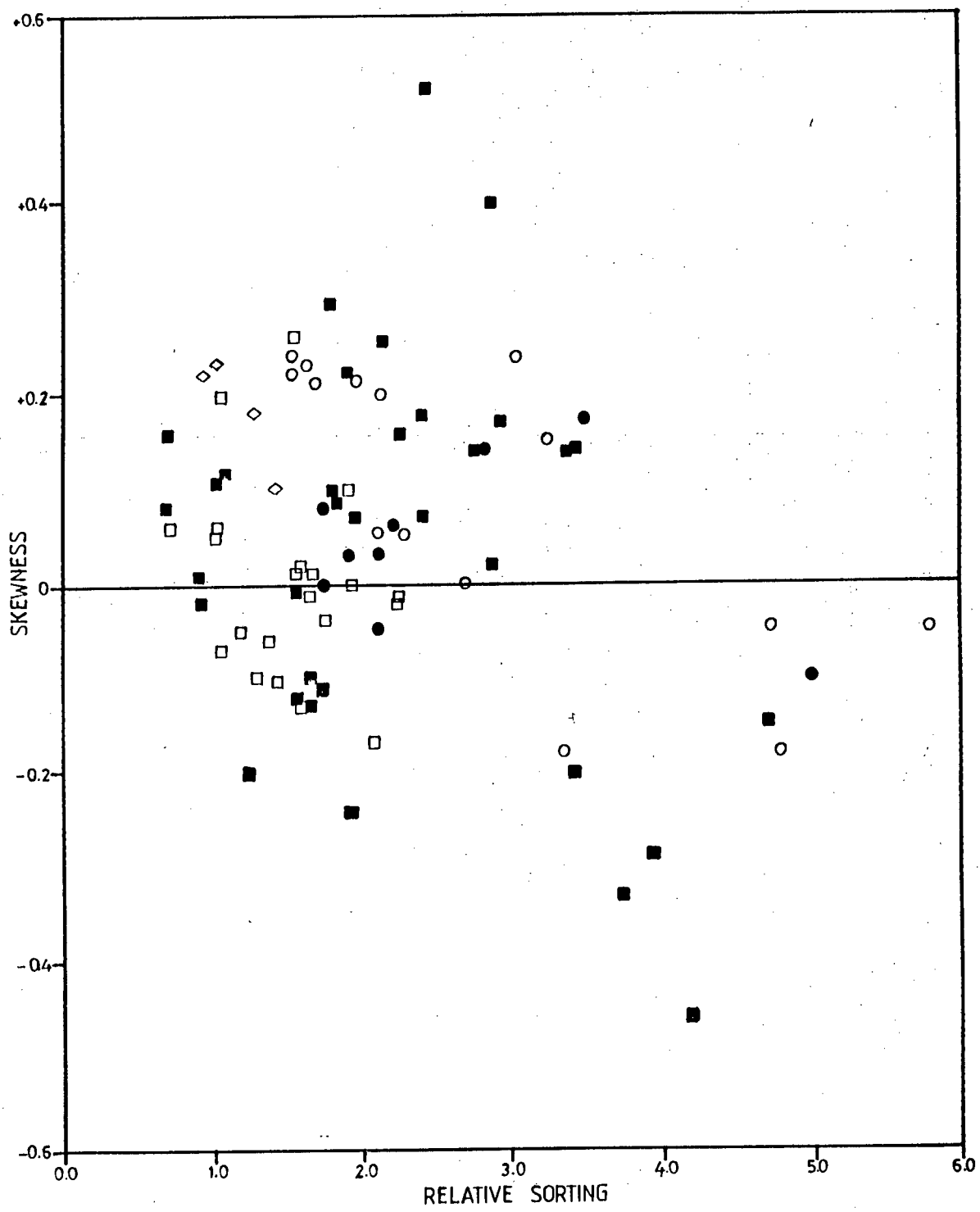

Figure 8-17. The relationship between skewness and relative sorting of the sand fractions. (For key, see figure 8-14).

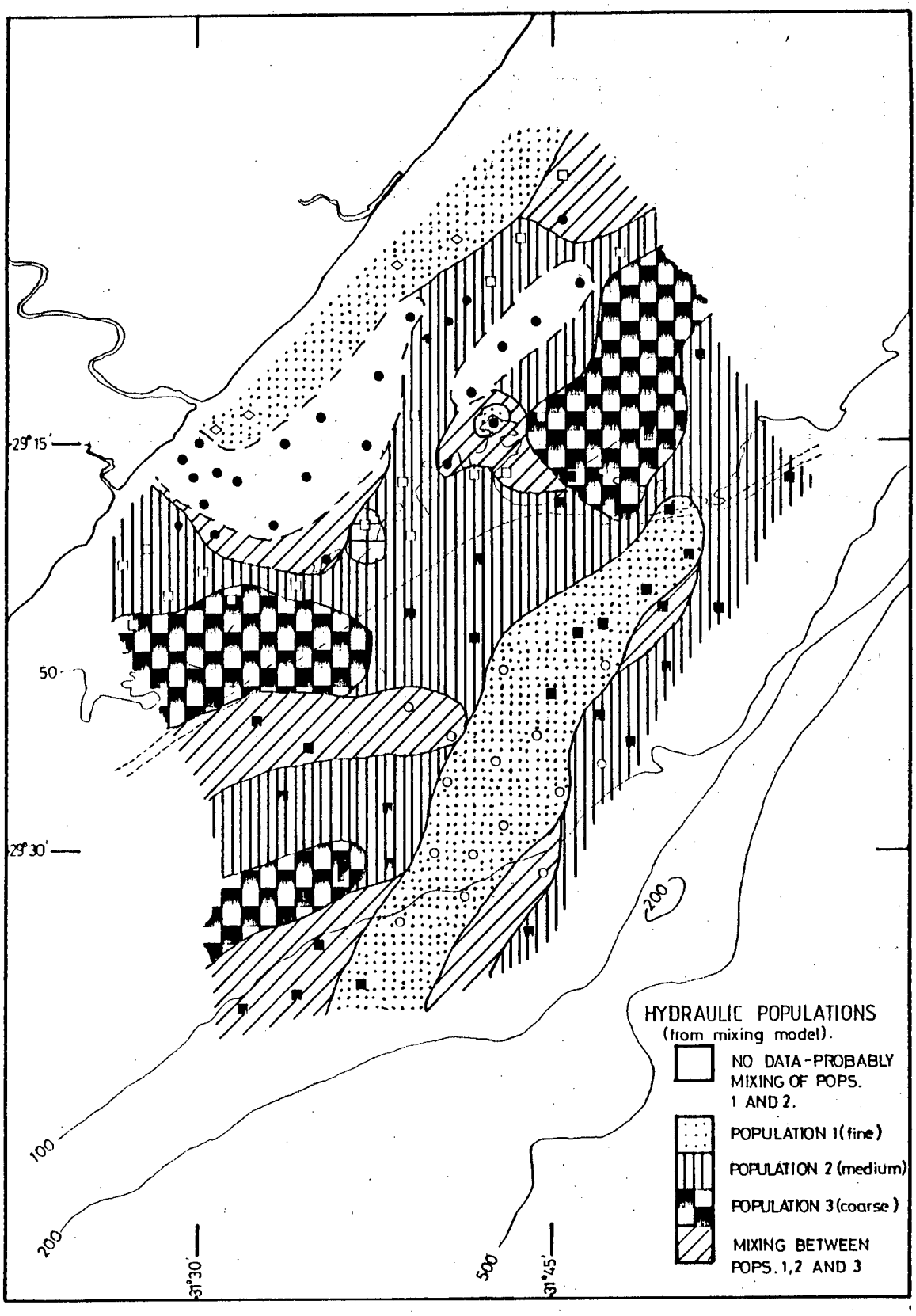

Figure 8-18. Hydraulic population distribution (from the mixing model).

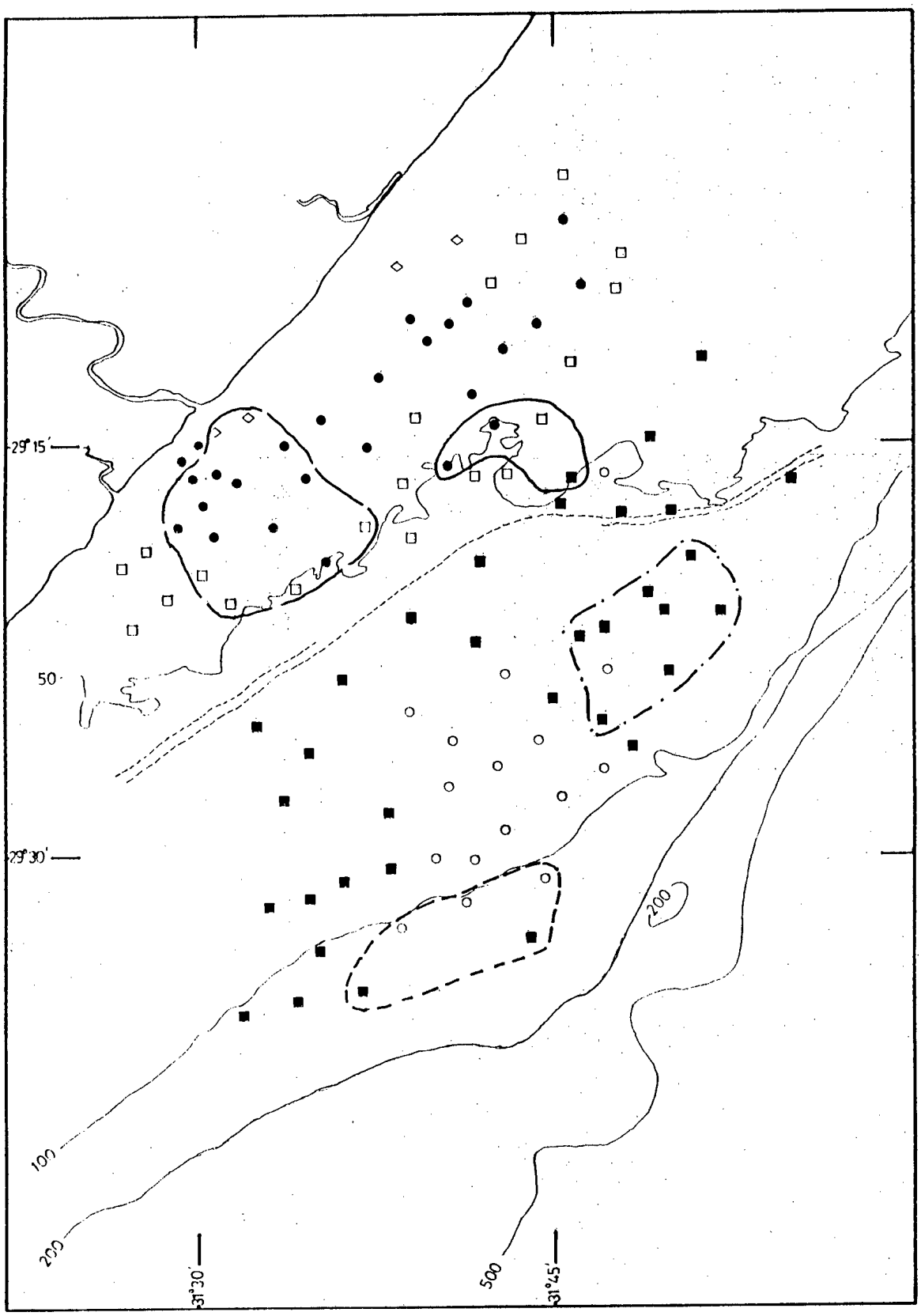

Figure 8-19. Areas used to test the mixing model.

same tests described above for all samples. Figure 8-20 shows trends existing in each of these four areas similar to that found when dealing with all of the samples, indicating that the mixing model is valid for samples from both the inner and outer shelves.

3.2 Cumulative Frequency Curves

Different populations of sand were also defined by grouping the cumulative frequency curves from the settling data as was done by Nota (1958) and Loring and Nota (1973). The groups of curves are shown in figure 8-21. The distribution of the groups on the continental shelf is shown in figure 8-22. Figure 8-22 does not vary markedly from figure 8-18, discussed above, but it does extend the area of mixing noticeably. This method of interpretation appears to indicate that the sand present in the nearshore mud belt is probably also of mixed origin, although the amount of sand involved is very small.

4. Discussion and Conclusions

In order to interpret the information discussed in the preceding sections, a review of the continental shelf history is necessary. The continental shelf off the coast of southeast Africa is classified as a high energy environment, with the major factor controlling sediment dispersal being the Agulhas Current and associated circulation patterns (Flemming, 1981). The submerged dune ridge that occurs along the 50 - 60 m isobath along most of the shelf provides evidence of a Pleistocene shoreline. This has been substantiated by side-

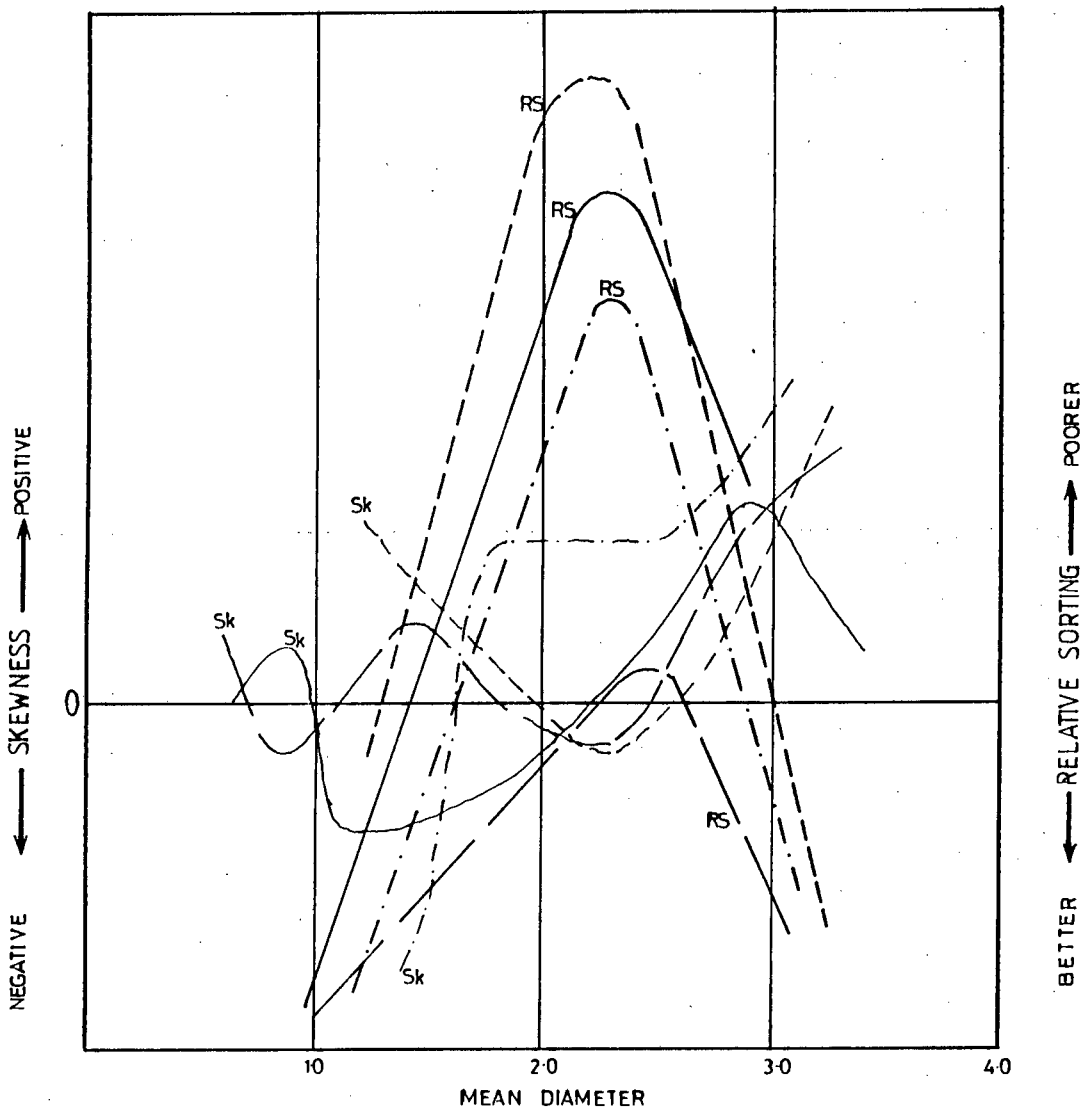

RELATIVE SORTING.		SKEWNESS.
———	MID-SHELF (NE)	———
——— ———	INNER-MID SHELF	——— ———
— — — — —	OUTER SHELF (SW)	— — — — —
—·—·—·—	OUTER SHELF (NE)	—·—·—·—

Figure 8-20. Size distribution characteristics of the areas used to test the mixing model.

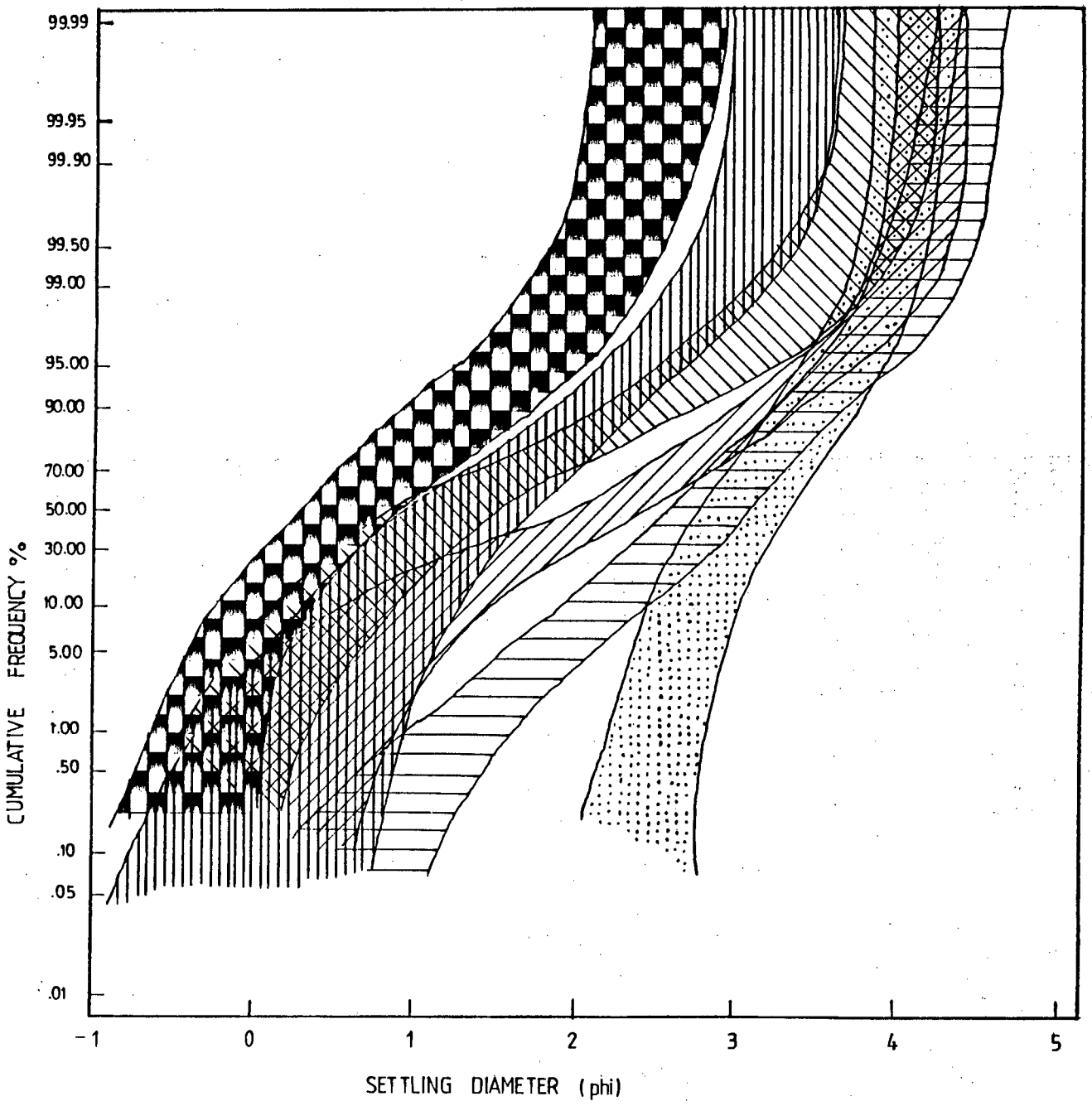

Figure 8-21. The groups of cumulative frequency curves used to define hydraulic populations.

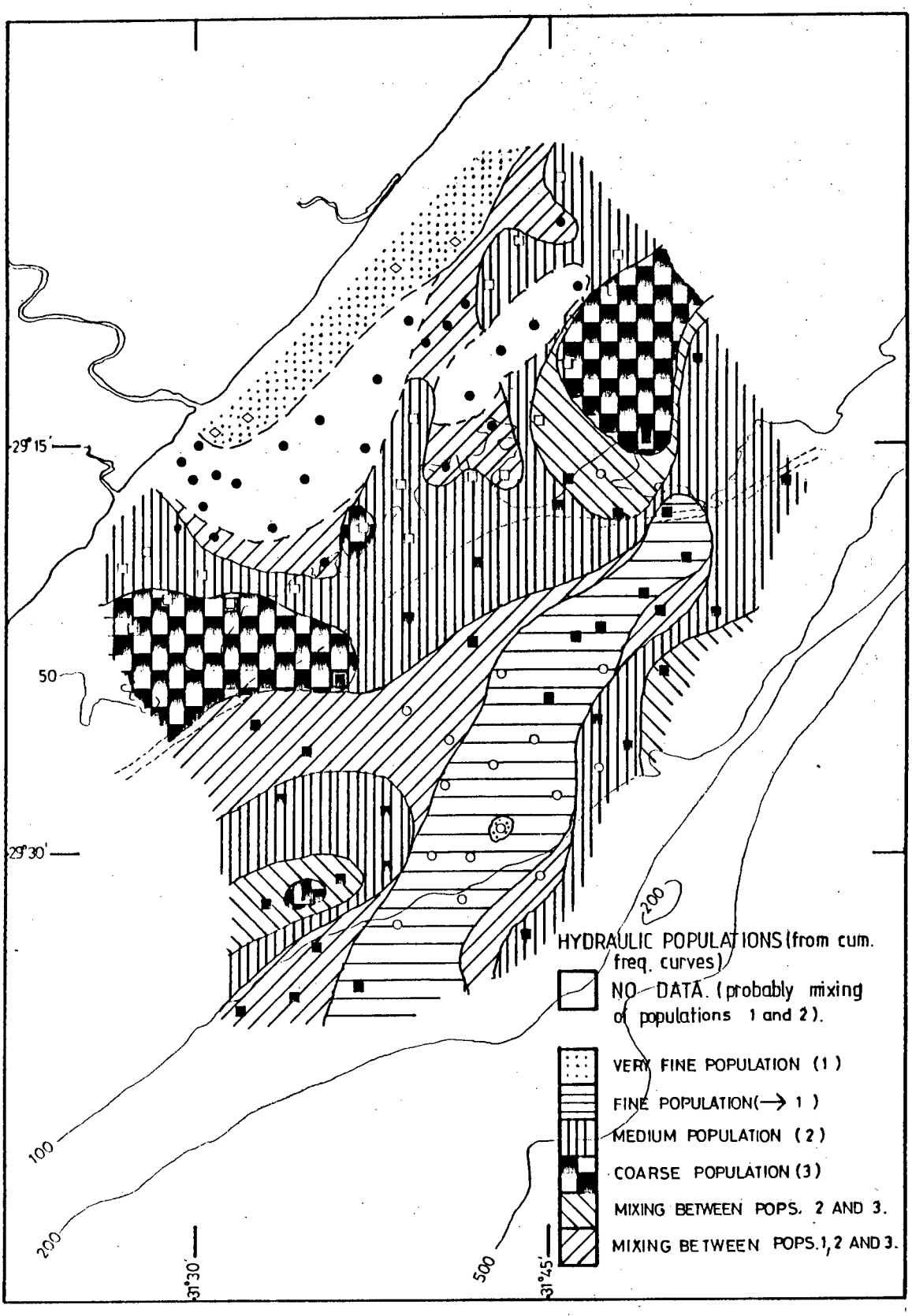

Figure 8-22. Hydraulic population distribution (from the cumulative frequency curve groups).

scan sonar records and dredge hauls that show rippled gravel deposits overlying muddy carbonaceous material dated at more than 40 650 yr BP (Flemming, 1978). Hutson (1980) has shown by micropaleontological evidence that the Agulhas Current was much weaker in the Pleistocene, only occurring as a seasonal phenomenon and even then not reaching much further south than Durban. From this information, a paleoenvironment can be reconstructed where the Tugela River mouth was situated on the present-day middle shelf with a large estuary behind it that was presumably a major depocentre for estuarine muds. The discharge from the river would have been deposited on the shelf in the present position of the outer shelf mud belt, with some sediment continuing on down the Tugela Canyon.

During the subsequent transgressions, the estuarine deposits were progressively covered by a thin veneer of alternating sands and gravels. Piston cores or vibro-cores, not available to this study, would be the only way to elucidate the nature of the Holocene transgressions. The Tugela Canyon, as a sediment export route, became inactive over this period, as suggested by its poor definition close to the shelf break. The shoreline receded towards its present position. At the same time, the Agulhas Current became stronger and the present-day hydrodynamic regime established itself. Sedimentary budgets calculated for the southeast African continental margin have estimated that as much as 90% of the suspended material supplied to the shelf is lost (Flemming and Hay, 1984). Mud is not being deposited on the open shelves of the east coast today except in a few small and relatively sheltered inner shelf regions.

It is thus very likely that the outer shelf mud belt is essentially a relict deposit from the Pleistocene, with minor modifications by modern processes. Once mud is deposited, it is bound with a cohesiveness so strong that it takes a current with the competency to move coarse gravel to erode it (McCave, 1972). The lower percentage of mud found in the surficial samples from the outer shelf mud belt suggests that either there was less mud present in the sediment initially or that some winnowing of the fines has occurred. It is possible that the outer mud is undergoing a slow but continuous process of erosion.

The inner mud belt forms the present-day depocentre for at least some of the suspended material discharged by the Tugela River. If, from the calculated figures of annual terrigenous input from the river by Flemming and Hay (1984), all suspended material supplied during the Holocene by the Tugela River was deposited in the inner shelf mud belt, it would have to comprise a 150 m thick column of mud (without allowing for compaction). As seismic records show a maximum thickness of mud of 14 m in the area, one must assume that over 90% of the suspended load is being lost. It would thus appear that the suspended fines become entrained into the predominantly north-flowing nearshore currents upon entering the ocean and that most of them slowly diffuse into the Agulhas Current to be carried away. Only in the course of heavy floods, carrying very high concentrations of fine sediment, does a fine bedload component develop which can then be trapped in the centre of the eddy where flow velocities are lowest.

The interpretation of the statistical size parameters substantiates the above discussion. The inner and outer shelf mud belts are distinctly separated by a sand belt composed of a reasonably well defined hydraulic end-member. The mixing occurring on the inner shelf is probably from onshore components of the wave and current regime combined with the abundant input of terrigenous fine material from the Tugela River. The outer shelf, on the other hand, presents a more complicated picture. From the mid-shelf progressing seawards, there appears to be mixing of the coarser components with the medium and finer-grained sands. The coarser populations are the result of the mixing of modern sands, possibly originating from the northern shelf sand stream, or residual sands with the gravel lag deposited during the transgressive-regressive sequence. The fine end-member existing in and around the outer shelf and belt could be a residual sediment from the Pleistocene Tugela River deposit that is now being slowly eroded by the Agulhas Current. This is indicated by an increasing grain size seaward of the outer shelf mud deposit. The present-day hydrodynamic regime would therefore seem very conducive to the considerable amount of mixing now found on the shelf, especially in the outer shelf regions of the study area.

CHAPTER IX MINERALOGY

1. Introduction

Qualitative bulk mineralogy was determined for all samples by X-ray diffraction. The mineralogical composition of each sample is given in Table 9-1. Interpretation of the X-ray diffractograms was limited by the great variability in intensity from given crystallographic planes in the feldspar series, as well as by interference from other minerals in the range of interplanar spacings used (viz. 2.10 - 29.45). Apparent relative abundances of the feldspars, clay minerals and carbonate minerals are noted in Table 9-1. However, as corrections were not made for variations in mass absorption coefficient of the samples, nor were peak areas calculated, these relationships are not accurate and are useful only as an indication of the mineral abundances. As the mineralogy was performed only as a check on the more detailed sedimentological and geochemical aspects of the study, the qualitative methods and the small angular range (3^{o} - $43^{o}2\theta$) used are considered adequate for this purpose. Example diffractograms are shown in figures 9-1a and b.

2. Mineralogical Composition

2.1 Quartz

Quartz was found to be the major constituent mineral of all the samples in the study area. This was expected from the previously established terrigenous classification given to the sediments by Flemming (1978). The outer shelf mud samples generally contain more quartz than the inner shelf

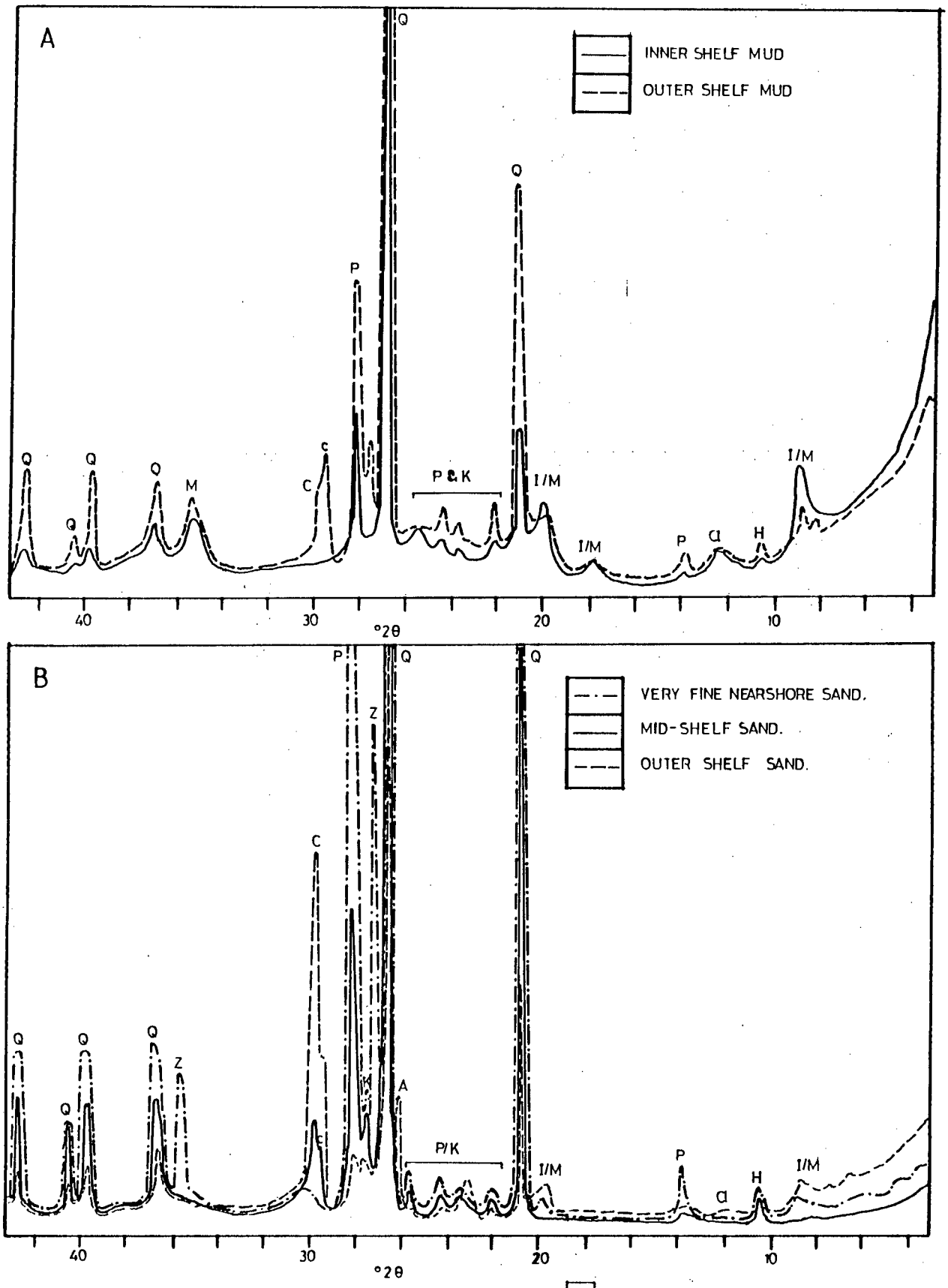

Figure 9-1. Sample X-ray diffractograms (A-inner and outer shelf muds; B-nearshore, mid-shelf, and outer shelf sands).

TABLE 9-1 : QUALITATIVE MINERALOGY OF THE TUGELA RIVER AND ADJACENT CONTINENTAL SHELF SEDIMENTS.

M-Major m-Minor t-Trace
P-Plagioclase feldspar K- K-feldspar I-Illite
C-Chlorite ML- Mixed-layer clays H-High-magnesian calcite L-Low-magnesian calcite

SAMPLE	QUARTZ	FELDSPARS	CLAYS	CALCITE	ARAGONITE	HORNBLENDE	MAGNETITE	PYRITE	ZIRCON
RIVER									
TR1RB	M	M P>K	m I>C,ML	t	-	t	-	-	-
TR2RB	M	M P>K	m I>C,ML	-	-	t	-	-	-
TR3RB	M	M K>P	t	-	-	m	-	-	-
TR3CR	M	M P~K	t	-	-	m	t	-	-
TR3LB	M	M P~K	t	-	-	m	m	-	-
TR4RB	M	M K>P	t	-	-	M	-	-	-
TR4CR	M	M P>K	t	-	-	m	-	-	-
TR4LB	M	M P>K	t	-	-	m	t	-	-
TR5RB	M	M K>P	t	-	-	m	t	t	-
INNER MUDS									
TM002	M	m P>K	M I>C,ML	t?	-	-	-	-	-
TM003	M	m P	M I>C,ML	t?	-	t	-	-	-
TM004	M	m P	M I>C,ML	t?	-	-	-	-	-
TM005	M	M P>K	m I>C,ML	t	-	-	-	-	-
TM006	M	M P>K	m I>C,ML	t	-	-	-	-	-
TM007	M	M P>K	m I~C,ML	t	-	m	-	-	-
TM008	M	M K>P	m I~C,ML	t	-	m	-	-	-
TM009	M	M P>K	m I>C,ML	m L	-	t	-	-	-
TM011	M	M P>K	M I>C,ML	t	-	-	-	-	-
TM012	M	M P>K	M I>C,ML	t	-	-	-	-	-
TM013	M	m K>P	M I>C,ML	t	-	-	-	-	-
TM015	M	m K>P	M I>C,ML	-	-	m	-	t	-
TM021	M	m P~K	M I>C,ML	M H>L	-	t	-	-	-
TM023	M	m P>K	M I>C,ML	M L>H	-	-	-	t	-
TM025	M	m P	m I>C,ML	M L>H	-	-	-	t	-

SAMPLE	QUARTZ	FELDSPARS	CLAYS	CALCITE	ARAGONITE	HORNBLENDE	MAGNETITE	PYRITE	ZIRCON
TM026	M	M P>K	m I>C,ML	m L>H	-	t	-	t	-
TM061	M	M K>P	t I>C,ML	m L>H	-	-	-	t	-
TM064	M	M K>P	m I>C,ML	-	-	t	-	-	-
TM065	M	M P>K	M I>C,ML	m L	-	t	-	-	-
TM068	M	M K>P	M I>C,ML	t	-	-	-	-	-
TM072	M	M P~K	M I>C,ML	-	-	m	-	t?	-
TM073	M	M K>P	M I>C,ML	t	-	t	-	t?	-
TM074	M	M P>K	M I>C,ML	-	-	t	-	-	-
TM075	M	m P>K	M I>C,ML	t?	-	m	-	-	-
TM076	M	M P>K	m I>C,ML	M L>H	-	t	-	-	-
TM078	M	M P>K	M I>C,ML	t	-	-	-	-	-
OUTER MUDS									
TM035	M	M K>P	t	m L>H	-	t	-	-	-
TM036	M	M K>P	m I>C,ML	M L>H	-	-	-	-	-
TM042	M	M K>P	t	M L>H	-	m	-	-	-
TM043	M	M K>P	t	m L>H	-	t	-	-	-
TM044	M	m P>K	m I>C,ML	M L>H	-	t	-	-	-
TM045	M	M P>K	m I>C,ML	m L	-	t	-	-	-
TM046	M	m P>K	t	M H>L	-	t	-	-	-
TM058	M	M P>K	m I>C,ML	m L>H	-	t	-	t	-
TM085	M	M P>K	m I>C,ML	m L	-	t	-	-	-
TM087	M	M P>K	m I>C,ML	m L>H	-	t	-	-	-
TM088	M	M P>K	m I>C,ML	m L>H	-	t	-	t	-
TM089	M	M P>K	t	m L	-	t	-	-	-
TM094	M	M K>P	t	m L	-	t	-	-	-
TM095	M	M K>P	t	m L>H	-	t	-	t?	-
TM096	M	M P>K	t	m H>L	-	t	-	t?	-
TM105	M	M P~K	t	M L>H	-	t	-	t	-

SAMPLE	QUARTZ	FELDSPARS	CLAYS	CALCITE	ARAGONITE	HORNBLENDE	MAGNETITE	PYRITE	ZIRCON
INNER SANDS									
TM010	M	M K>P	-	m L>H	-	m	-	-	-
TM014	M	M K>P	t	t	-	t	-	t?	-
TM016	M	M P>K	-	M H>L	-	t	-	-	-
TM017	M	M K>P	-	M H>L	-	t	-	-	-
TM018	M	m K>P	-	M H>L	-	t	-	-	-
TM019	M	M K>P	-	M L>H	-	t	-	-	-
TM020	M	M K>P	-	M L>H	-	-	-	t	-
TM022-1	M	M K>P	t	M H~L	-	t	-	-	-
TM022-2	M	M P~K	t	M L>H	-	-	-	-	-
TM024	M	M P>K	-	m H>L	-	t	-	t?	-
TM027	M	M P>K	-	m H	-	m	-	-	-
TM028	M	M P>K	t	m H>L	-	t	-	-	-
TM060	M	M K>P	-	m H>L	-	m	t?	-	-
TM062	M	M P>K	t	t	-	t	m	-	M
TM063	M	M P>K	t	t	-	t	t?	-	-
TM066	M	M P>K	t	M L>H	-	t	-	-	-
TM067	M	M K>P	-	m H>L	-	t	-	-	-
TM070	M	M P>K	t	t	-	M	t?	-	t
TM071	M	M P>K	t	t	-	m	t	-	-
TM077	M	M K>P	-	m L>H	-	t	-	-	-
TM079	M	M P>K	t	m L~H	-	M	t	t?	-
TM080	M	M K>P	t	m L~H	-	M	t?	t?	-
TM081	M	M P>K	-	m H	-	m	t?	-	-
TM098	M	M P~K	-	M L>H	-	t	-	-	-
TM099	M	m K>P	-	M L>H	-	t	-	-	-
OUTER SANDS									
TM029	M	M K>P	-	M H>L	-	t	-	-	-
TM030	M	m K~P	-	M H	t?	t	-	-	-

SAMPLE	QUARTZ	FELDSPARS	CLAYS	CALCITE	ARAGONITE	HORNBLENDE	MAGNETITE	PYRITE	ZIRCON
TM031	M	m P>K	t	M H>L	-	-	-	-	-
TM032	M	M P>K	t	M H~L	t?	t	-	-	-
TM033	M	M P>K	t	M H~L	-	-	-	-	-
TM034	M	M P>K	t	m H>L	-	t	-	-	-
TM037	M	m K>P	t	M L>H	t?	-	-	-	-
TM038	M	m K>P	-	M H>L	m	-	-	-	-
TM039	M	M K>P	-	M H>L	m	-	-	-	-
TM040	M	m K>P	t	M H>L	m	-	-	-	-
TM041	M	m K>P	t	M H>L	m	-	-	-	-
TM047	M	m K	t	M H>L	m	-	-	-	-
TM048	M	t	t	M H>L	m	-	-	-	-
TM051	M	M K>P	t	M L>H	t?	t	-	-	-
TM052	M	M P>K	t	m L~H	-	-	-	-	-
TM053	M	M P>K	t	M L>H	t	t	-	-	-
TM054	M	M K>P	t	m H>L	-	t	-	-	-
TM055	M	M P>K	t	m H>L	-	t	-	-	-
TM056	M	M P>K	t	m H>L	-	m	-	-	-
TM057	M	M K>P	-	m H>L	-	m	-	-	-
TM059	M	M P>K	-	M H>L	-	t	-	-	-
TM082	M	M K>P	t	m H>L	-	t	-	-	-
TM083	M	t	-	M H>L	m	t	-	-	-
TM084	M	M K>P	t	M H>L	t?	t	-	t	-
TM086	M	M P>K	t	M H>L	t?	t	-	t	-
TM090	M	m K>P	t	M H>L	m	-	-	-	-
TM091	M	m K>P	t	M L>H	t?	-	-	-	-
TM092	M	M P>K	t	M L>H	m	-	-	-	-
TM093	M	M P>K	t	M H>L	t	-	-	-	-
TM100	M	M P>K	t	m H>L	-	m	-	-	-
TM101	M	M K>P	-	M H>L	-	t	-	-	-

SAMPLE	QUARTZ	FELDSPARS	CLAYS	CALCITE	ARAGONJTE	HORNBLENDE	MAGNETITE	PYRITE	ZIRCON
TM102	M	m K>P	-	M H	m	t	-	t?	-
TM103	M	M P>K	t	m L>H	t?	t	-	-	-
TM104	M	M P>K	t	m L>H	t	t	-	-	-

muds, possibly due to dilution by the larger amounts of clay contained in the latter. The inner shelf sands are more quartz-rich than the outer shelf sands, undoubtedly due to the greater proportion of biogenic carbonate found in the outer shelf sediments. Windom (1976) suggested that the high concentrations of quartz found in sediments off the coast of South Africa are caused by both ice-rafting from Antarctica (most probably applicable further south from the study area) and transport of terrigenous material from the South African subcontinent by rivers and wind.

2.2 Feldspars

Feldspars were also found in all the sediments from the study area. Figure 9-2 shows the relative distribution of albitic plagioclase and orthoclase, the two major feldspars identified, and in which areas each is prevalent. Shepard (1963) found that where chemical weathering is not very intense, and/or where erosion is very rapid, feldspars may form a significant part of the sediments. As was discussed in chapter II section 3., the erosion rate within the Tugela River catchment is very high and this could explain the ubiquitous presence of feldspars in the sediments of the study area.

2.3 Clay Minerals

As the mineralogy of the clay fraction alone was not determined, identification of the clay minerals in the diffractograms may be somewhat inaccurate. Clay minerals must comprise more than $\pm$5% of the total sample in order to give

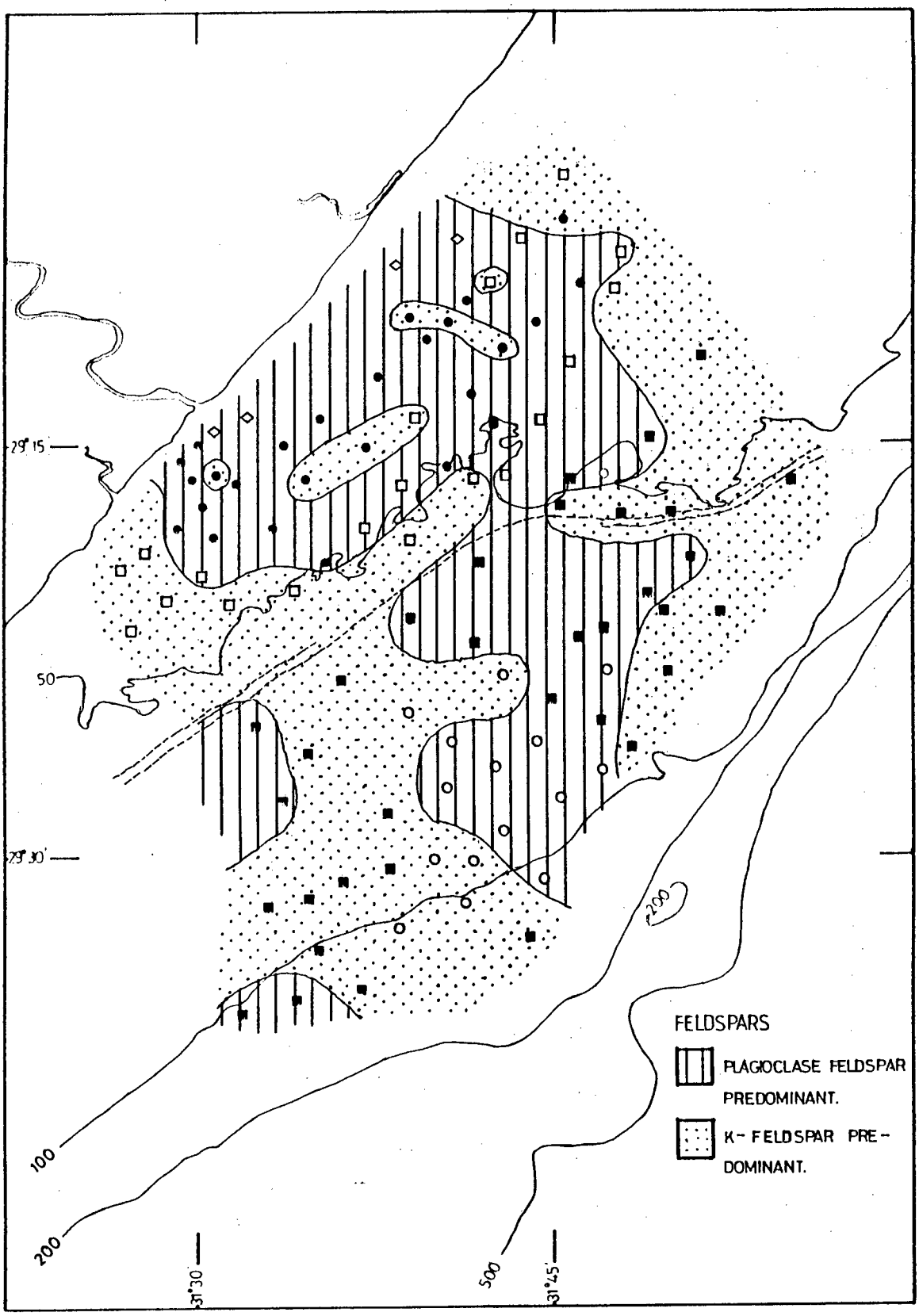

Figure 9-2. Relative distribution of feldspars.

rise to detectable peaks in bulk sediment analyses (Willis, pers. comm.). Those samples showing significant amounts of clay minerals are the estuarine and inner shelf mud samples. The outer shelf muds were found to contain lesser amounts of clay minerals. Trace amounts of clay were also recorded in the diffractograms of many inner and outer shelf sand samples, obviously dependent upon the amounts of mud present in these samples. The most abundant clay mineral found was illite. Lesser amounts of chlorite, kaolinite and mixed-layered clay were present although absolute identification of these minerals is impossible without heating and/or glycolation treatments (Carroll, 1970).

Illite is the most stable clay mineral in the marine environment (Degens, 1965). It is also the predominant clay mineral found in southwest Indian Ocean sediments (Windom, 1976). Most of the illite present in sedimentary environments comes from the alteration of potassium-bearing aluminosilicates such as micas and feldspars, though some of it may be formed by the chemical adsorption of potassium ions by montmorillonite (Mason, 1966). Kaolinite is also formed mainly by the breakdown of feldspars, but tends to favour an acid environment of formation in which all bases are removed in solution (Open University, 1978). The presence of both illite and kaolinite in the samples could be explained by the source of clay in the nearshore sediments being primarily the feldspars that make up almost 50% of the beach and river sands in the area (Maud, 1968). Chlorite usually is formed by physical weathering and is found mainly in the colder,

higher latitudes (Open University, 1978), thus it would be expected to be present in only small amounts, if at all, in the study area. Montmorillonite group minerals are formed mostly by the chemical weathering and alteration of basic rocks, both on continents and on the sea floor, their distribution thus being controlled by the distribution of basic rocks. Since the study area, including the catchment of the Tugela River, does not contain basic rocks, the presence of montmorillonite is not expected. However, it could be found in the study area combined with illite in a mixed-layered clay, and peaks indicating the presence of mixed-layered clay were found in the diffractograms of several samples.

2.4 Carbonate Minerals

The concentration of carbonate minerals in the sediments increases with distance from shore. The carbonate mineral content of sand samples on the mid- and outer shelf show high-magnesian calcite to be predominant over low-magnesian calcite. Aragonite, in trace and very minor amounts, is present only in the outer shelf sands, mostly in those along the shelf break. The outer shelf mud samples generally have more calcite than the inner shelf muds, with most of the samples from the latter group containing only trace amounts. It is interesting to note that low-magnesian calcite is the dominant species in the muds.

Siesser (1970) states that the sequence of decreasing carbonate mineral stability is low-magnesian calcite, aragonite, high-magnesian calcite. High-magnesian calcite and aragonite tend to undergo diagenesis in the marine environ-

ment, although their presence in relict sediments could simply be due to the addition of Recent skeletal material that has never been subaerially exposed, and hence not been leached of magnesium (Siesser, 1970). Leeder (1982) considers the presence of high-magnesian calcite and aragonite to be indicative of a low sediment deposition rate that does not permit burial diagenesis which would result in a change to low-magnesian calcite. Organisms extract proportionally more magnesium from warmer waters (Siesser, 1971), and, as discussed in chapter X, section 3.1.5, this mechanism appears to be a major sink for magnesium in the study area. Strontium preferentially substitutes in aragonitic skeletons over calcitic ones, and the distribution of strontium (fig. 10-26) closely follows that of aragonite (fig. 9-3).

2.5 Heavy Minerals

Hornblende was the major heavy mineral identified in the diffractograms and is more prevalent in the nearshore sediments than the outer shelf sediments, although trace amounts of hornblende were found in the outer shelf muds. Zircon was found to be present in two of the very fine nearshore sand samples. Trace amounts of magnetite were tentatively identified in the diffractograms of some of the inner shelf sands. In an investigation by Fromme (1977) of heavy minerals present along the Natal coast, magnetite was found to be the major constituent of the heavy mineral suite of the beach, surfzone and estuary sands. Fromme also identified several other heavy minerals present in the sands, the most frequently observed being ilmenite, hornblende, zircon, tourmaline and

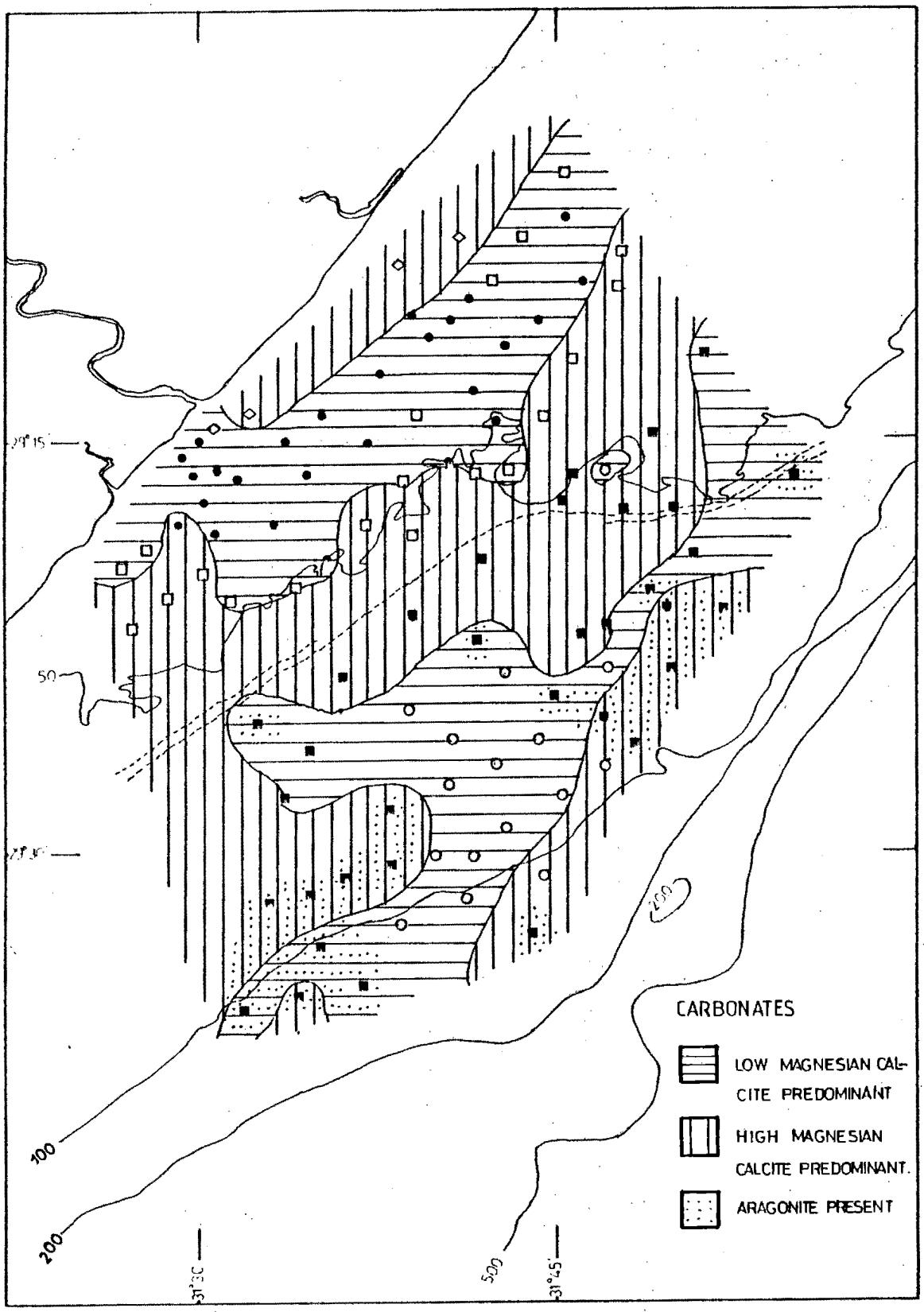

Figure 9-3. Relative distribution of carbonates.

rutile. He considered the total area of the Tugela River Mouth and the northeast-extending sand spit across the mouth to be a single source area for heavy minerals, with the mouth itself supplying fresh sediment by perennial discharge and the sand spit occasionally supplying sediment by wave-induced erosion. Fromme concluded that the distribution of heavy minerals in the vicinity of the Tugela River Mouth is due to the dominant northeast-flowing nearshore current, a result confirmed by this study.

2.6 Pyrite

Several mud samples and a few sand samples in the study area appear to contain trace amounts of pyrite. Pyrite usually forms by diagenetic sulphate reduction in the subsurface anoxic zone of muds (Leeder, 1982). It is possible that monosulphides are forming in the organic-rich muds off the mouth of the Tugela River. A relatively small amount of monosulphide imparts a black colouration to a sediment (Calvert, 1976), and, as described in Appendix A, Table A-2, the muds in this area are distinctively black. Monosulphides are the precursors to pyrite formation. Pyrite tends to impart a grey colour to sediments, and some pyrite was observed in a few of the grey outer shelf mud samples. Further speculation on the forms of iron sulphide present in the sediments, and to what extent they are present in the samples, is unwarranted in the absence of more detailed mineralogical and microscopic investigation.

3. Mineralogy of the Estuarine and River Sediments

The estuarine muds contain greater amounts of clay minerals than do the river sediments, as would be expected from the depositional processes known to occur in estuaries (see discussion in chap. X, section 4.). The proportions of quartz, feldspars and heavy minerals appear to increase upstream from the mouth. Magnetite and hornblende seem to be the most common heavy minerals in the river sediments, but as the X-ray diffractograms covered only a limited range of interplanar spacings (29.45 - 2.10), positive identification of other heavy minerals that diffract at higher 2θ angles was not possible.

4. Discussion and Conclusions

The qualitative mineralogy determined in this study supports the conclusions arrived at in the sedimentological discussions (chap. VIII, section 4.). The presence of quartz as the major mineral constituent of all the sediments in the study area substantiates the classification of these sediments as terrigenous. The carbonate minerals, with their increasing concentrations offshore, would appear indicative of little present-day deposition of terrigenous material occurring on the outer shelf, a supposition supported by the increasing high-magnesian calcite and aragonite contents near the shelf break. The dune ridge discussed in chapter VIII has been established as a Pleistocene shoreline, behind which the Tugela River once had a presumably large estuary. It is possible that this estuary trapped most of the clay supplied in the suspended load of the river as it flocculated

in the mixing fresh and saline waters in the estuary. As there is only a small estuary in existence today, it is unlikely that it is behaving similarly as a sink for the clay particles. This could explain why the present-day outer shelf mud belt contains more quartz and less clay than the inner shelf mud belt. The lack of clay in the outer shelf muds could also be accounted for by alteration and/or the winnowing action of the Agulhas Current.

Thus, the mineralogical evidence acquired in this study, like the sedimentological model presented in chapter VIII, supports the suggestions that the inner shelf mud belt is the present-day depocentre for some of the suspended material discharged from the Tugela River, and the mid- to outer shelf region is an area of predominantly relict sediment, where little or no Recent sedimentation is occurring outside of a minor biogenic carbonate input.

CHAPTER X GEOCHEMISTRY

1. Introduction

Chemical analyses, consisting of the determination of ten major elements (as oxides) and twenty-three minor and trace elements by XRFS, were performed on all samples. The samples were analysed for other trace elements as well, namely Mo, Se, Ge, Bi and W, but as the concentrations of these elements were generally below the lower limits of detection, they were excluded from the data table (Table 6-1) and not used in the geochemical interpretation. Analyses of CO_2 and organic matter, which together with H_2O+ comprised the loss on ignition (cf. chap. V, section 3.1), were also done on all samples.

The geochemical analyses were performed in order to determine the relationships that exist between variables and between samples in the study area. As it was not known which elements would prove useful in distinguishing between the inner and outer shelf muds, as many elements as possible were analysed. Detailed geochemistry of continental shelf sediments has not previously been done for bulk sediments off the southeast African coast; only specific analysis of glauconite (Birch, 1975), phosphorite and related sediments (Summerhayes, 1972b; Bremner, 1975), and carbonate minerals (Siesser, 1971) in other areas along the South African coast have been performed. It is believed that this baseline study will prove useful in determining future avenues of research in this region.

Interpretation of geochemical data on unconsolidated sediments has been found in the past to be a difficult, but not insurmountable, task, as evidenced in the reports of Hirst (1962a & b), Spencer et al. (1968), and Cook and Mayo (1980). Several techniques, predominantly of a statistical nature, have been used to help elucidate elemental relationships in a variety of depositional environments. This study uses several such statistical methods, as well as descriptions of the distributions of the elements, to arrive at a geochemical model of sedimentation in the area. The primary focus of the study was to determine whether a distinction between the inner shelf and outer shelf mud belts could be made. Thus, most of the discussion in the following section (2.) pertains only to the mud samples. Mention of the sand samples is made where relevant, but as the majority are of a quartzitic, terrigenous nature, they are considered to be essentially chemically inert. Exceptions are found in those samples containing notable amounts of heavy minerals and carbonate minerals, and will be dealt with as necessary.

Distributions and geochemical aspects of the analysed elements are discussed in section 3.. These are considered in two parts, the major elements and the minor and trace elements. Where possible, these distributions are related to the known mineralogy and the results of the statistical analysis. The geochemistry of the estuarine and river samples is discussed in section 4.. This is followed by a geochemical model of sedimentation derived from the geochemical data taken in conjunction with the sedimentological and

mineralogical results presented in chapters VIII and IX.

2. Statistical Analyses

The field of multivariate statistics has been widely applied to geological and geochemical problems. Good reviews of statistical techniques and applications may be found in Davis (1973) and Le Maitre (1982). A number of tests are available, although all are not necessarily applicable to any given problem. The validity of several statistical tests for specialised scientific studies has often been considered controversial, but if these tests are used with discernment there appears to be no question as to their usefulness in aiding the solving of problems comprised of several variables and numerous samples (Spencer et al., 1968). It should be noted that there are significant problems with closure in statistical tests any time a constant sum is used, viz. percentages that must add up to 100 (Davis, 1973). As no completely satisfactory method has yet been developed for dealing with this problem, it is mentioned here only as a cautionary note. The statistical tests used in this study were applied using the programs contained in the BMDP Statistical Software package (Dixon (ed.), 1981), which were found to be adequate for the needs of this project. The names of each program used may be found in the heading of the corresponding section. An initial statistical evaluation of the data was done to ascertain the nature of the frequency distributions of the variables, both for all the samples combined and separately for the two mud belts. Examples of some of the resulting histograms are given in Appendix C.

2.1 Statistics to Distinguish between the Inner and Outer Shelf Mud Groups

Statistical tests were done for both the concentrations of variables as found in the samples and on data that were recalculated on a carbonate-free basis. As the inner and outer shelf sediments vary considerably in carbonate content, it was felt that the dilution by carbonate in the outer shelf samples might mask true similarities or differences in the concentrations of other elements in the sediments. Although this procedure of recalculation is somewhat questionable in that many ions are not located entirely in either the terrigenous or carbonate fractions, it is useful for those elements likely to be concentrated in the terrigenous fraction (Cook and Mayo, 1980). As the primary objective of this examination was to see if a geochemical difference exists between the inner and outer shelf mud groups, and the average carbonate content of these two groups differs only by $\pm$4%, it will be shown that this dilution was not the sole cause of the geochemical differences found to exist between the two depositional areas.

2.1.1 Cluster Analysis (P2M)

The first statistical test used to distinguish between the two mud belts, as well as the other sediment groups present in the study area, was that of cluster analysis. This test forms clusters based on the Euclidean distance measure (the square root of the sum of squares of the differences between the values of the variables for two cases), initially considering each case as a separate cluster. Cluster

analysis was originally performed using all the major and trace element data and the textural data to confirm the grouping of samples that was done on the basis of textural analysis (after Shepard, 1954) combined with position on the shelf. The resulting dendrogram (fig. 10-1) shows a fairly well-defined distinction between the inner and outer mud groups, but little delineation between the sands. Definition of the sand groups (i.e. inner and outer shelf) was not expected as they have been found to consist of mixed populations (cf. chap. VIII). Subsequent clusters were formed using only the chemical data and only the textural data for all samples. As shown in figures 10-2 and 10-3, separation of the two mud belts was not achieved using either set of data alone. This test emphasizes the need for the combined usage of chemical data and textural data in classifying sediments and defining sedimentary transport dynamics (Holmes, 1982).

Cluster analysis is useful for an initial investigation of data and for objectively determining the grouping of samples previously determined on the basis of location combined with textural data for the mud samples. As the mud samples are of primary concern to this project, the cluster analysis provided a sound basis on which to continue further statistical analyses that require the samples to be arranged in groups.

2.1.2 Stepwise Discriminant Function Analysis (P7M)

Stepwise discriminant function analysis was used to

Figure 10-1. The results of cluster analysis using both chemical and textural variables.

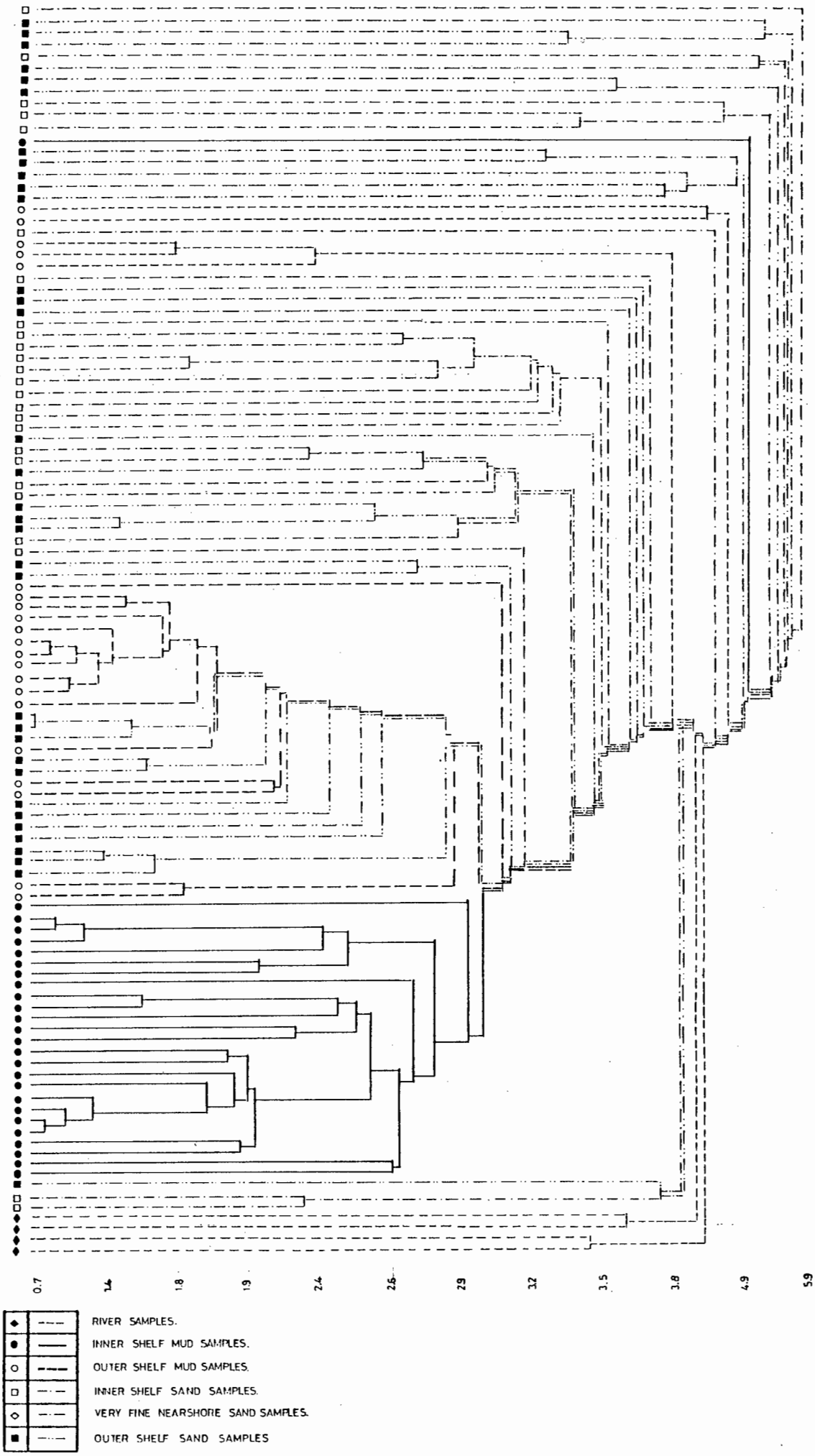

Figure 10-2. The results of cluster analysis using chemical data only.

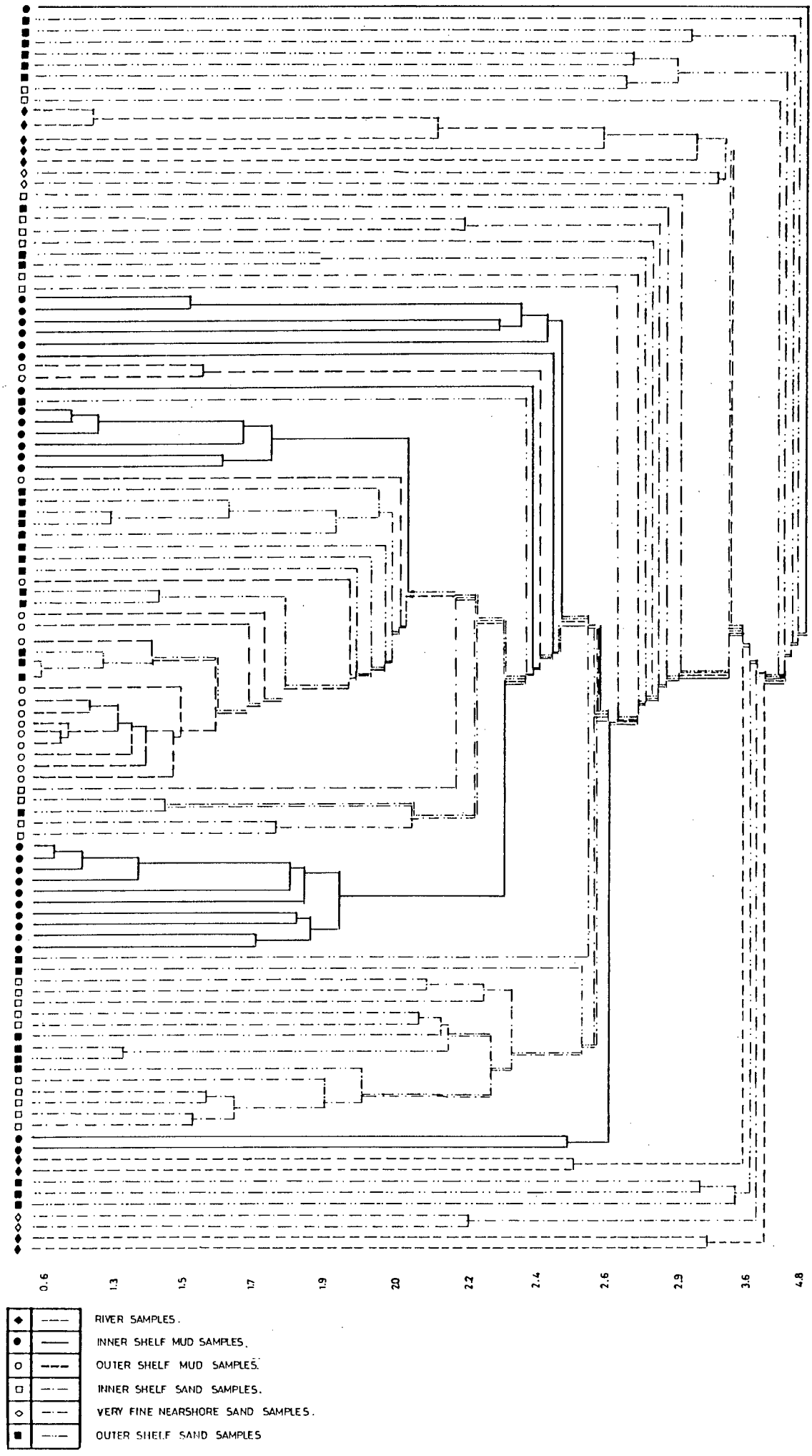

Figure 10-3. The results of cluster analysis using textural data only.

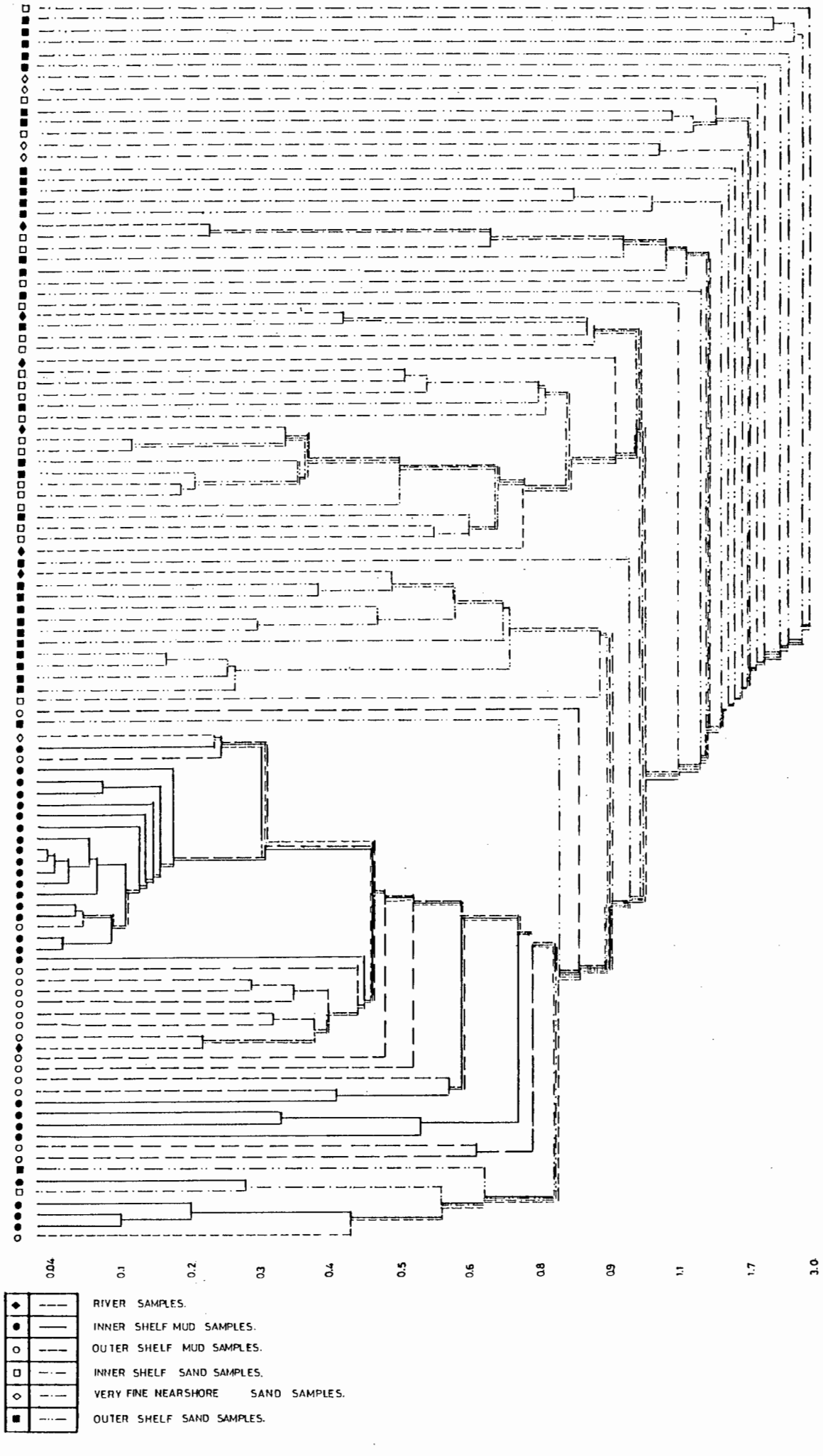

identify which variables are most effective in distinguishing between the sedimentary groups. Discriminant analysis assumes normality and independence of the variables, and although many of the variables in this study do not approach normal or lognormal distributions (cf. Appendix C), and several of the variables are not independent (section 2.2.2) it is still useful in determining if groups are distinct and if the samples are correctly classified in the groups.

The analysis operates by the entering and removing of variables on the basis of their F-scores, which account for the variance of the variable between groups. All samples were found to be correctly classified into the previously defined groups. The discriminant analysis was run several times in order to distinguish between all five sedimentary groups; between the river, inner and outer shelf mud groups; and between just the inner and outer shelf mud groups. Both the data as found and corrected on a carbonate-free basis were used. The discriminatory variables selected in distinguishing between all the groups were Rb, Br, Ba, K_2O and SiO_2. The plot given in the results of this analysis is shown in figure 10-4. Once again the mud groups are fairly well separated, but the sands are mixed. Ba, As and the ratio Fe/Al were the discriminatory variables in distinguishing between the river samples and the inner and outer shelf mud groups. The discriminatory variables selected to distinguish between the inner and outer shelf muds were Fe/Al, K/Al and Al_2O_3 for the original data (all variables given), and Ba and As for the carbonate-free data (trace elements

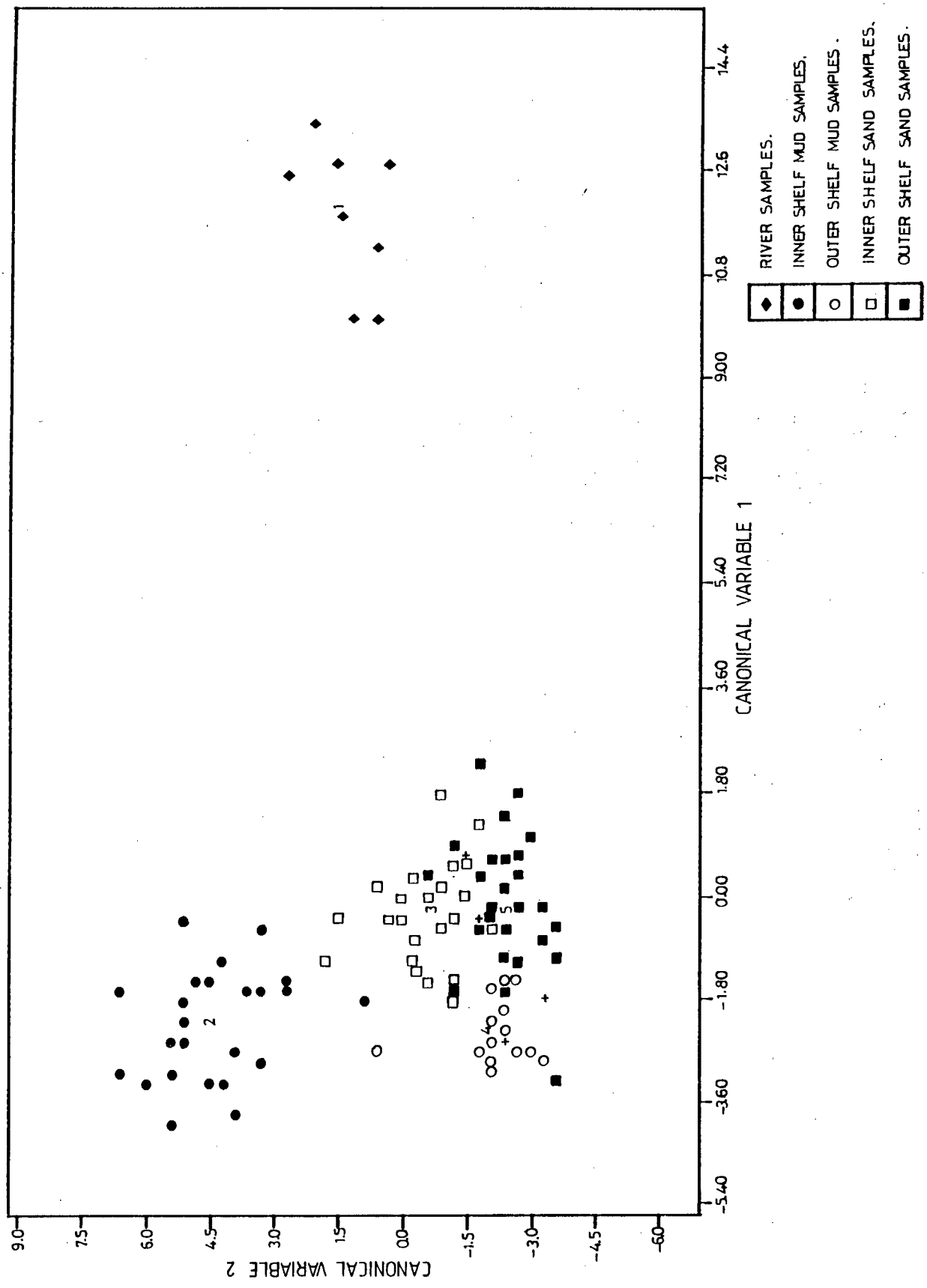

Figure 10-4. Plot of the results of discriminant function analysis using chemical variables (original data) for all samples.

only given). These choices appear to indicate that the elements associated with the clay minerals are the most discriminatory variables in almost all the analyses (cf. sections 2.2.2 and 3.1.3). The choice of Ba as a discriminatory variable is discussed in section 3.2.12.

The mid-shelf mud sample (TM058) discussed in chapter VIII, section 2.7 was found to consistently classify with the outer shelf mud group. As this sample lies inside of the reworked Pleistocene dune ridge (cf. fig. 6-2), it could possibly be an exposure of the mud deposited in the paleo-estuary of the Tugela River during the Pleistocene. As stated in chapter VIII, section 4., piston cores or vibro-cores would be the only way to conclusively support this supposition.

2.1.3 Mann-Whitney U-Tests (P3S)

The Mann-Whitney U-test is the non-parametric equivalent of Student's T-test, and is used to determine if two groups of samples are derived from the same population. The U-test is performed on a ranking of the variables (in order of increasing values) as opposed to the actual values of the variables themselves, and does not require an assumption of normality. The null hypothesis of this test is that the two groups tested have the same distribution (Siegel, 1956). This test was run only on the chemical variables, both as found in the sediment and corrected on a carbonate-free basis, in order to determine whether a purely statistical difference exists between the two mud groups. The results are given in

Table 10-1. Values were chosen to be significant at the 99% confidence level, i.e. if the level of significance (level of significance = 1 - confidence level) of a variable was found to be <0.01, the null hypothesis was rejected in favour of the conclusion that the two populations are different. As can be seen in Table 10-1, the majority (89% for the original data, 66% for the data on a carbonate-free basis) of variables are shown to be statistically different for both sets of data. The outer shelf mud has lower concentrations of all the variables except SiO_2, CaO, Na_2O, CO_2, Sr, Zr and Br compared to the inner shelf mud; the correction on a carbonate-free basis does not change the trend for any variable except MgO, which then shows a higher value in the outer mud group than in the inner mud group.

The Mann-Whitney U-test has 95% of the power efficiency of Student's T-test, and as such is one of the most powerful non-parametric tests. Therefore, since a sufficient number of samples is present in both mud groups (inner mud 26, outer mud 16), there appears to be little doubt as to the conclusion that the two mud groups are geochemically different. In the subsequent discussions of elemental distributions and relationships (section 3.), further evidence is proffered to substantiate this conclusion.

2.2 Statistics to Elucidate Geochemical Relationships

2.2.1 Spearman Rank Correlation Coefficients (P3S)

The Spearman rank correlation coefficients (r_s) were determined for all the variables in all samples, as well as

TABLE 10-1 : MANN-WHITNEY U-TEST RESULTS FOR THE INNER AND OUTER SHELF MUD BELTS, USING BOTH THE DATA AS FOUND IN THE SEDIMENTS AND DATA CORRECTED ON A CARBONATE-FREE BASIS. (D - Different at the 99% confidence level; S - Same at the 99% confidence level).

	INNER MUD BELT				OUTER MUD BELT				LEVEL OF SIGNIFICANCE			
			CARBONATE FREE				CARBONATE FREE					
VARIABLE	Mean	Co.Var.	Mean	Co.Var.	Mean	Co.Var.	Mean	Co.Var.	Original	Carbonate free	ORIGINAL	CARBONATE-FREE
SiO_2	58.81%	0.071	60.97%	-	59.98%	0.058	66.96%	-	.3647	.0002	S	D
TiO_2	0.88	0.120	0.91	-	0.81	0.074	0.90	-	.0038	.0659	D	S
Al_2O_3	16.60	0.168	17.15	-	12.59	0.106	14.04	-	.0000	.0007	D	D
Fe_2O_3	7.27	0.152	7.52	-	5.57	0.109	6.22	-	.0000	.0002	D	D
MnO	0.08	0.192	0.09	-	0.06	0.105	0.07	-	.0000	.0000	D	D
MgO	1.59	0.085	1.65	-	1.58	0.079	1.77	-	.3573	.1330	S	S
CaO	2.08	0.747	-	-	6.27	0.402	-	-	.0000	-	D	-
Na_2O	0.85	0.164	0.88	-	1.02	0.107	1.14	-	.0001	.0000	D	D
K_2O	2.25	0.118	2.32	-	1.95	0.077	2.18	-	.0015	.0316	D	S
P_2O_5	0.13	0.128	0.14	-	0.12	0.119	0.13	-	.0039	.2044	D	S
CO_2	1.51	0.715	-	-	4.57	0.468	-	-	.0000	-	D	-
H_2O+	5.38	0.228	5.55	-	3.55	0.183	3.96	-	.0000	.0001	D	D
Org.M	2.35	0.277	2.43	-	1.55	0.204	1.73	-	.0000	.0002	D	D
S	2103ppm	0.448	2185ppm	0.451	1542ppm	0.253	1728ppm	0.262	.0198	.1202	S	S
Rb	117	0.161	121	0.148	96	0.104	108	0.081	.0012	.0172	D	S
Sr	145	0.379	-	-	333	0.345	-	-	.0000	-	D	-
Y	30	0.145	31	0.126	22	0.080	25	0.062	.0000	.0000	D	D
Zr	226	0.237	233	0.231	292	0.140	327	0.141	.0001	.0000	D	D
Nb	15	0.148	16	0.132	13	0.103	15	0.063	.0012	.0120	D	S
U	3.1	0.238	3.2	0.243	3.0	0.214	3.4	0.232	.8968	.3785	S	S
Th	14	0.115	14	0.105	12	0.077	14	0.086	.0015	.1543	D	S
Pb	24	0.133	25	0.121	21	0.083	24	0.076	.0053	.1083	D	S
Zn	80	0.181	82	0.167	56	0.136	63	0.109	.0000	.0000	D	D
Cu	36	0.247	37	0.231	19	0.163	22	0.146	.0000	.0000	D	D
Ni	58	0.191	60	0.176	43	0.138	48	0.119	.0000	.0005	D	D
Co	27	0.123	28	0.105	19	0.092	21	0.070	.0000	.0000	D	D
Cr	152	0.122	157	0.109	134	0.092	150	0.776	.0022	.1083	D	S
V	128	0.148	132	0.133	93	0.112	104	0.092	.0000	.0000	D	D
Ba	462	0.123	477	0.103	393	0.100	437	0.055	.0003	.0034	D	D
Sc	23	0.146	23	0.139	18	0.090	21	0.087	.0001	.0065	D	D
Br	22	0.512	22	0.525	45	0.187	51	0.185	.0000	.0000	D	D
Ga	20	0.178	21	0.165	15	0.129	16	0.103	.0000	.0002	D	D
La	38	0.139	39	0.125	25	0.123	28	0.113	.0000	.0000	D	D
Ce	84	0.115	87	0.106	62	0.102	69	0.088	.0000	.0000	D	D
Nd	42	0.129	44	0.113	30	0.116	33	0.110	.0000	.0000	D	D
As	14	0.215	14	0.218	11	0.178	12	0.173	.0010	.0172	D	S

for all the variables in each of the sedimentary groups (viz. river, inner muds, inner sands, outer muds, outer sands) except for the two estuarine samples. The latter samples do not constitute a statistically significant group as the standard deviation of one or more variables is equal to zero. The Spearman rank correlation is a non-parametric test with 91% of the efficiency of the parametric Pearson's r correlation, and was used because of the sensitivity of the Pearson's test to non-normality of data. The results for all samples together are shown in Table 10-2, the correlation coefficients determined by Pearson's test are shown in Table 10-3 for comparison. The results for the individual groups are presented in Tables 10-4 to 10-8. Only results significant at the 95% confidence level are shown in the tables, with values significant at the 99% confidence level underlined. Values of significance for the number of samples in each separate group are given in the corresponding tables. These correlations are discussed where applicable in section 3..

2.2.2 R-Mode Factor Analysis (P4M)

R-mode factor analysis is so-called because it uses the Pearson's r correlation coefficient to determine factors which account for the preponderance of variation between variables. These factors are then rotated orthogonally to emphasize (maximize) loadings on the major factors determined. Factor analysis is considered by many to be a useful method of interpretation in geology as it can consolidate a large number of variables into a workable number of mathematical factors (Spencer, 1966; Spencer et al., 1968; Summerhayes, 1972a).

TABLE 10-2 : SPEARMAN RANK CORRELATION COEFFICIENTS FOR ALL SAMPLES COMBINED.
Only values significant at the 95% confidence level are shown (>.306).
Values significant at the 99% confidence level (>.432) are underlined.

	SiO_2	TiO_2	Al_2O_3	Fe_2O_3	MnO	MgO	CaO	Na_2O	K_2O	P_2O_5
SiO_2	1.000									
TiO_2		1.000								
Al_2O_3	-.359	.894	1.000							
Fe_2O_3	-.353	.849	.947	1.000						
MnO					1.000					
MgO	-.552					1.000				
CaO		-.748	-.719	-.708	-.525	-.313	1.000			
Na_2O	.702							1.000		
K_2O		.841	.906	.813			-.694		1.000	
P_2O_5	-.620	.613	.750	.764		.343	-.347	-.415	.653	1.000
CO_2	-.329	-.698	-.633	-.641	-.528		.976	-.327	-.601	
H_2O+	-.655	.691	.870	.846			-.420	-.406	.742	.830
Org.M	-.569	.723	.901	.853			-.525	-.317	.768	.763
S	-.786		.313			.332		-.573		.466
Rb	-.431	.849	.966	.889			-.625		.939	.760
Sr		-.704	-.672	-.694	-.579		.977		-.643	-.347
Y		.964	.915	.853			-.736		.838	.660
Zr		.605	.357					.443	.376	
Nb		.977	.927	.862			-.737		.887	.668
U	-.369	.782	.752	.692			-.491		.713	.595
Th	-.415	.910	.881	.814			-.617		.830	.679
Pb	-.426	.749	.860	.846			-.608		.812	.761
Zn	-.399	.886	.988	.957			-.699		.864	.767
Cu	-.356	.860	.976	.947			-.731		.840	.713
Ni	-.313	.873	.972	.962			-.757		.834	.715
Co		.859	.926	.942	.372		-.842		.793	.629
Cr		.853	.764	.837	.462		-.773		.651	.541
V		.901	.922	.953	.410		-.820		.806	.680
Ba		.743	.677	.603	.368	-.399	-.856		.771	.281
Sc	-.365	.864	.963	.954			-.674		.828	.757
Br	-.660	.338	.519	.498	-.405	.334			.418	.617
Ga	-.397	.878	.993	.949			-.685		.893	.772
La	-.311	.922	.930	.853			-.715		.857	.704
Ce	-.404	.913	.927	.864			-.652		.854	.746
Nd	-.392	.922	.921	.853			-.668		.839	.724
As	-.346				.311	.463		-.369	.082	.369
Gravel		-.652	-.574	-.510	-.306		.730		-.569	
VCS		-.406	-.353	-.299			.394		-.329	
CS		-.794	-.734	-.616			.595		-.734	-.453
MS	.340	-.802	-.736	-.639			.465		-.795	-.570
FS			-.313	-.368	-.404		.336		-.387	-.391
VFS		.548	.433	.307	-.337			.336	.434	
Mud	-.485	.870	.970	.914			-.618		.886	.797

	CO_2	H_2O+	Org.M	S	Rb	Sr	Y	Zr	Nb	U
CO_2	1.000									
H_2O+		1.000								
Org.M	-.414	.879	1.000							
S	.327	.575	.539	1.000						
Rb	-.521	.873	.889	.406	1.000					
Sr	.957	-.393	-.475		-.570	1.000				
Y	-.665	.758	.784		.874	-.690	1.000			
Zr					.347		.512	1.000		
Nb	-.666	.754	.781		.904	-.691	.964	.560	1.000	
U	-.432	.649	.670	.334	.765	-.455	.781	.404	.793	1.000
Th	-.532	.781	.790	.370	.829	-.571	.944	.443	.921	.824
Pb	-.509	.793	.817	.361	.868	-.569	.788		.784	.712
Zn	-.611	.885	.911	.351	.951	-.653	.912	.351	.918	.748
Cu	-.659	.858	.910		.921	-.688	.891	.315	.886	.714
Ni	-.690	.830	.891		.908	-.713	.888	.330	.889	.716
Co	-.785	.757	.813		.838	-.810	.877	.306	.864	.670
Cr	-.771	.541	.577		.666	-.782	.815	.387	.803	.642
V	-.772	.742	.787		.841	-.809	.906	.337	.889	.715
Ba	-.851	.343	.461		.626	-.812	.698	.423	.733	.502
Sc	-.592	.857	.874	.316	.914	-.645	.882	.343	.883	.715
Br		.665	.606	.609	.609		.348		.402	.490
Ga	-.594	.887	.905	.350	.970	-.639	.905	.340	.915	.746
La	-.630	.783	.826	.308	.904	-.673	.964	.437	.947	.765
Ce	-.557	.830	.853	.393	.919	-.614	.957	.420	.943	.790
Nd	-.580	.814	.843	.362	.901	-.624	.965	.435	.942	.774
As		.265		.333		-.008		-.442		
Gravel	.705		-.438		-.510	.669	-.632	-.412	-.640	-.430
VCS	.377				-.334	.324	-.403	-.383	-.409	
CS	.529	-.561	-.602		-.737	.508	-.795	-.520	-.813	-.665
MS	.401	-.617	-.597		-.771	.408	-.778	-.475	-.803	-.725
FS		-.364				.386				
VFS			.361		.469		.512	.665	.526	.496
Mud	-.520	.901	.921	.417	.967	-.563	.886	.365	.913	.769

	Th	Pb	Zn	Cu	Ni	Co	Cr	V	Ba	Sc
Th	1.000									
Pb	.795	1.000								
Zn	.879	.853	1.000							
Cu	.853	.833	.975	1.000						
Ni	.836	.848	.975	.983	1.000					
Co	.797	.792	.933	.949	.964	1.000				
Cr	.729	.678	.763	.763	.819	.840	1.000			
V	.831	.820	.919	.926	.954	.962	.925	1.000		
Ba	.607	.544	.615	.665	.669	.704	.662	.711	1.000	
Sc	.839	.843	.965	.946	.966	.920	.809	.936	.592	1.000
Br	.467	.535	.539	.462	.455			.314		.532
Ga	.880	.870	.989	.970	.967	.917	.754	.913	.632	.967
La	.930	.778	.925	.901	.890	.868	.755	.883	.679	.890
Ce	.946	.806	.928	.895	.884	.851	.743	.874	.610	.897
Nd	.948	.779	.923	.900	.884	.855	.743	.872	.633	.882
As	.006	.303								
Gravel	-.507	-.468	-.569	-.561	-.600	-.621	-.556	-.607	-.685	-.538
VCS	-.353		-.374	-.336	-.366	-.382		-.332	-.310	-.355
CS	-.758	-.597	-.733	-.673	-.687	-.659	-.534	-.645	-.577	-.691
MS	-.791	-.657	-.708	-.652	-.648	-.594	-.571	-.646	-.567	-.669
FS		-.405		-.313	-.325	-.328	-.349	-.383	-.307	
VFS	.532	.322	.430	.382	.367				.322	.353
Mud	.882	.860	.969	.942	.934	.868	.695	.865	.579	.931

	Br	Ga	La	Ce	Nd	As	Gravel	VCS	CS	MS
Br	1.000									
Ga	.556	1.000								
La	.384	.920	1.000							
Ce	.478	.925	.976	1.000						
Nd	.425	.914	.977	.986	1.000					
As						1.000				
Gravel		-.548	-.593	-.549	-.563		1.000			
VCS		-.350	-.403	-.382	-.389		.607	1.000		
CS	-.354	-.722	-.786	-.773	-.775		.681	.661	1.000	
MS	-.450	-.726	-.731	-.751	-.748		.458		.771	1.000
FS						-.495		-.371		
VFS	.423	.427	.459	.467	.485	-.444	-.392	-.431	-.647	-.658
Mud	.619	.970	.900	.922	.911		-.519	-.317	-.737	-.759

	FS	VFS	Mud
FS	1.000		
VFS	.356	1.000	
Mud	-.324	.457	1.000

TABLE 10-3 : PEARSON'S CORRELATION COEFFICIENTS FOR ALL SAMPLES COMBINED.
Only values significant at the 99% confidence level are shown.

	SiO_2	TiO_2	Al_2O_3	Fe_2O_3	MnO	MgO	CaO	Na_2O	K_2O	P_2O_5	CO_2	H_2O+	Org.M
SiO_2	1.000												
TiO_2		1.000											
Al_2O_3		.799	1.000										
Fe_2O_3		.784	.954	1.000									
MnO	.268			.256	1.000								
MgO	-.663					1.000							
CaO	-.652	-.640	-.607	-.599	-.341	.488	1.000						
Na_2O	.667	.277				-.316	-.422	1.000					
K_2O		.778	.921	.822			-.633		1.000				
P_2O_5	-.431	.582	.764	.780		.277	-.247	-.301	.696	1.000			
CO_2	-.681	-.621	-.569	-.573	-.354	.484	.994	-.458	-.593		1.000		
H_2O+	-.470	.600	.900	.865			-.316	-.436	.771	.788	-.293	1.000	
Org.M	-.382	.614	.867	.833			-.374	-.327	.734	.711	-.332	.846	1.000
S	-.671		.359	.289	-.274	.319	.259	-.486	.288	.416	.296	.527	.560
Rb	-.258	.764	.972	.896			-.537		.949	.770	-.495	.887	.831
Sr	-.674	-.592	-.567	-.570	-.374	.487	.988	-.403	-.595		.986	-.290	-.330
Y		.935	.883	.837			-.588		.831	.642	-.554	.745	.742
Zr	.259	.631				-.236	-.277	.590			-.280		
Nb		.955	.910	.864			-.652		.884	.689	-.623	.747	.745
U		.791	.716	.665			-.394		.686	.571	-.371	.608	.584
Th		.909	.784	.736			-.429		.756	.605	-.396	.677	.660
Pb	-.295	.667	.858	.849	.238		-.429		.795	.750	-.397	.793	.770
Zn		.794	.990	.968			-.582		.882	.775	-.547	.907	.871
Cu		.710	.953	.934	.243		-.560	-.275	.815	.699	-.520	.891	.889
Ni		.772	.962	.967	.253		-.609		.814	.730	-.577	.864	.871
Co		.784	.924	.951	.324		-.686		.780	.650	-.659	.799	.827
Cr		.828	.713	.825	.416		-.651		.591	.516	-.650	.528	.541
V		.833	.936	.973	.356		-.668		.811	.699	-.642	.802	.791
Ba	.412	.682	.625	.568	.268	-.477	-.813	.372	.724	.272	-.793	.340	.443
Sc		.785	.961	.959			-.594		.835	.775	-.566	.866	.838
Br	-.480	.315	.434	.414	-.376	.265		-.240	.386	.563		.496	.446
Ga	-.236	.776	.994	.956			-.577		.908	.783	-.540	.913	.864
La		.870	.925	.870			-.580		.862	.707	-.539	.818	.817
Ce	-.251	.878	.928	.880			-.518		.860	.754	-.480	.844	.821
Nd	-.236	.881	.918	.869			-.523		.845	.713	-.484	.830	.819
As	-.361				.313	.418	.243	-.367		.338	.257		
Gravel	-.356	-.400	-.317	-.260		.245	.534		-.287		.521		
VCS		-.440	-.355	-.354			.430		-.241		.426	-.263	-.303
CS		-.618	-.577	-.499			.460		-.501	-.373	.433	-.469	-.513
MS	.334	-.694	-.682	-.618			.249		-.717	-.602	.321	-.601	-.587
FS	.251		-.329	-.324	-.281	-.212			-.331	-.301		-.365	-.280
VFS		.528				-.242		.632	.238		-.195		
Mud	-.313	.774	.968	.896			-.491		.897	.769	-.451	.898	.867

	S	Rb	Sr	Y	Zr	Nb	U	Th	Pb	Zn	Cu	Ni	Co
S	1.000												
Rb	.439	1.000											
Sr	.292	-.494	1.000										
Y	.253	.837	-.544	1.000									
Zr			-.248	.479	1.000								
Nb	.241	.892	-.603	.944	.435	1.000							
U	.331	.735	-.351	.761	.433	.796	1.000						
Th	.333	.791	-.380	.915	.571	.889	.828	1.000					
Pb	.400	.864	-.407	.746		.767	.658	.698	1.000				
Zn	.380	.956	-.542	.877		.901	.704	.780	.856	1.000			
Cu	.321	.881	-.525	.848		.824	.603	.710	.798	.951	1.000		
Ni	.268	.887	-.568	.854		.865	.644	.731	.827	.965	.975	1.000	
Co		.831	-.650	.858		.853	.619	.714	.783	.933	.947	.967	1.000
Cr		.613	-.628	.763	.361	.766	.591	.684	.629	.731	.700	.792	.815
V		.856	-.636	.888		.878	.669	.764	.822	.941	.934	.965	.970
Ba		.562	-.781	.678	.377	.688	.428	.526	.471	.569	.620	.629	.671
Sc	.327	.916	-.557	.839		.876	.688	.745	.837	.962	.924	.962	.922
Br	.487	.539				.408	.477	.401	.478	.437	.273	.359	
Ga	.390	.975	-.539	.864		.895	.704	.775	.869	.992	.948	.957	.913
La	.365	.894	-.535	.958	.341	.924	.751	.888	.773	.925	.893	.883	.877
Ce	.423	.915	-.472	.940	.333	.937	.788	.909	.797	.931	.869	.875	.854
Nd	.376	.885	-.475	.960	.349	.927	.755	.907	.768	.921	.887	.881	.871
As	.252				-.390				.285				
Gravel		-.386	.531	-.361		-.410	-.278	-.264		-.327	-.287	-.327	-.351
VCS		-.322	.392	-.402		-.441	-.312	-.360	-.280	-.390	-.324	-.373	-.396
CS	-.249	-.578	.392	-.602	-.297	-.671	-.532	-.610	-.431	-.601	-.506	-.542	-.533
MS	-.347	-.714		-.680	-.316	-.726	-.670	-.699	-.595	-.650	-.561	-.586	-.536
FS		-.314			.258				-.367	-.289	-.356	-.326	-.297
VFS				.390	.779	.393	.381	.463					
Mud	.452	.968	-.446	.841		.901	.735	.781	.840	.955	.895	.907	.853

	Cr	V	Ba	Sc	Br	Ga	La	Ce	Nd	As	Gravel	VCS	CS
Cr	1.000												
V	.886	1.000											
Ba	.614	.665	1.000										
Sc	.777	.943	.556	1.000									
Br		.267		.471	1.000								
Ga	.703	.928	.580	.963	.465	1.000							
La	.705	.892	.627	.883	.285	.915	1.000						
Ce	.694	.876	.550	.896	.423	.924	.977	1.000					
Nd	.703	.883	.593	.872	.324	.907	.980	.983	1.000				
As			-.316							1.000			
Gravel	-.345	-.318	-.362	-.317		-.308	-.334	-.317	-.325	.342	1.000		
VCS	-.342	-.360		-.384		-.345	-.393	-.425	-.420		.552	1.000	
CS	-.342	-.479	-.339	-.558	-.381	1.568	-.626	-.651	-.636	.320	.508	.721	1.000
MS	-.489	-.587	-.421	-.643	-.522	-.671	-.651	-.703	-.677				.284
FS		-.331		-.273		-.327				-.450		-.277	-.332
VFS			.333				.235	.250	.255	-.423		-.230	-.359
Mud	.616	.857	.520	.920	.565	.964	.882	.912	.891		-.299	-.365	-.610

	MS	FS	VFS	Mud
MS	1.000			
FS		1.000		
VFS	-.451	.230	1.000	
Mud	-.715	-.333		1.000

TABLE 10-4 : SPEARMAN RANK CORRELATION COEFFICIENTS FOR THE RIVER SAMPLES.
Only values significant at the 95% confidence level (>.714) are shown.
Values significant at the 99% confidence level (>.893) are underlined.

	SiO_2	TiO_2	Al_2O_3	Fe_2O_3	MnO	MgO	CaO	Na_2O	K_2O	P_2O_5
SiO_2	1.000									
TiO_2	-.955	1.000								
Al_2O_3	-.928	.828	1.000							
Fe_2O_3		.810		1.000						
MnO				.778	1.000					
MgO				.928	.889	1.000				
CaO				.821	.963	.892	1.000			
Na_2O								1.000		
K_2O	-.714		.892						1.000	
P_2O_5	-.836		.854						.872	1.000
CO_2										
H_2O+	-.928	.846	.892						.750	.781
Org.M										
S			.750						.821	.818
Rb	-.714		.892						1.000	.872
Sr	-.785		.821						.857	.982
Y	.991	.936	.955						.756	.816
Zr	-.892	.756	.964						.857	.818
Nb	-.928	.846	.892						.750	.781
U										.790
Th	-.964	.882	.964						.821	.909
Pb			.785						.892	.727
Zn	-.991	.936	.900							.844
Cu	-.991	.936	.900							.844
Ni	-.982	.990	.872	.763						.750
Co	-.821	.882		.892		.821				
Cr				.964	.815	.964	.857			
V		.790		.991	.822	.955	.846			
Ba	-.714		.892						1.000	.872
Sc	-.954	.963	.785	.804						.733
Br	-.776		.896						.896	.852
Ga	-.964	.900	.857							.836
La	-.882	.736	.900						.882	.990
Ce	-.857		.964						.964	.927
Nd	-.774		.846						.900	.908
As										
Gravel										
VCS										
CS	.714		-.714						-.714	
MS	.785	-.774		-.750						
FS										
VFS	-.892	.774	.857						.714	.745
Mud	-.892	.756	.928						.892	.982

	CO_2	H_2O+	Org.M	S	Rb	Sr	Y	Zr	Nb	U
CO_2	1.000									
H_2O+		1.000								
Org.M	.821		1.000							
S	.750	.714	.714	1.000						
Rb		.750		.821	1.000					
Sr				.750	.857	1.000				
Y		.955			.756	.756	1.000			
Zr		.857			.857	.785	.919	1.000		
Nb		1.000		.714	.750		.955	.857	1.000	
U						.879				1.000
Th		.857		.714	.821	.892	.955	.928	.857	
Pb	.857		.750	.785	.892	.750		.750		
Zn		.955				.774	.981	.864	.955	
Cu		.955				.774	.981	.864	.955	
Ni		.872				.709	.963	.818	.872	
Co		.750					.774		.750	
Cr										
V										
Ba		.750		.821	1.000	.857	.756	.857	.750	
Sc		.879					.925	.729	.879	
Br					.896	.896	.783	.836		.841
Ga		.964				.750	.955	.821	.964	
La		.846		.846	.882	.955	.872	.864	.846	.717
Ce		.857		.857	.964	.892	.882	.928	.857	
Nd		.864		.937	.900	.828	.800	.792	.864	
As										
Gravel										
VCS										
CS		-.892			-.714		-.756	-.750	-.892	
MS						-.714	-.720			-.767
FS		.785						.714	.785	
VFS		.964			.714		.919	.892	.964	
Mud		.821		.821	.892	.964	.882	.892	.821	.748

	Th	Pb	Zn	Cu	Ni	Co	Cr	V	Ba	Sc
Th	1.000									
Pb	.714	1.000								
Zn	.937		1.000							
Cu	.937		1.000	1.000						
Ni	.927		.963	.963	1.000					
Co			.846	.846	.872	1.000				
Cr						.785	1.000			
V					.743	.919	.955	1.000		
Ba	.821	.892							1.000	
Sc	.860		.963	.963	.971	.954		.811		1.000
Br	.896	.836	.723	.723	.730				.896	
Ga	.892		.991	.991	.927	.857				.954
La	.937	.738	.890	.890	.798				.882	.774
Ce	.928	.857	.846	.846	.763				.964	
Nd	.810	.738	.809	.809					.900	
As						.785				.729
Gravel										
VCS										
CS			-.774	-.774					-.714	
MS	-.750		-.774	-.774	-.818	-.857		-.738		-.860
FS			.720	.720						
VFS	.821		.919	.919	.818				.714	.823
Mud	.964	.785	.882	.882	.818				.892	.767

	Br	Ga	La	Ce	Nd	As	Gravel	VCS	CS	MS
Br	1.000									
Ga		1.000								
La	.844	.882	1.000							
Ce	.896	.821	.955	1.000						
Nd	.723	.828	.936	.937	1.000					
As						1.000				
Gravel							1.000			
VCS							.763	1.000		
CS		-.821	-.738	-.750	-.828			.801	1.000	
MS		-.750								1.000
FS		.750							-.821	
VFS		.928	.810	.821	.810				-.928	
Mud	.896	.857	.991	.964	.900					

	FS	VFS	Mud
FS	1.000		
VFS	.892	1.000	
Mud		.785	1.000

TABLE 10-5 : SPEARMAN RANK CORRELATION COEFFICIENTS FOR THE INNER SHELF MUD SAMPLES.
Only values significant at the 95% confidence level (>.329) are shown.
Values significant at the 99% confidence level (>.465) are underlined.

	SiO_2	TiO_2	Al_2O_3	Fe_2O_3	MnO	MgO	CaO	Na_2O	K_2O	P_2O_5
SiO_2	1.000									
TiO_2	-.343	1.000								
Al_2O_3	-.886	.597	1.000							
Fe_2O_3	-.899	.488	.968	1.000						
MnO	-.444	.399	.558	.605	1.000					
MgO	-.757		.711	.796	.406	1.000				
CaO	.546	-.729	-.783	-.692	-.615		1.000			
Na_2O	.769		-.537	-.563		-.534		1.000		
K_2O	.757	.748	.919	.858	.639	.583	-.848	-.372	1.000	
P_2O_5	-.693	.336	.640	.725	.403	.731		-.454	.560	1.000
CO_2	.438	-.786	-.706	-.604	-.558		.972		-.792	
H_2O+	-.898	.533	.942	.925	.516	.699	-.744	-.565	.847	.621
Org.M	-.688		.617	.614		.498	-.438	-.422	.500	.432
S		-.380								
Rb	-.853	.537	.922	.915	.436	.764	-.671	-.452	.821	.686
Sr	.666	-.697	-.874	-.817	-.602	-.464	.955		-.872	-.348
Y	-.635	.689	.813	.742	.645	.380	-.952		.894	
Zr	.582		-.420	-.495		-.469		.745		-.417
Nb	-.425	.814	.642	.594	.419	.408	-.582		.751	.653
U	-.409					.439				.566
Th	-.733	.484	.723	.722	.413	.461	-.729		.640	
Pb	-.829	.437	.858	.901	.463	.701	-.561	-.431	.740	.754
Zn	-.886	.588	.989	.973	.582	.739	-.779	-.524	.921	.659
Cu	-.821	.637	.959	.930	.606	.629	-.878	-.422	.931	.545
Ni	-.872	.584	.988	.971	.540	.735	-.785	-.504	.905	.650
CO	-.685	.627	.818	.797	.627	.482	-.896		.813	.365
Cr	-.864	.502	.950	.942	.428	.777	-.678	-.551	.839	.640
V	-.865	.580	.982	.973	.584	.717	-.786	-.527	.907	.633
Ba	-.299	.761	.551	.450	.615		-.872		.723	
Sc	-.912	.411	.905	.900		.823	-.553	-.641	.759	.726
Br		-.382				.386	.554	-.345		.573
Ga	-.905	.538	.969	.971	.551	.760	-.730	-.567	.895	.705
La	-.798	.548	.890	.876	.567	.617	-.806	-.405	.879	.491
Ce	-.856	.453	.830	.880	.498	.726	-.551	-.493	.753	.737
Nd	-.730	.691	.870	.857	.654	.512	-.850		.880	.447
As						.390	.336			.604
Gravel		-.373	-.335		-.607		.541		-.426	
VCS										
CS	.590	-.729	-.747	-.668	-.414	-.372	.666		-.775	-.500
MS	.561	-.764	-.709	-.627	-.496	-.282	.760		-.815	-.402
FS	.489	-.889	-.746	-.626	-.583	-.286	.881		-.882	
VFS										
Mud	-.622	.807	.802	.740	.500	.554	-.698		.849	.657

	CO_2	H_2O+	Org.M	S	Rb	Sr	Y	Zr	Nb	U
CO_2	1.000									
H_2O+	-.673	1.000								
Org.M	-.334	.585	1.000							
S			.363	1.000						
Rb	-.600	.903	.588		1.000					
Sr	.906	-.839	-.501		-.804	1.000				
Y	-.910	.777	.576		.694	-.908	1.000			
Zr		-.436	-.341		-.451			1.000		
Nb	-.624	.590	.329		.631	-.591	.600		1.000	
U			.395		.400				.333	1.000
Th	-.673	.776	.587		.737	-.785	.762			
Pb	-.480	.841	.690		.906	-.697	.633	-.463	.604	.451
Zn	-.693	.947	.602		.906	-.868	.817	-.404	.651	
Cu	-.815	.927	.616		.871	-.936	.901	-.341	.660	
Ni	-.705	.940	.614		.917	-.881	.808	-.418	.652	
CO	-.835	.799	.646		.743	-.919	.913		.560	
Cr	-.597	.913	.569		.885	-.802	.709	-.404	.575	.342
V	-.705	.926	.568		.895	-.883	.801	-.437	.615	
Ba	-.886	.508	.335		.417	-.746	.878		.571	
Sc	-.463	.900	.592		.913	-.691	.583	-.540	.547	.409
Br	.581			.331			.497	-.412		.391
Ga	-.649	.951	.567		.946	-.839	.772	-.476	.625	.311
La	-.715	.867	.673		.806	-.865	.879	-.340	.560	
Ce	-.472	.810	.681		.782	-.649	.672	-.383	.592	.334
Nd	-.798	.822	.509		.748	-.893	.890		.588	
As							-.331			.392
Gravel	.523			.340		.499	-.457			
VCS										.444
CS	.671	-.670		.386	-.706	.694	-.648		-.747	
MS	.752	-.645	-.337		-.674	.725	-.778		-.663	
FS	.885	-.665		.409	-.651	.824	-.850		-.724	
VFS	-.337			.418			.407			
Mud	-.666	.710	.441	-.354	.789	-.746	.696		.844	.403

	Th	Pb	Zn	Cu	Ni	Co	Cr	V	Ba	Sc
Th	1.000									
Pb	.683	1.000								
Zn	.727	.855	1.000							
Cu	.781	.819	.961	1.000						
Ni	.732	.858	.990	.965	1.000					
Co	.814	.727	.828	.897	.835	1.000				
Cr	.699	.804	.950	.908	.966	.736	1.000			
V	.728	.846	.980	.964	.988	.830	.959	1.000		
Ba	.571	.408	.545	.663	.531	.761	.396	.541	1.000	
Sc	.637	.823	.897	.830	.911	.655	.930	.891		1.000
Br									-.677	
Ga	.735	.876	.973	.938	.970	.787	.942	.964	.469	.920
La	.768	.808	.906	.945	.901	.906	.847	.899	.621	.786
Ce	.666	.838	.859	.810	.853	.752	.794	.824	.390	.796
Nd	.776	.719	.891	.898	.875	.908	.793	.877	.722	.675
As		.303							-.429	
Gravel				-.403	-.352	-.385		-.387	-.544	
VCS										
CS	-.428	-.607	-.719	-.694	-.698	-.599	-.619	-.689	-.564	-.633
MS	-.580	-.619	-.691	-.708	-.666	-.653	-.559	-.662	-.773	-.518
FS	-.565	-.509	-.722	-.784	-.715	-.733	-.613	-.727	-.850	-.531
VFS	.413								-.475	
Mud	.498	.689	.789	.790	.793	.683	.718	.777	.558	.725

	Br	Ga	La	Ce	Nd	As	Gravel	VCS	CS	MS
Br	1.000									
Ga		1.000								
La		.880	1.000							
Ce		.852	.822	1.000						
Nd		.841	.882	.803	1.000					
As	.795					1.000				
Gravel	.382						1.000			
VCS								1.000		
CS		-.698	-.571	-.552	-.697				1.000	
MS	.333	-.670	-.613	-.549	-.734				.847	1.000
FS	.506	-.683	-.691	-.508	-.767		.553		.768	.847
VFS						-.361				-.418
Mud		.779	.718	.704	.697		-.410		-.774	-.717

	FS	VFS	Mud
FS	1.000		
VFS		1.000	
Mud	-.838		1.000

TABLE 10-6 : SPEARMAN RANK CORRELATION COEFFICIENTS FOR THE INNER SHELF SAND SAMPLES.
Only values significant at the 95% confidence level (>.329) are shown.
Values significant at the 99% confidence level (>.465) are underlined.

	SiO_2	TiO_2	Al_2O_3	Fe_2O_3	MnO	MgO	CaO	Na_2O	K_2O	P_2O_5
SiO_2	1.000									
TiO_2		1.000								
Al_2O_3		.789	1.000							
Fe_2O_3		.735	.816	1.000						
MnO		.433		.493	1.000					
MgO		.555	.556	.811	.681	1.000				
CaO	-.376	-.820	-.869	-.761	-.400	-.512	1.000			
Na_2O	.345	-.741	-.841	-.692	-.508	-.543	-.903	1.000		
K_2O		-.377	-.453				-.375		1.000	
P_2O_5		.509	.494	.577	.467	.501	-.342	.461		1.000
CO_2	-.377	-.843	-.865	-.777	-.478	-.587	.985	-.917		-.394
H_2O+	-.572		-.531	-.558		-.385				.355
Org.M		.423	.688	.543		.373	-.530	.448		
S	-.667	-.438			-.598		-.527	-.589		
Rb		.614	.776	.456			-.660	.537	.771	
Sr	-.350	-.782	-.804	-.757	-.425	-.527	.905	-.829	.338	-.381
Y		.950	.837	.697	.386	.530	-.823	.767		.500
Zr		.836	.441				-.488	.437	.464	.343
Nb		.910	.738	.579			-.706	.607	.519	.365
U		.745	.768	.505			-.651	.718	.454	.486
Th		.759	.634	.497			-.647	.474	.425	
Pb		.729	.796	.808	.504	.599	-.771	.728		.486
Zn		.812	.948	.841		.643	-.874	.795		.437
Cu		.679	.917	.812		.606	-.837	.742		
Ni		.764	.894	.888	.331	.728	-.877	.794		.436
Co		.746	.895	.911	.391	.750	-.846	.772		.408
Cr		.893	.767	.795	.580	.741	-.830	.811		.542
V		.908	.837	.845	.565	.697	.884	.863		.554
Ba		.410	.331				-.418	.393	.857	
Sc		.809	.853	.915	.449	.780	-.783	.718		.501
Br	-.594		.375	.515		.499				
Ga		.799	.970	.807		.593	-.875	.834	.382	.435
La		.746	.683	.404			-.561	.507	.462	.341
Ce		.822	.771	.524			-.639	.603	.473	.462
Nd		.809	.746	.503			-.645	.565	.499	.384
As				.399	.509	.527				
Gravel	-.493	-.401					.448	-.369		
VCS										
CS		-.366	-.389				.365			
MS		-.519	-.538				.525	-.544	-.562	
FS										
VFS		.415	.396				-.509	.402		
Mud		.767	.920	.724		.415	-.718	.673	.522	.526

	CO_2	H_2O+	Org.M	S	Rb	Sr	Y	Zr	Nb	U
CO_2	1.000									
H_2O+		1.000								
Org.M	-.489	.399	1.000							
S	-.561	.380		1.000						
Rb	-.599	.437	-.568		1.000					
Sr	.924		-.357	.630	-.510	1.000				
Y	-.840	.350	.542	-.358	-.636	-.761	1.000			
Zr	-.506			-.357	.503	-.433	.754	1.000		
Nb	-.688	.352	.471		.749	-.626	.914	.837	1.000	
U	-.659	.338	.336	-.373	.637	-.668	.802	.602	.778	1.000
Th	-.632	.344	.454		.712	-.574	.786	.667	.838	.536
Pb	-.762	.356	.595	-.360	.608	-.670	.738	.449	.650	.592
Zn	-.875	.571	.692		.682	-.796	.870	.436	.743	.683
Cu	-.831	.580	.717		.704	-.766	.737		.619	.558
Ni	-.881	.494	.695		.562	-.800	.789	.348	.633	.555
Co	-.855	.562	.651		.556	-.805	.774	.335	.629	.575
Cr	-.882		.362	-.560	.391	-.863	.867	.574	.688	.671
V	-.925		.473	-.538	.482	-.891	.881	.594	.719	.670
Ba	-.360			-.374	.604	-.352	.334	.584	.497	.377
Sc	-.804	.518	.606		.470	-.764	.800	.438	.656	.625
Br		.743	.490	.454						
Ga	-.861	.492	.684		.751	-.784	.850	.456	.754	.747
La	-.565		.536		.660	-.459	.794	.707	.831	.665
Ce	-.659	.409	.530		.697	-.554	.866	.736	.864	.718
Nd	-.658	.400	.534		.740	-.535	.840	.730	.853	.642
As										
Gravel	.451			.352		.360	-.475	-.381	-.338	
VCS										
CS	.343		-.389		-.500					
MS	.505			.404	-.515	.613	-.515	-.352	-.495	-.392
FS				.353			-.528	-.465	-.536	-.632
VFS	-.504				.492	-.407	.483		.407	
Mud	-.703	.615	.689		.787	-.654	.807	.504	.785	.781

	Th	Pb	Zn	Cu	Ni	Co	Cr	V	Ba	Sc
Th	1.000									
Pb	.590	1.000								
Zn	.701	.757	1.000							
Cu	.661	.757	.940	1.000						
Ni	.585	.774	.961	.921	1.000					
Co	.616	.768	.950	.926	.963	1.000				
Cr	.602	.709	.821	.700	.813	.801	1.000			
V	.623	.788	.851	.761	.857	.844	.960	1.000		
Ba	.351								1.000	
Sc	.501	.759	.888	.807	.900	.907	.851	.883		1.000
Br		.385	.353	.425	.338	.404				.435
Ga	.622	.810	.957	.905	.921	.897	.782	.832		.873
La	.781	.493	.685	.543	.549	.540	.556	.612		.548
Ce	.802	.562	.753	.637	.615	.635	.647	.703	.367	.620
Nd	.846	.564	.744	.648	.611	.623	.620	.676	.394	.574
As										
Gravel	-.340		-.338		-.331		-.373	-.391		
VCS	-.499									
CS	-.622		-.444	-.356						
MS	-.445	-.416	-.393	-.430		-.342	-.448	-.518	-.574	-.406
FS	.330									
VFS	.639	.347	.444	.484	.371		.368	.360		
Mud	.627	.692	.855	.795	.775	.770	.649	.718	.348	.773

	Br	Ga	La	Ce	Nd	As	Gravel	VCS	CS	MS
Br	1.000									
Ga	.329	1.000								
La		.656	1.000							
Ce		.707	.941	1.000						
Nd		.687	.917	.981	1.000					
As	-.525		-.448	-.330	-.323	1.000				
Gravel	.412		-.413	-.394	-.384	.412	1.000			
VCS			-.415	-.418	-.483	.429	.525	1.000		
CS		-.362	-.672	-.614	-.631	.709	.672	.779	1.000	
MS		-.469	-.388	-.450	-.393					1.000
FS			.380	.352	.381	-.499		-.619	-.693	
VFS		.368	.380	.453	.522	-.374	-.493	-.712	-.726	
Mud	.434	.876	.709	.814	.790				-.419	-.486

	FS	VFS	Mud
FS	1.000		
VFS	.378	1.000	
Mud		.363	1.000

TABLE 10-7 : SPEARMAN RANK CORRELATION COEFFICIENTS FOR THE OUTER SHELF MUD SAMPLES.
Only values significant at the 95% confidence level (>.425) are shown.
Values significant at the 99% confidence level (>.601) are underlined.

	SiO_2	TiO_2	Al_2O_3	Fe_2O_3	MnO	MgO	CaO	Na_2O	K_2O	P_2O_5
SiO_2	1.000									
TiO_2		1.000								
Al_2O_3		.789	1.000							
Fe_2O_3		.701	.877	1.000						
MnO		.533	.565	.686	1.000					
MgO	-.847					1.000				
CaO		-.686	-.814	-.567		-.769	1.000			
Na_2O	.915			-.501			-.975	1.000		
K_2O		.675	.848	.598				-.723	1.000	
P_2O_5	-.630	.491	.688	.747	.480				-.969	1.000
CO_2		-.660	-.785	-.517		.468	.950	-.494	.498	
H_2O+		.442	.718	.713				-.533		.659
Org.M	-.444		.661	.867	.553			-.704		.702
S	-.679					.567				.452
Rb		.603	.857	.757	.565		-.715		.721	.695
Sr		-.757	-.849	-.667			.958		-.952	
Y		.901	.817	.698	.471		-.674		.688	
Zr								.473		-.631
Nb		.793	.865	.670	.463		-.758		.802	-.528
U						.511				.546
Th	-.517		.554	.606	.444			-.502		.662
Pb		.576	.715	.611	.543		-.613		.588	.615
Zn		.795	.918	.929	.645		-.634		.688	.791
Cu	-.435	.643	.884	.901	.650		-.554	-.584	.576	.844
Ni		.764	.917	.899	.582		-.638	-.533	.657	.851
Co		.772	.828	.755	.471		-.698		.699	.571
Cr		.754	.849	.923	.643		-.562	-.487	.560	.718
V		.799	.875	.883	.620		-.675		.657	.685
Ba	.559	.508	.638			-.631	-.891		.898	
Sc		.588	.831	.854	.571		-.487	-.536	.554	.837
Br			.505	.614	.487					.576
Ga		.729	.901	.909	.575		-.633		.675	.800
La		.713	.758	.713			-.597	-.456	.670	.637
Ce	-.434	.719	.766	.859	.632		-.453	-.482	.474	.730
Nd		.632	.722	.723	.447		-.439	-.525	.488	.701
As	-.625		.593	.710	.534			-.786		.861
Gravel	-.483						.631	-.454	-.495	
VCS								-.449		
CS	-.496	-.481	-.539			.589	.838	-.480	-.822	
MS	-.665					.662	.698	-.641	-.677	
FS										
VFS	.855			-.450		-.758		.952		-.531
Mud		.592	.883	.773	.553		-.744		.739	-.680
										.660

	CO_2	H_2O+	Org.M	S	Rb	Sr	Y	Zr	Nb	U
CO_2	1.000									
H_2O+	-.462	1.000								
Org.M		.553	1.000							
S				1.000						
Rb	-.672	.494	.660		1.000					
Sr	.941	-.504	-.432		-.709	1.000				
Y	-.600	.570			.643	-.719	1.000			
Zr		-.471	-.515					1.000		
Nb	-.825	.655	.448		.799	-.812	.767		1.000	
U										1.000
Th		.721		.427	.559		.495	-.440	.496	
Pb	-.518		.446		.907	-.602	.626		.634	
Zn	-.625	.726	.725		.813	-.748	.828		.816	
Cu	-.497	.789	.740	.426	.758	-.620	.700	-.465	.657	
Ni	-.548	.692	.713	.464	.787	-.698	.834		.702	
Co	-.610	.715	.504		.597	-.724	.890		.673	
Cr	-.449	.705	.754	.486	.655	-.620	.804		.611	
V	-.546	.633	.694	.462	.695	-.710	.846		.647	
Ba	-.920				.621	-.804	.480		.673	
Sc	-.435	.693	.644	.424	.806	-.537	.719		.637	
Br			.808		.758			-.486	.462	
Ga	-.572	.653	.764		.868	-.683	.812		.748	
La	-.578	.670		.666	.482	-.697	.781		.593	
Ce		.677	.647	.476	.613	-.508	.818		.549	
Nd		.786	.498	.571		-.510	.787		.502	
As		.672	.702	.492	.654		.488	-.563	.406	
Gravel	.553				-.460	.501				
VCS										
CS	.805				-.482	.737	-.528		-.644	
MS	.712			.430		.547			-.522	
FS	.451	-.486			-.469			.757	-.486	
VFS		-.454	-.517	-.673				.550		
Mud	-.702	.660	.738		.900	-.741	.637	-.462	.829	

	Th	Pb	Zn	Cu	Ni	Co	Cr	V	Ba	Sc
Th	1.000									
Pb	.474	1.000								
Zn	.610	.688	1.000							
Cu	.722	.636	.886	1.000						
Ni	.594	.721	.922	.945	1.000					
Co	.544	.508	.799	.791	.835	1.000				
Cr	.577	.570	.846	.886	.919	.876	1.000			
V	.503	.649	.838	.863	.924	.901	.976	1.000		
Ba		.496	.462	.333		.507			1.000	
Sc	.767	.764	.860	.870	.892	.697	.819	.780		1.000
Br		.573	.550	.534	.476		.441			.509
Ga	.586	.769	.946	.863	.931	.811	.868	.866	.480	.907
La	.502	.457	.793	.739	.826	.784	.737	.755		.743
Ce	.707	.540	.845	.858	.860	.881	.911	.876		.826
Nd	.554		.755	.820	.834	.895	.849	.838		.713
As	.673	.565	.700	.820	.773	.578	.681	.631		.767
Gravel		-.477							-.684	
VCS						-.506			-.816	
CS									-.807	
MS									-.430	
FS										-.505
VFS	-.489			-.478						.684
Mud	.486	.703	.796	-.555	-.511	.700	-.480	.756	.623	
				.794	.777		.724			

	Br	Ga	La	Ce	Nd	As	Gravel	VCS	CS	MS
Br	1.000									
Ga	.616	1.000								
La		.744	1.000							
Ce		.859	.731	1.000						
Nd		.733	.848	.863	1.000					
As	.603	.736	.538	.693	.648	1.000				
Gravel							1.000			
VCS								1.000		
CS							.551	.462	1.000	
MS							.669		.830	1.000
FS	-.439			-.439	-.482	-.486		-.431		-.561
VFS						-.802			-.563	-.461
Mud	.768	.816	.458	.614	.539	.634				

	FS	VFS	Mud
FS	1.000		
VFS		1.000	
Mud	-.601		1.000

TABLE 10-8 : SPEARMAN RANK CORRELATION COEFFICIENTS FOR THE OUTER SHELF SAND SAMPLES.
Only values significant at the 95% confidence level (>.306) are shown.
Values significant at the 99% confidence level (>.432) are underlined.

	SiO_2	TiO_2	Al_2O_3	Fe_2O_3	MnO	MgO	CaO	Na_2O	K_2O	P_2O_5
SiO_2	1.000									
TiO_2		1.000								
Al_2O_3		.882	1.000							
Fe_2O_3		.842	.867	1.000						
MnO	.516				1.000					
MgO	-.584	-.333	-.445			1.000				
CaO	-.941	-.529	-.511	-.448	-.425	.575	1.000			
Na_2O	.905	.543	.522	.411	.434	-.575	-.936	1.000		
K_2O		.605	.811	.624		-.602	-.434	.469	1.000	
P_2O_5	-.431		.355	.455	-.611				.317	1.000
CO_2	-.941	-.526	-.507	-.443	-.426	.561	.995	-.935	-.420	
H_2O+	-.332	.600	.688	.679	-.472				.450	.603
Org.M		.667	.746	.704	-.476				.496	.550
S	-.856				-.344	.431	.773	-.739		
Rb		.775	.925	.758	-.377	-.480	-.333	.327	.884	.408
Sr	-.963	-.425	-.423	-.393	-.443	.555	.973	-.909	-.394	.309
Y		.915	.858	.743			-.319	.348	.579	
Zr		.970	.795	.742		-.337	-.443	.468	.541	
Nb		.974	.914	.839		-.372	-.468	.485	.681	
U										
Th		.717	.760	.629	-.388				.562	.361
Pb			.494	.439					.639	.376
Zn		.917	.931	.882		-.311	-.412	.400	.645	.401
Cu		.870	.922	.876			-.365	.342	.615	.390
Ni	.320	.896	.913	.856			-.568	.530	.582	
Co	.484	.854	.809	.801			-.702	.682	.481	
Cr	.563	.804	.699	.753			-.705	.677	.458	
V	.492	.825	.814	.814			-.679	.661	.540	
Ba	.785	.500	.632	.450		-.739	-.838	.830	.776	
Sc	.319	.893	.928	.828		-.361	-.551	.538	.633	
Br	-.387	.543	.626	.656	-.723				.430	.658
Ga		.890	.980	.880		-.409	-.462	.461	.796	.392
La		.852	.896	.775		-.324			.612	.377
Ce		.828	.829	.748	-.349				.572	.365
Nd		.821	.818	.739	-.375				.522	.419
As		-.707	-.582	-.473	.320	.391	.392	-.398	-.349	
Gravel	-.502	-.512	-.321		-.309	.419	.599	-.611		.319
VCS	-.334	-.532	-.372			.343	.478	-.470		
CS		-.754	-.665	-.547		.428	.502	-.447	-.416	
MS		-.535	-.579	-.398		.342		-.306	-.635	-.319
FS		.578	.447	.354		-.409	-.379	.350		
VFS		.730	.705	.555	-.403	-.413			.544	
Mud		.845	.910	.813	-.416				.673	.491

	CO_2	H_2O+	Org.M	S	Rb	Sr	Y	Zr	Nb	U
CO_2	1.000									
H_2O+		1.000								
Org.M		.788	1.000							
S	.777		.379	1.000						
Rb	-.322	.697	.765		1.000					
Sr	.972			.847		1.000				
Y	-.320	.716	.751		.814		1.000			
Zr	-.437	.565	.631		.718	-.337	.889	1.000		
Nb	-.460	.661	.722		.848	-.364	.934	.948	1.000	
U		.359	.353	.311			.322		.311	1.000
Th		.743	.772		.822		.857	.695	.775	.469
Pb		.468	.336		.624		.411		.379	
Zn	-.406	.711	.780		.854		.890	.861	.935	.323
Cu	-.367	.770	.830		.837		.888	.794	.876	
Ni	-.571	.606	.706		.769	-.457	.861	.797	.869	
Co	-.704	.420	.517		.607	-.600	.756	.746	.804	
Cr	-.712	.327	.352	-.429	.526	-.670	.674	.727	.743	
V	-.689	.427	.493	-.310	.641	-.616	.746	.711	.774	
Ba	-.835			-.658	.568	-.825	.355	.410	.496	
Sc	-.547	.609	.699		.783	-.444	.861	.807	.883	
Br		.799	.784		.694		.605	.533	.611	.422
Ga	-.459	.733	.736		.934	-.374	.871	.817	.924	
La		.733	.845		.854		.912	.818	.880	
Ce		.785	.852		.826		.924	.812	.867	
Nd		.791	.881		.802		.930	.802	.859	.348
As	.389	-.376	-.391		-.500	.313	-.627	-.759	-.726	
Gravel	.573					.505	-.403	-.529	-.484	
VCS	.453					.360	-.491	-.528	-.508	
CS	.479	-.350	-.518		-.586	.352	-.716	-.743	-.763	
MS		-.431	-.431		-.578		-.493	-.552	-.588	-.317
FS	-.355		.369		.384		.501	.634	.605	
VFS		.596	.667		.717		.732	.741	.785	.404
Mud		.777	.907		.900		.889	.790	.890	.353

	Th	Pb	Zn	Cu	Ni	Co	Cr	V	Ba	Sc
Th	1.000									
Pb	.494	1.000								
Zn	.784	.409	1.000							
Cu	.787	.395	.909	1.000						
Ni	.698	.342	.906	.940	1.000					
Co	.518		.807	.818	.934	1.000				
Cr	.454		.660	.709	.811	.842	1.000			
V	.545	.311	.740	.828	.915	.917	.929	1.000		
Ba		.361	.430	.409	.524	.551	.591	.617	1.000	
Sc	.676		.900	.919	.955	.870	.783	.876	.571	1.000
Br	.754	.433	.738	.664	.506					.484
Ga	.791	.515	.948	.919	.895	.786	.692	.784	.570	.904
La	.820	.419	.915	.928	.878	.750	.586	.714	.362	.874
Ce	.854	.450	.873	.896	.810	.679	.538	.636		.789
Nd	.864	.411	.888	.903	.828	.689	.526	.636		.796
As	-.509		-.691	-.536	-.542	-.542	-.420	-.364		-.541
Gravel			-.371		-.383	-.507	-.400	-.339	-.423	-.396
VCS			-.472	-.325	-.463	-.569	-.311	-.350		-.450
CS	-.536		-.762	-.607	-.701	-.723	-.436	-.518	-.372	-.683
MS	-.460		-.560	-.441	-.422	-.349			-.411	-.485
FS	.324		-.585	-.383	-.441	.465				.444
VFS	.657	.320	.796	.624	.598	.510	.317	.348		.614
Mud	.856	.457	.930	.918	.856	.715	.551	.681	.337	.851

	Br	Ga	La	Ce	Nd	As	Gravel	VCS	CS	MS
Br	1.000									
Ga	.687	1.000								
La	.675	.898	1.000							
Ce	.695	.854	.943	1.000						
Nd	.721	.835	.943	.972	1.000					
As	-.483	-.602	-.585	-.587	-.588	1.000				
Gravel		-.315				.508	1.000			
VCS		-.378	-.453	-.425	-.420	.478	.858	1.000		
CS	-.370	-.666	-.727	-.705	-.691	.712	.704	.824	1.000	
MS	-.382	-.556	-.466	-.450	-.483	.553			.385	1.000
FS	.351	.459	.529	.508	.502	-.796	-.671	-.769	-.847	-.326
VFS	.625	.730	.743	.758	.766	-.736	-.506	-.576	-.760	-.650
Mud	.765	.915	.931	.924	.934	-.564		-.368	-.681	-.561

	FS	VFS	Mud
FS	1.000		
VFS	.754	1.000	
Mud	.456	.765	1.000

However, it should be noted that there are arguments against the use of factor analysis in geology (Temple, 1978; Le Maitre, 1982), although most of the objections put forth do not apply to sedimentary environments. Spencer and others (1968) showed how mathematical factors could be identified with environmental factors, indicating relationships between these environmental factors and the elemental distributions. Summerhayes (1972a) also found relationships existing between mathematical factors and environmental factors, stating that the associations of the factors are controlled or influenced by mineral provenance, chemical and physical depositional processes and the degree of geochemical coherence between certain elements. In this study, similar relationships were identified between the mathematical factors representing the elemental and textural data and the mineralogy and sedimentology of the study area.

Six factors explain 89.2% of the variance of the chemical and textural data of this study. Loadings of the variables on the factors (viz. correlations of the variables with the factors) are presented in Table 10-9. It should be noted that the loadings of the variables on each factor represent the correlation of the variable to the factor and not correlations between the variables themselves. The factors are diagrammatically summarized in figure 10-5.

Factor 1 accounts for 56.2% of the variance of the data, and is readily identified from the distribution of factor 1 scores (fig. 10-6) as a clay mineral factor. This is further

TABLE 10-9 : SORTED ROTATED FACTOR LOADINGS FROM THE FACTOR ANALYSIS PERFORMED ON THE CHEMICAL AND TEXTURAL DATA. LOADINGS LESS THAN 0.25 ARE OMITTED.

	FACTOR 1	FACTOR 2	FACTOR 3	FACTOR 4	FACTOR 5	FACTOR 6
Al_2O_3	.982					
Ga	.980					
Zn	.976					
Cu	.961					
Mud	.959					
Rb	.955					
Ni	.951					
Ce	.943					
Fe_2O_3	.941					
Sc	.941					
La	.941					
Nd	.940					
H_2O+	.927					
V	.923				.285	
Co	.911					
Org.M.	.901					
K_2O	.893	-.268				
Y	.893		.354			
Nb	.893		.328			
Pb	.859					.260
Th	.814		.487			
P_2O_5	.793					.322
TiO_2	.784		.532			
U	.719		.414			
M.Sand	-.694		-.436			
Cr	.690	-.270	.285		.484	
SiO_2	-.325	-.902				
Sr	-.459	.844				
CO_2	-.458	.842				
CaO	-.499	.826				
MgO		.693			.560	
Ba	.578	-.662				-.254
S	.443	.597			-.267	
Zr			.912			
V.F.Sand			.872			
Na_2O		-.576	.658			
V.C.Sand	-.289			.815		
C.Sand	-.528			.707		
Gravel		.373		.637		
F.Sand	-.365		.258	-.621		
MnO		-.312			.772	
Br	.423	.317				.733
As		.261	-.374	.396	.382	.403
%VARIANCE EXPLAINED	56.2%	14.2%	7.9%	4.8%	3.3%	2.4%
CUMULATIVE PROPORTION OF TOTAL VARIANCE	56.2%	70.8%	78.7%	83.5%	86.8%	89.2%

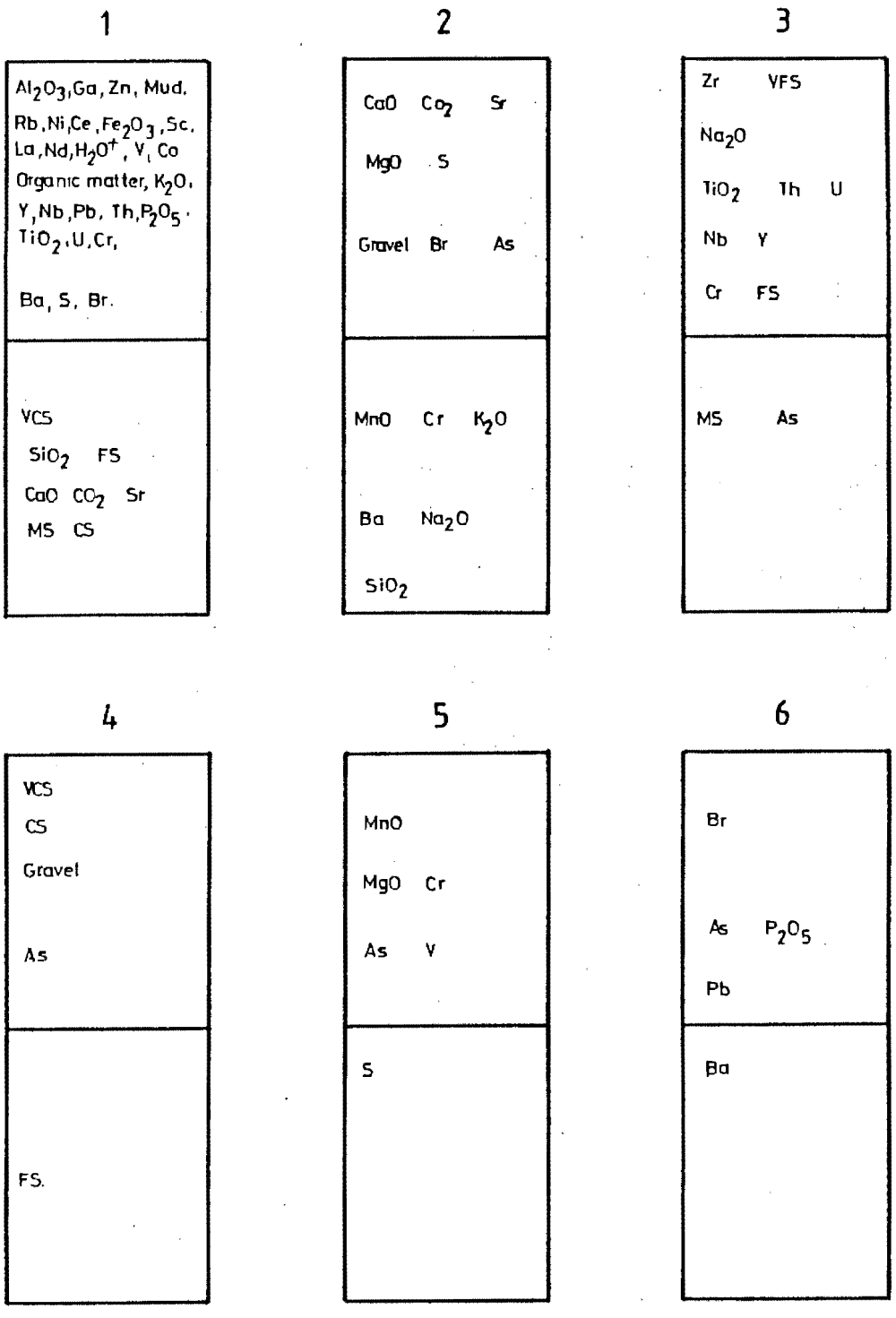

Figure 10-5. Graphic representation of factors.

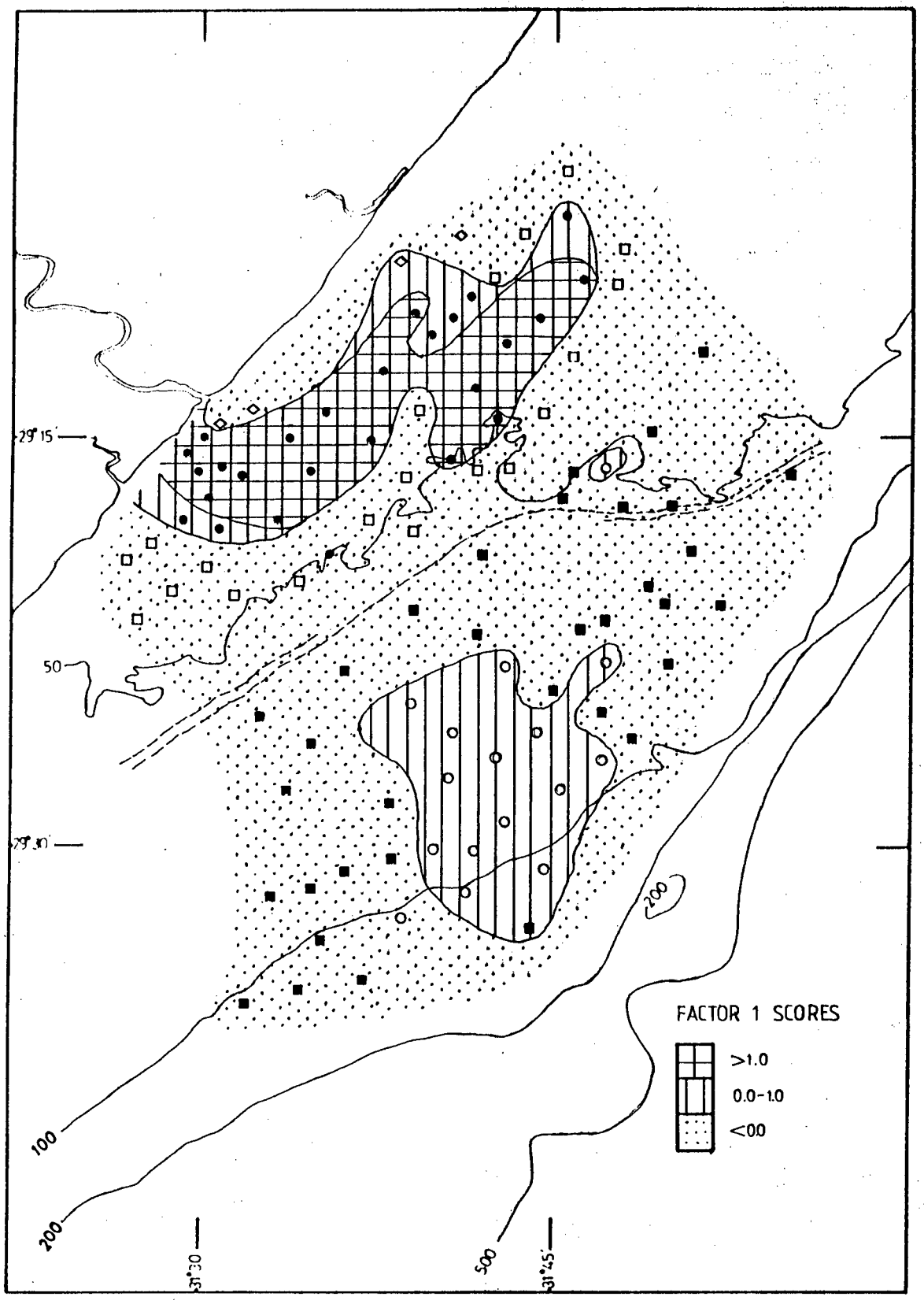

Figure 10-6. Distribution of factor 1 (clay mineral factor) scores.

evidenced by the high positive loadings on the factor of mud, Al_2O_3, and numerous cations with the factor, all of which are known to be associated with clay minerals in the sedimentary environment (Hirst, 1962b; Förstner et al., 1978). The negative loadings of medium, coarse and very coarse sand, as well as the carbonate mineral constituents of CaO, CO_2, and Sr, indicate an antipathetic relationship of the coarse fractions and carbonates to the clays.

Factor 2 is a bipolar factor representing both quartz-feldspar and the carbonate minerals. CaO, CO_2, MgO and Sr are all highly positively correlated to this factor, while SiO_2 is even more strongly negatively loaded. Ba, Na_2O and K_2O are also negatively correlated to factor 2, showing an association of feldspars and quartz. The mineralogical discussion (chap. IX) also inferred such a relationship. It is interesting to note the very weak positive correlation of gravel with factor 2, presumably due to the number of shell fragments that fall into this size range. The distribution of factor 2 scores is shown in figure 10-7, and corresponds closely to the distributions of the carbonate mineral components CaO, CO_2 and Sr shown in section 3..

Factor 3 may be regarded as a heavy mineral factor as indicated by the positive correlations of Zr, TiO_2, Th, Y, Nb, U, Cr and Na_2O to it. The moderately high loading of Na_2O on the factor may be explained by its presence in hornblende. Very fine sand is strongly positively loaded on factor 3, with a weak positive loading of fine sand also seen,

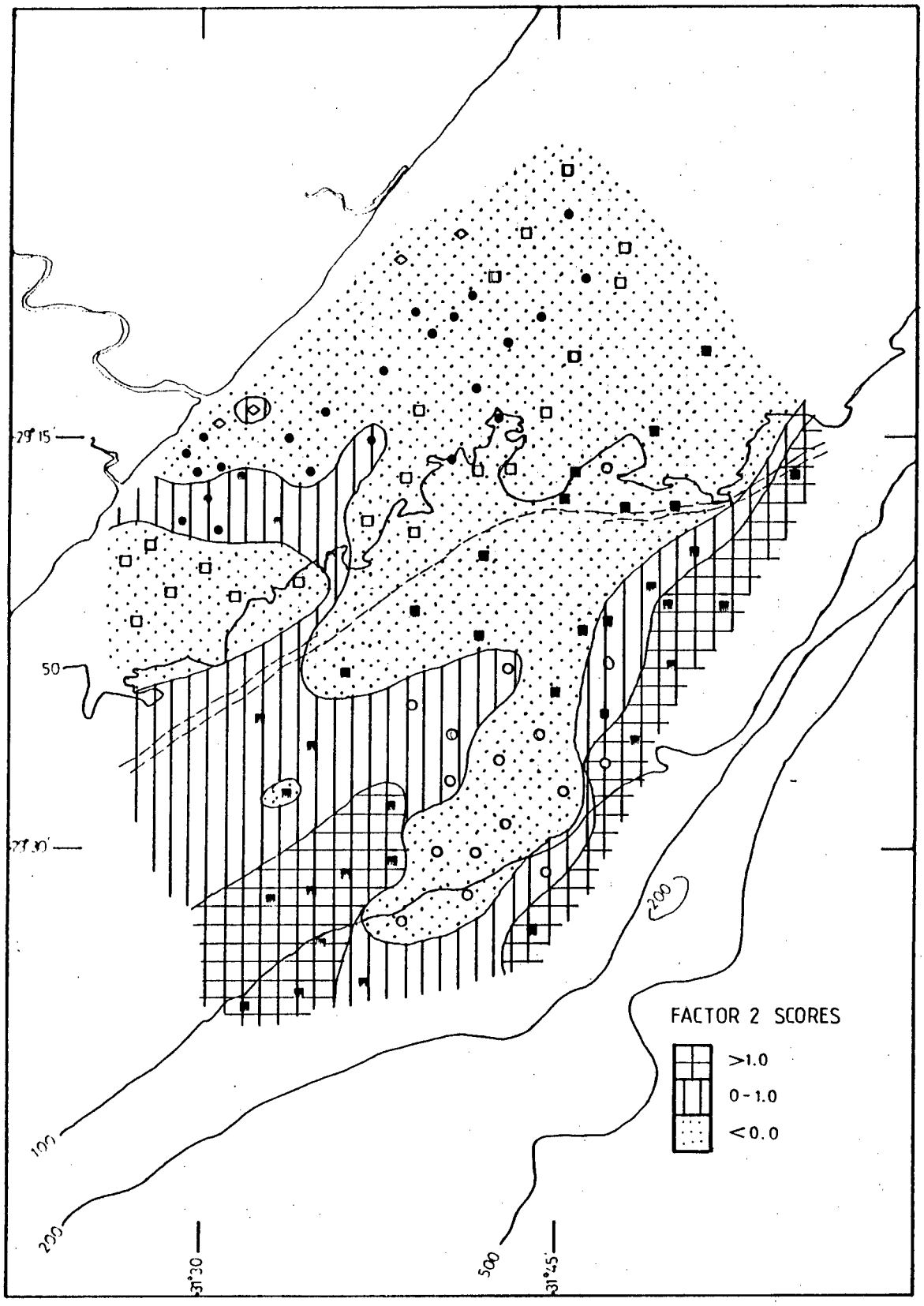

Figure 10-7. Distribution of factor 2 (quartz/feldspar-carbonate factor) scores.

while medium sand is negatively correlated to the factor. This suggests that the heavy minerals are fine-grained and thus associated with the finer fractions of the sediments. The distribution of factor 3 scores is presented in figure 10-8, and clearly shows the very fine nearshore sands to be an area of heavy mineral concentration, as suggested in chapter IX, with a secondary area of concentration coinciding with the position of the outer shelf mud belt. The high positive heavy mineral scores in the outer shelf region are further evidence that this area was a nearshore region in the Pleistocene.

Factor 4 is most probably a textural factor. Very coarse sand, gravel and coarse sand are all positively loaded on factor 4, with fine sand being negatively loaded, showing an antipathetic relationship between the coarse and fine fractions. Arsenic is also positively correlated to factor 4, suggesting a possible association of this element with the coarser sediment fractions.

Factor 5 shows positive loadings of MgO, MnO, Cr, V and As, with a negative loading of S. This factor could represent manganese mineral formation, however it appears likely that this factor simply represents the relationships of these elements in the study area rather than a specific mineralogical or environmental association.

Factor 6 shows a high positive loading of Br, with lesser positive loadings of P_2O_5, As and Pb, and a negative loading of Ba. As is discussed in section 3., Br concentrations

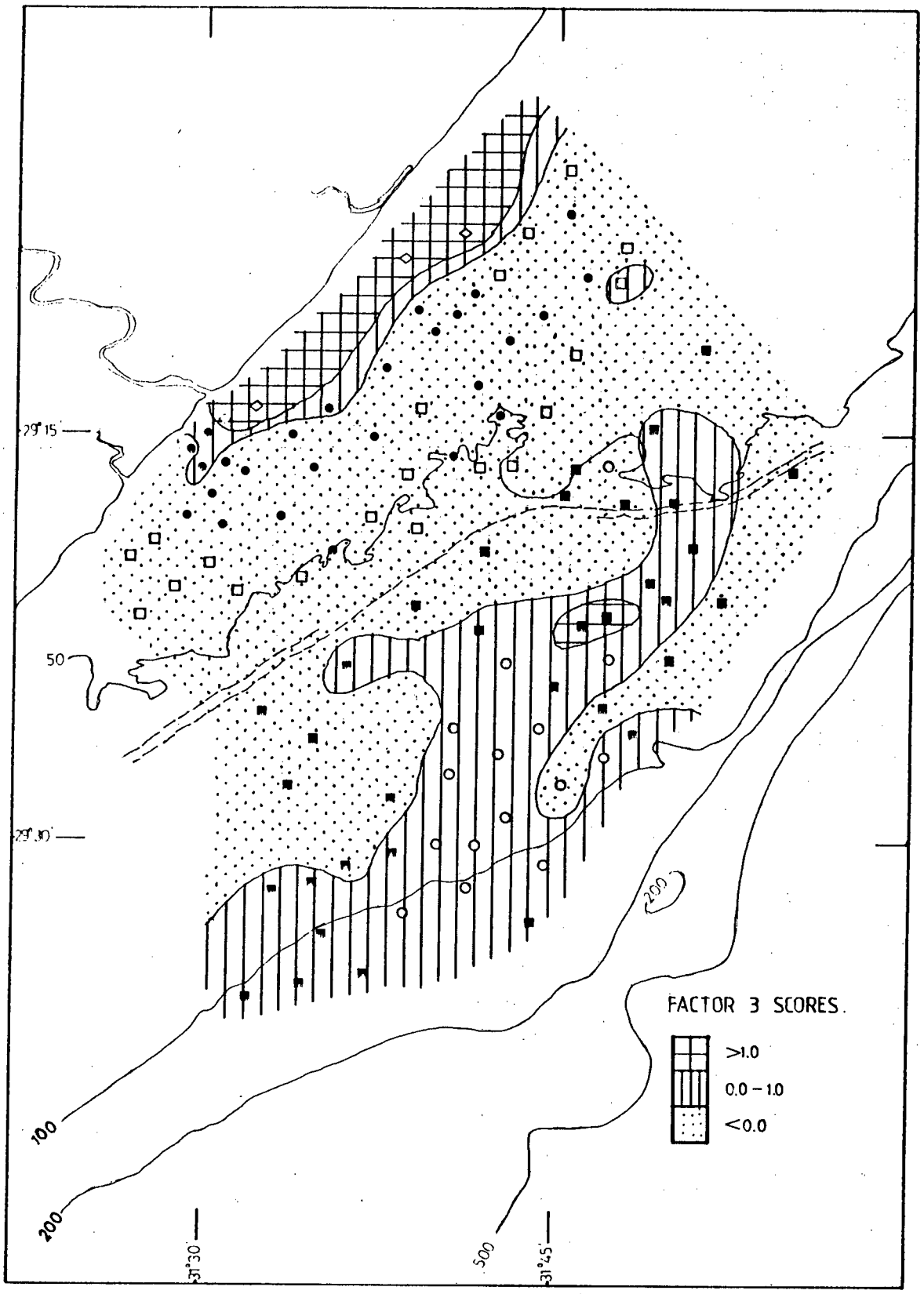

Figure 10-8. Distribution of factor 3 (heavy mineral factor) scores.

increase significantly towards the outer shelf while Ba decreases, possibly indicating that this factor is related to the residence times of the sediments on the shelf and to diagenesis.

3. Elemental Distributions and Geochemistry

The elemental distributions are, as would be expected, closely linked to the mineralogical trends discussed in chapter IX. The data as found in the samples are used in the following discussion, rather than the data recalculated on a carbonate-free basis. As shown in the various statistical tests in section 2., carbonate is not the major distinguishing variable in identifying different sedimentary groups in the study area, particularly the mud sample groups. Thus, it is believed that the data as found in the samples gives a better representation of the geochemistry of the sediments in the area than the data corrected on any basis.

There are several good references available on the fate of various elements during weathering, trsnsportation and sedimentation; examples are Keith and Degens (1959), Degens (1965), Mason (1966) and Krauskopf (1967). The paths that elements follow during depositional cycles are governed by their chemical properties, such as the relative stability of their ions in water, as well as by the physical and chemical properties of minerals. The fates of the major elements during sedimentation are: SiO_2 concentrates in resistate sediments; Al_2O_3 in the hydrolysates (clay minerals); iron and manganese in the oxidates; calcium and magnesium in the

carbonates; sodium tends to remain in solution and eventually accumulates in the oceans; potassium is adsorbed by clays (Mason, 1966).

Garrels and Mackenzie (1971) give an excellent explanation of the changes that occur in the transformation of igneous rocks to sediments. They classified sediments by using the established world average compositional values of various types of sediments and sedimentary rocks in a logarithmic plot of SiO_2/Al_2O_3 against $Na_2O + CaO/K_2O$. The sediments of this study have been plotted in the same manner and compared to the plot of world average values (fig. 10-9) The inner shelf and estuarine muds plot within the field of argillaceous sediments, while most of the outer shelf muds are closely grouped within the area defined as siliceous sediment. The inner shelf sands are all within the siliceous sediment field, as are several of the mid- to outer shelf sands. Those sands falling outside of the siliceous field could probably be defined as calcareous, following the suggestion of Cook and Mayo (1980) that the calcareous compositional field for sediments may not be as discrete as described by Garrels and Mackenzie.

The distributions and geochemistry of the major elements are discussed below, followed by a similar examination of the minor and trace elements.

3.1 Major Elements

The average major element compositions of the sedimentary groups in this study, along with world average composi-

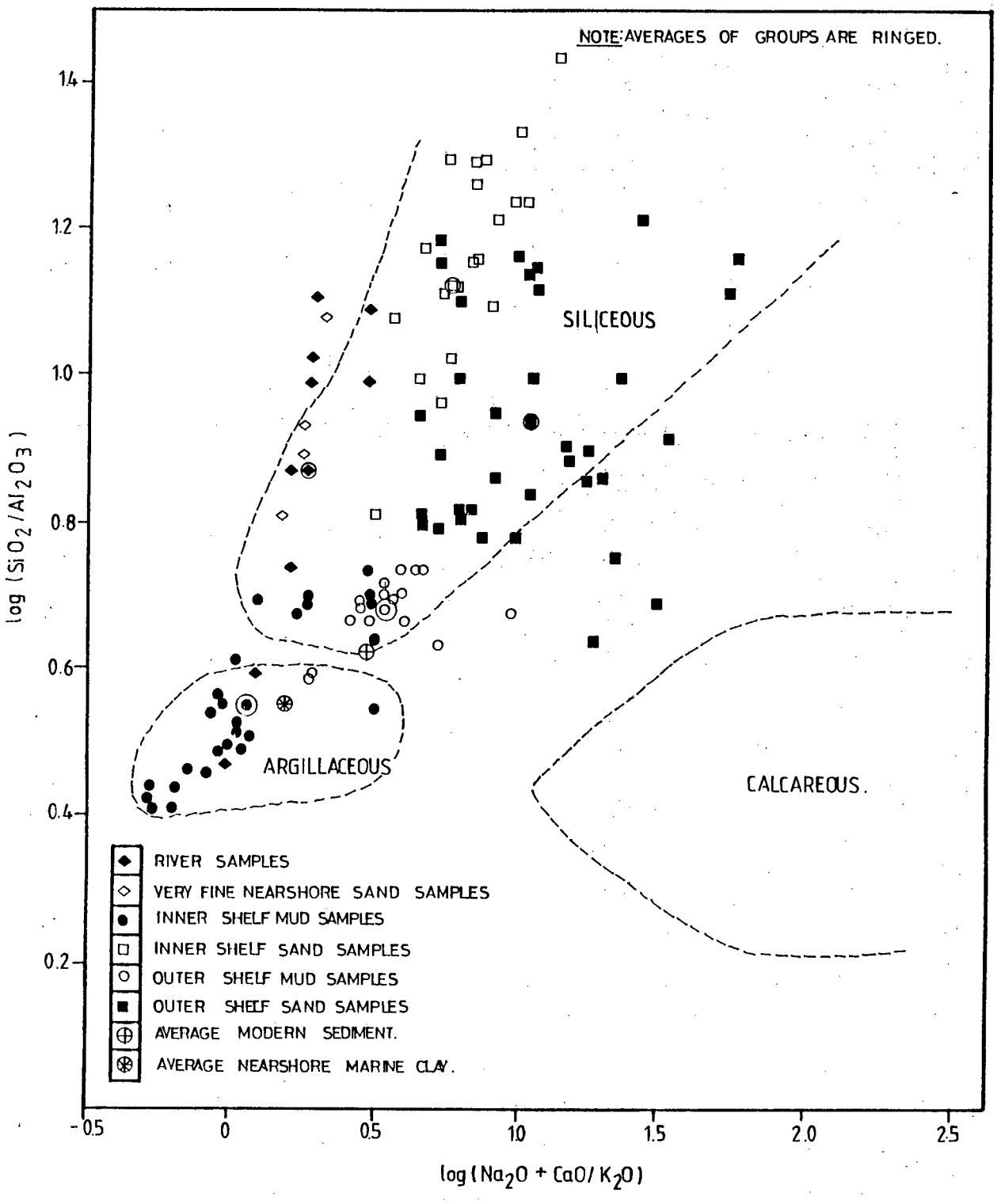

Figure 10-9. The relationship between log (SiO_2/Al_2O_3) and log (Na_2O + CaO/K_2O) for the study area sediments. The silicious, calcareous and argillaceous fields are those defined by Garrels and Mackenzie (1971).

tions for the major sedimentary rock types, are presented in Table 10-10.

3.1.1 SiO_2

The high percentages of SiO_2 present in the majority of the samples, along with the mineralogical data (chap. IX), show that most of the SiO_2 in the study area is present as quartz. Hirst (1962a) found indications from the analyses of silicon in his study of the Gulf of Paria sediments that silicon varies antipathetically with the clay mineral content. This appears to be the case in this study area as well, as evidenced by the negative loading of SiO_2 on the clay mineral factor and a negative correlation between SiO_2 and Al_2O_3 in the inner mud samples where the highest clay mineral content was found. The quartz-feldspar/carbonate factor shows quartz to be even more strongly antipathetically related to the carbonate minerals, conclusively indicating its terrigenous origin. There has been no evidence found in this study or others on the region to suggest biogenic SiO_2 formation.

It is interesting to note that SiO_2 correlates significantly with the fine, medium and coarse sand fractions in the inner shelf muds, but correlates highly only with very fine sand in the outer shelf muds (Tables 10-5 and 10-7). These correlations indicate that the presence of fine-grained crystalline quartz is more prevalent in the very fine sand fraction of the outer muds than in the inner muds. This was confirmed by observations of the sand fractions from both groups under a binocular microscope. The greater proportion

TABLE 10-10 : MAJOR ELEMENT COMPOSITIONS (% OXIDES).

OXIDE	ESTUARY	RIVER	INNER SHELF MUDS	INNER SHELF SANDS	OUTER SHELF MUDS	OUTER SHELF SANDS	1 AVERAGE SEDIMENT	2 AVERAGE MUDSTONE	3 AVERAGE SANDSTONE	4 AVERAGE LIMESTONE	5 AVERAGE SHALE
SiO_2	57.82	77.74	58.81	74.10	59.98	55.77	59.9	63.5	77.6	5.20	58.90
TiO_2	0.98	0.63	0.88	0.51	0.81	0.46	-	0.8	0.4	0.06	0.78
Al_2O_3	16.90	8.43	16.60	5.96	12.59	6.73	13.8	17.4	7.1	0.80	16.70
Fe_2O_3*	8.47	4.55	7.27	3.22	5.57	3.60	6.4	7.3	3.4	0.50	6.50
MnO	0.14	0.07	0.08	0.08	0.06	0.06	-	-	-	0.05	0.09
MgO	1.50	1.34	1.60	1.32	1.58	1.79	2.1	2.3	1.2	7.90	2.60
CaO	1.42	1.89	2.08	6.49	6.27	14.87	4.2	1.2	3.1	42.60	2.20
Na_2O	0.54	1.24	0.85	1.07	1.02	0.94	1.3	2.0	1.2	0.05	1.60
K_2O	1.73	1.52	2.24	1.38	1.95	1.32	2.0	3.4	1.3	0.33	3.60
P_2O_5	0.14	0.08	0.14	0.09	0.12	0.10	-	-	0.1	0.04	0.16
(CO_2	0.90	0.60	1.51	4.58	4.57	11.51	4.0	0.2	2.5	41.60	1.30
L.O.I. (H_2O+	5.74	0.92	5.38	1.06	3.55	2.03	6.3	2.4	2.1	0.77	5.00
(OrgM	3.38	0.90	2.35	0.38	1.55	0.87	-	-	-	-	-
TOTAL	99.66	99.91	99.79	100.24	99.62	100.05	99.6	100.5	100.0	99.90	99.43

* as total iron

1) Garrels, R.M. and Mackenzie, F.T. (1971). Evolution of Sedimentary Rocks, 397 pp. W.W.Norton and Co., Inc., N.Y.

2) Shaw, D.M. (1956). Geochemistry of pelitic rocks, Part III. Major elements and general geochemistry. Bull. Geol. Soc. Amer. 67, 919-934.

3) Pettijohn, F.J. (1963). Chemical composition of sandstones - excluding carbonate and volcanic sands. In Data of Geochemistry, (ed. M. Fleischer), U.S.Geol. Survey Prof. Paper 440-S.

4) Clarke, F.W. (1924). Data of Geochemistry. U.S. Geol. Survey Bull. 770.

5) Wedepohl, K.H. (1969). Composition and Abundance of Common Sedimentary Rocks. In Handbook of Geochemistry, Vol. I, (ed. K.H. Wedepohl), pp. 250-271. Springer-Verlag, Berlin.

of quartz found in the outer shelf mud samples (chap. IX, section 2.1) substantiates these correlations.

Comparison of the SiO_2 values for the different sedimentological groups in the area to world averages (cf. Table 10-10) shows that the river samples, along with the majority of the inner and mid-shelf sands, could be classified as sandstones (>70% SiO_2). The inner and outer shelf mud values are slightly lower than the average SiO_2 value for shales of 63.5%, but compare favourably to the average SiO_2 value of 59.9% for the average sediment. Some of the outer shelf sands contain as little as 25% SiO_2 due to their high carbonate contents. Such concentrations are too low to permit these samples to be classified as either sandstones or shales, but also are too high to compare with the SiO_2 value for limestones of 5.2%. The distribution of SiO_2 in the study area is shown in figure 10-10.

3.1.2 TiO_2

The distribution of TiO_2 (fig. 10-11) shows that it is primarily correlated to the mud fraction and secondarily associated with the very fine sand fraction (see figs. 8-9 and 8-10). TiO_2 is positively loaded on both the clay mineral factor and the heavy mineral factor. The majority of titanium is incorporated in the clay fraction, although it is unlikely that TiO_2 is chemically bonded to the clay minerals. However, its presence is most likely explained by the mixing of clay minerals with amorphous or finely dispersed crystalline titanium oxide (probably ilmenite and rutile in this area) or

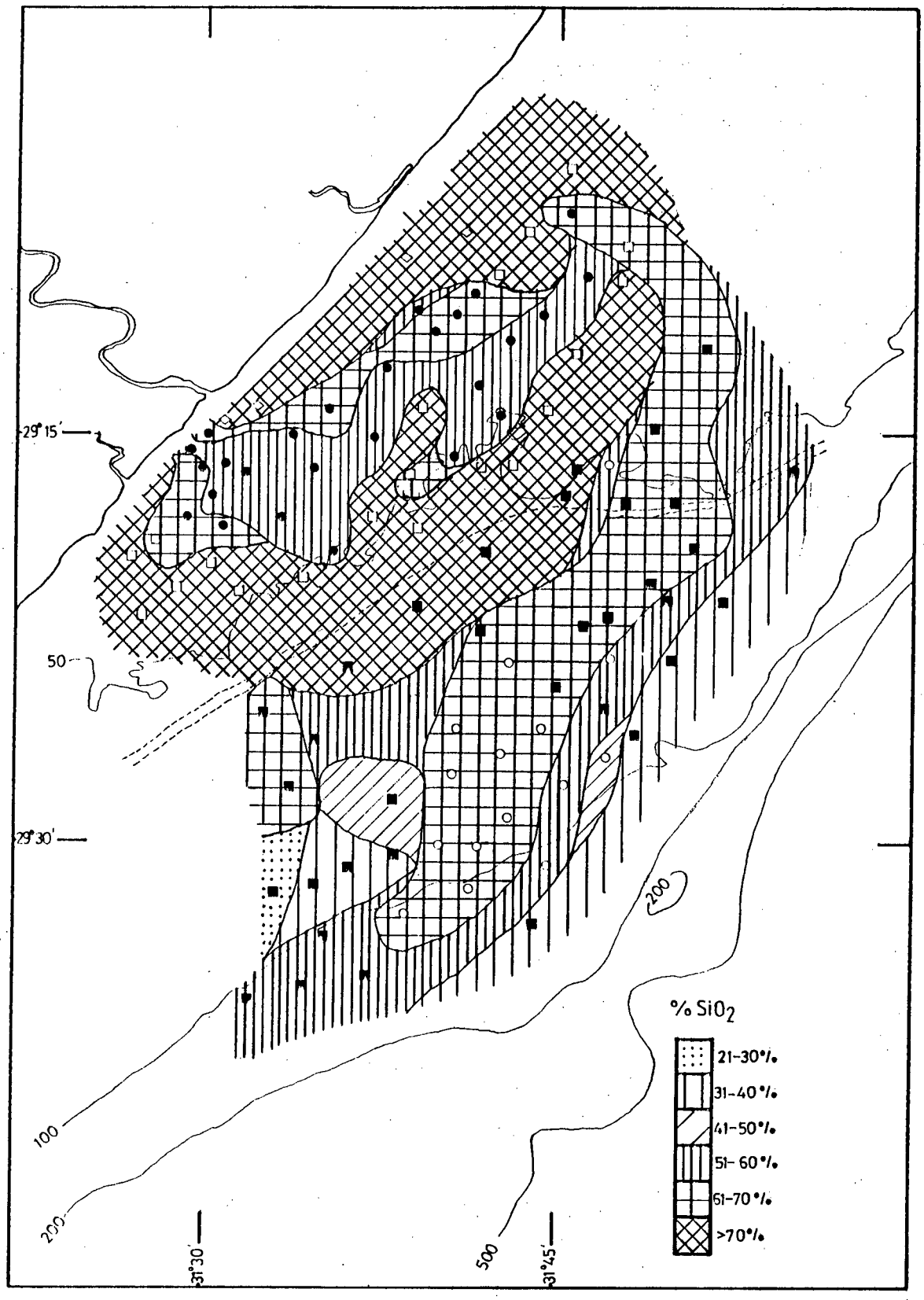

Figure 10-10. Distribution of SiO_2.

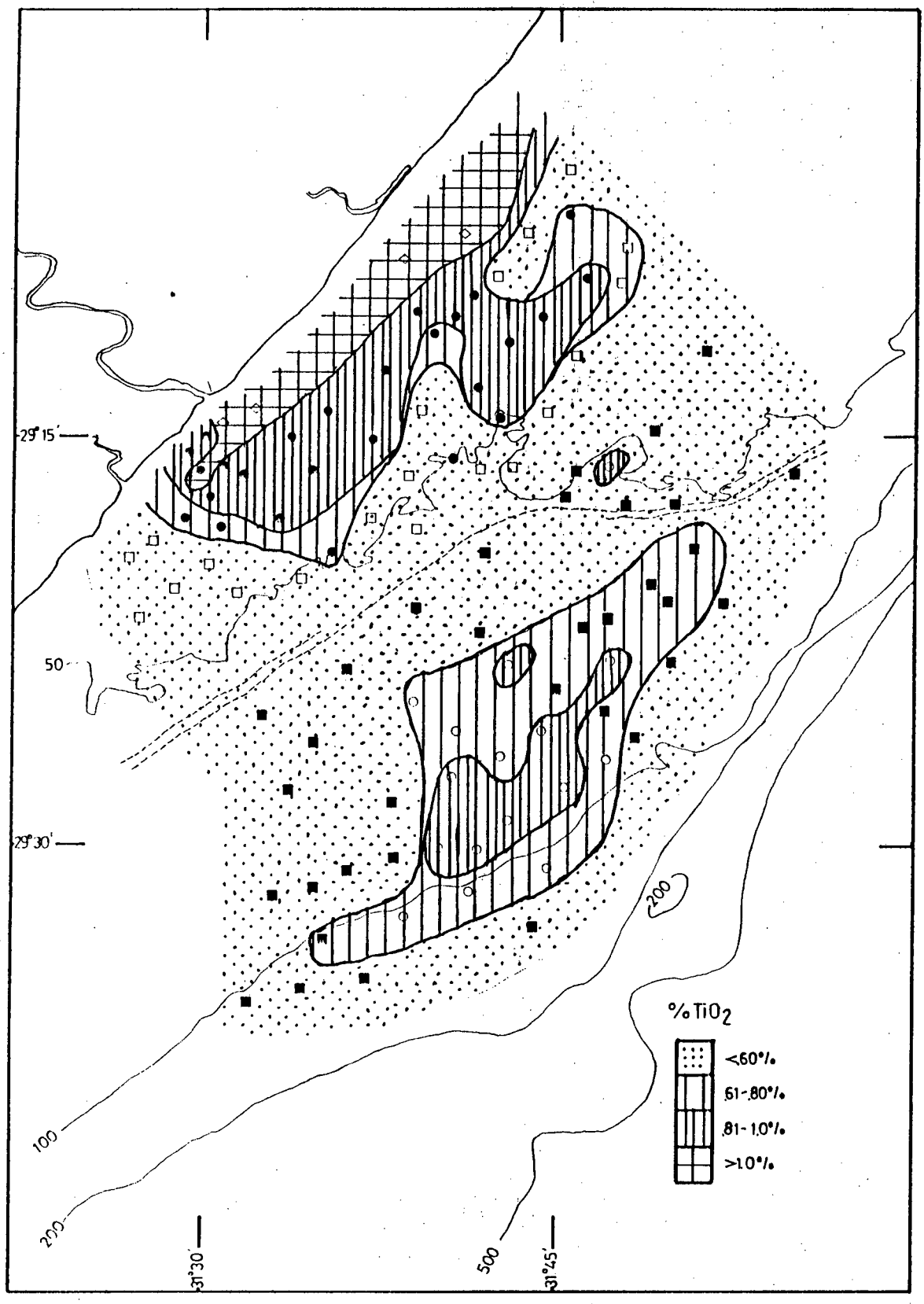

Figure 10-11. Distribution of TiO_2.

titanium dioxide hydrate released during weathering (Degens, 1965). The highest concentration of TiO_2 (>1.0%) is predictably found in the very fine nearshore sands due to their proximity to the river mouth which is the source of the heavy minerals in the area. The high concentration of the nearestshore muds (0.91 - 1.0% TiO_2) suggests that there is a significant amount of fine-grained detrital TiO_2 present, although this could not be confirmed from the X-ray diffractograms. The presence of TiO_2 in these mud samples could be from association with the clay minerals as discussed above, or from the physical mixing of the muds with the very fine nearshore sands. The outer shelf muds also show reasonably high TiO_2 concentrations (0.71 - 0.90%, averaging 0.81%). This would be expected if the outer mud belt was the paleodepocentre for the Tugela River, as the heavy mineral composition of the drainage basin would not have changed from the Pleistocene to the present.

3.1.3 Al_2O_3

The Al_2O_3 frequency distribution shows a distinctly bimodal trend (cf. Appendix C), with the sands containing 2.4 - 11% and the muds 12 - 21%. The highest concentrations of Al_2O_3 are found in the inner mud belt (fig. 10-12), undoubtedly a result of the total amounts of clay minerals and feldspar present there. Moir (1976) found that less clay was present in the outer shelf mud samples, which is supported in this study by the lesser average concentration of Al_2O_3 found in those samples. Hirst (1962b) used aluminum as an indicator of total clay mineral content, and Förstner (pers.

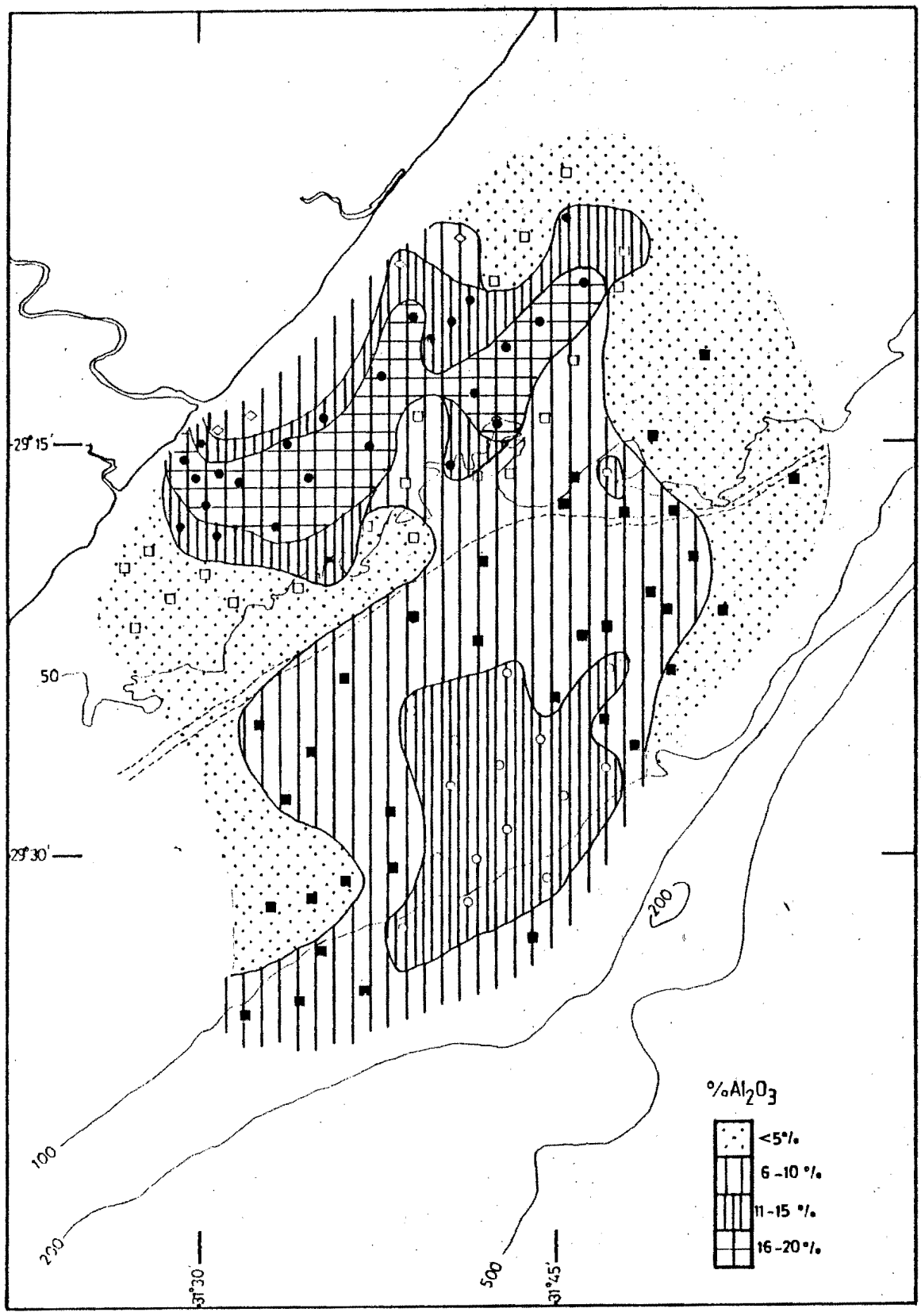

Figure 10-12. Distribution of Al_2O_3.

comm.) considers Al_2O_3 content to be the best representative of clay due to its immobility in the sedimentary environment. Further support of this correlation is found in the factor analysis (section 2.2.2), which shows Al_2O_3 to have the highest loading on the clay mineral factor.

3.1.4 Fe_2O_3 and MnO

Total iron was calculated as Fe_2O_3 due to the generally oxidised nature of surficial marine sediments. Fe_2O_3 varies with Al_2O_3 in all the sediments with slight deviations shown for the estuarine muds and the very fine nearshore sands that are enriched in heavy minerals (fig. 10-13). The mineralogy (chap. IX) shows that some of these samples contain magnetite, as was found by Fromme (1977). The high concentrations of Fe_2O_3 in the inner shelf mud belt (fig. 10-14), as well as the highly positive loading on the clay mineral factor, suggests that the iron in the region is predominantly associated with the clay mineral fraction. Förstner (pers. comm.) found that a high correlation of iron with aluminum is often indicative of homogeneity of clay minerals in an area. Iron that is not associated with the clays may be accounted for as ferruginous coatings on quartz and/or calcite grains; iron staining was observed in some mid-shelf sand samples. There is also the possibility of authigenic pyrite and/or monosulphides forming in the more reduced sectors of the mud column (Calvert, 1976). Pyrite was detected in some X-ray diffractograms (chap. IX, section 2.6), but as analyses for Fe^{2+} were not performed, its presence cannot be confirmed chemically.

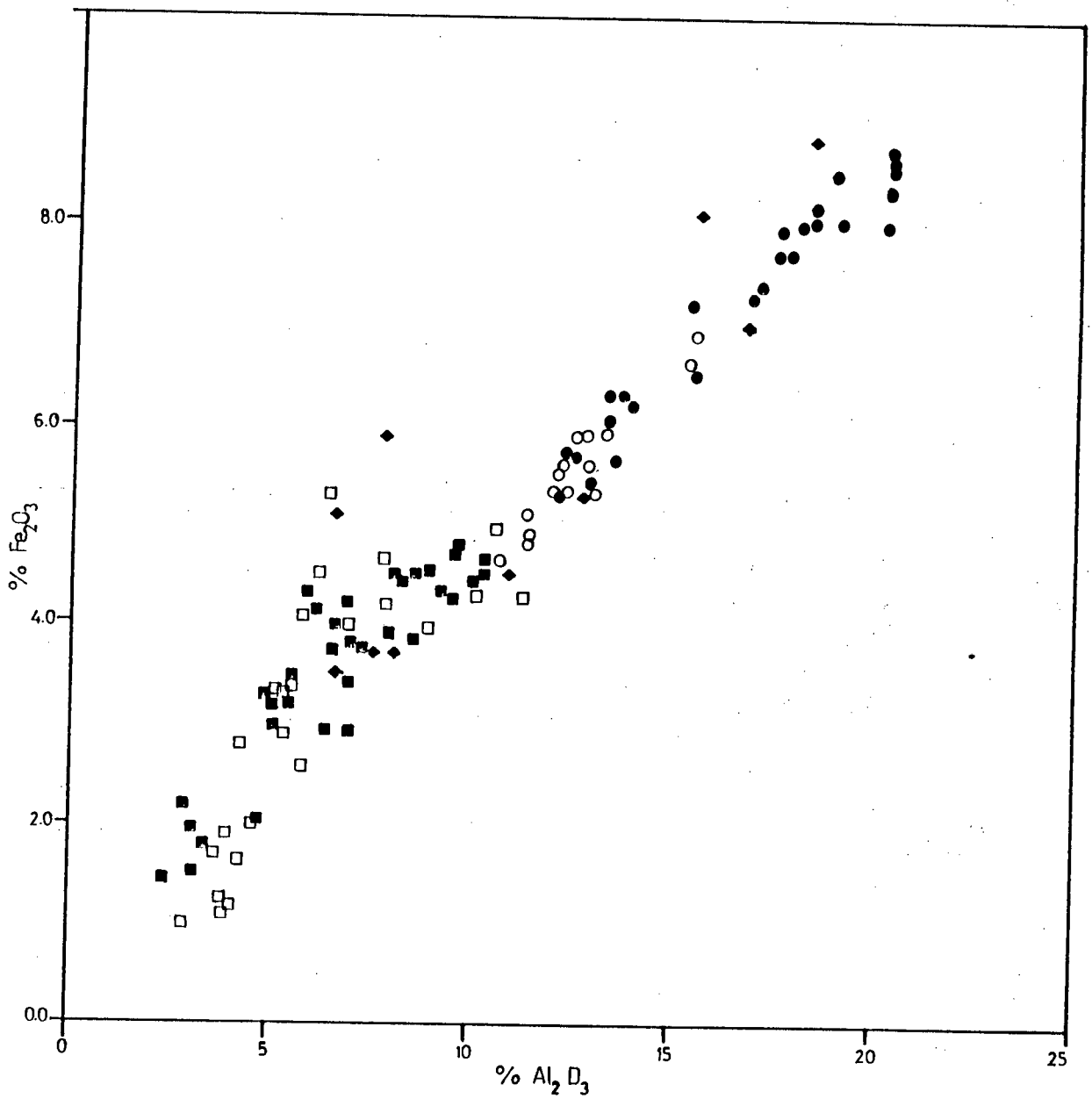

Figure 10-13. The relationship between Fe_2O_3 and Al_2O_3 contents of the study area sediments.

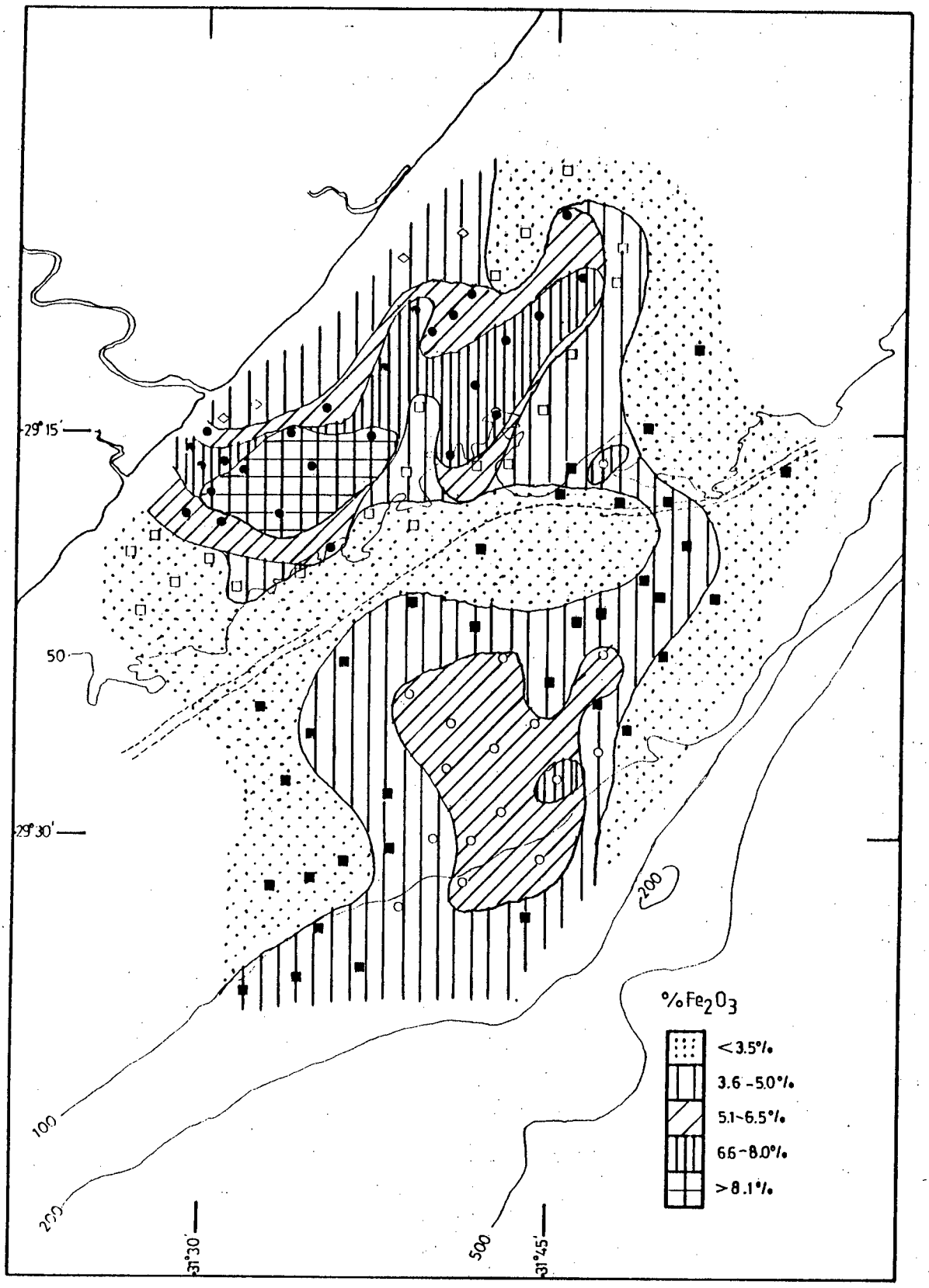

Figure 10-14. Distribution of Fe_2O_3 (Fe_2O_3 representing total iron content).

The MnO distribution (fig. 10-15) does not follow that of Fe_2O_3 closely. The highest concentrations of MnO (0.1 - 0.2%) are found in the generally coarse sands in the northeast and southwest mid-shelf regions of the study area, as well as in the river muds and in some of the mud samples immediately off the mouth of the Tugela. The mid-shelf sands show an antipathetic relation of MnO concentration to Fe_2O_3 concentration, while in the estuarine and inner muds the MnO and Fe_2O_3 concentration are sympathetic. This may be explained by theories on fractionation of iron and manganese in the exogenic cycle found in Degens (1965) and Keith and Degens (1959). Keith and Degens discuss how manganese and iron are closely associated in igneous rocks but are both dissolved to some extent under weathering and sedimentation conditions. Iron tends to remain behind or be transported in suspended form. Manganese tends to be transported in a dissolved state or adsorbed on clays. Iron and manganese ions respond differently to changes in pH and redox potential (Eh), resulting in different minerals of the iron and manganese family being deposited in sediments according to specific environmental conditions (Degens, 1965).

The presence of higher MnO concentrations in the coarse sands of the mid-shelf could be interpreted environmentally as indicative of regions of slow or non-deposition in the Recent, accompanied by a slow accumulation of manganese oxides that might possibly be the initial growths of continental shelf ferromanganese nodules. The accumulation of Mn relative to Fe increases in areas of low detrital deposition (Wedepohl,

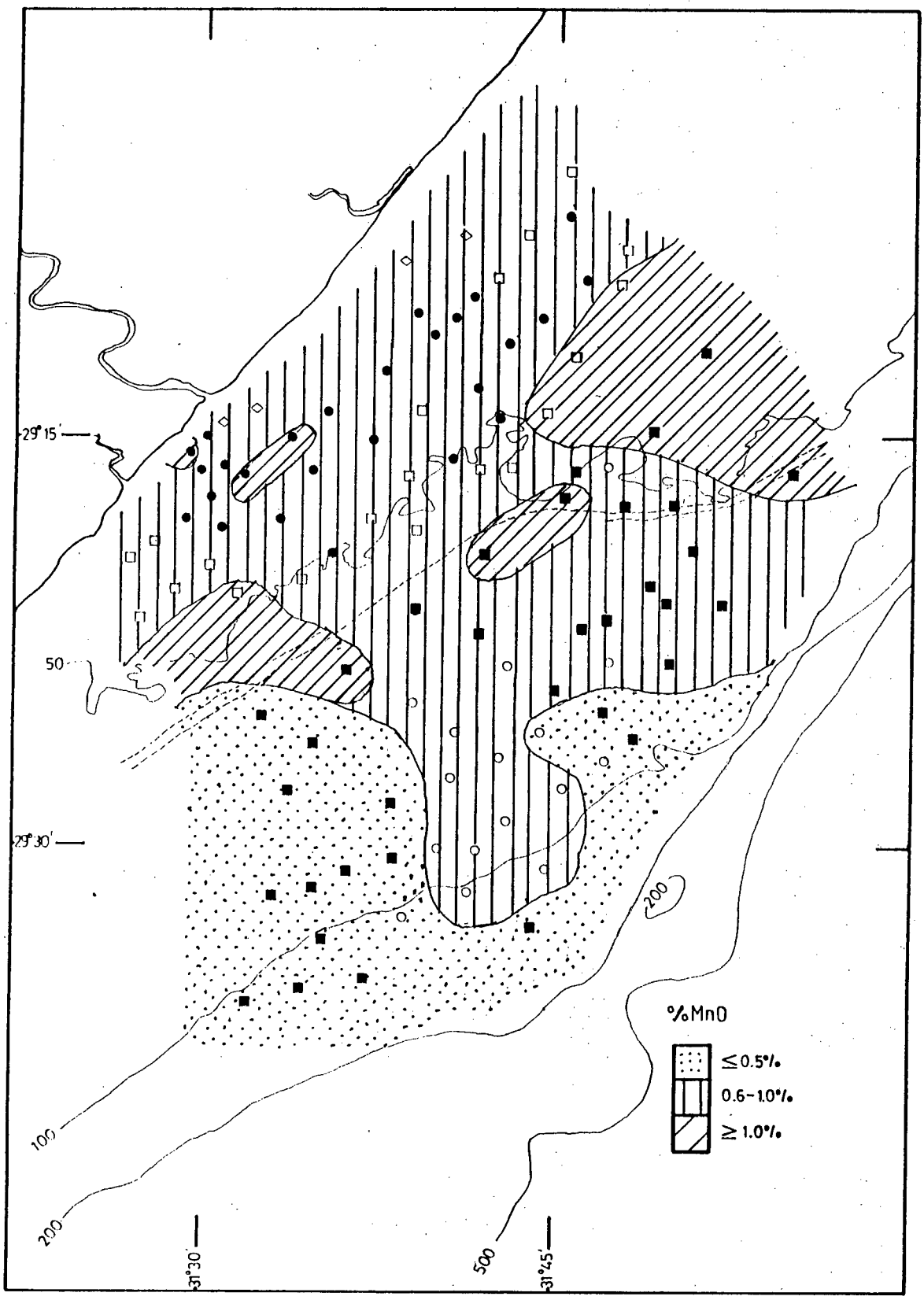

Figure 10-15. Distribution of MnO.

1978). Thus Mn/Fe (Fe representing total iron) in these areas tends to be higher than for areas of high deposition. The Mn/Fe ratios for the sands of the study area (Table 10-11) would appear to support the interpretation of slow or non-deposition on the mid-shelf, as the average Mn/Fe ratio for the inner sand group is higher than for the other sedimentary groups. Although no evidence of the common constituent minerals of such concretions (manganite as $\gamma MnO \cdot OH$ and δMnO_2) were noted in the X-ray diffractograms, manganese coatings on some grains were observed under the microscope in some of the mid-shelf sand samples.

3.1.5 CaO, CO_2 and MgO

CaO and CO_2 are both highly positively correlated on the quartz-feldspar/carbonate factor, as well as being highly correlated with each other in all the continental shelf samples. These correlations, along with the fact that virtually all the samples containing more than 10% CaO are located on the outer shelf and along the shelf break (fig. 10-16), are evidence that the major proportion of CaO is present in the area as $CaCO_3$ (calcite and aragonite) of predominantly biogenic origin. This is confirmed by the sympathetic distribution of CO_2 (fig. 10-17) to that of CaO, and the mineralogy determined on those samples containing high concentrations of CaO. It is interesting to note that the carbonate mineral components (viz. CaO, CO_2 and Sr) correlate with the gravel, very coarse sand and coarse sand in the mid- to outer shelf sands and with medium sand in the inner shelf sands. The mineralogy is significant in stating a biogenic origin of the

TABLE 10-11 : AVERAGE Mn/Fe RATIOS FOR THE SEDIMENTARY GROUPS IN THE STUDY AREA. (Fe = total Fe).

	$\frac{Mn}{Fe}$
Average Estuarine	0.018
Average River	0.019
Average Inner Shelf Muds	0.013
Average Inner Shelf Sands	0.033
(Four Very Nearshore Sands	0.019)
(Other Inner Shelf Sands	0.036)
Average Outer Shelf Muds	0.013
Average Outer Shelf Sands	0.024
Shales (in Clarke, 1924)*	0.013
Sandstones (in Clarke, 1924)*	0.007
Igneous Rocks (in Goldschmidt, 1937)*	0.020
Deep Sea Clays (in Wedepohl, 1978)	0.095

* As quoted in Hirst (1962a).

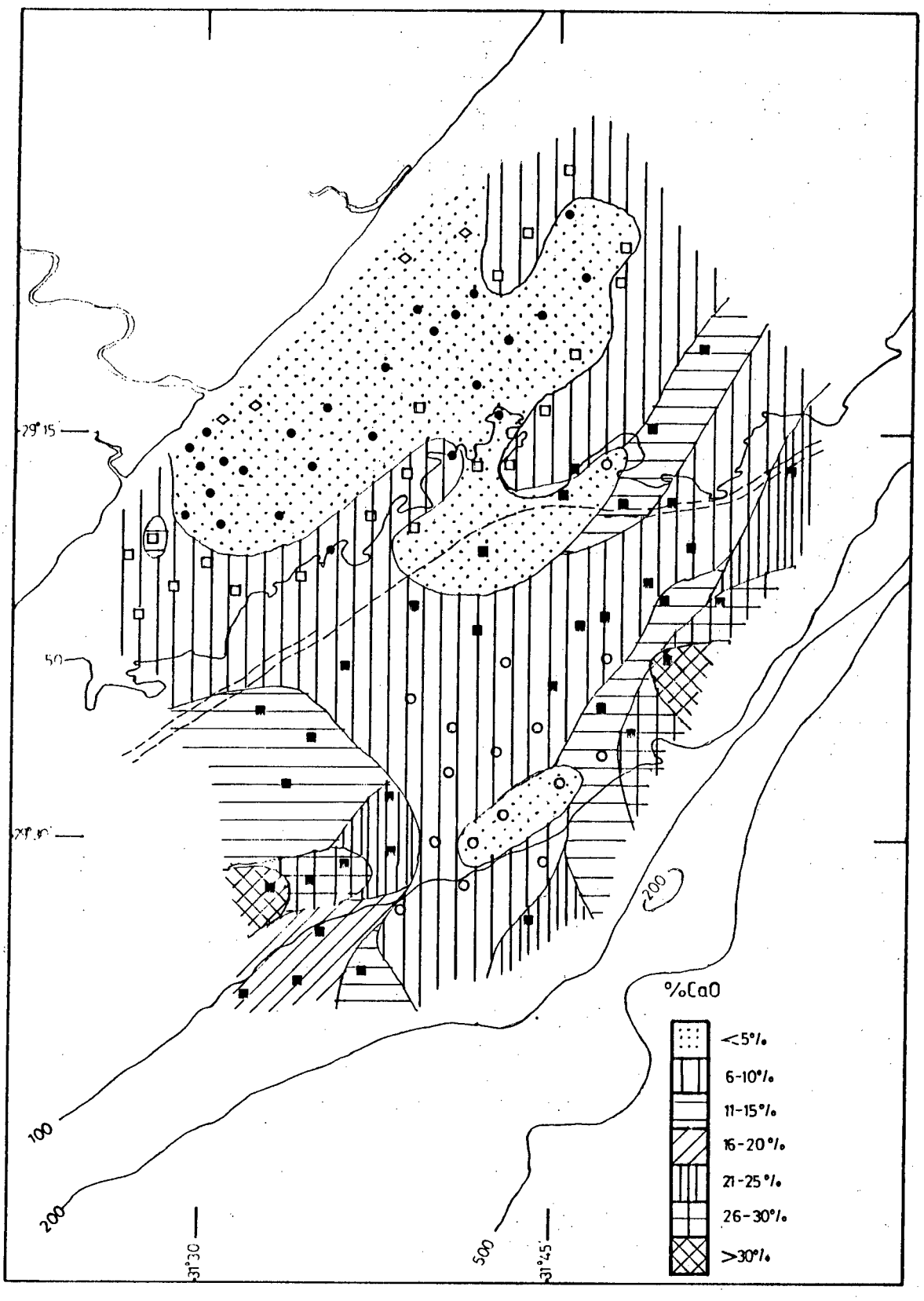

Figure 10-16. Distribution of CaO.

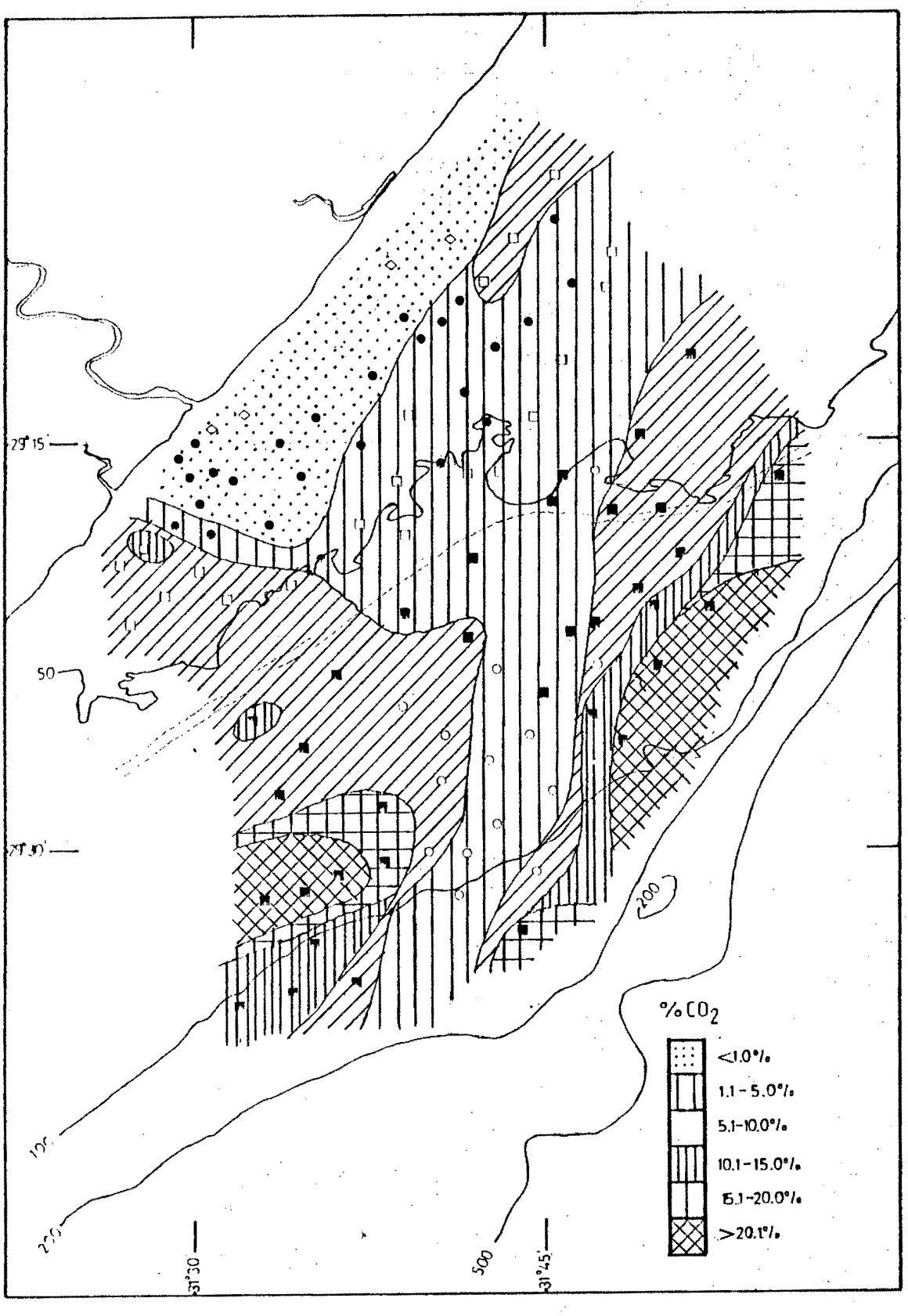

Figure 10-17. Distribution of CO_2.

carbonates, due to the presence of a greater proportion of high-Mg calcite relative to low-Mg calcite shown in the diffractograms of the outer shelf sands. High-Mg calcite is almost always formed by the concentration of Mg by organisms, the exception being the inorganic formation of dolomite (Siesser, 1971). No dolomite was identified in these samples. Any remaining CaO left over after assignment to $CaCO_3$ would presumably be accounted for by detrital feldspar (plagioclase) and possibly $Ca_3(PO_4)_2$, although the presence of collophane was not detected in the diffractograms, possibly due to the overlap of its peaks with those of other minerals.

The distribution of MgO (fig. 10-18) is not as well defined as that of CaO, although an apparent sympathetic relationship exists between the two oxides in the outer shelf sediments which show high CaO concentrations. The plot of CaO against MgO (fig. 10-19) shows a good correlation for these outer shelf sand samples compared to the rest of the sediments. This association was expected, from the presence of high-Mg calcite in these outer shelf samples and the fact that the outer shelf sand group is the only sedimentary group that shows a significant positive correlation of CaO with MgO (cf. Tables 10-5 to 10-8). MgO concentrations in the other groups, mainly the inner shelf muds, could be due to an association of MgO with the clays (it is usually found in chlorites and montmorillonites).

3.1.6 K_2O and Na_2O

K_2O is highly loaded on the clay mineral factor, as

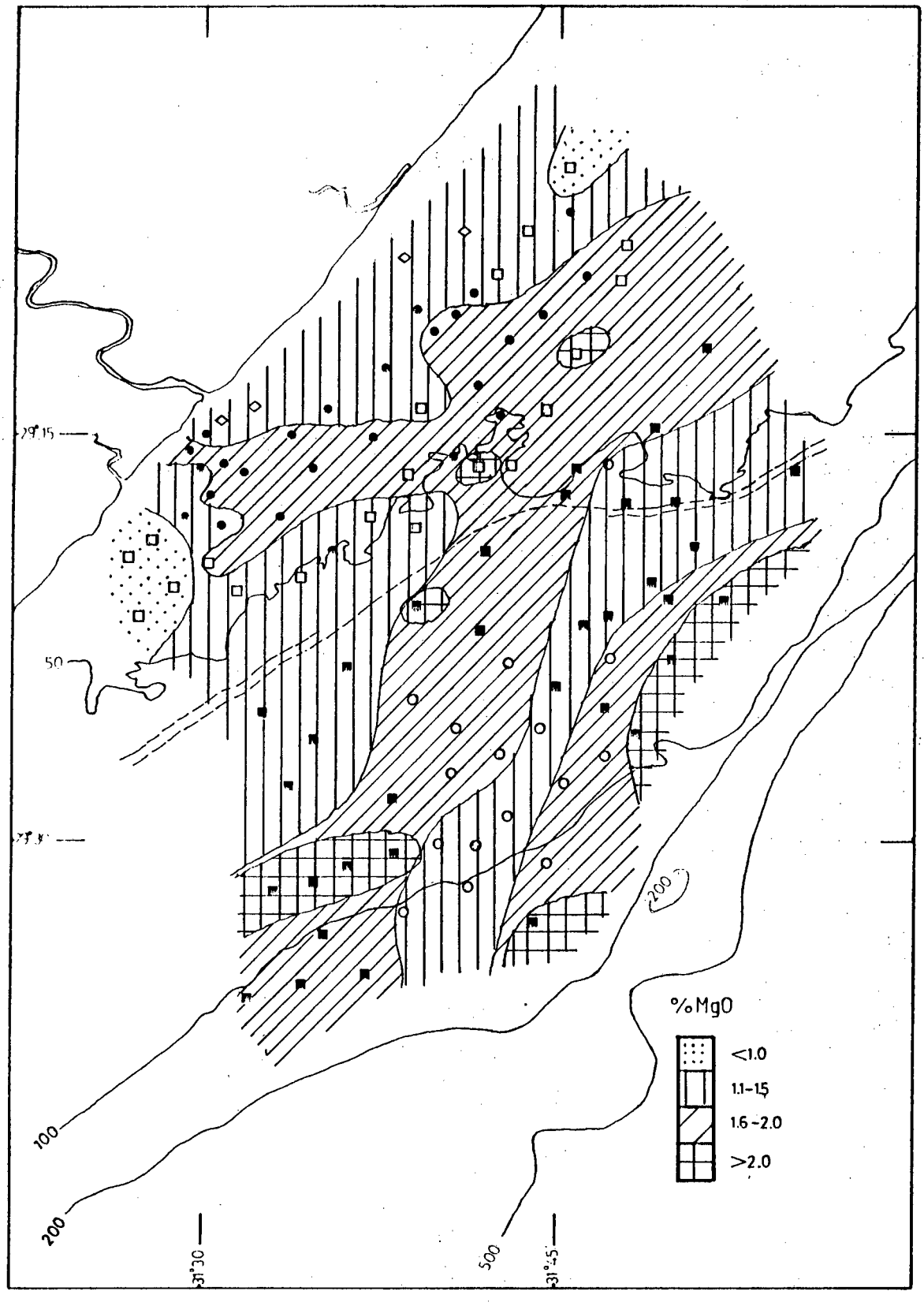

Figure 10-18. Distribution of MgO.

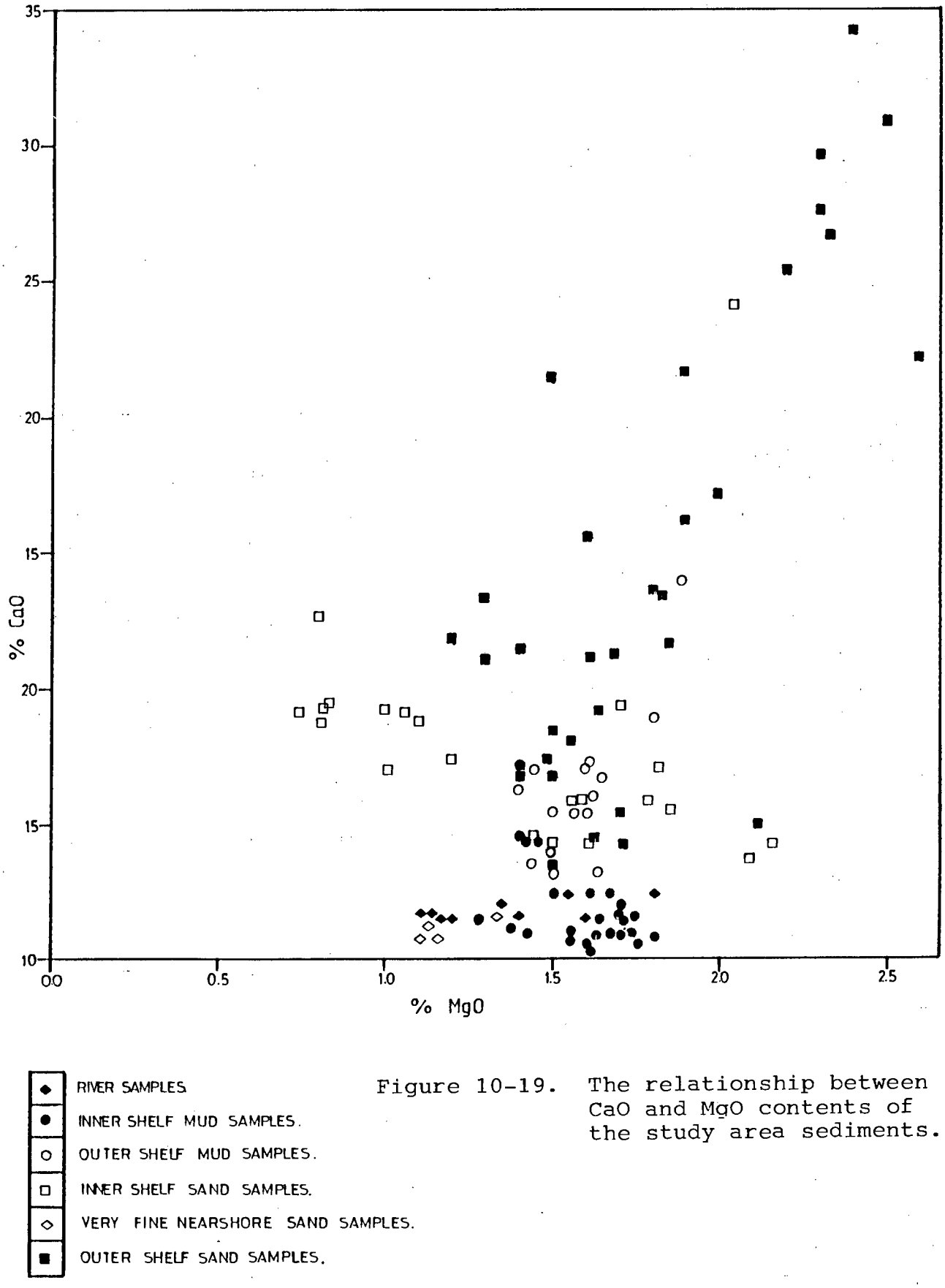

Figure 10-19. The relationship between CaO and MgO contents of the study area sediments.

would be expected from the known behaviour of potassium in substituting in clays (Mason, 1966). Its distribution (fig. 10-20) shows that the highest concentrations of K_2O lie in the mud belts, being more concentrated in the inner shelf mud belt than in the outer shelf mud belt. K_2O is highly correlated with Al_2O_3 in all groups except the inner sands, further indicating that it is predominantly located in the clay minerals, presumably mostly in illite. Any K_2O not accounted for in the clay minerals is explicable by the presence of K-feldspar in many of the samples. The fact that Na_2O is more highly correlated with Al_2O_3 than K_2O in the inner shelf sand samples is undoubtedly due to the greater proportion of plagioclase feldspar to K-feldspar present.

The Na_2O concentration is very low and varies only slightly over the study area (fig. 10-21). The highest concentrations of Na_2O are found in the four very fine nearshore sand samples, suggesting that it is associated with the hornblende and plagioclase found in these samples. This is supported by the relatively large hornblende peaks shown in the diffractograms of these samples (chap. IX, section 2.5). The rest of the Na_2O is most likely associated with the plagioclase (albite) present in many samples. It is unlikely that sodium is located in the clays, as the montmorillonite content of the samples was found to be low or non-detectable; also the loading of Na_2O on the clay mineral factor is zero.

Sodium is almost always depleted relative to potassium in sediments (compared to igneous rocks) due to its being

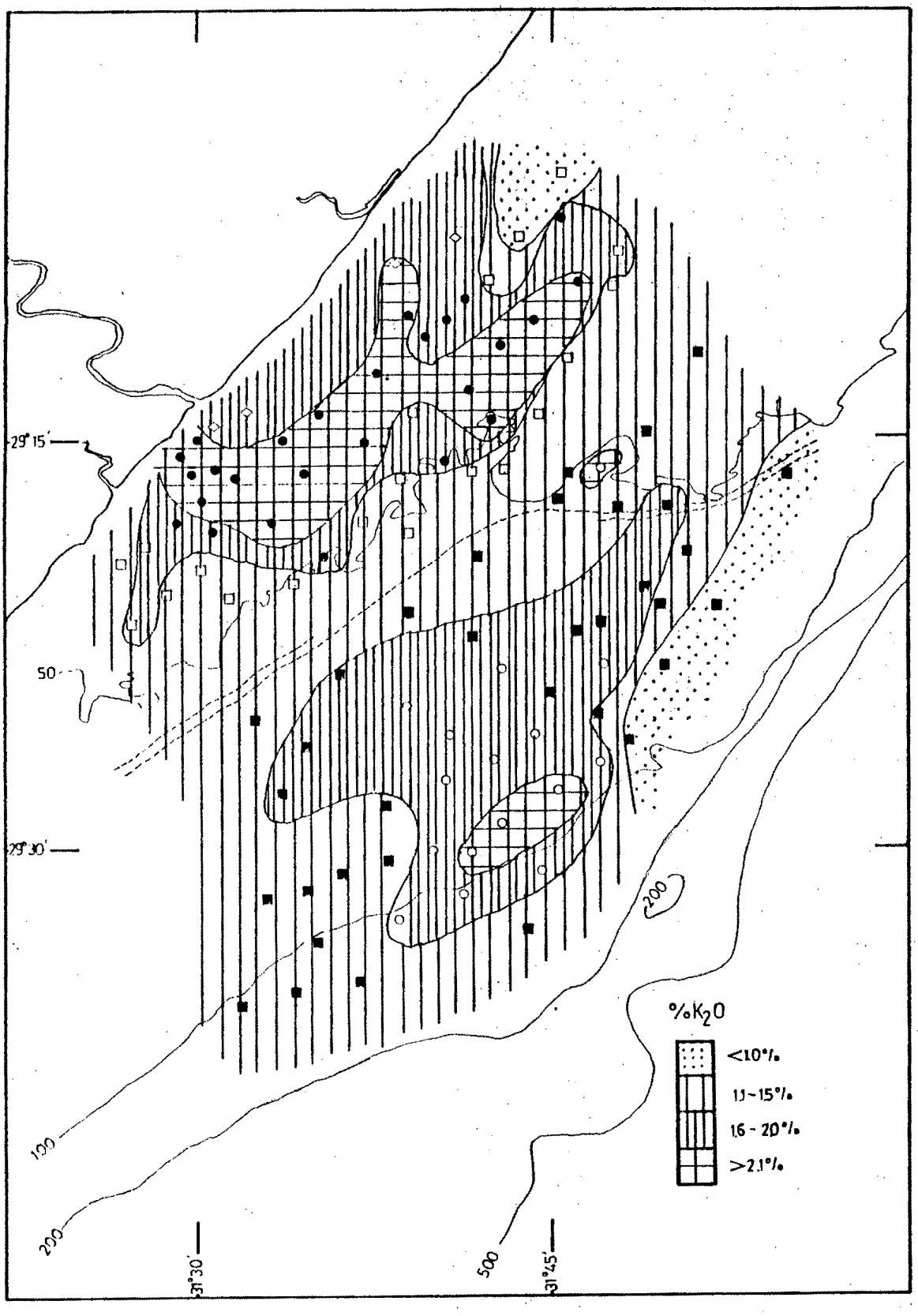

Figure 10-20. Distribution of K_2O.

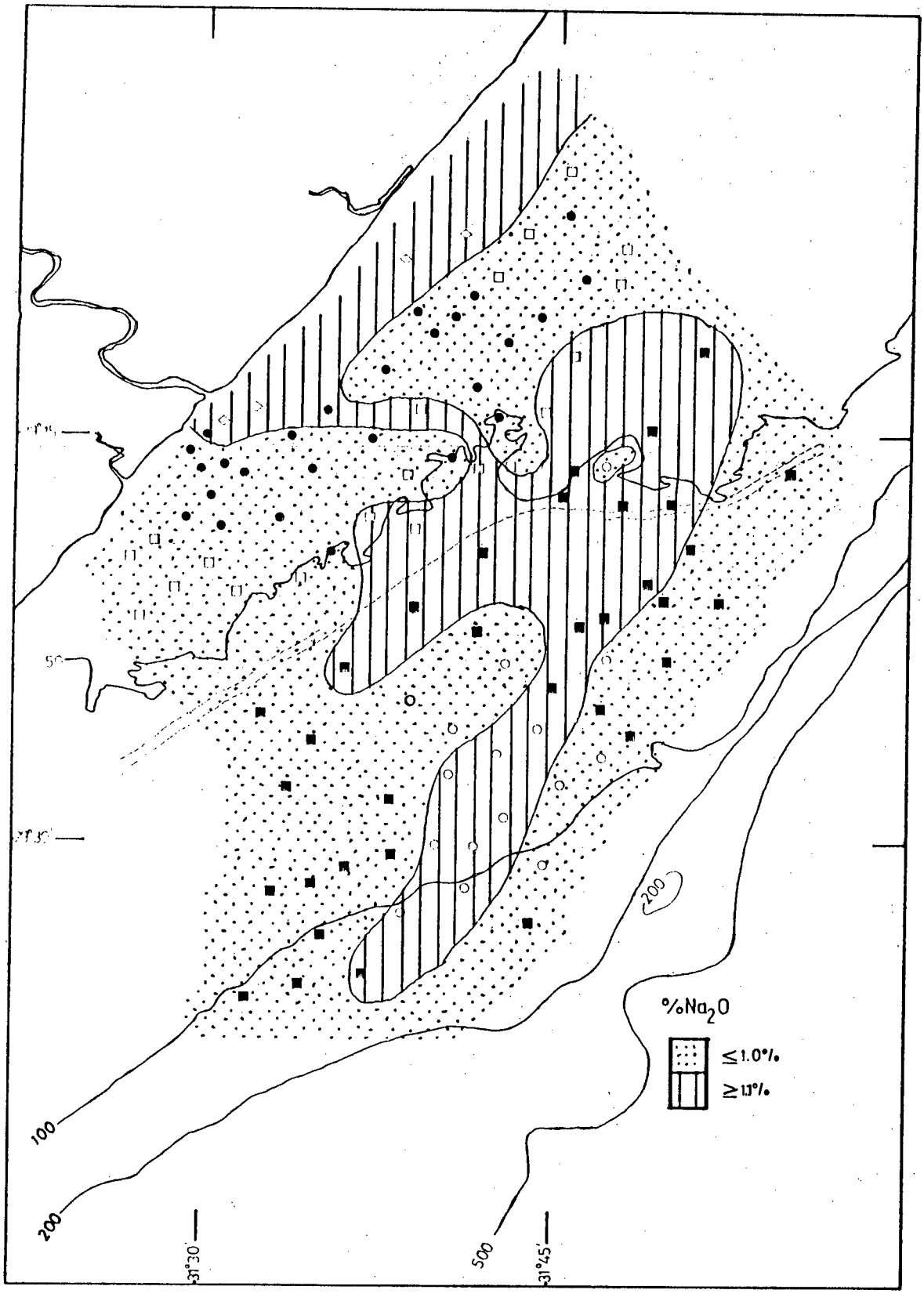

Figure 10-21. Distribution of Na_2O.

readily solubilized into oceanic waters (Mason, 1966). All the sediments show low Na/K ratios (Table 10-12), which, following the interpretation of Hirst (1962a), may be taken as an indication of slow depositional rates accompanied by increased cation exchange of K for Na. As Hirst (1962a) states that similar clay content is essential in drawing conclusions using the Na/K ratio, an interpretation of slow depositional rates may not be applicable to this study due to the difference in clay content between the inner and outer shelf mud samples. It might be better to interpret the Na/K ratios determined in this study in terms of their inverses, viz. K/Na, which would reflect the greater stability to weathering of K-feldspar over plagioclase.

3.1.7 P_2O_5

P_2O_5 is moderately loaded on the clay mineral factor. On the inner shelf, its distribution (fig. 10-22) follows closely that of the mud, with more dispersion of P_2O_5 evident on the outer shelf. The average concentration of P_2O_5 in the muds (inner muds 0.14%, outer muds 0.12%) is comparable with that for the average shale (0.16%; Wedepohl, 1969), although most sample concentrations are slightly lower. The phosphate could be associated with finely disseminated apatite, although, as stated earlier, neither apatite nor collophane was positively identified in the X-ray diffractograms. P_2O_5 is positively correlated with Al_2O_3 in all of the continental shelf sediment groups (cf. Tables 10-5 to 10-8), suggesting that it may be associated with the clay minerals. P_2O_5 may also be supplied by plant material associated with the organic matter

TABLE 10-12 : AVERAGE Na/K RATIOS FOR THE SEDIMENTARY GROUPS IN THE STUDY AREA.

	Na/K
Average Estuarine	0.284
Average River	0.743
Average Inner Shelf Muds	0.344
Average Inner Shelf Sands	0.700
(Four Very Nearshore Sands	0.776)
(Other Inner Shelf Sands	0.685)
Average Outer Shelf Muds	0.485
Average Outer Shelf Sands	0.665
Argillaceous Sediments (in Rankama & Sahama, 1950)*	0.360
Igneous Rocks (in Rankama & Sahama, 1950)*	1.090

* As quoted in Hirst (1962a).

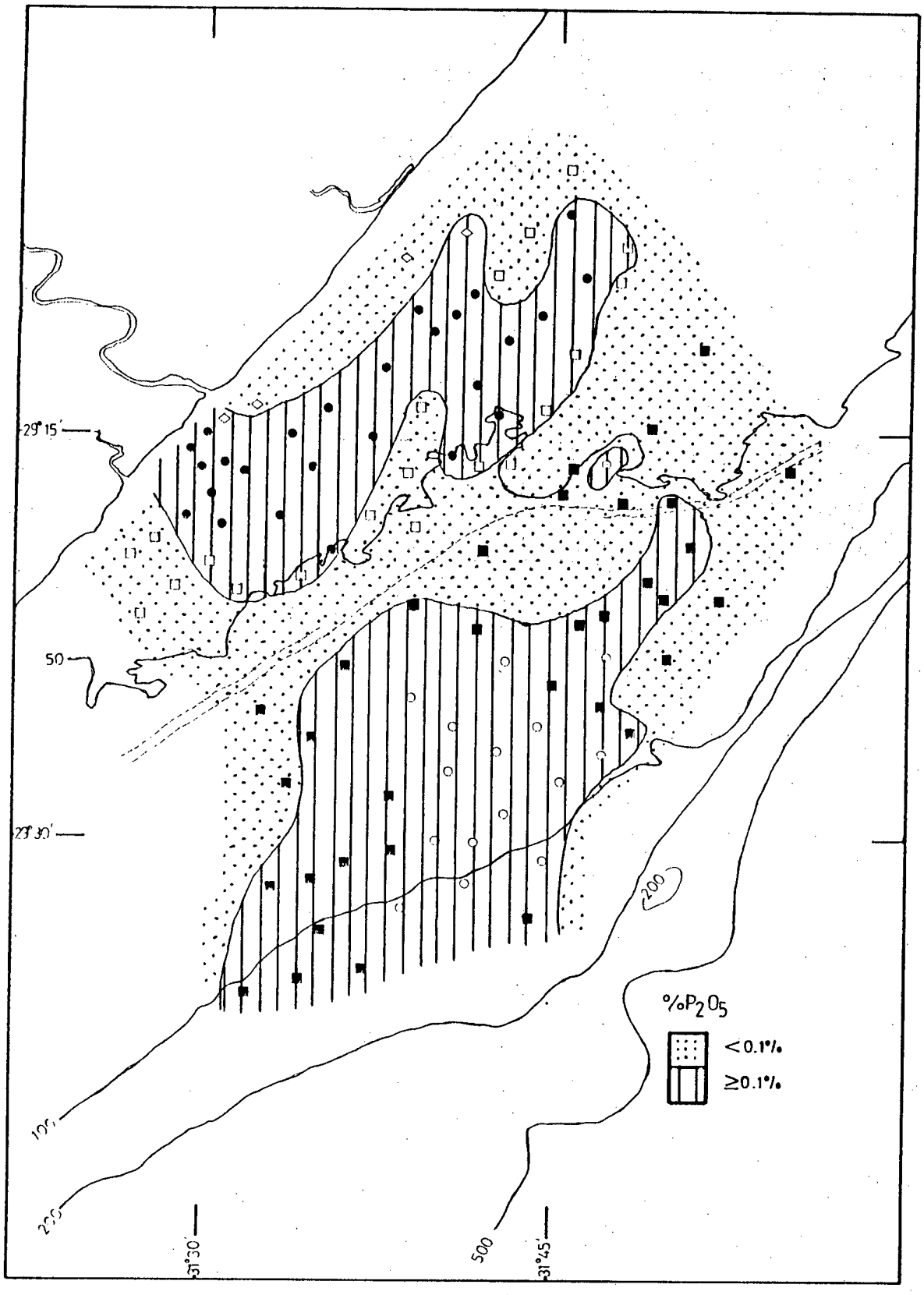

Figure 10-22. Distribution of P_2O_5.

found in the muds. Significant correlations of P_2O_5 with organic matter, however, are only shown in the outer shelf muds and sands, possibly due to phytoplankton input (Degens, 1965).

3.1.8 Organic Matter and H_2O+

The distribution of organic matter is shown in figure 10-23. The region of highest organic matter content (>2.6%) is clearly associated with the river input, reflected by the black colour of the samples taken in the vicinity of the river mouth (Appendix A, Table A-2). The black colour probably results from the decomposition of the organic matter, creating a reducing environment in which sulphides (which are black) may be precipitated. As the organic fraction is largely detrital (Riley and Chester, 1971), this association would be expected. The organic matter concentrations are relatively high over the whole area of the inner shelf mud belt (1.6 - 4.3%), with concentrations of 1.6 - 2.1% found in the outer shelf mud samples. Degens (1965) states that the average organic matter content of shales is 2.1%, showing the values obtained in this study not to be anomalous. Organic matter is highly loaded on the clay mineral factor, as might be expected from its usual relationship to mud in the sedimentary environment. A major transport mechanism for organic matter is by its coating clay particles. Organic matter is more well correlated to Al_2O_3 in both the outer shelf and the inner shelf muds, further supporting the association of organic matter to the clay minerals. Small twigs and leaves were found in the 63 μm sieve when separating the mud from the

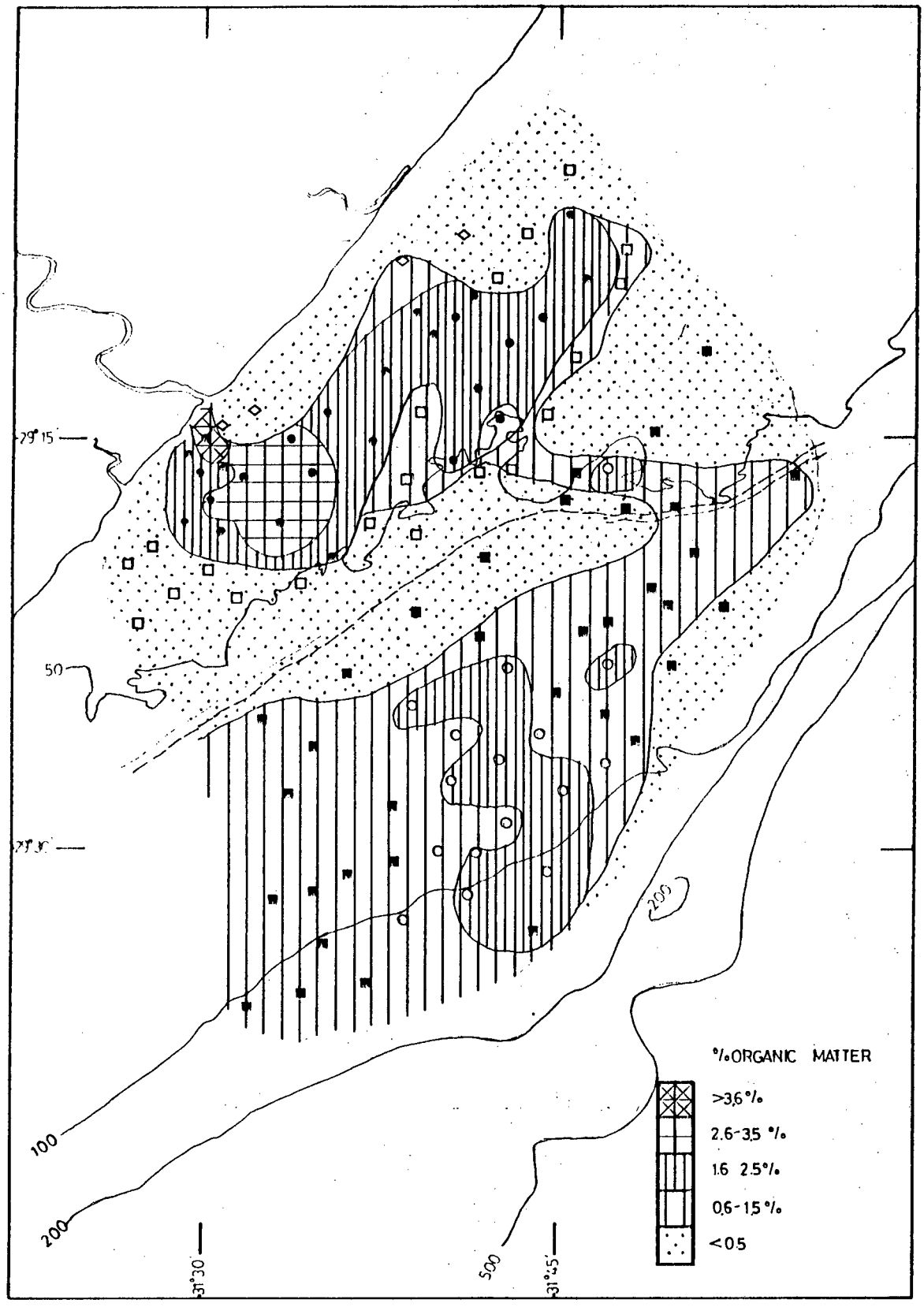

Figure 10-23. Distribution of organic matter.

sand, particularly in the inner shelf mud samples.

H_2O+ is highly positively correlated with the clay mineral factor, and it can safely be assumed that most, if not all, of the water is located in the intersheet positions of the clay minerals or present in the octahedral layers as OH^- ions.

3.2 Minor and Trace Elements

The average minor and trace element compositions of the sedimentary groups found in this study, along with the world-wide averages for shale, sandstone and carbonate rocks, are presented in Table 10-13.

3.2.1 Sulphur

Sulphur is positively loaded on both the clay mineral factor and the quartz-feldspar/carbonate factor (0.443 and 0.597 respectively). The distribution of sulphur (fig. 10-24) shows an association of sulphur with the inner shelf mud samples, although a negative correlation is shown between S and mud in Table 10-5. The relatively high concentrations of sulphur in some of the mid- to outer shelf sand samples are the obvious cause of the correlation of this element with the carbonate mineral components in the sand sample groups (Tables 10-6 and 10-8). Sulphur is generally not geochemically associated with carbonate minerals, and, as there was a lack of identifiable pyrite or monosulphides in most of these sand samples, the relationship is inexplicable from the results of this study. It should be noted that other researchers also found anomalous sulphur results from their analyses

TABLE 10-13 : MINOR AND TRACE ELEMENT CONCENTRATIONS (ppm).

ELEMENT	ESTUARY	RIVER	INNER SHELF MUD	INNER SHELF SANDS	OUTER SHELF MUD	OUTER SHELF SANDS	WORLDWIDE AVERAGES * SHALE	SANDSTONE	CARBONATE
S	561	154	2103	679	1542	1581	2400	240	1200
Rb	86	54	117	45	96	52	140	60	3
Sr	115	158	145	305	333	677	300	20	610
Y	34	18	30	16	22	15	26	40	30
Zr	235	268	226	337	292	208	160	220	19
Nb	16	8.7	15	6.5	13	6.1	11	0.0X	0.3
U	2.4	1.6	3.0	1.4	3.0	1.5	3.7	0.45	2.2
Th	14	7.3	14	6.7	12	7.2	12	1.7	1.7
Pb	22	16	24	14	21	15	20	7	9
Zn	78	37	80	24	56	30	95	16	20
Cu	56	16	36	6.1	19	8.1	45	X	4
Ni	88	35	58	19	43	22	68	2	20
Co	36	19	27	12	19	12	19	0.3	0.1
Cr	211	152	152	97	134	89	90	35	11
V	158	88	128	59	93	57	130	20	20
Ba	611	558	462	370	393	278	580	X0	10
Sc	28	12	23	9.9	18	11	13	1	1
Br	13	<1.0	22	4.7	45	20	4	1	6.2
Ga	20	8.9	20	6.3	15	7.5	19	12	4
La	38	18	38	16	25	15	92	30	X
Ce	80	38	84	36	62	39	59	92	11.5
Nd	46	21	42	19	30	20	24	37	4.7
As	7.4	3.1	14	12	11	12	13	1	1

* Turekian, K.K. & Wedepohl, K.H. (1961). Distribution of the elements in some major rock units of the Earth's crust. Bull. Geol. Soc. Amer. 72, 175-92.

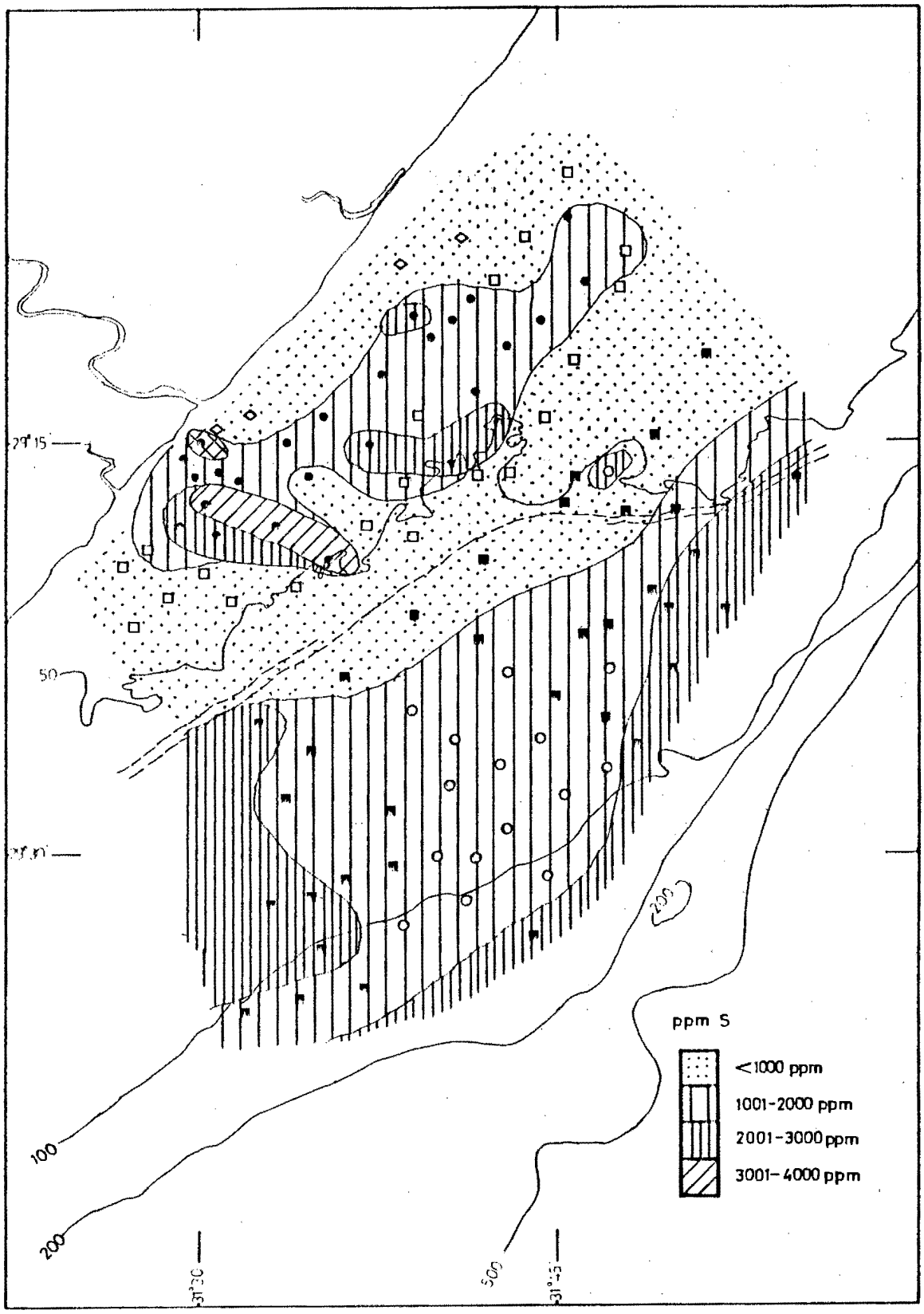

Figure 10-24. Distribution of sulphur.

run at the same time as the study samples, indicating a possible analytical problem. Thus, the reliability of the sulphur data is questionable, and not too much emphasis should be placed upon them.

3.2.2 Rubidium

Rubidium correlates very well with Al_2O_3 in all the sedimentary groups and is highly positively loaded on the clay mineral factor, indicating that its presence in the study area is primarily due to its substitution (for potassium) in and adsorption onto the clays. Hirst (1962b) suggested that clays have a higher adsorptive capacity for rubidium than for potassium, supported in this study by rubidium having a higher loading (0.955) on the clay mineral factor than potassium (0.893). Rubidium that is not associated with the clay minerals may be accounted for by its presence in K-feldspar and mica. The highest concentrations of rubidium are found in the inner shelf mud belt (fig. 10-25), which has already been shown to contain more clay than does the outer shelf mud belt (cf. section 3.1.3). The rubidium contents of the sediment groups in the study area (Table 10-13) are somewhat depleted compared to the average value of 140 ppm for shales, probably due to dilution by quartz.

Rubidium is geochemically coherent with potassium, being similar in ionic charge (both +1), ionic radius (Rb^+ 0.147 nm, K^+ 0.145 nm), and bonding properties (Mason, 1966). The K/Rb ratios for the sedimentary groups in this study show a characteristic enrichment of rubidium relative to potassium in

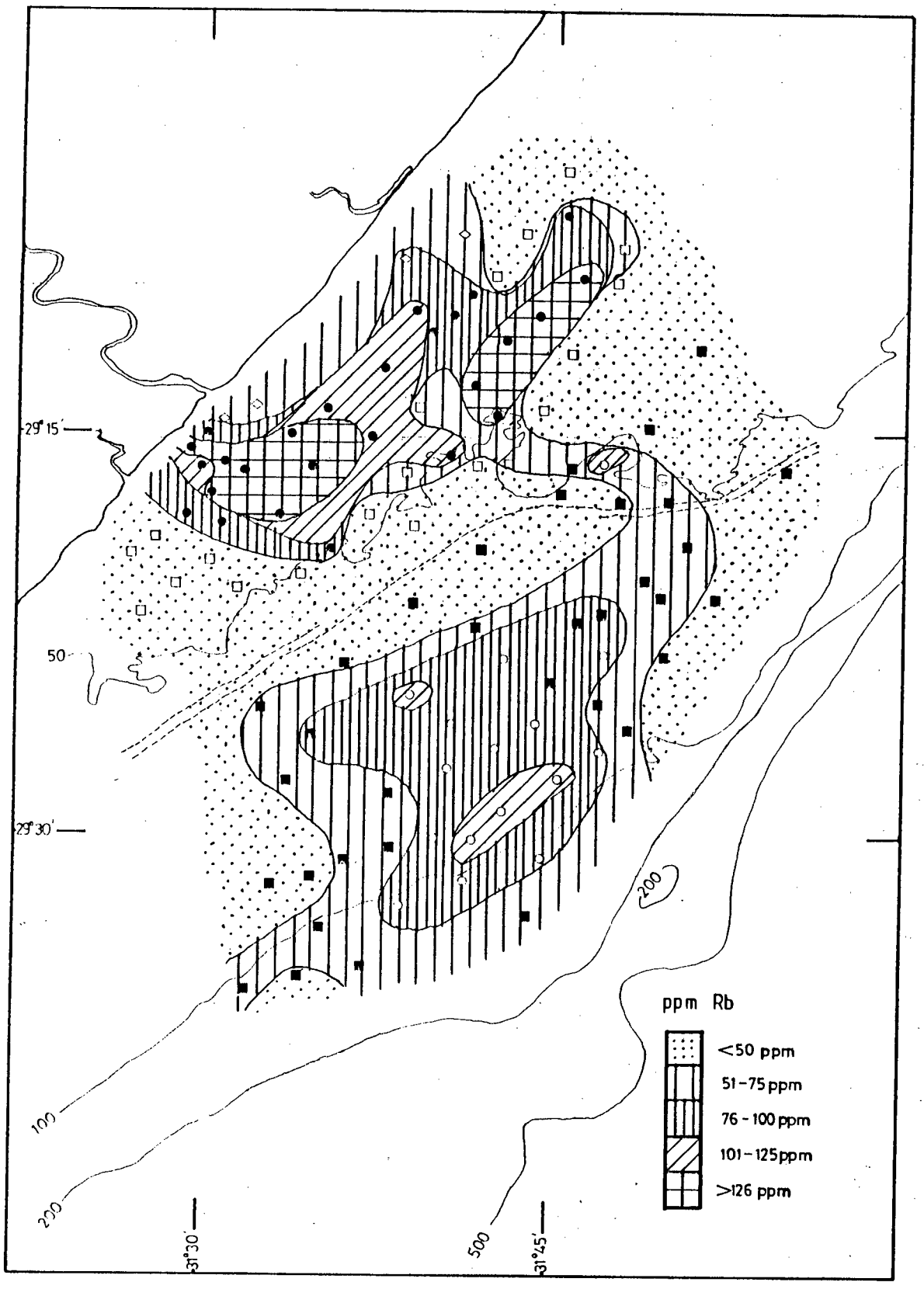

Figure 10-25. Distribution of rubidium.

the muds as compared with the sands. The estuarine, inner and outer shelf muds have average K/Rb values of 165, 161 and 169 respectively, compared to the average value for shales of 150 (Heier and Billings, 1978). The values are well within the range used to identify marine shales (150 - 200) quoted by Heier and Billings (1978). The average K/Rb values for the inner and outer shelf sands are 262 and 219 respectively, comparable to the values of 230 - 260 found for sands by Hirst (1962b) in the Gulf of Paria sands. The river sands have an average K/Rb value of 234.

3.2.3 Strontium

The strontium distribution (fig. 10-26) shows a well-defined seaward increase in concentration, following the distributions of CaO and CO_2 closely. This is due to the isomorphic substitution of Sr (ionic radius 0.116 nm) for Ca (ionic radius 0.103 nm) in the carbonate structure, preferentially entering aragonite over calcite. Strontium is the most highly positively loaded variable on the quartz-feldspar/carbonate factor, further substantiating its close association with the carbonate minerals in the study area.

There is the possibility of some association of strontium with the clays in the mud samples. Cook and Mayo (1980) hypothesized that there may be limited substitution of Sr for K in the clays, or that Sr may be adsorbed onto the clay particle surfaces. The strongly negative loading of Sr (-0.459) on the clay mineral factor, due to its strong relationship with CaO_2, would tend to rule out such a relationship between

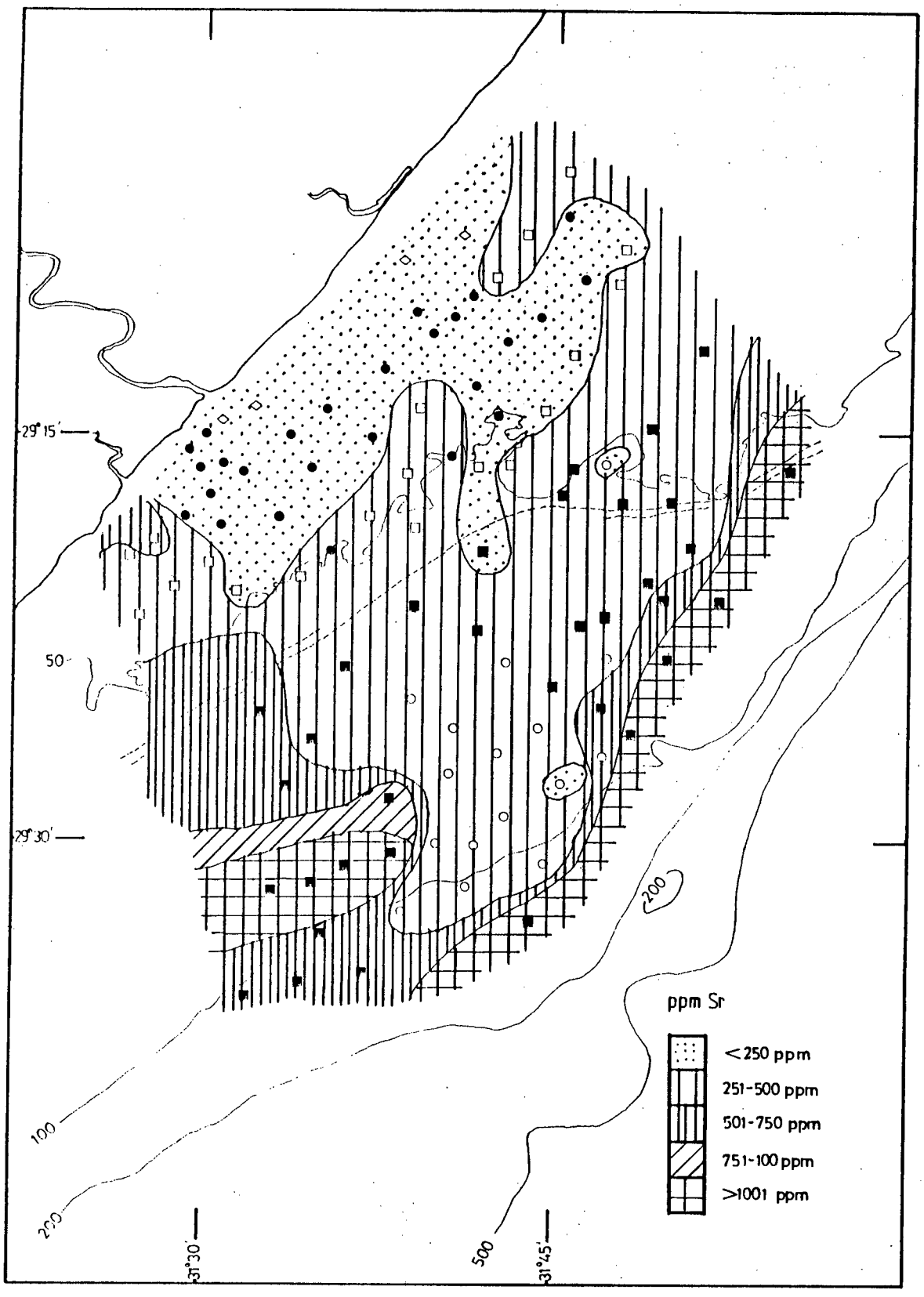

Figure 10-26. Distribution of strontium.

strontium and the clay minerals in the continental shelf samples. However, a high correlation of Sr with mud is seen in the river samples (Table 10-4), probably because there is no carbonate component to hide the Sr-clay relationship in the river environment.

3.2.4 Yttrium

The highest concentrations of Y (>30 ppm) are found in the very fine nearshore sands, with the outer shelf mud samples also showing fairly high (20 - 26 ppm) concentrations. Yttrium has a high positive loading on the clay mineral factor, and it shows significant correlations in all the sedimentary groups with Al_2O_3, TiO_2, Fe_2O_3 and several other elements that are related to the clays. Thus it seems likely that yttrium is predominantly associated with the clay minerals in the study area. The distribution of yttrium (fig. 10-27), together with its positive loading on the heavy mineral factor, suggests an additional association of Y with the heavy minerals in the nearshore sands and in the outer shelf muds. Yttrium has been found in hornblende (Mason, 1966). More detailed research into the heavy mineral fraction would have to be done to substantiate this suggestion.

3.2.5 Zirconium

The zirconium distribution is shown in figure 10-28. All the mud samples are enriched in Zr relative to the average value for shales of 160 ppm; they are even enriched relative to the average value for South African shales given by Erlank et al. (1978) as 200 ppm. The highest zirconium concentra-

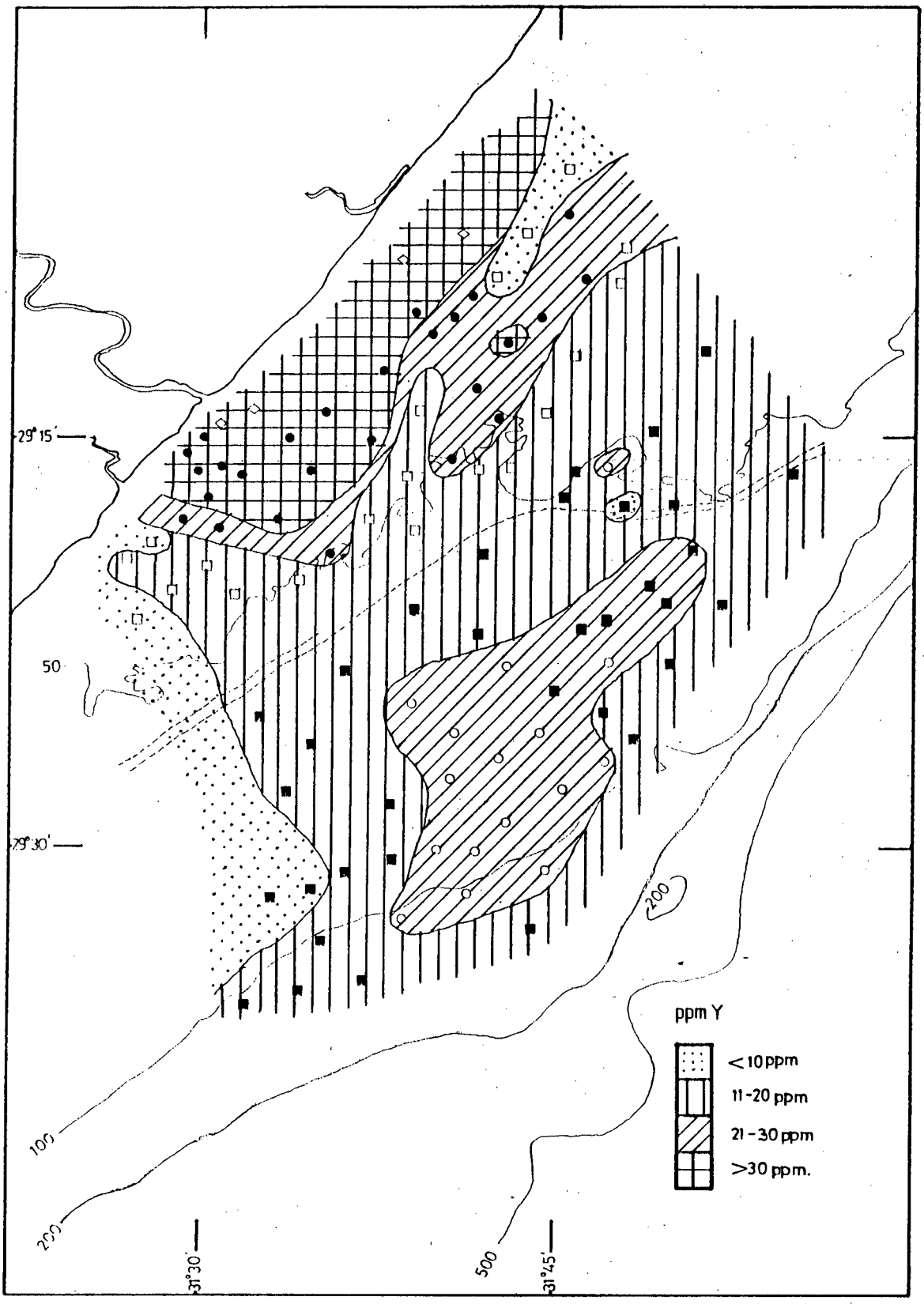

Figure 10-27. Distribution of yttrium.

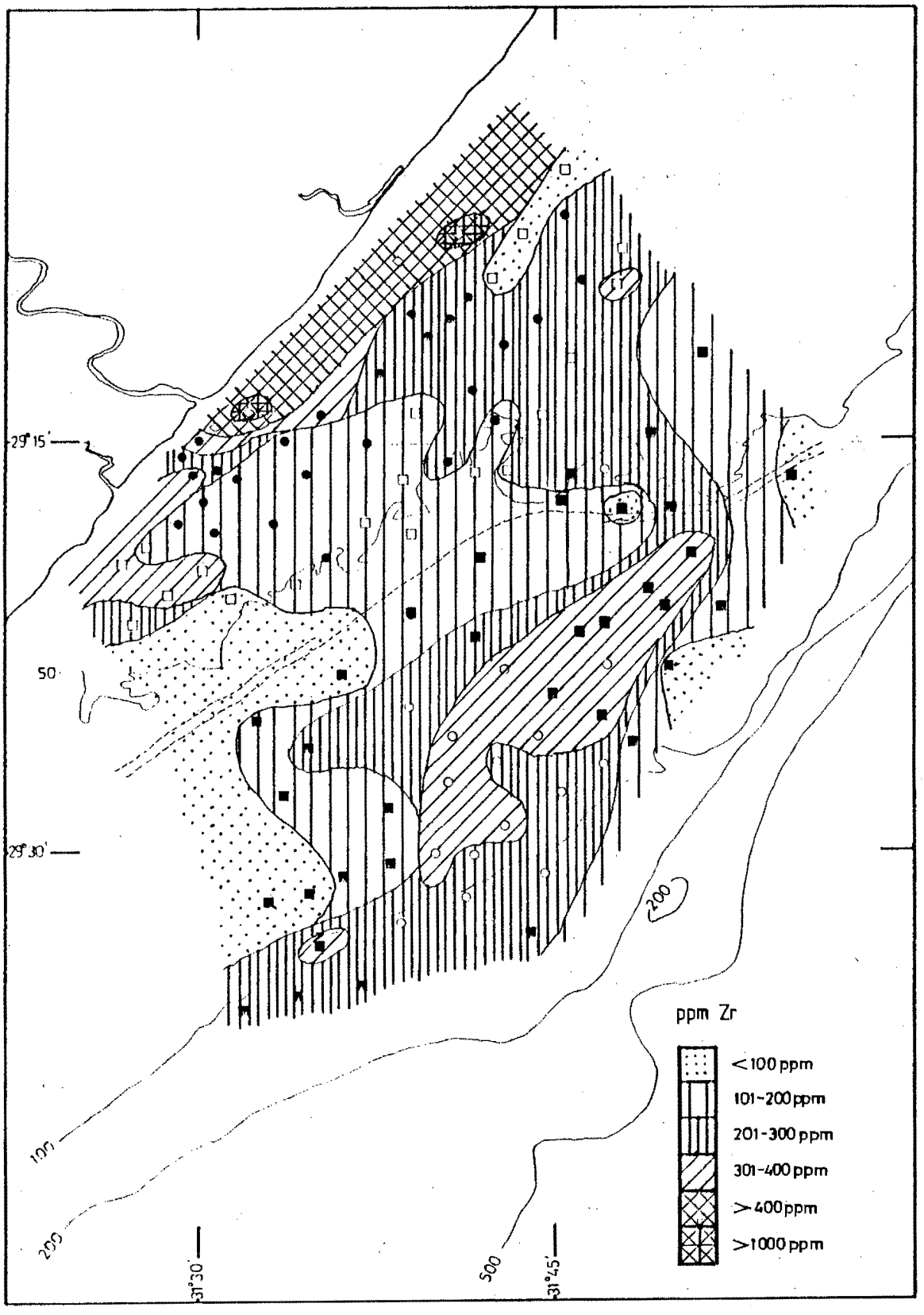

Figure 10-28. Distribution of zirconium.

tions (700 - 1500 ppm) are found in the four very fine nearshore sands, confirming this region as a heavy mineral province. Zircon was identified in the X-ray diffractograms of two of these samples (cf. chap IX, section 2.5). The area of Zr concentration >300 ppm coinciding with the position of the outer shelf mud belt could be significant in identifying this region as a Pleistocene depocentre. Holmes (1971) found the Zr content of sediments to be a fairly reliable indicator of ancient shoreline deposits. Although the concentrations of Zr in the outer mud samples are much less than those in Holmes' study (he used values >1000 ppm), the fact that the concentration of Zr in the outer shelf muds is higher than the surrounding mid- and outer shelf sands would appear meaningful. Zirconium concentration is dependent on the provenance of the sediment rather than depositional processes (Hirst, 1962b), and as such, adds further verification to the previously stated hypothesis of the outer shelf mud belt being the relict Pleistocene depocentre of the Tugela River.

3.2.6 Niobium

Niobium is significantly correlated to Al_2O_3 in all the sedimentary groups, and its distribution follows that of Al_2O_3 quite closely (fig. 10-29, cf. 10-12). Thus, it seems likely that the niobium present in the study area is predominantly associated with the clays. Further evidence of this association is the high positive loading of Nb on the clay mineral factor. The average values of the estuarine, inner shelf and outer shelf muds (Table 10-13) show slight enrichment of Nb over the average value for shales of 11 ppm. The high con-

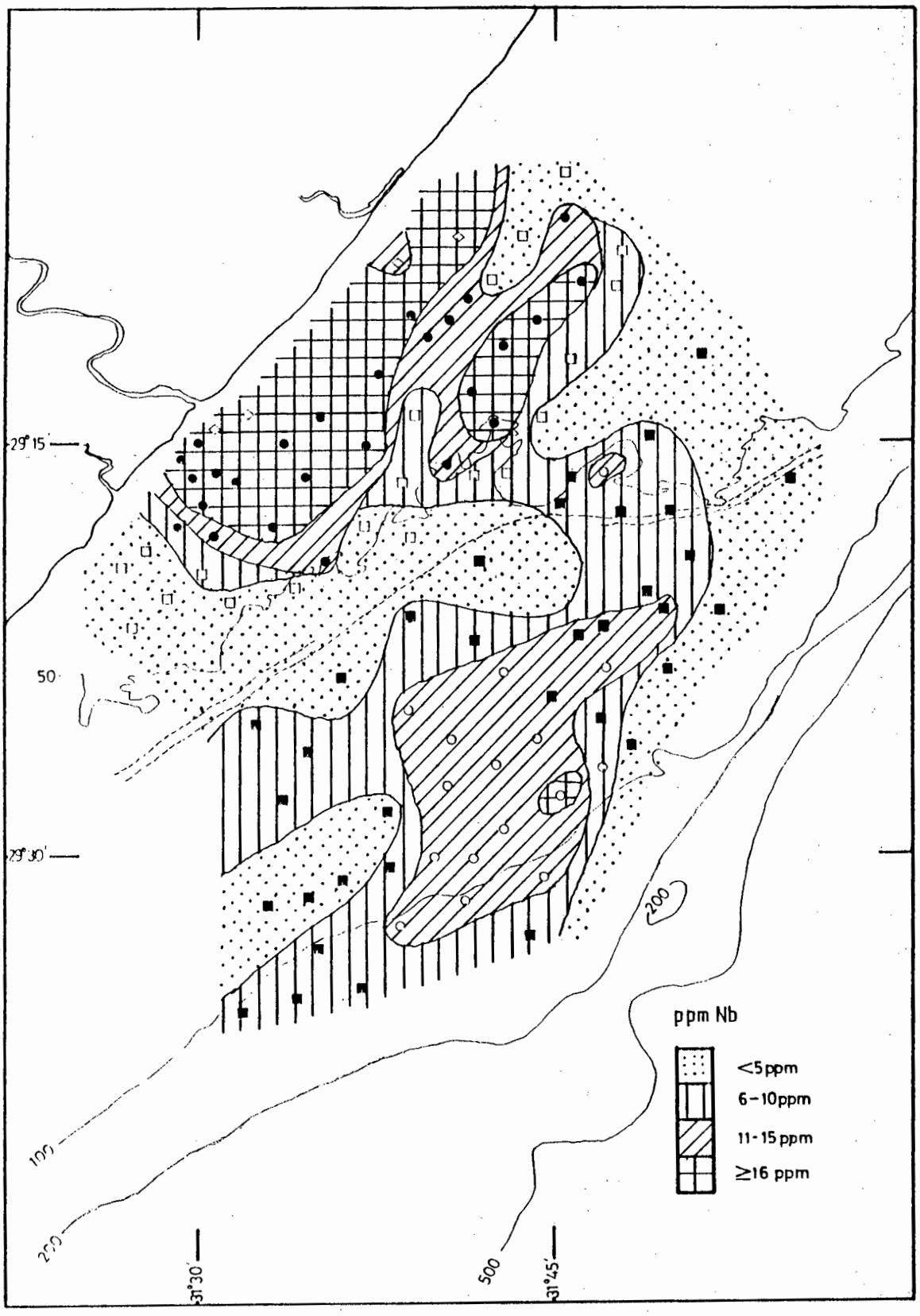

Figure 10-29. Distribution of niobium.

centrations of niobium in the four very fine nearshore sand samples and in the nearest-shore muds (16 - 18 ppm) could possibly indicate a secondary association of niobium to the heavy minerals and the factor analysis (section 2.2.2) shows Nb to be positively correlated with the heavy mineral factor. Niobium has been found as an accessory element in ilmenite (Mason, 1966) and perhaps is indicative of the presence of ilmenite in these samples.

3.2.7 Uranium and Thorium

Uranium and thorium are correlated with each other in the sand samples (Tables 10-4 to 10-8), and their distributions are generally similar over the study area (figs. 10-30 and 10-31). Many samples have concentrations of U below the detection limit, and few samples exceed the average value of U for shales of 3.7 ppm. The highest concentrations of uranium are found in the very fine nearshore sands and muds, as well as in some of the outer shelf muds. Uranium is positively loaded on the clay mineral factor, and has been found to concentrate in the clays (generally illite) of black shales (Mason, 1966), and in the anoxic zone of marine sediments in restricted basins (Rogers and Adams, 1978). A smaller positive loading of uranium is found on the heavy mineral factor, although which heavy mineral(s) it might be associated with is not clear from the results of this study.

Thorium concentrations are generally close to the average value for shales (12 ppm) in the inner and outer shelf mud samples (14 and 12 ppm, respectively), with the exception

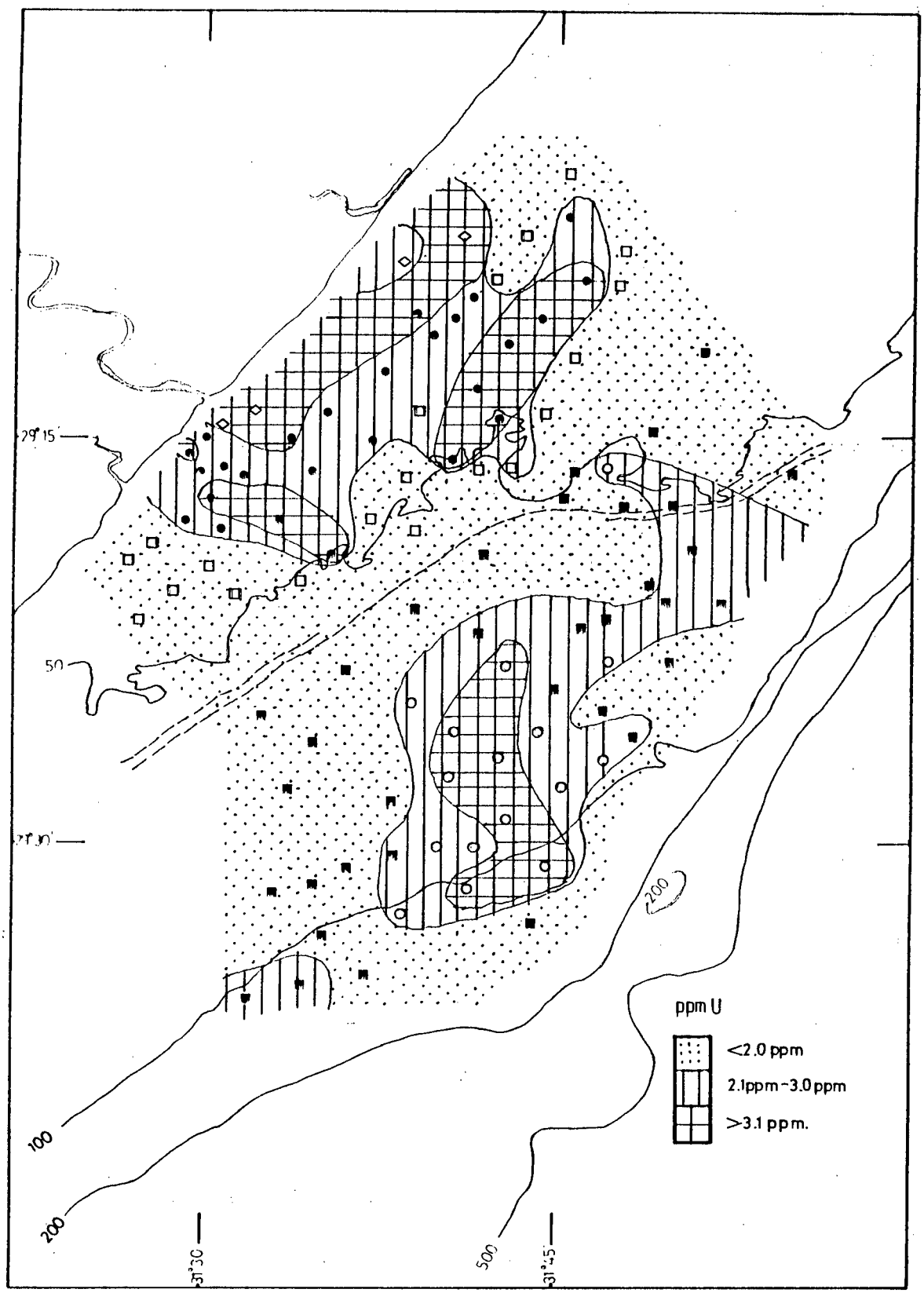

Figure 10-30. Distribution of uranium.

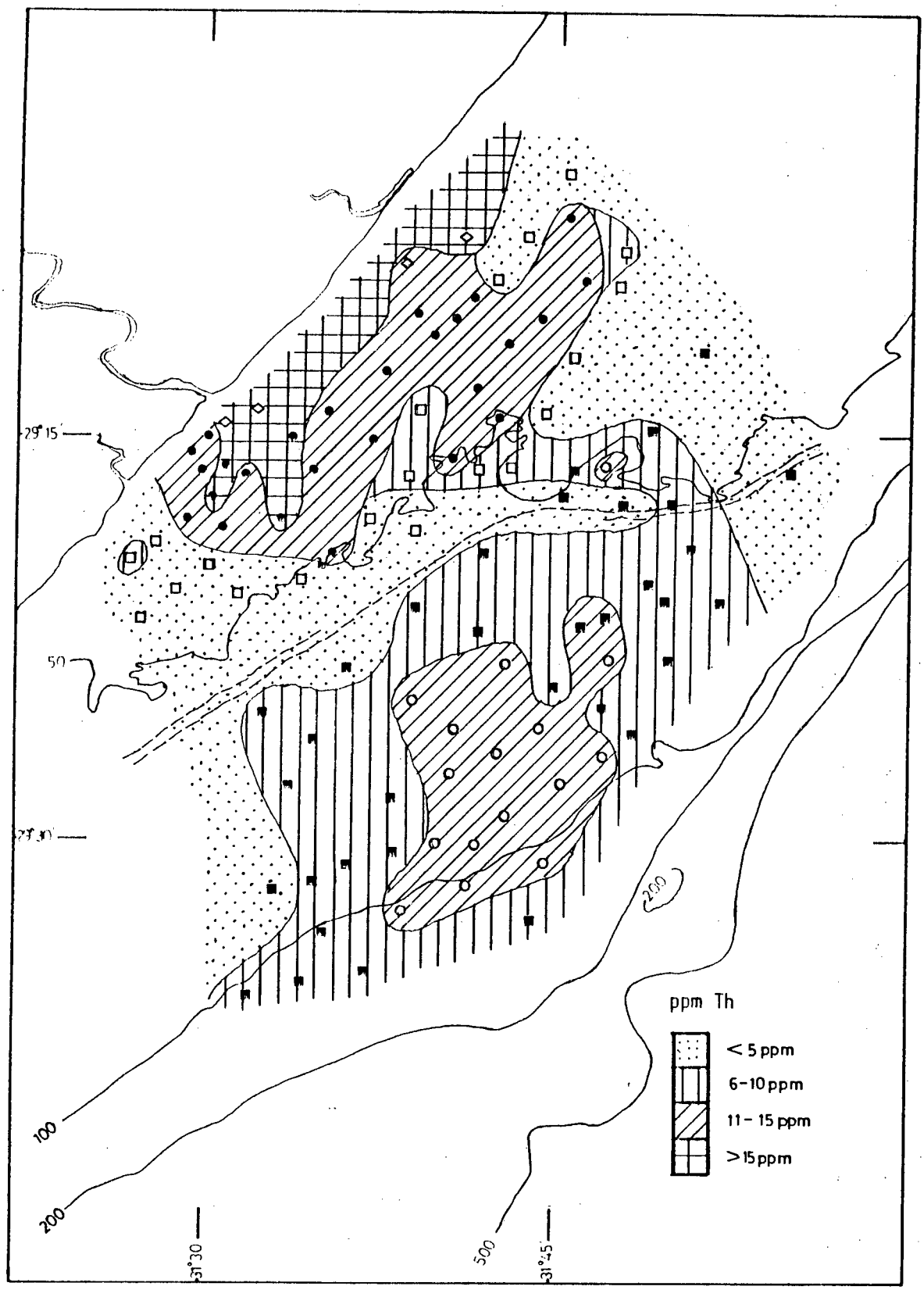

Figure 10-31. Distribution of thorium.

again being found in the four very fine nearshore sands and a few nearshore mud samples. Thorium is positively loaded on the clay mineral factor, and is for the most part well correlated with Al_2O_3, suggesting that its presence in the study area is accounted for by its association with the clays. The enrichment of thorium in the very nearshore samples, as well as its positive loading on the heavy mineral factor, show Th to also be associated with the heavy minerals. Which heavy minerals cannot be determined from the results of this study, but it is interesting to note that the correlation of Th with TiO_2 in the inner and outer shelf sands is highly positive, suggesting that it is possibly related to ilmenite or rutile.

3.2.8 Lead

Lead is highly positively loaded on the clay mineral factor, and its distribution (fig. 10-32) further indicates its concentration in the mud fraction (Pb is significantly correlated to mud in all the continental shelf sediment groups (Tables 10-5 to 10-8)). Hirst (1962b) quotes Wedepohl's suggestion that clay minerals contain the bulk lead content of sediments, being adsorbed onto the clay particles, and usually concentrating in illite. Holmes (1982) has shown that lead quickly achieves a total chemical equilibrium with respect to mud in marine sediments due to its rapid adsorbance onto the clays. The inner and outer shelf sands have an average lead content of 14 and 15 ppm respectively, which is notably higher than the average value for sandstones of 7 ppm.

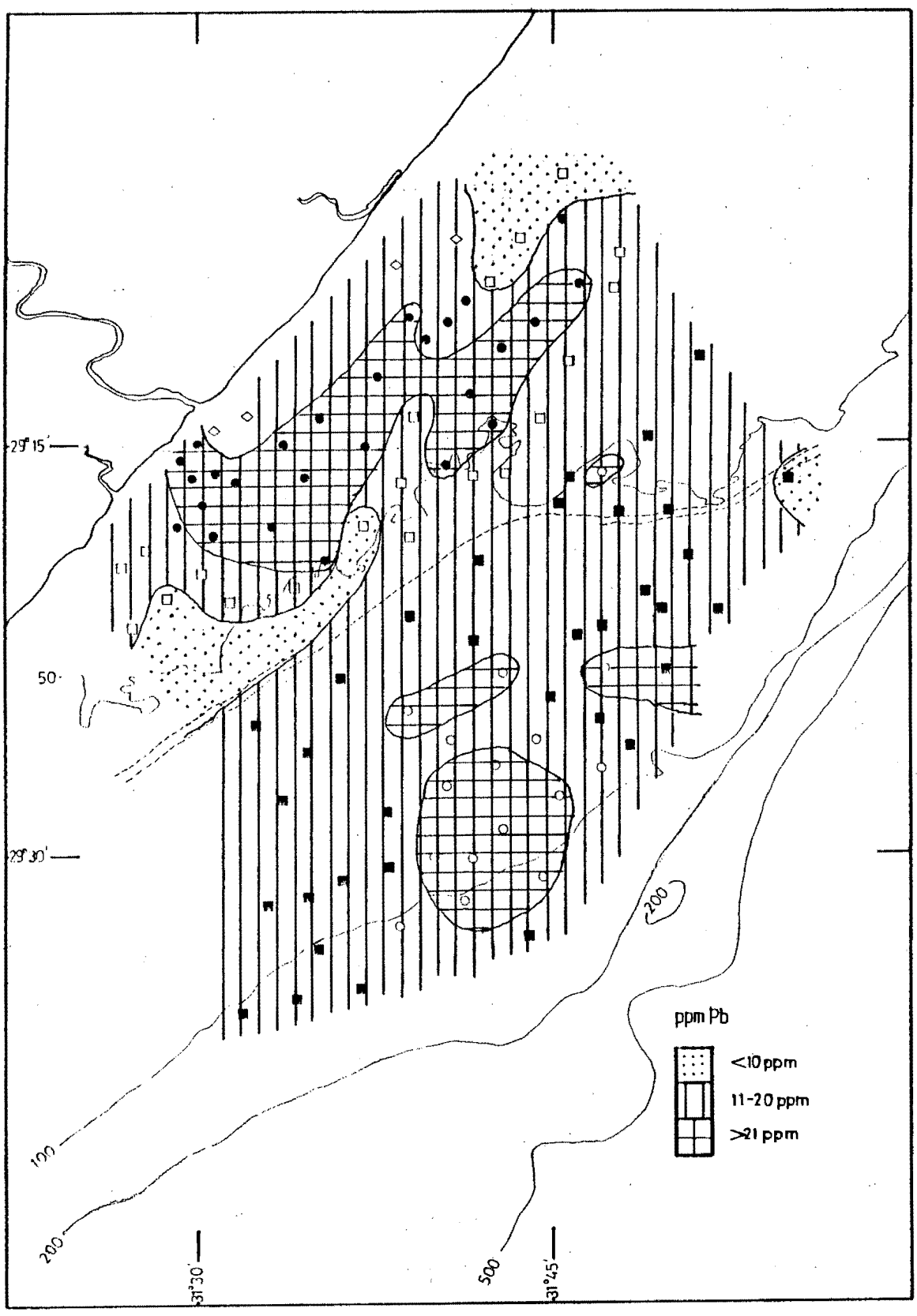

Figure 10-32. Distribution of lead.

3.2.9 Zinc, Copper and Nickel

Zinc, copper and nickel are all highly correlated with the clay mineral factor, leaving little doubt that these elements are closely associated with the clay minerals in the clay fraction in the study area. They are also highly correlated with each other and with organic matter in all of the continental shelf sediment groups. The correlations of Zn, Cu and Ni with organic matter are probably due to enrichment by adsorption on clay particles coated with organic material (cf. section 3.1.8), precipitation effects during sedimentation, or entrainment in organo-metallic complexes (Keith and Degens, 1959). Recent research has shown that a group of metal-binding proteins called metallothioneins, which occur in several marine invertebrate species, are effective in the removal of toxic metals such as Cu, Zn, Hg and Cd from the marine environment (Roesijadi, 1980; Capuzzo, 1981). The values of Zn in the inner and outer shelf muds (80 and 56 ppm respectively) are somewhat lower than the average value for shales (95 ppm), although the nearest-shore muds close to the Tugela River Mouth have concentrations of 90 - 100 ppm (fig. 10-33). Zinc correlates significantly with several major and trace elements (cf. Tables 10-4 to 10-8), many of which are probably second-order correlations that result from a common association of these elements, and zinc, with the clays. Wedepohl (1978) cites several examples of high correlation between Zn and Fe_2O_3 that have been found in past studies, and similar correlations of Zn with Fe_2O_3 were found in all the sedimentary groups of this study.

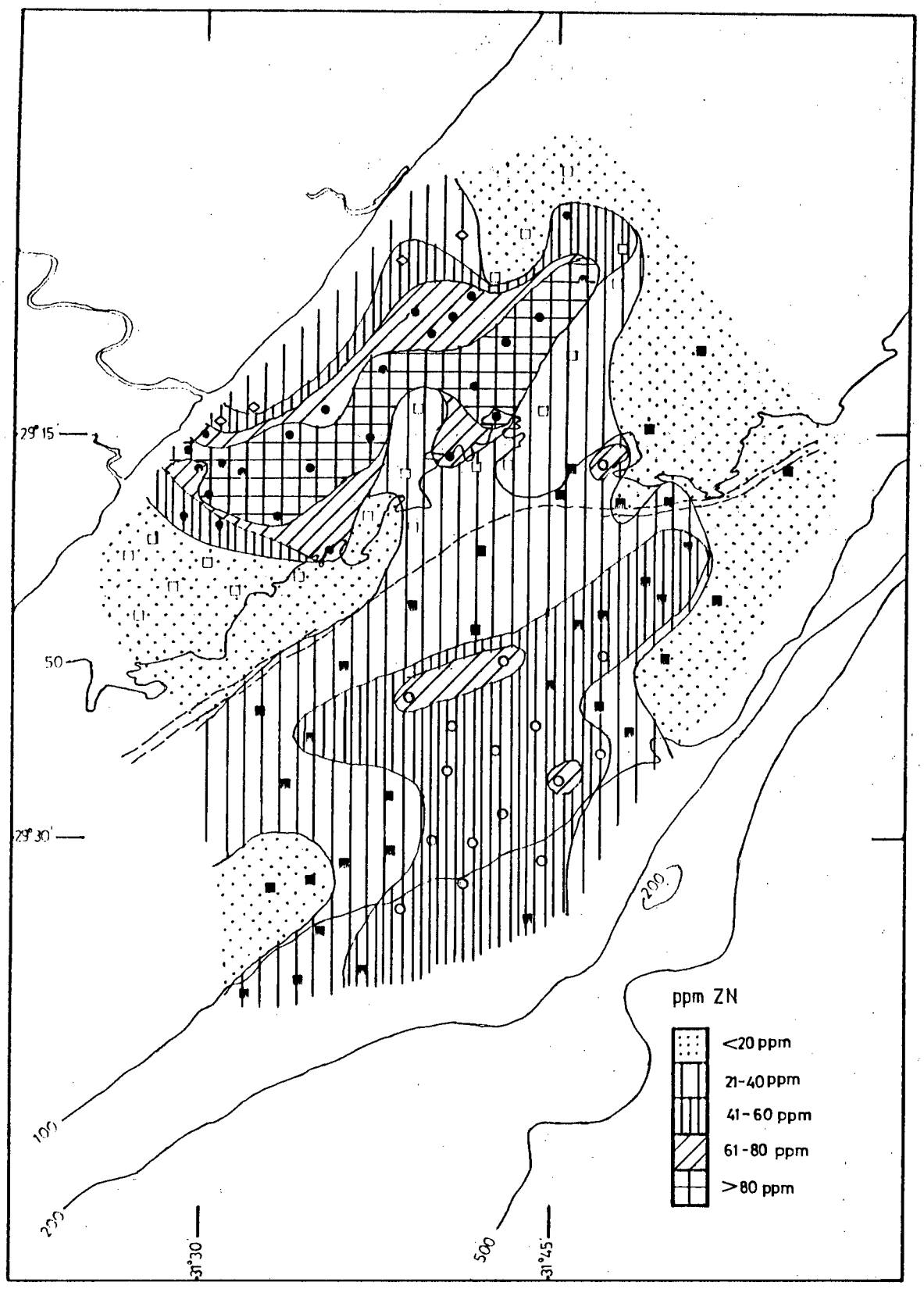

Figure 10-33. Distribution of zinc.

Copper also shows a number of significant correlations with many major and trace elements for the same reasons as does zinc. Hirst (1962b) suggests that copper enters depositional areas primarily structurally combined in the lattices of clay minerals, generally favouring illite as its host. Gibbs (1973) also found that the major transport mechanism for copper was incorporation into crystalline structures. Thus, the distribution of copper (fig. 10-34) may be readily explained by the flocculation and deposition of clays close to the river mouth, with decreasing copper concentration occurring simultaneously with decreasing clay content with increasing distance from the river mouth. The copper distribution closely follows that of Fe_2O_3 (cf. fig. 10-14), suggesting an association of the two elements either in the clays or in ferric oxides. Copper is effectively adsorbed by both iron and manganese oxides, as well as by clay minerals (Wedepohl, 1978). The copper values of the outer shelf muds (average 19 ppm) are roughly half that of the inner shelf muds (average 36 ppm). Copper concentration in both areas is depleted relative to the average value for shales of 45 ppm.

Nickel, like zinc and copper, shows a number of significant correlations with several other major and trace elements. Nickel is less positively correlated with most of these elements, with the exception of Fe_2O_3 with which it is more strongly correlated than are Zn and Cu. The nickel values in the muds closest to the river mouth are fairly close to the average value for shales of 68 ppm (the average inner mud Ni value being 58 ppm), but the nickel concentrations in the

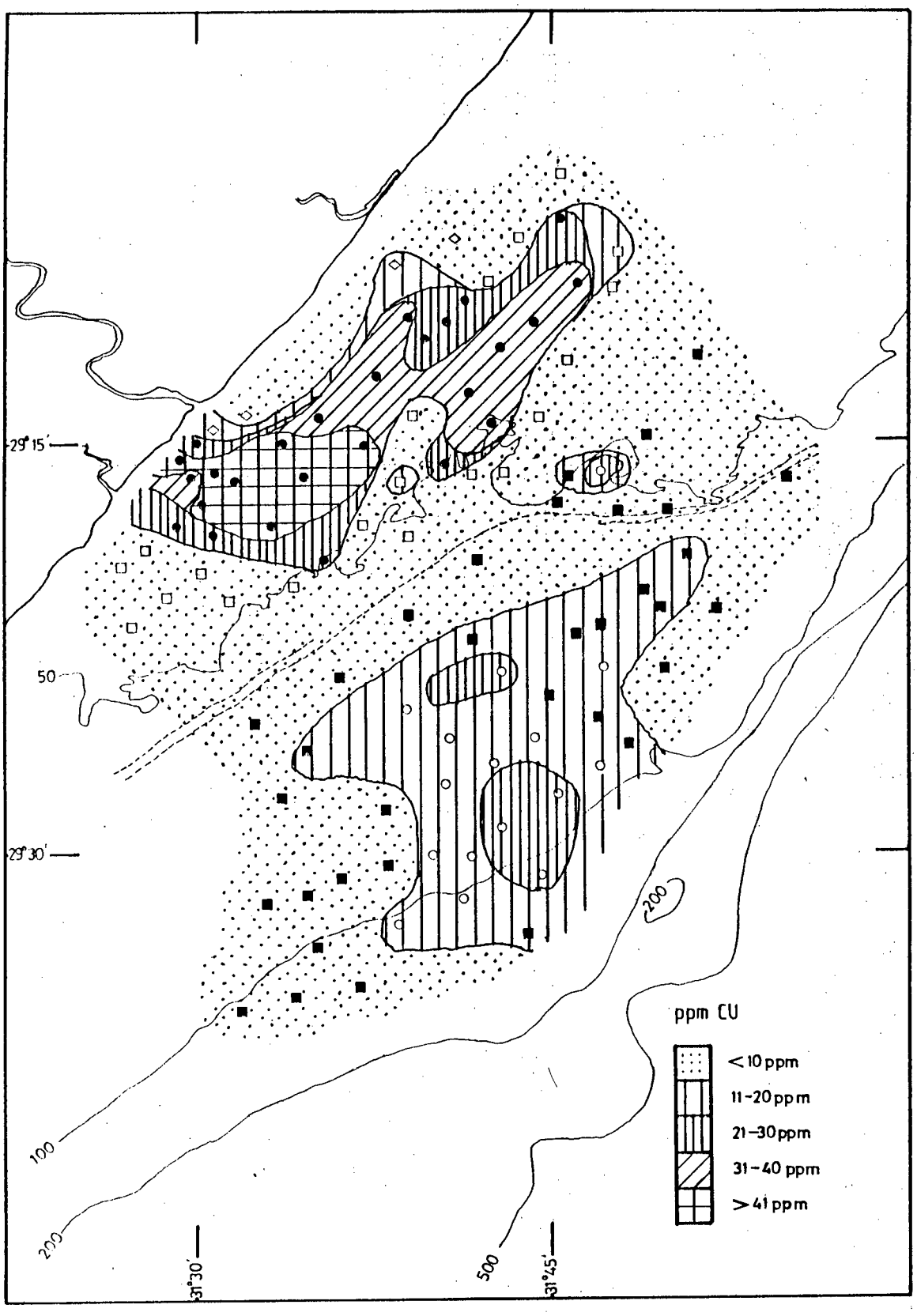

Figure 10-34. Distribution of copper.

outer shelf mud belt are considerably lower with an average value of 43 ppm. The distribution of nickel (fig. 10-35), like that of copper, follows the iron distribution; explicable by the similar chemical behaviour of Ni and Cu as a result of their similar ionic radii (Cu^{2+} 0.072 nm, Ni^{2+} 0.069 nm). Gibbs (1973) categorizes nickel with iron as an element whose dominant mechanism of transport is precipitation and coprecipitation on solids, with adsorption being the secondary mechanism. It appears as though the Ni present in the study area is most probably associated with the clay minerals. Nickel is relatively stable in solution during weathering and initial transportation, which could explain the high concentrations found close to the river mouth via its association with precipitating clay particles.

3.2.10 Cobalt

Cobalt is also enriched in the nearshore muds (>28 ppm) of the study area compared to the outer shelf muds and the average value given for shales (both 19 ppm). Cobalt is highly positively loaded on the clay mineral factor and has significant correlations with mud in all the sedimentary groups, inferring that it is associated with the clays. Nicholls and Loring (1962) found strong relationships between both cobalt and nickel and organic matter that they suggested were due to adsorption rather than biological concentration. Both Ni and Co are significantly correlated with organic matter in all the sediment groups except the outer shelf muds in this study. Gibbs (1973) considers Co, like Cu, to be incorporated into the crystalline structures of the clays. The distribution of

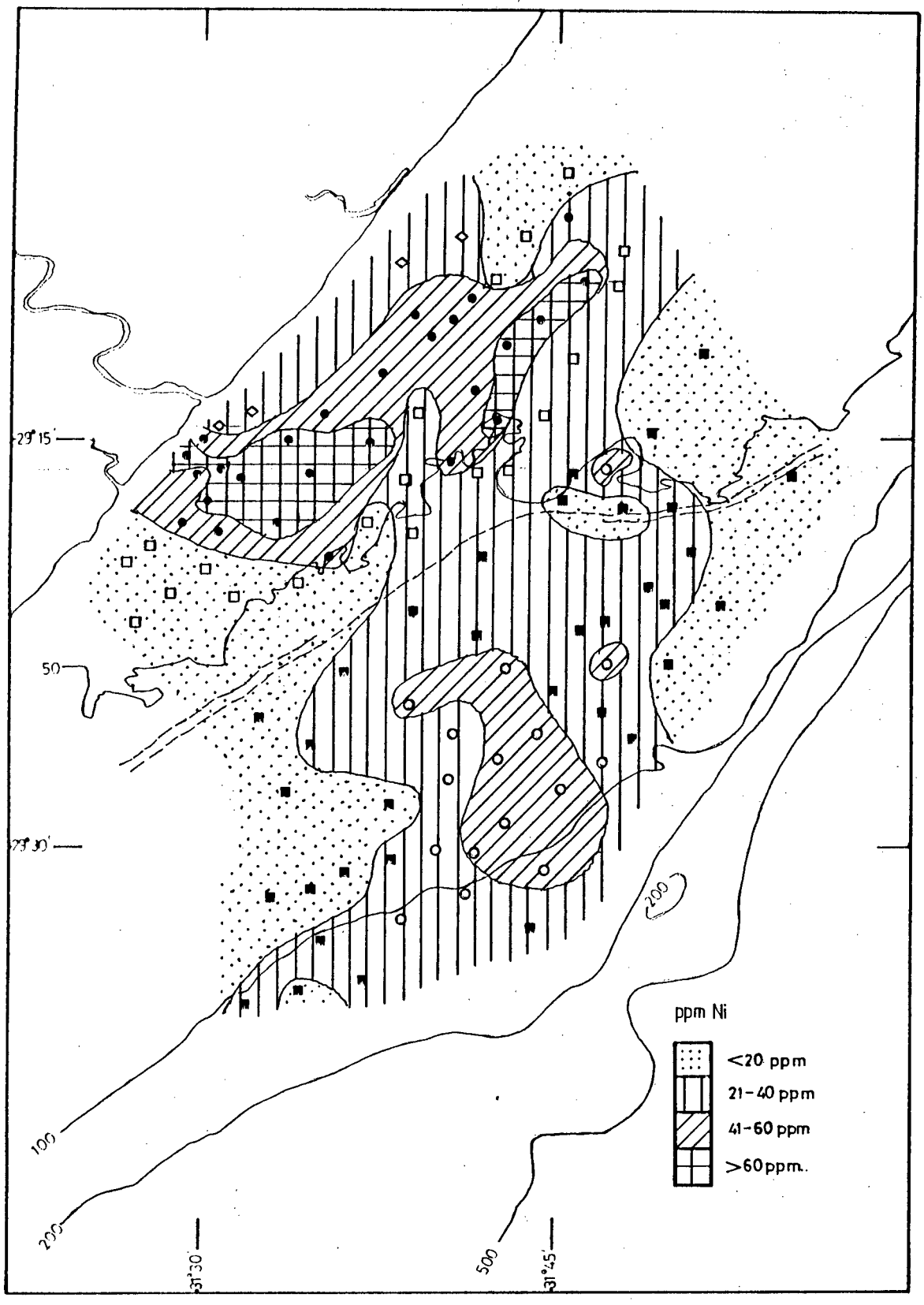

Figure 10-35. Distribution of nickel.

Co (fig. 10-36) is somewhat similar to those of Fe_2O_3 and Ni. This would be expected because of its similar ionic radius (Co^{3+} 0.063 nm, Fe^{3+} 0.064 nm) and resulting analogous chemical behaviour.

3.2.11 Chromium and Vanadium

Chromium is positively loaded on both the clay mineral factor and the heavy mineral factor, as well as on factor 5. Cr appears to be enriched in all the sediments of the study area (fig. 10-37), with the inner and outer shelf muds having average values of 152 and 134 ppm respectively (average shale 90 ppm), and the inner and outer shelf sand values averaging at 97 and 89 ppm (average sandstone 35 ppm). Shiraki (1978) gives the average Cr values for Recent shallow water clayey sediments as 60 ppm and sandy sediments as 26 ppm, making the enrichment of the study area sediments even more notable. Two of the very fine nearshore sand samples have anomalously high concentration of chromium (>190 ppm). This is explainable in these previously classified heavy mineral samples by Cr being a known accessory element in magnetite (Mason, 1966). Many of the inner shelf mud samples have Cr concentrations in excess of 150 ppm, probably due to contributions from its incorporation primarily in the clay minerals (Hirst, 1962b) and secondarily in the fine-grained heavy minerals associated with the clay-sized fraction.

Vanadium is much more significantly positively loaded on the clay mineral factor than chromium. It is also less positively loaded on factor 5 than Cr, and is not loaded at all on the heavy mineral factor, as evidenced by its distribution

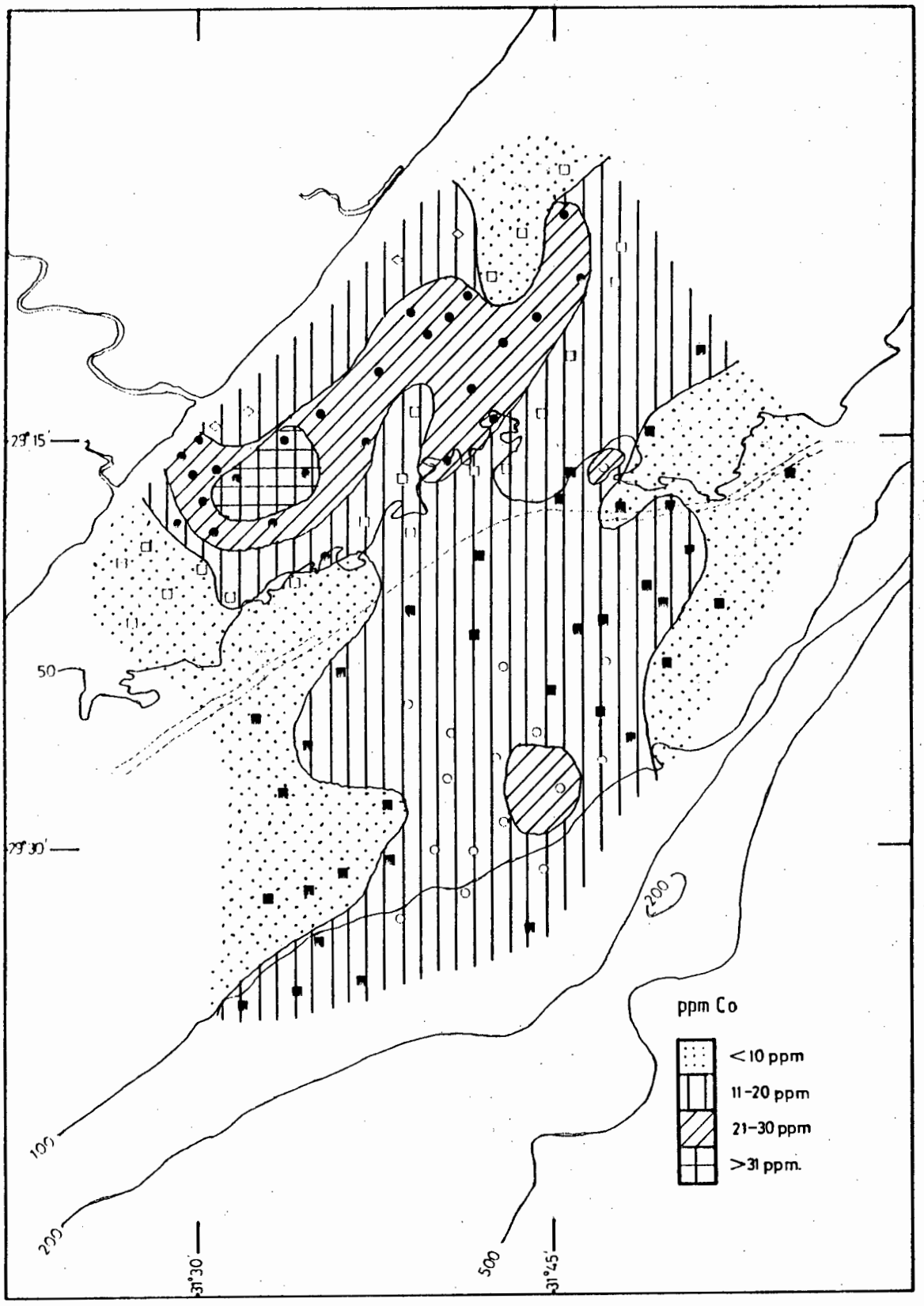

Figure 10-36. Distribution of cobalt.

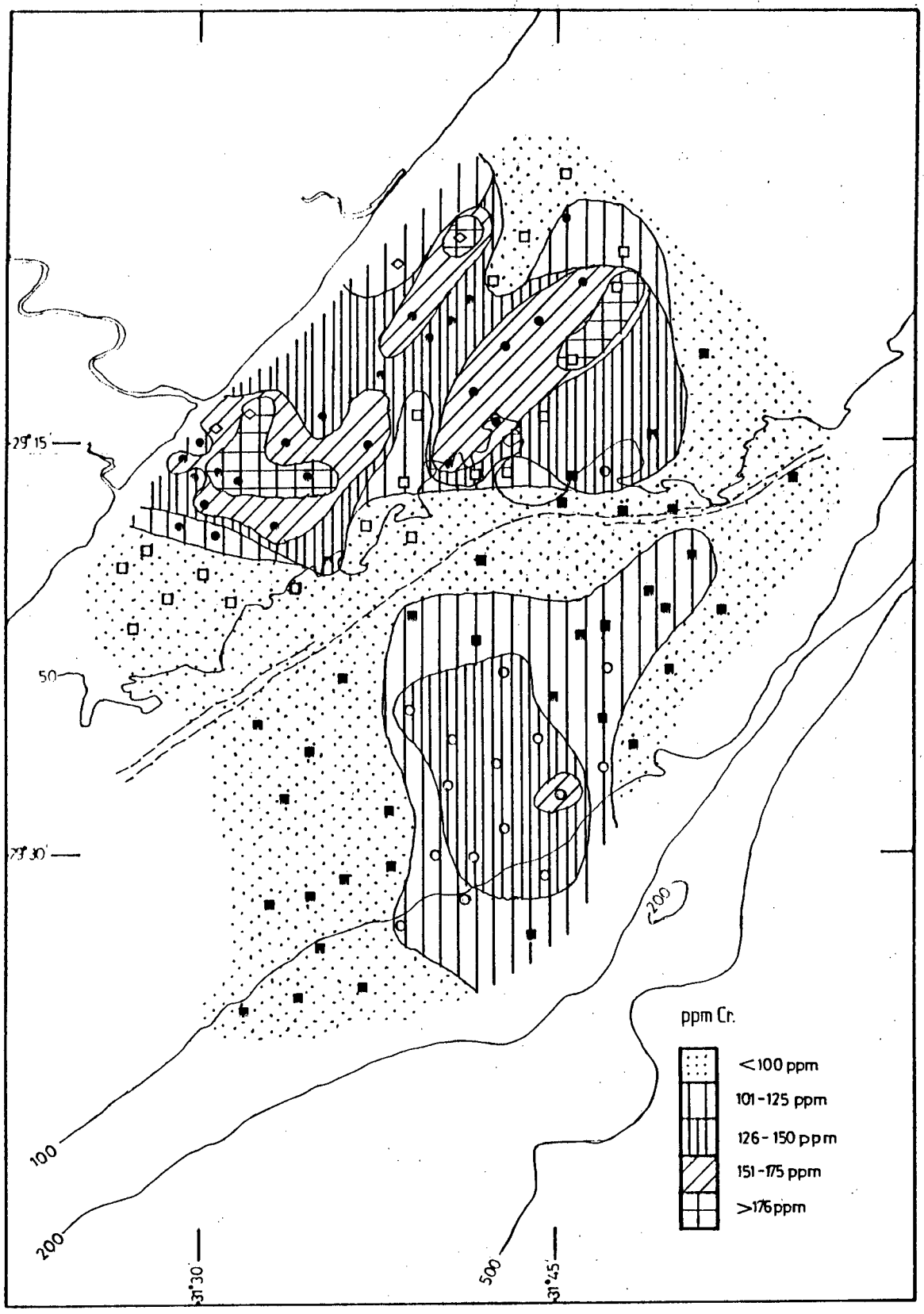

Figure 10-37. Distribution of chromium.

(fig. 10-38), which does not show enrichment in the nearshore sands. Chromium and vanadium are highly correlated with each other in all the sediment groups, and this is evidently a relationship that exists predominantly in the clay minerals. The concentrations of vanadium found in the mud samples (Table 10-13) agree well with the range of 100 - 150 ppm given for Recent clays by Landergren (1978). Vanadium is significantly correlated to organic matter in all of the continental shelf sedimentary groups, as would be expected from the known relationship of vanadium to organic materials previously established by the presence of vanadyl porphyrin complexes found in oils, sediments, and sedimentary rocks (Landergren, 1978).

3.2.12 Barium

As stated in the statistical analysis section (2.), barium was one of the most discriminatory variables found in the stepwise discriminant function analysis. Partial explanation for this is found in the factor analysis, which shows a significantly positive loading of Ba on the clay mineral factor and an even more significant negative loading on the quartz-feldspar/carbonate factor. The frequency distribution for this element within the two mud groups is distinctly bimodal (cf. Appendix C), although overlap does exist. Barium is not thought to be bound in clay minerals, though many studies have shown barium to be preferentially concentrated in clays over sands and silts (Puchelt, 1978). Puchelt reviews the positioning of barium in various minerals and cites indications which point to a correlation of barium with mica, due to a parallelism found between the amount of illite and the

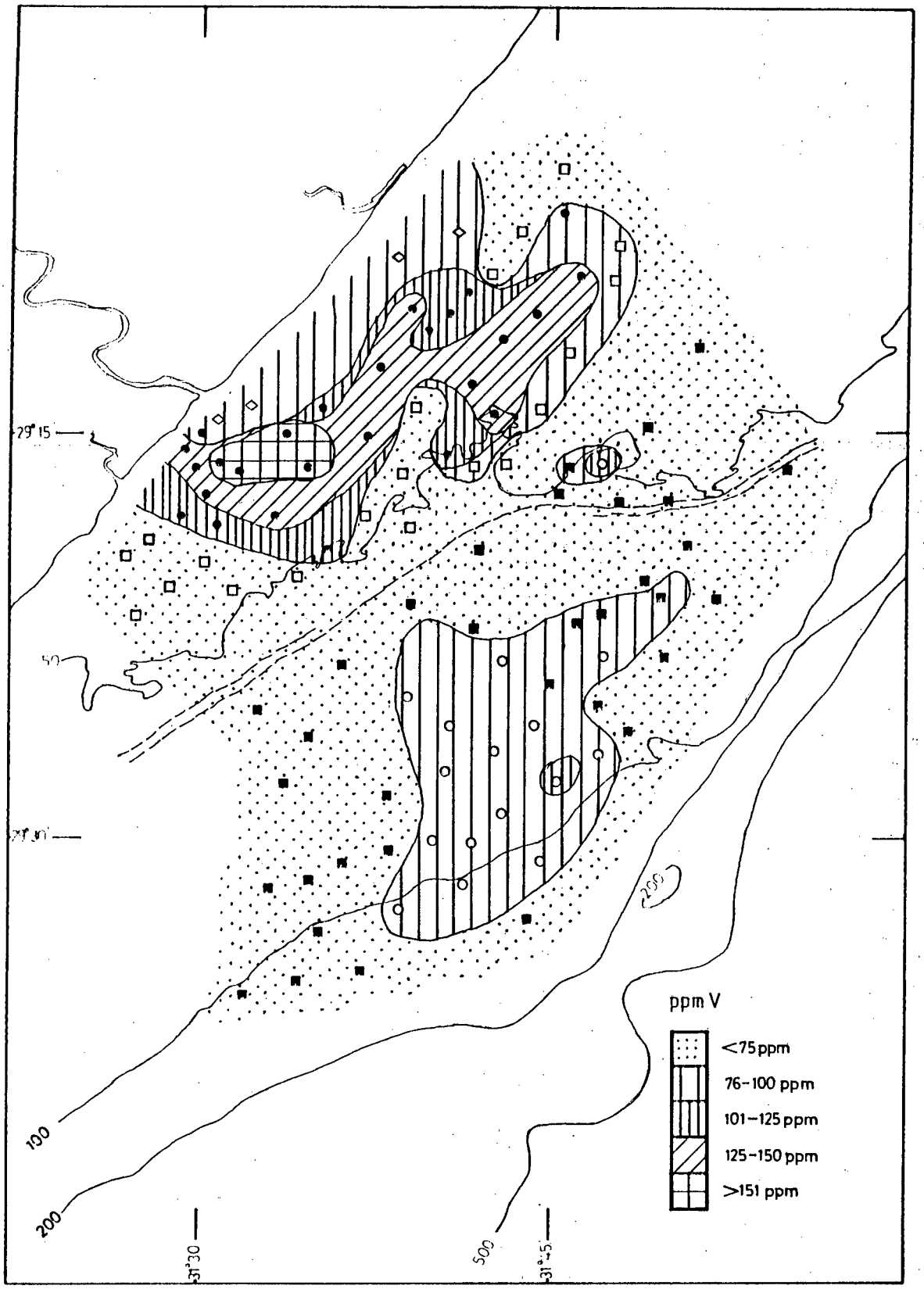

Figure 10-38. Distribution of vanadium.

concentration of barium. It is believed that this is due to barium and potassium having similar ionic radii (Ba^{2+} 0.146 nm; K^{+} 0.145 nm), while barium has a higher charge, leading to the preferential adsorption of barium into illite. Hirst (1962b) quotes Rankama and Sahama (1950) in stating that barium is so strongly adsorbed in nearshore areas as to be largely removed from solution, such rapid adsorption being aided by flocculating clay minerals acting as scavengers. It appears as though this mechanism could be operative in the study area, but it does not explain the highest concentrations of barium that are found in the very fine nearshore sands (fig. 10-39). This anomaly could be due to substitution of Ba for potassium in mica or feldspar (Mason, 1966) in these sands. Thus, barium is probably primarily associated with the high clay content found in the inner shelf mud belt, and secondarily with the detrital minerals found in the nearshore sands that are mixing into the inner shelf muds (chap. VIII). One could deduce from this that the choice of Ba as a discriminating variable in distinguishing between the inner and outer shelf muds is due to the difference in the proportion of clay minerals and unaltered detrital mica and feldspars between these two depositional areas. It would appear that the clay and fresh detrital mineral content is much more important than the carbonate content in determining this distinction.

3.2.13 Scandium

Scandium is highly positively loaded on the clay mineral factor, and its concentration in both the inner and outer

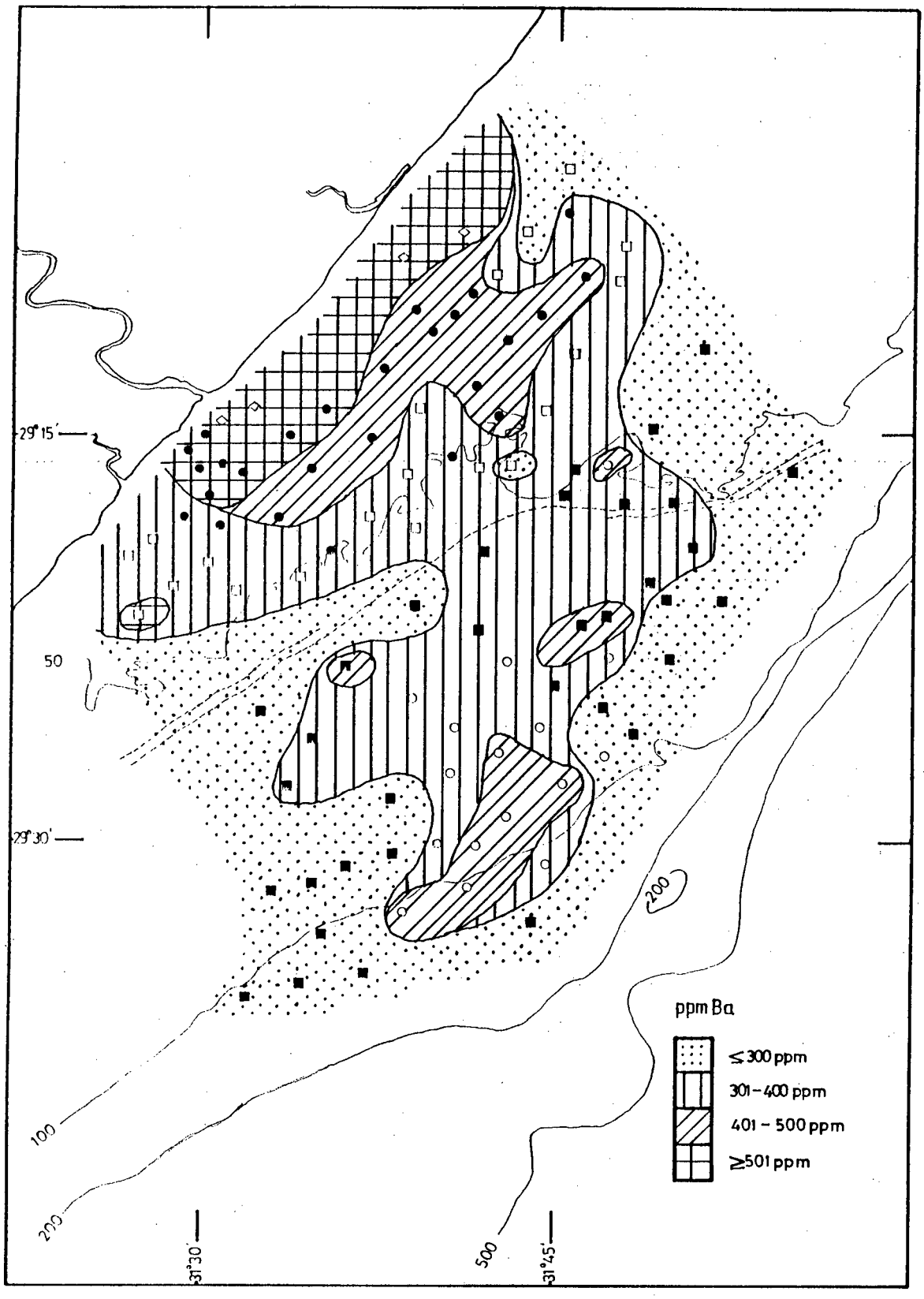

Figure 10-39. Distribution of barium.

shelf muds (averages of 23 and 18 ppm respectively) is enriched relative to the average value for shales of 13 ppm (fig. 10-40). It has been fairly well documented that scandium is chiefly contained in the clay fraction of Recent sediments, being adsorbed by clay minerals and hydrous aluminum and iron oxides (Frondel, 1978). In this study, scandium correlates highly with Al_2O_3 and Fe_2O_3 in all the continental shelf sediment groups (Tables 10-5 to 10-8), as well as, to a lesser extent, to a number of other major and trace elements previously stated to be associated with the clays.

3.2.14 Bromine

Bromine is a very interesting element in the study area as it is the only trace element that shows a distinct enrichment in the outer shelf muds relative to the inner shelf muds (fig. 10-41). The average concentrations of both the inner and outer shelf muds (22 and 45 ppm respectively) are much higher than the average value given for shales of 4 ppm (probably due to the greater availability of Br in the marine environment), although they are depleted compared to the average values for marine sediments given in Fuge (1978) of 77 - 128 ppm. Bromine is positively loaded on both the clay mineral factor and the quartz-feldspar/carbonate factor, but its most significant correlation is with factor 6, on which it is the most highly loaded variable. Bromine is significantly correlated to CaO, CO_2, P_2O_5 and As in the inner shelf mud group, probably accounting for its positive loading on the quartz-feldspar/carbonate factor. The inner shelf sand group shows correlations of Br with Fe_2O_3, MgO, organic matter and As.

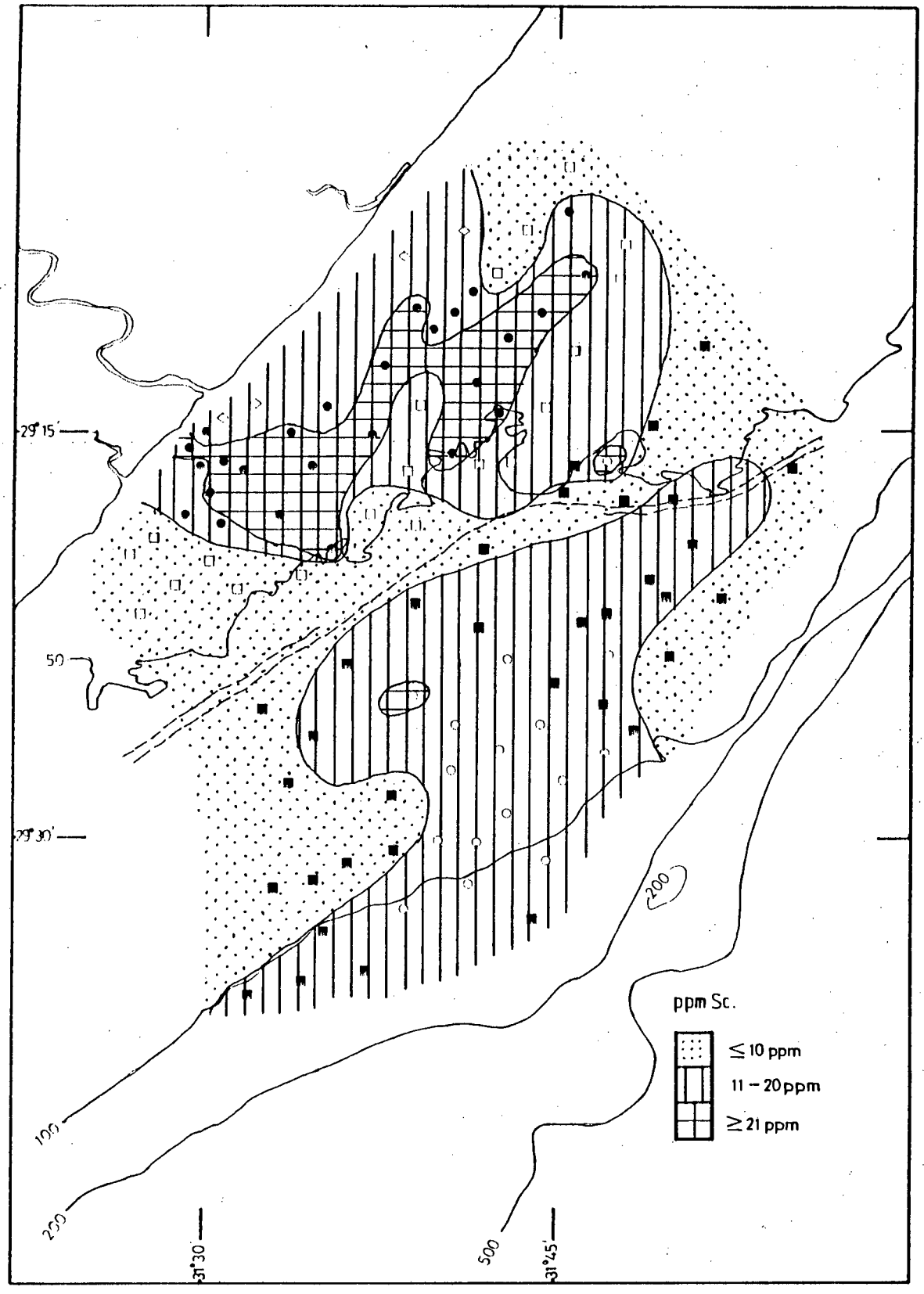

Figure 10-40. Distribution of scandium.

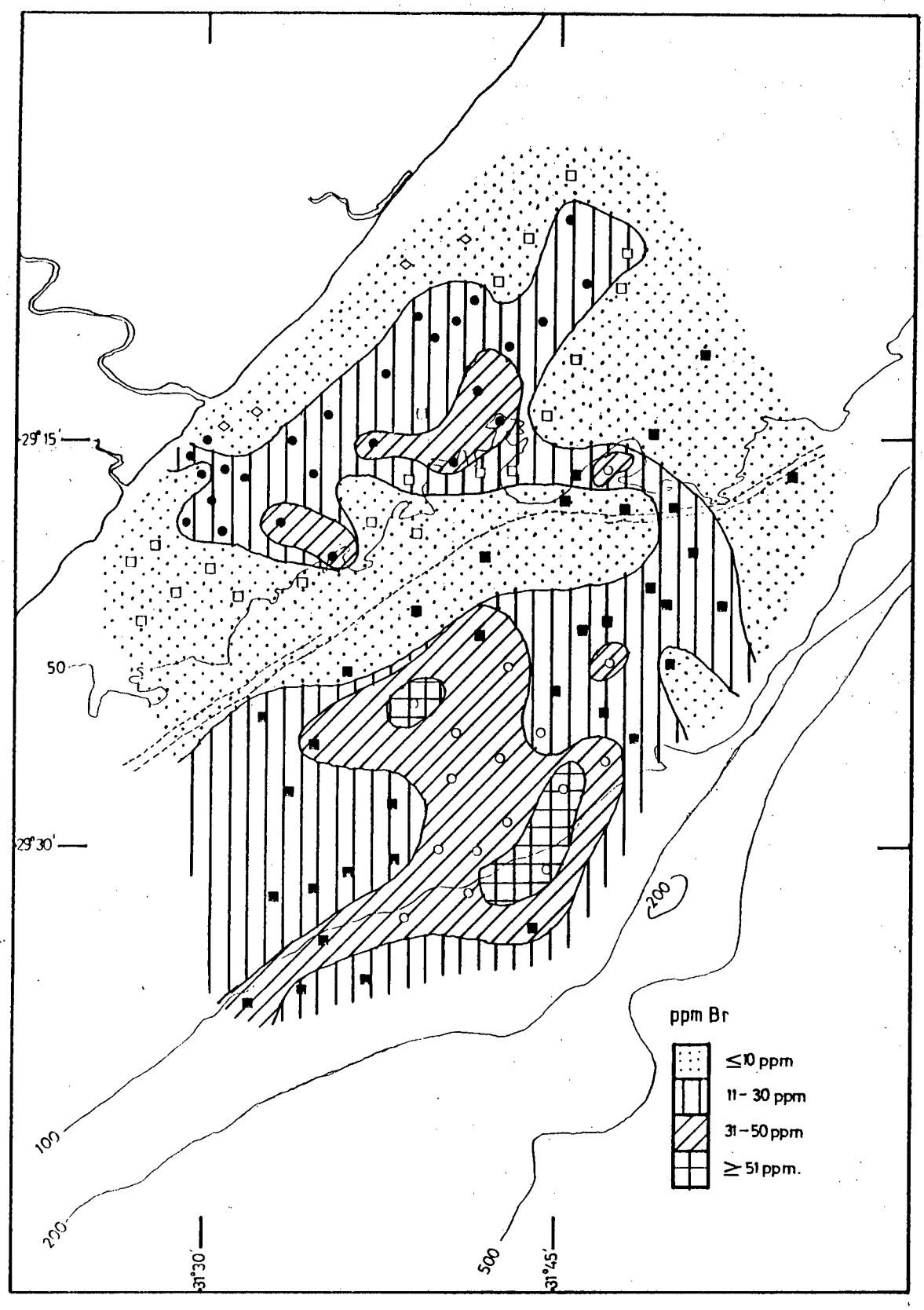

Figure 10-41. Distribution of bromine.

In the outer shelf mud and sand groups, bromine is highly correlated with organic matter and mud, as well as several second-order correlations resulting from its association with these two variables (cf. Tables 10-4 to 10-8).

The geochemical associations for bromine do not appear to have been as extensively studied as those for other trace elements. Fuge (1978) cites several studies which express doubt at the ability of bromine to occupy regular lattice sites in most rock forming minerals, generally it remains in residual liquids and concentrates in connate waters. The geochemistry of bromine is very similar to that of chlorine in igneous rocks and volcanic gases, but is more similar to that of iodine in sediments. Both iodine and bromine are found to be enriched in organic-rich soils and sediments; a strong correlation of Br with organic carbon has been shown to exist in sedimentary rocks and some Recent sediments. The plot of bromine against organic matter for the sediments of this study (fig. 10-42) graphically shows the close relationship between Br and organic matter in the outer shelf sediments. Bromine does concentrate in the soft parts of some marine organisms, mainly molluscs and coelenterates, and it may also be adsorbed onto decaying organic material. Diagenetic reactions occurring in the older outer shelf sediments involving organic material enriched in Br could possibly be responsible for the enrichment of Br in these sediments, although documentation of such reactions could not be found in the literature.

3.2.15 Gallium

Gallium is very highly positively correlated to Al_2O_3

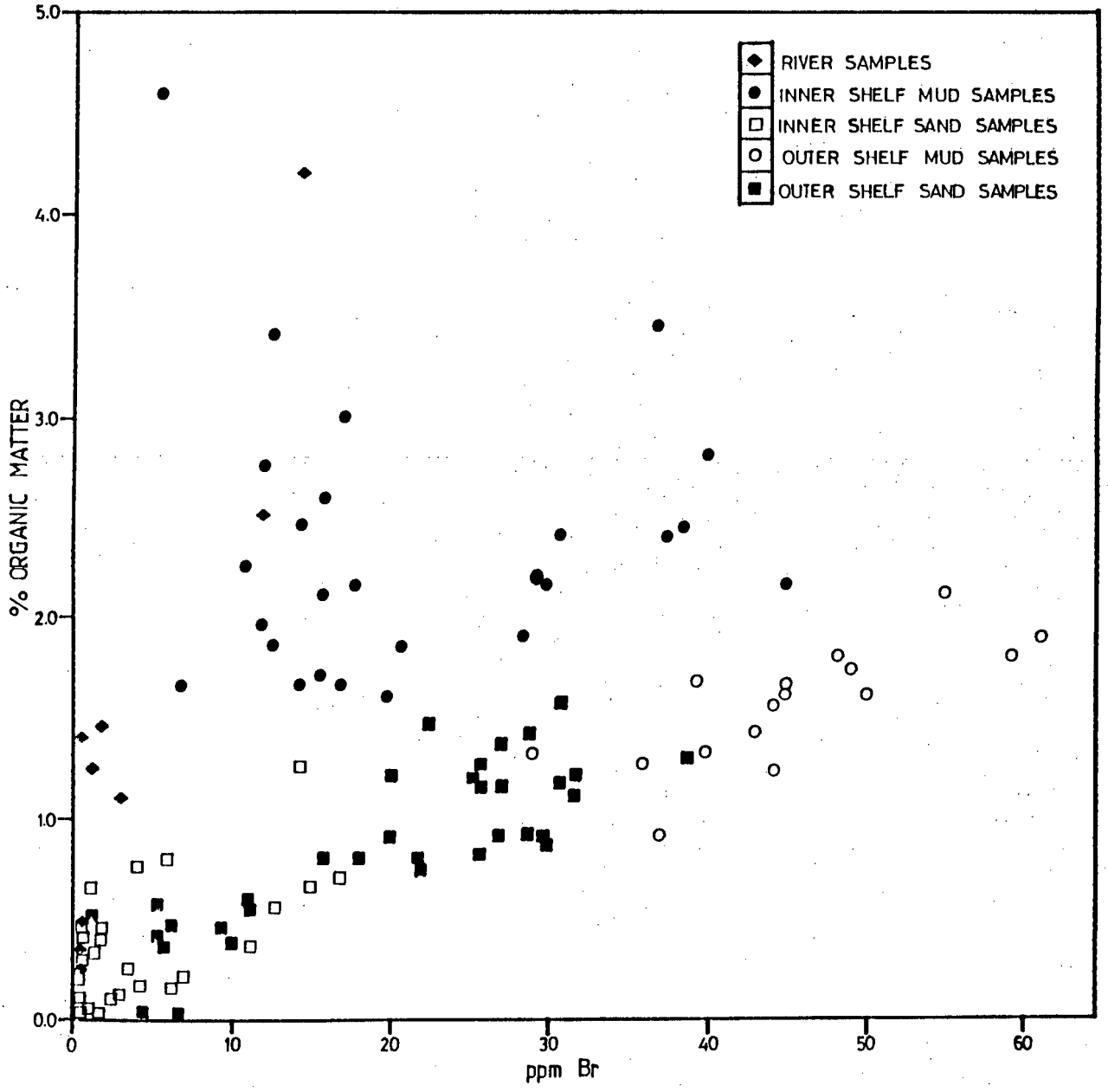

Figure 10-42. The relationship between bromine and organic matter contents of the study area sediments.

and is the second most highly loaded variable on the clay mineral factor after Al_2O_3. This is because the geochemistry of gallium is dominated by its chemical similarity to aluminum (ionic radius Al^{3+} 0.051 nm, Ga^{3+} 0.062 nm). Gallium probably enters the depositional area in the lattices of the clay minerals, with little separation occurring between gallium and aluminum during weathering and transportation (Hirst, 1962b). The gallium concentration in the inner shelf mud belt averages 20 ppm (average shale 19 ppm), with the outer shelf mud belt average being lower at 15 ppm as expected (fig. 10-43). Gallium is not known to accumulate in organisms (Burton and Culkin, 1978), thus the significant correlations of gallium with organic matter in the continental shelf samples found in this study could be attributed to a secondary reflection of the association of Ga with the clays and aluminum.

3.2.16 Rare Earth Elements (La, Ce and Nd)

The only rate earth elements which could be determined by XRF in this study were lanthanum, cerium and neodymium. All three elements are highly positively loaded on the clay mineral factor, and their distributions (figs. 10-44, 10-45 and 10-46) show the highest concentrations of these elements occurring in the inner shelf mud belt. Some of the highest concentrations of all three rare earth elements are found in the very fine nearshore sands, probably because of their incorporation in the heavy minerals, most likely hornblende (Mason, 1966). There appears to be a notable depletion of La in the muds (inner shelf mud average 38 ppm; outer shelf muds average 25 ppm) compared to the average value for shales of

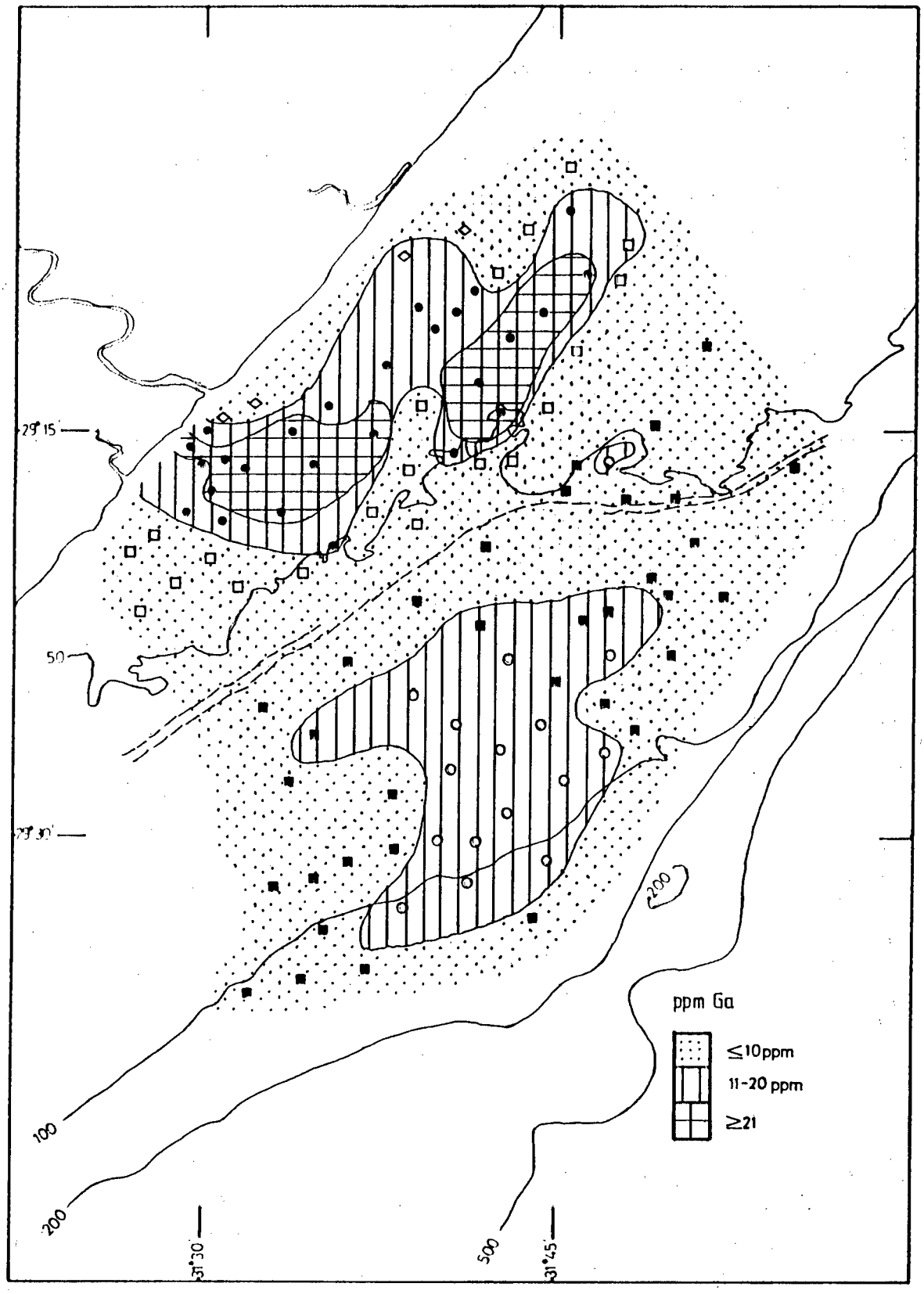

Figure 10-43. Distribution of gallium.

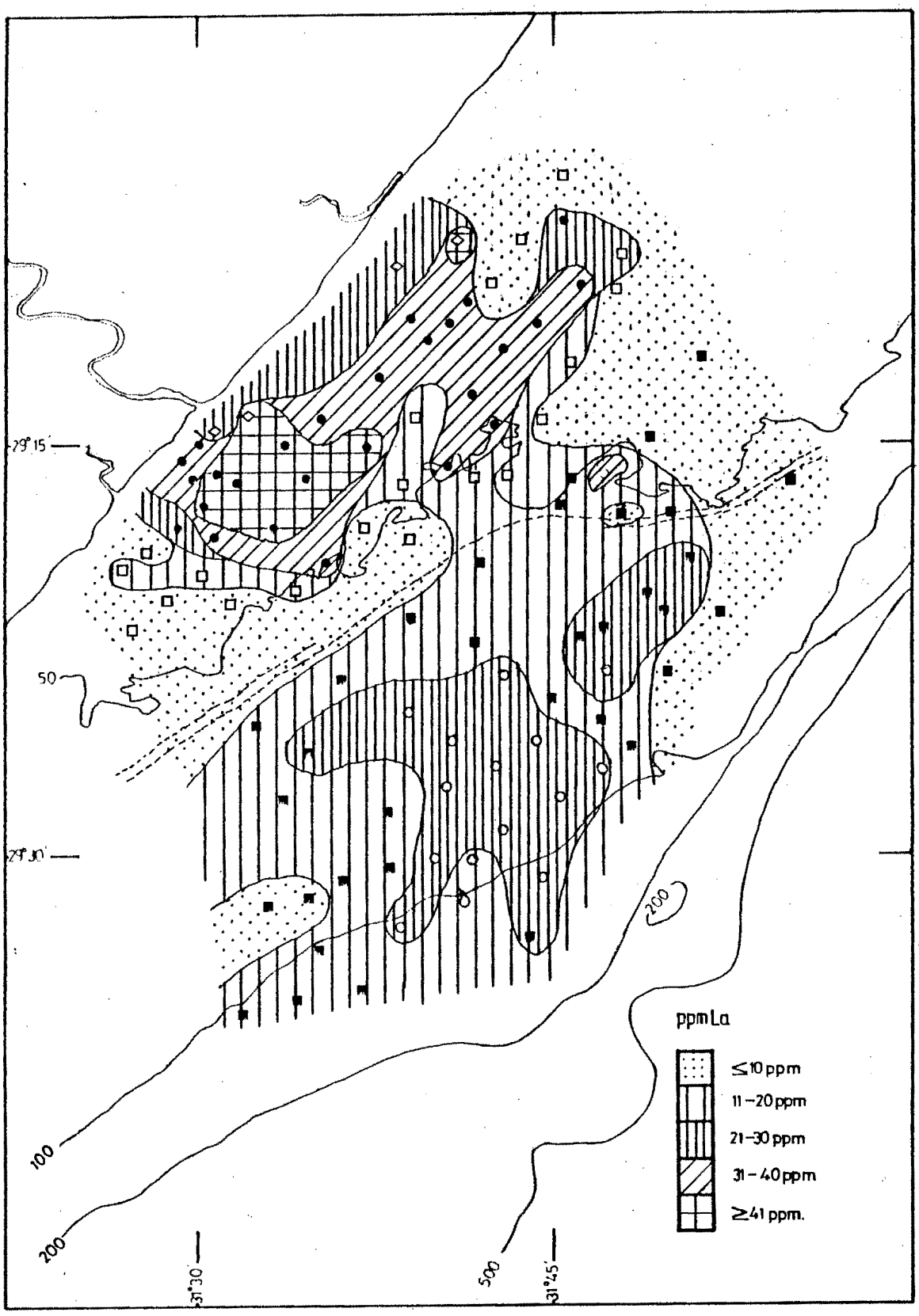

Figure 10-44. Distribution of lanthanum.

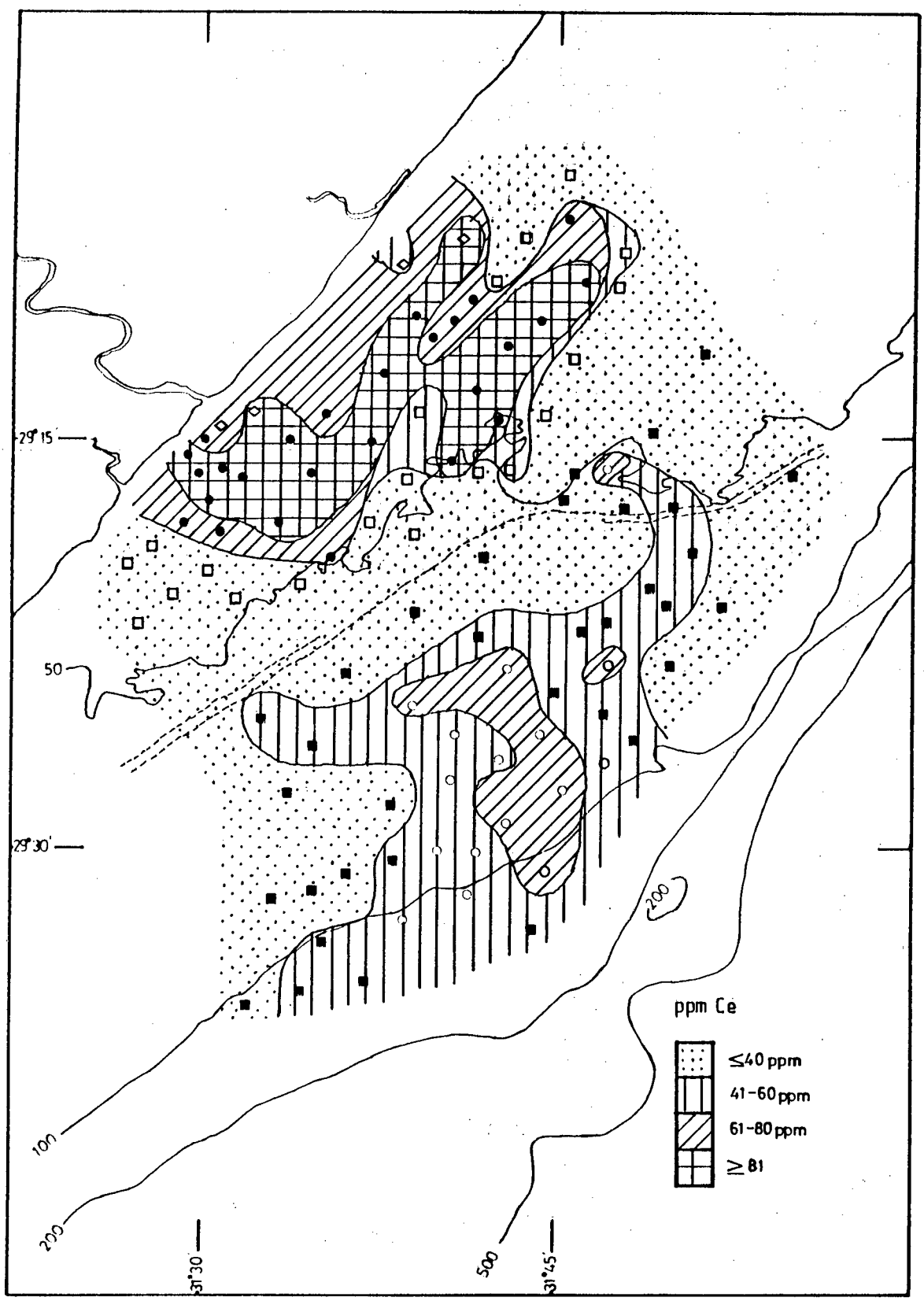

Figure 10-45 Distribution of cerium.

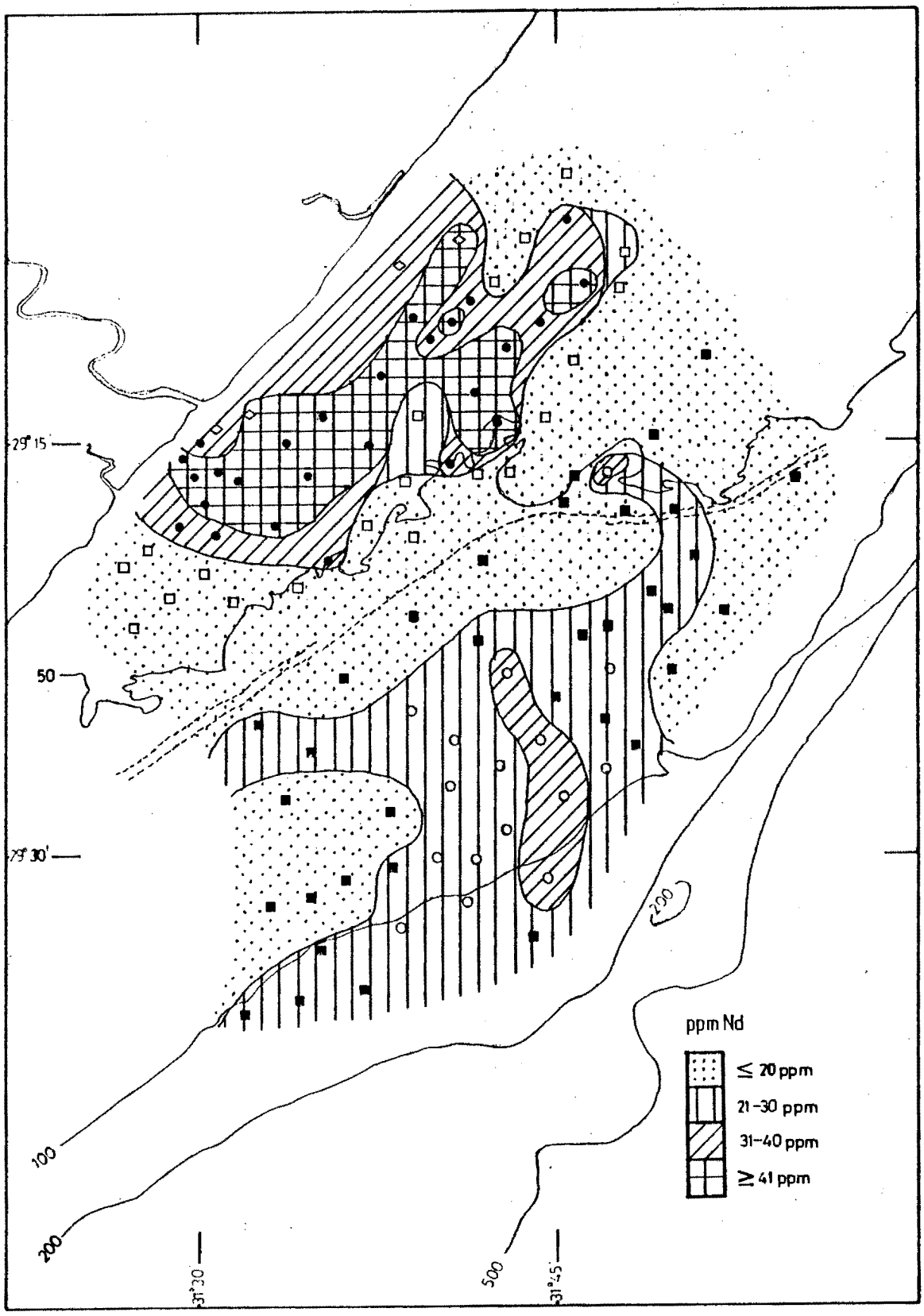

Figure 10-46. Distribution of neodymium.

92 ppm. Both Ce and Nd are enriched in the inner shelf mud belt (averages of 84 ppm and 42 ppm respectively) relative to the outer shelf mud belt (averages of 62 ppm and 30 ppm) and the average shale values of 59 ppm for Ce and 24 ppm for Nd. Although La has been known to substitute for Ca in carbonates (Cook and Mayo, 1980), this does not appear to be of consequence in this area. The associations of these elements to the clay mineral factor, as well as their being correlated with a number of other elements that have been shown to be preferentially contained in the clays (cf. Tables 10-5 to 10-8), suggest that the presence of these rare earth elements in the study area may be accounted for by their adsorption on the clay minerals.

3.2.17 Arsenic

Arsenic is not correlated with the clay mineral factor at all, showing low positive loadings on the quartz-feldspar/carbonate factor, the textural factor, and factors 5 and 6, with a negative loading on the heavy mineral factor. The frequency distribution of arsenic is virtually normal (cf. Appendix C). Arsenic correlates with different variables in each of the four continental shelf sediment groups. In the inner shelf sand group As correlates significantly only with MgO, Br and coarse sand, while in the outer shelf sand group As is only correlated with the gravel, very coarse sand, coarse sand and medium sand fractions. Arsenic correlates with P_2O_5 and Br in the inner shelf mud group. The outer shelf mud group is the most interesting for As, as in these samples As is highly correlated with mud and organic matter,

as well as with several other elements that are also associated with the mud fraction.

Generally, arsenic has been found to be present in iron sulfides, in clay minerals (possibly in adsorbed form) and in organic matter in shales (Onishi, 1978). The average values for the inner and outer shelf mud groups are 14 and 11 ppm respectively, agreeing quite well with the average value for shales of 13 ppm. The highest concentrations of arsenic (>20 ppm) in the study area are found in some of the mid- and outer shelf samples, most of which have high carbonate contents and a large coarse sediment fraction (fig. 10-47). This is unusual in that the values for carbonate-rich sediments generally average around 1 ppm, and it would seem to indicate that As is not concentrated in the carbonate itself, but in other components comprising the coarse fraction. The concentration of As in these samples could be due to the ferruginous coatings on grains mentioned earlier (section 3.1.4), as the hydrous oxides of iron and manganese are known to be effective scavengers of arsenic (Degens, 1965).

4. Geochemistry of the Estuarine and River Sediments

The limited extent of the estuary was discussed in chapter II, section 2.. Even though the estuary is small, and non-existent during floods, the geochemistry of the two estuarine samples and the seven river samples indicate that estuarine processes are active in the transitional area between the river environment and the marine environment. Most of the trace elements determined show an increase in concen-

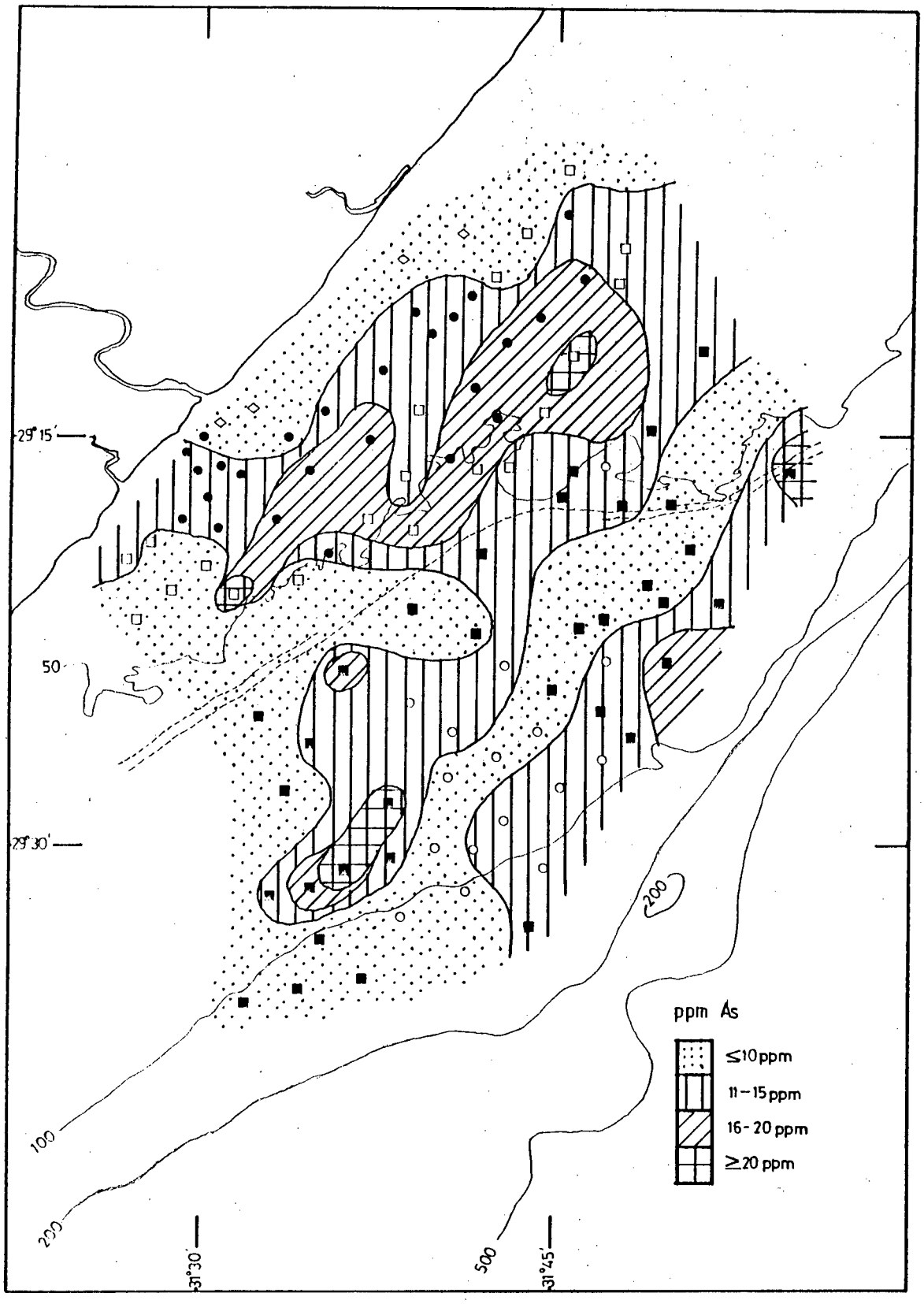

Figure 10-47. Distribution of arsenic.

tration in the estuarine samples compared to the river sediments, probably related to the higher proportion of fines in these samples. The estuarine sediments are also enriched in several of the trace elements compared to the continental shelf sediments. This enrichment is caused by the numerous chemical reactions and physical processes that occur in estuaries, some of which are discussed below. There are many good references containing detailed information on these processes; for example, Dyer (1972), Cronin (1975) and Burton and Liss (1976).

Two of the most important processes that occur in the estuarine environment are the flocculation of clay particles and the transformation of dissolved organic matter to particulate organic matter. An excellent explanation of flocculation may be found in Burton (1976). Essentially, this process results from the reduction of repulsive forces between charged particles upon entering a more saline environment, increasing the tendency of these particles to adhere when they collide. The number of collisions tends to be increased in an estuary because of turbulence in the mixing waters and the generally higher concentrations of particulate material (Burton, 1976). Flocculation is a particularly effective and important process in the deposition of argillaceous sediments in estuarine and nearshore environments. Much of the fine-grained sediment found in these areas can be directly attributed to the processes of flocculation (Pryor, 1975).

One of the first major chemical reactions occurring in

the estuarine environment is that of cation exchange, which predominantly affects the clay minerals (Open University, 1978). The occurrence of such exchanges in the study area, some due to adsorption on the clay mineral surfaces and some due to incorporation into the crystalline lattices, is probably a major cause of the increase in concentration shown by most of the trace elements analysed in the estuarine sediments over the river sediments. Another important chemical process in estuaries is the precipitation of iron and manganese oxides and hydroxides, which is caused by the increase of pH and Eh in the zone where river water mixes with sea water. Iron and manganese oxides are well known scavengers of several trace elements, and coprecipitation of Cu, Ni, Co, Cr and V with these oxides has been documented (eg. De Groot et al., 1976).

Compared to the continental shelf mud samples, the estuarine muds are markedly enriched in Fe_2O_3, MnO, Cu, Ni, Co, Cr and V relative to Al_2O_3. The high concentrations of these metals could be attributed to the processes of coprecipitation with iron and manganese oxides and/or the adsorption on clay minerals. The latter mechanism is most likely the dominant one for two reasons:

1) the river water is already quite basic upon entering the estuary (cf. chap II, section 4.), lessening the effect of the change in pH normally experienced in mixing estuarine waters, and implying that the reactions begin further upstream; and
2) other trace elements that are usually associated with iron oxides, notably arsenic, were found to be depleted

in the estuarine samples compared to the continental shelf samples.

The enrichment of these metals is undoubtedly enhanced by the contributions of metal and other pollutants from the sources mentioned in chapter II, section 4..

Barium also shows a degree of enrichment in the estuarine muds compared to the continental shelf mud samples, probably due both to its adsorption on clays and to the greater proportion of unaltered detrital mica and feldspars in these sediments. White (1970) considered Ba to be a characteristic element in distinguishing estuarine and very nearshore sediments from other continental shelf sediments. It would appear from the high concentrations of Ba found in the estuarine and very nearshore sediments found in this study (cf. this chap. section 3.2.12 and fig. 10-39) that this region shows a similar characterization. It is interesting to note that Ba, as does Rb, correlates perfectly (1.000) with K_2O in the seven river samples, indicating that the concentrations of these elements in the river sediments are completely due to their substitution for potassium in detrital micas and feldspars.

A substantial decrease in Na_2O occurs in the estuarine muds compared to the river sediments. Sodium is released during the transition from rock to soil, and is very mobile in the aqueous environment (Mason, 1966). The average Na/K ratio for the estuarine samples in only 0.284 compared to an average value for the river samples of 0.743, the difference

being more likely due to the feldspar compositions of the sediments rather than indicative of depositional rates, because of the large discrepancy between the clay contents of the two groups.

Calcium is known to be lost from estuarine sediments to sea water (Open University, 1978), and a decrease in CaO content is observed from the upstream samples to those from the river mouth. CaO correlates positively to MgO and MnO in the river samples (Table 10-4), indicating that it is probably associated with plagioclase feldspar and heavy minerals (hornblende) in these sediments (cf. chap. IX). Strontium also increases in concentration upstream from the estuary and is probably substituting for Ca in the feldspars (Mason, 1966), although the highly positive correlation of Sr with mud (0.964) in the river samples suggests that it is primarily concentrated in the clay fractions of these sediments.

In general, the elemental distributions and relationships in the estuarine and river sediments, although subjected to some different processes than the continental shelf sediments, appear to be controlled basically by the same mineral-element associations found in the factor analysis (section 2.2.2) and discussed in section 3.. Slight differences from the previous discussion (section 3.) are found in the river sediments, due to their greater proportions of quartz, feldspar and heavy minerals, but the primary association of most of the trace elements and several of the major oxides with the clay minerals appears to remain true as evidenced by the enrichment of

many elements in the clay-rich estuarine muds.

5. Discussion and Conclusions

A composite geochemical model is presented in figure 10-48. This schematically representative model of geochemical sedimentation in the study area is based upon the hydraulic sedimentary populations determined in chapter VIII, section 3. (depicted in figures 8-18 and 8-22) as well as the mineralogy (chap. IX) and the elemental distributions and geochemical associations discussed in the preceding sections.

The Tugela River sediments are composed mostly of quartz and feldspars, with a notable proportion of heavy minerals. The geochemistry of these predominantly sandy sediments is governed by their mineralogy, with the majority of the trace elements and several major oxides being principally associated with the clay fractions of the sediments. Na_2O, CaO, K_2O, Rb and Ba are primarily associated with the feldspars, K_2O, Rb and Ba secondarily with detrital micas, and Fe_2O_3, Co, Cr, V and possibly MnO and MgO probably associated with the heavy minerals. The estuarine muds show enrichment of several of the trace elements that have been discussed in sections 3. and 4. as being associated with the clay minerals. It may be concluded that the estuarine samples are essentially mixtures of the quartz, feldspars and heavy minerals found in the river sediments, with the greatest proportion of the mud composed of the newly-formed and detrital clay floccules. There may also be a minor contribution of precipitating iron and manganese oxides, although this was not conclusively established.

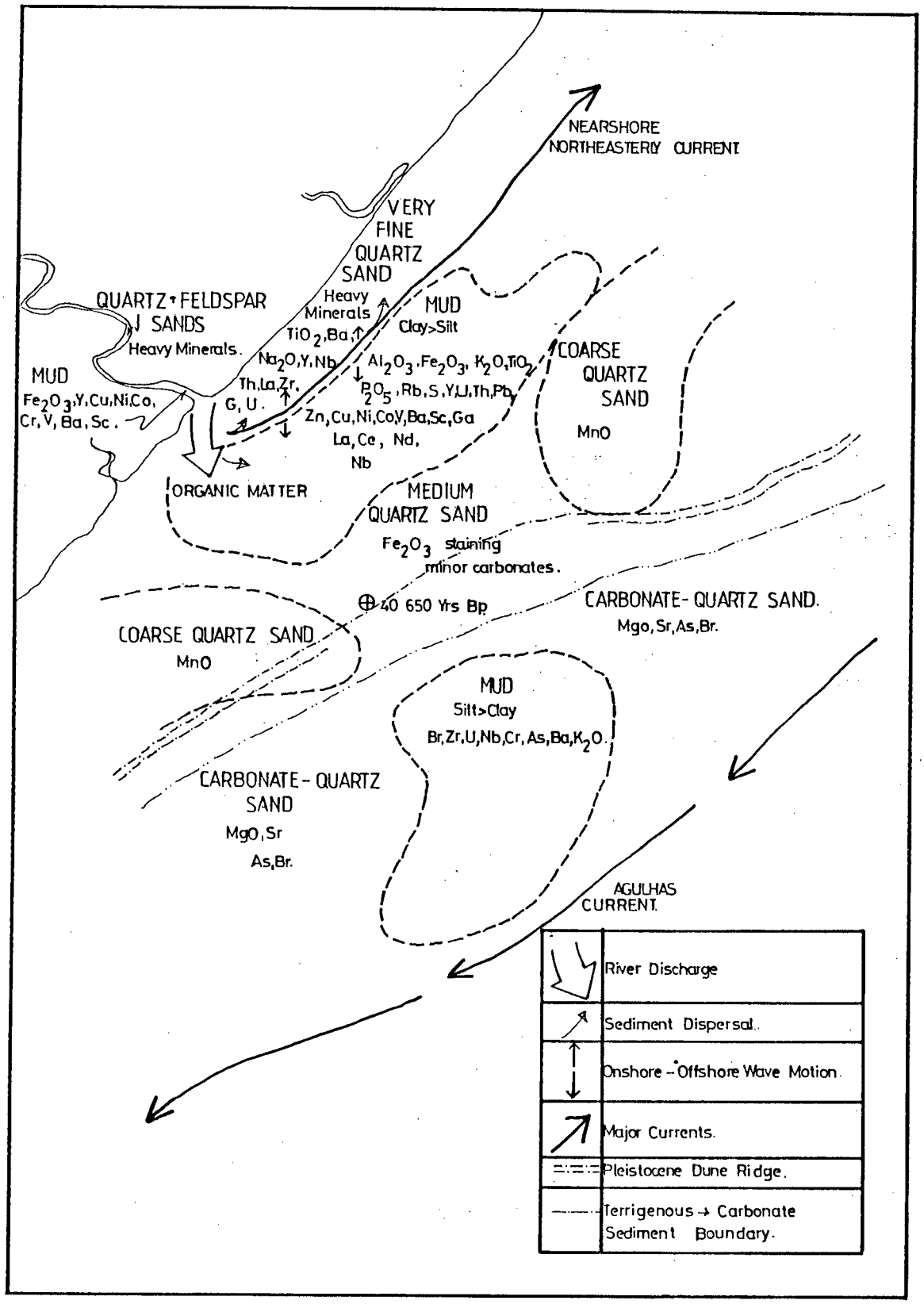

Figure 10-48. Geochemical model of sedimentation (schematic).

The very fine nearshore sands are of a quartzitic and feldspathic nature, containing a prominant heavy mineral fraction. The high concentrations of several elements in these samples, notably TiO_2, Na_2O, Zr, Cr, U, Th, Y, Nb, La, and Ba, have all been found to be primarily associated with the heavy and detrital mineral fractions of these sands. These four nearshore sediment samples are representative of present-day bedload deposition from the Tugela River that is transported in a northeasterly direction along the coast by the dominantly northeast-flowing nearshore current.

The inner shelf mud belt is comprised predominantly of clay with some silt and sand. There appears to be a minor input of finely disseminated heavy minerals occurring along the nearshore edge of the mud belt (chap. VIII, section 3.2) and the introduction of a minor biogenic carbonate input in the more seaward regions. The clay minerals, although not individually identified (chap IX, section 2.3), have been shown to be the major controlling factor of the geochemical difference between the inner and outer shelf muds (cf. this chap. section 3.2.12). Al_2O_3, Fe_2O_3, MnO, TiO_2, K_2O, organic matter, Rb, Ba, S, P_2O_5, Ga, Zn, Cu, Ni, Co, V, La, Ce, Nd, Pb, Sc, U, Th, Y, and Rb are all enriched in the inner shelf mud samples relative to the other continental shelf sediments. These elements have been shown to be associated with the clay minerals present in the sediments (sections 2. and 3.), confirming the factor analysis (section 2.2.2) conclusion that the clays account for most of the variance (56.2%) of most of the elements in the study area. Possible secondary associa-

tions of the elements listed above are with iron and manganese colloids and in the finely disseminated heavy minerals. The inner shelf mud belt is a Recent deposit that accounts for some of the suspended material discharged from the Tugela River. The largest amount of deposition coincides with the times of flood discharges from the river, when the largest amount of sediment is contributed and forced beyond the northeasterly nearshore current to become deposited inside the cell of eddy circulation where flow velocities are the lowest.

The mid-shelf sands are mostly quartzitic with a slightly larger carbonate component than the nearer-shore sediments. The very coarse and coarse sands found in the northeastern and southwestern regions of the study area were shown to have minor enrichment of MnO, and had Mn/Fe ratios indicative of slow or non-deposition. Iron staining was observed in some of the samples from these regions (cf. this chap. section 3.1.4). These sands are for the most part relict, deposited in the area during the transgressive-regressive sequences that occurred in the Pleistocene. The only date available for the sediments of the study area, 40 650 yr BP, was taken on the mid-shelf (cf. fig. 6-2), and along with the presence of the partially-buried Pleistocene dune ridge, almost certainly proves these sediments to be of Pleistocene age.

The area of mud on the outer shelf contains much less clay than the inner shelf mud belt, and larger proportions of quartz and carbonate minerals. These muds are enriched to some degree in many of the clay-associated elements compared

to the surrounding sands, but have concentrations far less than those found in the inner shelf muds. Diagenetic reactions involving the alteration and/or winnowing away of the mud in the outer shelf mud belt have produced a few elemental relationships not seen in the inner mud belt. The percentage mud in the outer shelf belt correlates well with such elements as Br and As; the percentage mud in the inner shelf mud group does not correlate with these elements at all, (cf. Tables 10-5 and 10-7). These correlations could possibly be attributed to the longer period of residence of the outer shelf mud samples on the shelf, with more time having been available for diagenetic processes affecting the compositions of pore waters and the organic matter present to occur. This mud belt is believed to represent the paleodepocentre for some of the suspended and bedload material from the Tugela River at a time when the mouth was located on the mid-shelf. This is in agreement with the acceptance of the Pleistocene dune ridge as a paleo-shoreline, and the data showing a region of heavy mineral concentration coinciding with the position of the present-day outer shelf mud belt. The lesser amount of clay found in the outer shelf muds is thought to be due either to retention of the clay in the paleoestuary of the Tugela River, or the winnowing action of the Agulhas Current causing erosion. The close association of the very fine sand fraction to the mud fraction in these samples would lend preference to the first theory, as hydraulically they could be classified with the very fine nearshore sands discussed above. The visual appearance of these muds, i.e. grey, stiff and compacted (cf. Appendix A, Table A-2), also lend support to the statement

that they are relict. The grey colour of the outer shelf mud samples could be indicative of diagenetic iron sulphide formation during a period of higher deposition in the area.

The outer shelf sands are composed largely of quartz with a major biogenic carbonate component. There appears to be some concentration of sulphur in these sands, but as stated earlier in this chapter (cf. section 3.2.1), the analyses may not be trustworthy. MgO and Sr are concentrated in the outer shelf sands, the latter element being concentrated primarily along the shelf break where the samples showed detectable amounts of aragonite (cf. chap. IX, section 2.4). The outer shelf sands may be classified as relict, with virtually no Recent deposition occurring except for the biogenic carbonate precipitation. Strong correlations between CaO, CO_2 and Sr (the carbonate mineral components) and the gravel, very coarse and coarse sand fractions in the mid-outer shelf sands (cf. Table 10-8) infers that some of the coarse sediments are a result of the breaking up of carbonate beach rock formed during the existence of the Pleistocene barrier-lagoon complexes (cf. chap. III, section 3.). These carbonate-rich coarse sediments were subsequently mixed with the thin sheets of gravels and sands deposited during the transgressive-regressive sequences. From the hydraulic population determinations, there appears to be a significant amount of this mixing occuring in the sediments on the mid-outer shelf, undoubtedly to a large part caused by the combined effects of the Agulhas Current and the related eddy system in the region.

Holmes (1982) found that the use of chemical data in combination with textural data was a much better way of determining sediment transport paths than the use of textural data alone. Suggested sediment transport paths operative in the study area are shown in figure 10-48. The major paths defined are those involving the northeasterly-flowing nearshore current, which carries much of the suspended and fine bedload material discharged from the Tugela and the Agulhas Current, the latter being more of a destructive than constructive component of the sediment dynamics in the area. Mixing between the very fine nearshore sands and the nearshore edge of the inner shelf mud belt is depicted by broken arrows representing the on and off-shore components of the waves in the nearshore region. The eddy system is not shown in figure 10-48 because of its intermittent nature (cf. chap. IV, section 3.), and the uncertainty of its exact position.

CHAPTER XI SUMMARY OF MAIN CONCLUSIONS AND RECOMMENDATIONS FOR FUTURE RESEARCH

1. Summary of Main Conclusions

The following is a summary of the main conclusions drawn in the preceding three chapters.

1.1 Sedimentology

A review of the sedimentology of the area (presented in chap. VIII) in conjunction with information taken from other sources (cf. chap. IV) allows the reconstruction of a paleo-environment for the study area. It appears as though the Tugela River Mouth was situated on the present-day middle shelf, with a large estuary behind it that was presumably a major depocentre for estuarine muds. The discharge from the river would have been deposited on the shelf in the present position of the outer shelf mud belt. During subsequent transgressive-regressive sequences, the estuarine deposits were progressively covered by a veneer of alternating sands and gravels. It is thus likely that the outer shelf mud belt is essentially a relict deposit from the Pleistocene, with minor modifications by modern processes, while the inner shelf mud belt forms the present-day depocentre for at least some of the suspended and bedload materials discharged from the Tugela River. The inner and outer shelf mud deposits are distinctly separated by a sand belt composed of a reasonably well-defined hydraulic end-member. The present-day hydrodynamic regime seems very conducive to the considerable amount of mixing now found on the shelf, as determined by interpretation

of the statistical parameters from the particle-size analyses.

1.2 Mineralogy

The presence of quartz as the major mineral constituent of all the sediments in the study area substantiates the classification of these sediments as terrigenous. The carbonate minerals, with their increasing concentration offshore, appear to be indicative of little present-day deposition of terrigenous material occurring on the outer shelf. This supposition is supported by the increasing high-magnesian calcite and aragonite contents near the shelf break. The outer shelf mud belt contains more quartz and a lower proportion of clay minerals than the inner shelf mud belt. This could be explained by the trapping of the clay supplied by the Tugela River in its large Pleistocene paleoestuary and/or the winnowing action of the Agulhas Current on the present-day outer shelf mud belt.

1.3 Geochemistry

A geochemical distinction between the inner shelf and outer shelf mud belts was found. The clay minerals, although not individually identified, have been shown to be the major controlling factor of this geochemical difference. The geochemical data was found to support the textural and mineralogical data in the identification of the inner shelf mud belt as a Recent deposit representing the present-day depocentre for the Tugela River and the outer shelf mud belt as a relict deposit representing the Pleistocene paleodepocentre for material from the Tugela River.

1.4 General

It can thus be seen that the use of chemical data combined with textural data in a sedimentologically complex region such as the study area allows a better distinction between groups of sediments and environments of deposition than the use of either set of data alone. The sediments from this area had previously been thought to be unclassifiable on the basis of textural data alone, due to their mixed nature and the complex hydrodynamic regime (cf. chap. IV). The use of multi-variate statistics on a data set consisting of both chemical and textural variables has permitted the classification of the inner shelf sediments as predominantly modern and the outer shelf sediments as relict. This classification agrees with that of other sediments from the continental shelf off the east coast of South Africa (Flemming, 1978), and shows the usefulness of geochemistry in solving a sedimentological problem.

2. Recommendations for Future Research

2.1 The <63 μm Fraction

In studies of this type, it would probably prove more rewarding to concentrate primarily on the <63 μm (mud) fraction. As it was found in this study that the clay minerals are the major factor controlling the geochemical difference between the two mud belts, bulk sediment chemistry may be considered redundant in future research of this kind. Hydraulic particle-size analyses of the <63 μm fraction of the samples (similar to the analyses performed on the 63 μm-2 mm fraction in this study) would prove useful in the interpreta-

tion of the sediment dynamics in the predominantly muddy areas.

2.2 Cores

Vibro-cores or piston cores should be recovered from the study area, particularly from the mid-shelf region, to elucidate the nature of the transgressive-regressive sequences and to conclusively prove the existence of a paleoestuary for the Tugela River. Such cores were not taken as part of this study as the number of samples generated from them becomes unrealistic for the scope of a M.Sc. project.

2.3 Organic Matter

Detailed study of the organic materials found in the samples would also be an interesting avenue of research in the future. Several trace elements were found to be associated with the organic matter in the study area sediments, particularly Br in the outer shelf samples. Determination of the nature of the organic matter in these sediment samples could possibly explain such associations in a manner that geochemical analyses alone cannot.

ACKNOWLEDGEMENTS

This project was sponsored by the Department of Geochemistry, University of Cape Town, and the National Research Institute of Oceanology (NRIO). I wish to thank the Department of Geochemistry for access to laboratory space and analytical equipment; NRIO for arranging and financing ship time for sampling; and the Department of Geology for access to the X-ray diffractometre and photocopying facilities. Special thanks are due to the University of Cape Town for providing financial support through a research scholarship and a research associateship.

I gratefully acknowledge the help of Mr. Nico Snyman, Natal Conservation Officer, who was our guide to the Tugela River area and who was most accommodating in finding access points to the often difficult river sampling sites desired. His knowledge of the history and the ecology of the area made the sampling trip most enjoyable and interesting.

Thanks are extended to the captain and crew of the CSIR's Research Vessel Meiring Naude for their helpfulness and fellowship at sea. Dr. Keith Martin of NRIO deserves special thanks for playing the role of project supervisor while at sea, and for many helpful discussions on the project in the following year and a half.

Dr. Burg Flemming of NRIO is thanked for suggesting the project, organising the ship time, discussions of the work,

and reviewing the sedimentology chapter. I wish to thank Dr. Garth Eagle, also of NRIO, for his helpful criticism of the manuscript. Mr. Mathew Smith deserves acknowledgement for his patient help and instruction in the sedimentology laboratory.

I particularly wish to thank my supervisor, Prof. J.P. Willis, for his help in the analytical and interpretative phases of this work, and for his evaluation and discussions with me of the manuscript. I wish also to acknowledge the help received from other staff members in the Department of Geochemistry, especially Profs. A.J. Erlank and A.R. Duncan and Drs. H.S. Smith and D.L. Reid, during the course of this project. The research assistants, secretary and my fellow students in Geochemistry deserve acknowledgement for their help in the laboratories and for useful discussions of my thesis work and of geochemistry in general.

I wish to also thank: Mrs. G. Woodborne for assuming the daunting task of typing the manuscript and tables, and for doing a superb job; Mr. C. Maritz for spending part of a holiday weekend fixing the typewriter after it broke at a crucial time in the preparation of the text; and Mr. Barry Yudaken for assistance with the drafting.

The most important acknowledgements go to the people to whom this thesis is dedicated, my parents and my husband. My heartfelt thanks go to my parents for the many years of financial and moral support they have given me, and to my

husband, Theunis Stander, whose considerable help with the drafting along with his encouraging and patient support of my work has made this thesis possible.

REFERENCES

Begg,G. (1978). The Estuaries of Natal. Natal Town and Regional Planning Report 41, 657 pp.

Birch,G.F. (1975). Sediments on the continental margin off the west coast of South Africa. Joint GSO/UCT Mar.Geosci. Group Bull., Geol.Dept.Univ. Cape Town, 6, 142 pp.

Birch,G.F. (1979). The "Karbonat-Bombe" : a precise, rapid and cheap instrument for determining calcium carbonate in sediments and rocks. Joint GSO/UCT Mar.Geosci.Unit Tech.Rep., Geol.Dept.Univ. Cape Town, 11, 122-126.

Bremner,J.M. (1975). Faecal pellets, glauconite, phosphate and bedrock from the Kunene-Walvis continental margin. Joint GSO/UCT Mar.Geol.Prog.Tech.Rep., Geol.Dept.Univ. Cape Town, 7, 59-68.

Burton,J.D. (1976). Basic properties and processes in estuarine chemistry. In: Burton,J.D. and Liss,P.S. (eds.). Estuarine Chemistry. Academic Press, London, pp. 1-36.

Burton,J.D. and Liss,P.S. (eds.) (1976). Estuarine Chemistry. Academic Press, London, 229 pp.

Burton,J.D. and Culkin,F. (1978). Gallium (31). In: Wedepohl,K.H. (ed.), Handbook of Geochemistry, Vol. II-3. Springer-Verlag, Berlin.

Calvert,S.E. (1976). The mineralogy and geochemistry of nearshore sediments. In: Riley,J.P. and Chester,R. (eds.) Chemical Oceanography, Vol. 6, 2nd edn. Academic Press, London, pp. 187-280.

Capuzzo,J.M. (1981). Predicting pollution effects in the marine environment. Oceanus 24(1), 25-33.

Carroll,D. (1970). Clay minerals: A guide to their X-ray identification. Geol.Soc.Amer.Special Paper 126, 80 pp.

Cook,P.J. and Mayo,W. (1977). Sedimentology and Holocene history of a tropical estuary (Broad Sound, Queensland). Bur.Miner.Resour.Geol.Geophys.Bull., Aust.Govt.Publ.Serv., 170, 206 pp.

Cook,P.J. and Mayo,W. (1980). Geochemistry of a tropical estuary and its catchment - Broad Sound, Queensland. Bur. Miner.Resour.Geol.Geophys.Bull., Aust.Govt.Publ.Serv., 182, 211 pp.

Clarke,F.W. (1924). Data of geochemistry. U.S.Geol.Surv.Bull. 770.

Cronin,L.E. (ed.) (1975). Estuarine Research, Vol.I. Chemistry, Biology and the Estuarine System. Academic Press, N.Y., 738 pp.

Davis,J.C. (1973). Statistics and Data Analysis in Geology. John Wiley and Sons, Inc., N.Y., 550 pp.

Degens,E.T. (1965). Geochemistry of Sediments. Prentice-Hall Englewood Cliffs, N.J., 342 pp.

De Groot,A.J., Salomons,W. and Allersma,E. (1976). Processes affecting heavy metals in estuarine sediments. In: Burton,J.D. and Liss,P.S. (eds.), Estuarine Chemistry. Academic Press, London, pp. 131-157.

Dixon,W.J. (ed.) (1981). BMDP Statistical Software 1981. Univ. of Calif. Press, Berkeley, 725 pp.

Du Toit,S.R. and Leith,M.J. (1974). The J(c)-1 bore-hole on the continental shelf near Stanger, Natal. Trans.geol. Soc.S.Afr. 77, 247-252.

Dyer,K.R. (ed.) (1972). Estuarine Hydrography and Sedimentation. Cambridge Univ. Press, Cambridge, 230 pp.

Erlank,A.J., Smith,H.S., Marchant,J.W., Cardoso,M.P. and Ahrens,L.H. (1978). Zirconium (40). In: Wedepohl,K.H. (ed.), Handbook of Geochemistry, Vol. II-4. Springer-Verlag, Berlin.

Flemming,B.W. (1977) Depositional processes in Saldahna Bay and Langebaan Lagoon. C.S.I.R. Res.Rep., Stellenbosch, 362, 215 pp.

Flemming,B.W. (1978). Underwater sand dunes along the southeast African continental margin - observations and implications. Mar.Geol. 26, 177-198.

Flemming,B.W. (1980). Sand transport and bedform patterns on the continental shelf between Durban and Port Elizabeth (southeast African continental margin). Sedimt.Geol. 26, 179-205.

Flemming,B.W. (1981). Factors controlling shelf sediment dispersal along the southeast African continental margin. Mar.Geol. 42, 259-277.

Flemming,B.W. and Hay,R. (1984). On the bulk density of South African marine sands. Joint GSO/UCT Mar.Geol.Unit Tech. Rep., Geol.Dept.Univ.Cape Town, 14. (In press).

Flemming,B.W. and Thum,A.B. (1978). The settling tube - a hydraulic method for grain size analysis of sands. Kieler Meeresforschungen 4, 82-95.

Folk,R.L. (1954). The distinction between grain size and mineral composition in sedimentary rock nomenclature. J.Geol. 62, 344-359.

Förstner,U., Müller,G. and Stoffers,P. (1978). Heavy metal contamination in estuarine and coastal sediments: sources, chemical association and diagenetic effects. In: Goldberg,E.D. (ed.), Biogeochemistry of Estuarine Sediments. UNESCO, pp. 49-69.

Förstner,U. and Wittmann,G.T.W. (1981). Metal pollution in the Aquatic Environment. Springer-Verlag, Berlin, 486 pp.

Fromme,G.A.W. (1977). Mineral tracing tests as a mean to determine the littoral sand transport. Unpubl.C.S.I.R. Rep.

Frondel,C. (1978). Scandium (21). In: Wedepohl,K.H. (ed.), Handbook of Geochemistry, Vol. II-2. Springer-Verlag, Berlin.

Fuge,R. (1978). Bromine (35). In: Wedepohl,K.H. (ed.), Handbook of Geochemistry, Vol. II-3. Springer-Verlag, Berlin.

Garrels,R.M. and Mackenzie,F.T. (1971). Evolution of Sedimentary Rocks. Norton, N.Y., 397 pp.

Gibbs,R.J. (1973). Mechanisms of trace metal transport in rivers. Science 180, 71-73.

Golterman,H.L., Sly,P.G. and Thomas,R.L. (1983). Study of the Relationship between Water Quality and Sediment Transport - A Guide for the Collection and Interpretation of Sediment Quality Data. UNESCO. (In press).

Goodlad,S.W. (1978). The bathymetry of the Natal Valley off the Natal and Zululand coasts (Southern Africa). Joint GSO/UCT Mar.Geol.Prog.Tech.Rep., Geol.Dept.Univ.Cape Town, 10, 96-104.

Goodlad,S.W. (1979). Some aspects of deep current activity in the mid-Natal Valley. Joint GSO/UCT Mar.Geosci.Unit Tech. Rep., Geol.Dept.Univ.Cape Town, 11, 91-98.

Harris,T.F.W. (1964). Notes on Natal coastal waters. S.Afr. J.Sci. 60, 237-241.

Heier,K.S. and Billings,G.K. (1978). Rubidium (37). In: Wedepohl,K.H. (ed.)., Handbook of Geochemistry, Vol. II-4. Springer-Verlag, Berlin.

Heydorn,A.E.F. (ed.) (1976). Ecology of the Agulhas Current region - an assessment of biological responses to environmental parameters in the southwest Indian Ocean. Proc. 1st Interdisciplinary Conf.Mar.Freshwater Res. S.Afr., 55 pp.

Hirst,D.M. (1962a). The geochemistry of modern sediments from the Gulf of Paria - I. The relationship between the mineralogy and the distribution of major elements. Geochim. cosmochim. Acta 26, 309-334.

Hirst,D.M. (1962b). The geochemistry of modern sediments from the Gulf of Paria - II. The location and distribution of trace elements. Geochim.cosmochim.Acta 26, 1147-1187.

Hobday,D.K. (1980). Geological evolution and geomorphology of the Zululand coast. In: Allanson,B.R. (ed.), Lake Sibaya, Monographiae Biologicae 36, Junk Publ., The Hague, pp. 1-20.

Hobday,D.K. and Orme,A.R. (1974). The Port Durnford Formation: A major Pleistocene barrier-lagoon complex along the Zululand coast. Trans.geol.Soc.S.Afr. 77, 141-149.

Holmes,C.W. (1971). Zirconium on the continental shelf: possible indicator of ancient shoreline deposition. Geol.Surv. Res., U.S.Geol.Surv.Prof.Paper 750-C, C7 - C12.

Holmes,C.W. (1982). Geochemical indices of fine sediment transport, northwest Gulf of Mexico. J.sedimt.Petrol. 52, 307-321.

Hutson,W.H. (1980). The Agulhas Current during the Late Pleistocene: analysis of modern faunal analogs. Science 207, 64-66.

Keith,M.L. and Degens,E.T. (1959). Geochemical indicators of marine and freshwater sediments. In: Abelson,P.H. (ed.), Researches in Geochemistry, pp. 38-61.

Kemp,P.H. (1967). Hydrobiological studies on the Tugela River system. Part VI. Acidic drainage from mines in the Natal coalfields. Hydrobiologia 24, 393-425.

Kleeman,A.W. (1967). Error in the chemical analyses of rocks. J.Geol.Soc.Aust. 14, 43-47.

Krauskopf,K.B. (1967). Introduction to Geochemistry. McGraw-Hill Book Co., N.Y., 721 pp.

Landergren,S. (1978) - Vanadium (23). In: Wedepohl,K.H. (ed.), Handbook of Geochemistry, Vol. II-2. Springer-Verlag, Berlin.

Leeder,M.R. (1982). Sedimentology: Process and Product. George Allen and Unwin Publ. (Ltd.), London, 344 pp.

Le Maitre,R.W. (1982). Numerical Petrology: Statistical Interpretation of Geochemical Data. Elsevier Sci. Publ. Co., Amsterdam, 281 pp.

Loring,D.H. and Nota,D.J.G. (1973). Morphology and sediments of the Gulf of St. Lawrence. Bull.Fish.Res.Bd.Canada 182, 115 pp.

Mason,B. (1966). Principles of Geochemistry. 3rd edn. John Wiley and Sons, Inc., N.Y., 329 pp.

Maud,R.R. (1968). Quaternary geomorphology and soil formation in coastal Natal. Z.Geomorph. 7, 155-199.

McCave,I.N. (1972). Transport and escape of fine-grained sediment from shelf areas. In: Swift,D.J.P., Duane,D.B. and Pilkey,O.H. (eds.), Shelf Sediment Transport: Process and Pattern. Dowden, Hutchinson and Ross, Inc., Stroudsberg, PA, pp. 225-248.

Middleton,E.A. and Oliff,W.D. (1961). Suspended silt loads in the Tugela River. Trans.S.Afr.Inst.Civil Engrs. 3(12), 237-244.

Moir,G.J. (1975). Bathymetry of the upper continental margin between Cape Recife (34°S) and Ponto Do Ouro (27°S). Joint GSO/UCT Mar.Geol.Prog.Tech.Rep., Geol.Dept.Univ. Cape Town, 7, 68-78.

Moir,G.J. (1976). Preliminary textural and compositional analyses of surficial sediments from the upper continental margin between Cape Recife (34°S) and Ponto Do Ouro (27°S), South Africa. Joint GSO/UCT Mar.Geol.Prog.Tech. Rep., Geol.Dept.Univ.Cape Town, 8, 68-75.

Morgans,J.F.C. (1956). Notes on the analysis of shallow-water soft substrata. J.anim.Ecol. 24, 367-387.

Müller, G. and Gastner,M. (1971). The "Karbonat-Bombe", a simple device for the determination of carbonate content in sediments, soils and other materials. Neus Jahrbuch für Mineralogie 10, 466-469.

Murgatroyd,A.L. (1979). Geologically normal and accelerated rates of erosion in Natal. S.Afr.J.Sci. 75, 395-396.

Nicholls,G.D. and Loring,D.H. (1962). The geochemistry of some British Carboniferous sediments. Geochim.cosmochim. Acta 26, 181-223.

Nicholson,J. (1983). Effects of Tugela on sedimentary processes. (Abstr.) Jnt. Symp. Sandy Beaches and Ecosystems. Port Elizabeth.

Nota,D.J.G. (1958). Sediments on the Western Guiana Shelf. Unpubl. Doctoral Thesis, Univ. of Utrecht, 98 pp.

Oliff,W.D. (1960) Hydrobiological studies on the Tugela River System. Part I. The main Tugela River. Hydrobiologia 14, 281-385.

Onishi,H. (1978). Arsenic (33). In: Wedepohl,K.H. (ed.). Handbook of Geochemistry, Vol. II-3. Springer-Verlag, Berlin.

Open University. (1978). Oceanography, Units 11 and 12: Sediments. The Open University Press, Milton Keyes, 58 pp and 50 pp.

Orme,A.R. (1973). Barrier and lagoon systems along the Zululand coast, South Africa. In: Coates,D.R. (ed.), Coastal Geomorphology. Publs Geomorph., State Univ. N.Y., pp. 181-212.

Orme,A.R. (1974). Estuarine sedimentation along the Natal coast, South Africa. U.S. Office nav.Res.Tech.Rep. 5, 45 pp.

Pearce,A.F. (1976). The gross features of the East Coast Shelf circulation. C.S.I.R.Res.Rep., Stellenbosch, 346, 18 pp.

Pearce,A.F., Schumann,E.H. and Lundie,G.S.H. (1978). Features of the shelf circulation off the Natal coast. S.Afr.J. Sci. 74, 328-331.

Pearson,T.H. (1980). Marine pollution effects of pulp and paper industry wastes. Helgoländer Meeresunters 33, 340-365.

Pettijohn,F.J. (1963). Chemical composition of sandstones - excluding carbonate and volcanic sands. In: Fleischer,M. (ed.), Data of Geochemistry. U.S.Geol.Surv.Prof.Paper 440-S.

Pryor,W.A. (1975). Biogenic sedimentation and alteration of argillaceous sediments in shallow marine environments. Bull.geol.Soc.Am. 86, 1244-1254.

Puchelt,H. (1978). Barium (56). In: Wedepohl,K.H. (ed.), Handbook of Geochemistry, Vol. II-4. Springer-Verlag, Berlin.

Roesijadi,G. (1980-1981). The significance of low molecular weight metallothionein-like proteins in marine invertebrates : current status. Mar.Environ.Res. 4, 167-179.

Rogers,J.J.W. and Adams,J.A.S. (1978). Uranium (92). In: Wedepohl,K.H. (ed.), Handbook of Geochemistry, Vol. II-5. Springer-Verlag, Berlin.

Shaw,D.M. (1956). Geochemistry of pelitic rocks. Part III. Major elements and general geochemistry. Bull.Geol.Soc. Am. 67, 919-934.

Shepard,F.P. (1954). Nomenclature based on sand-silt-clay ratios. J.sedimt.Petrol. 24, 151-158.

Shepard,F.P. (1963). Submarine Geology. 2nd edn. Harper and Row, N.Y., 557 pp.

Shiraki,K. (1978). Chromium (24). In: Wedepohl,K.H. (ed.), Handbook of Geochemistry, Vol. II-3. Springer-Verlag, Berlin.

Siegel,S. (1956). Nonparametric Statistics for the Behavioral Sciences. McGraw-Hill Book Co., Inc., N.Y. 312 pp.

Siesser,W.G. (1970). Petrology and mineralogy of carbonate sediments. SANCOR Mar.Geol.Prog.Tech.Rep., Geol.Dept. Univ.Cape Town, 2, 44-58.

Siesser,W.G. (1971). Carbonate sediments and rocks. SANCOR Mar.Geol.Prog.Tech.Rep., Geol.Dept.Univ.Cape Town, 3, 45-58.

South African Committee for Stratigraphy (SACS). (1980). Stratigraphy of South Africa. Part I. (Comp. L.E. Kent). Lithostratigraphy of the Republic of South Africa, South West Africa/Namibia, and the Republics of Bophuthatswana, Transkei and Venda. Handbk.geol.Surv.S.Afr. 8, 690 pp.

Spencer,D.W. (1966). Factors affecting element distributions in a Silurian graptolite band. Chem.Geol. 1, 221-249.

Spencer,D.W., Degens,E.T. and Kulbicki,G. (1968). Factors affecting element distributions in sediments. In: Ahrens,L.H. (ed.), Origin and Distribution of the Elements. Pergamon Press, Oxford, pp. 981-998.

Summerhayes,C.P. (1972a). Geochemistry of continental margin sediments from northwest Africa. Chem.Geol. 10, 137-156.

Summerhayes,C.P. (1972b). Studies of the mineralogy and geochemistry of unconsolidated sediments from around southern Africa. Part I. Aspects of the mineralogy and geochemistry of Agulhas Bank sediments. SANCOR Mar.Geol.Prog. Tech.Rep., Geol.Dept.Univ.Cape Town, 4, 64-81.

Temple,J.T. (1978). The use of factor analysis in geology. Mathl.Geol. 10, 379-387.

Wedepohl,K.H. (1969). Composition and abundance of common sedimentary rocks. In: Wedepohl,K.H. (ed.), Handbook of Geochemistry, Vol. I. Springer-Verlag, Berlin, pp. 250-271.

Wedepohl,K.H. (1978). Manganese (25), Copper (29), Zinc (30). In: Wedepohl,K.H. (ed.), Handbook of Geochemistry, Vol. II-3. Springer-Verlag, Berlin.

White,S.M. (1970). Mineralogy and geochemistry of continental shelf sediments off the Washington-Oregon coast. J.sedimt. Petrol. 40, 38-54.

Windom,H.L. (1976). Lithogenous materials in marine sediments. In: Riley,J.P. and Chester,R. (eds.), Chemical Oceanography, Vol. 5, 2nd edn. Academic Press, London, pp. 103-135.

APPENDICES

APPENDIX A.

TABLE A-1 : SAMPLE LOG FOR THE RIVER SAMPLES.
All samples were taken on 25 March 1982.

SAMPLE	APPROX. DEPTH(m)	VISUAL DESCRIPTION
TR1RB	1	mud, very organic, brown mud on top (see figure A-1)
TR2RB	1	dark mud, organic
TR3RB	1	muddy sand
TR3CR	1.25	muddy sand
TR3LB	1	dark brown, slightly (fine) sandy mud
TR4RB	0.5-1	slightly muddy sand
TR4CR	0.5	slightly muddy sand
TR4LB	1	dark brown muddy sand
TR5RB	1	slightly muddy sand

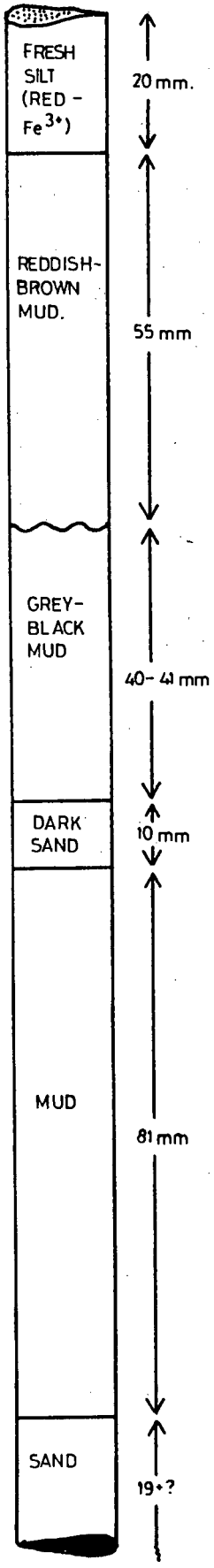

FIG. A-1 : DIAGRAM OF TR1RB HAND-CORE (TO SCALE).

APPENDIX A.

TABLE A-2 : SAMPLE LOG FOR THE CONTINENTAL SHELF SAMPLES.

DATE	TIME	STATION	DEPTH(m)	LATITUDE	LONGITUDE	VISUAL DESCRIPTION
29-3-82	1818-1827	2	34	29°17,2	31°30,2	dark grey mud w/4mm brown cover (v.org.rich)
"	1847-1855	3	32	29°16,3	31°31,6	dark grey mud w/2-3mm brown mud cover
"	1922-1927	4	28	29°14,9	31°33,5	lighter grey mud w/dusting of brown mud on top
"	1945-1950	5	31	29°13,9	31°35,0	grey mud w/thin veneer of brown mud on top
"	2017-2025	6	35	29°12,4	31°37,4	grey mud w/thin veneer of brown mud
"	2045-2050	7	35	29°11,0	31°39,6	grey mud w/~2cm brown mud on top
"	2101-2106	8	34	29°10,4	31°40,4	grey mud w/1cm brown mud on top
"	2117-2122	9	32	29°09,6	31°41,25	grey mud w/thin veneer of brown mud
"	2132-2137	10	30	29°09,0	31°42,4	slightly muddy medium - coarse sand
"	2209-2214	11	44	29°09,0	31°46,1	grey mud w/thin veneer of brown mud
"	2235-2240	12	44	29°10,4	31°44,2	grey mud w/thin veneer of brown mud
"	2255-2300	13	43	29°11,4	31°42,8	grey mud w/thin veneer of brown mud
"	2335-2342	14	40	29°13,9	31°39,1	muddy medium sand w/thin veneer of brown mud
30-3-82	0025-0030	15	37	29°16,1	31°34,4	slightly sandy grey mud
"	0112-0117	16	42	29°19,7	31°30,4	medium sand
"	0130-0137	17	41	29°20,6	31°28,8	medium sand
"	0153-0158	18	41	29°21,6	31°27,4	medium sand
"	0220-0225	19	36	29°19,5	31°26,9	medium sand
"	0236-0241	20	36	29°18,8	31°27,8	medium-coarse sand
"	0253-0259	21	36	29°17,9	31°29,2	fine sandy mud w/thin brown mud veneer
"	0335-0345	22	51	29°20,2	31°34,1	2 drops - (1) muddy fine sand (2) medium sand
"	0348	23	51	29°19,3	31°35,3	fine sandy grey mud
"	0426-0432	24	47	29°17,9	31°36,9	medium sand
"	0510-0514	25	50	29°15,6	31°40,4	grey mud w/~2mm brown mud on top
"	0543-0546	26	48	29°14,2	31°42,4	grey mud w/fine dusting brown mud on top
"	0629-0631	27	44	29°11,8	31°45,8	medium sand
"	0712-0715	28	42	29°07,9	31°47,8	sandy greyish-brown mud (Note heavy minerals, esp. ilm.)
"	0758-0800	29	45	29°11,7	31°51,4	medium-coarse sand
"	0847-0854	30	60	29°16,3	31°55,0	medium-fine sand, some shell frag.
"	0936-0945	31	60	29°19,1	31°50,9	sandy grey-black mud
"	1000-1006	32	61	29°20,4	31°49,0	slightly sandy greenish grey mud - compact
"	1025-1031	33	62	29°21,6	31°47,2	fine sandy mud - dark green w/fresh brown surface layer
"	1039-1044	34	62	29°22,0	31°46,1	dark grey mud w/thin layer brown mud
"	1110-1116	35	66	29°23,3	31°42,9	dark grey mud
"	1144-1152	36	70	29°24,6	31°38,8	dark grey mud
"	1224-1233	37	67	29°26,1	31°34,6	fine sandy mud
"	1322-1330	38	71	29°31,8	31°32,9	coarse sand
"	1345-1405	39	75	29°31,5	31°34,7	coarse sand
"	1420-1430	40	78	29°30,9	31°36,1	slightly muddy medium sand
"	1448-1458	41	77	29°30,5	31°38,1	muddy medium sand-sandy mud
"	1515-1523	42	79	29°30,0	31°39,9	slightly sandy mud
"	1545-1550	43	85	29°30,2	31°41,6	brown/grey mud
"	1608-1611	44	82	29°29,1	31°43,0	sandy (very fine) grey mud
"	1642-1644	45	90	29°27,8	31°45,2	grey mud
"	1702-1715	46	90	29°26,8	31°47,0	2 drops - (1) shelly w/some mud (2) shelly stiff mud - sampled
"	1730	47	90	29°26,0	31°48,4	muddy shelly sand
"	1902-1912	48	133 126)	29°33,0	31°44,0	shelly stiff mud NB.separate echmoderm sample btl.
"	2138-2155	51	124) 124 123)	29°34,9	31°37,0	3 small samples - slightly muddy fine sand
"	23 -2328	52	70	29°27,9	31°33,7	fine-medium (coarse) dark green muddy sand
"	2357-0010	53	67	29°25,3	31°32,5	fine-medium (coarse) dk.green muddy sand - partly shelly
31-3-82	0040-0055	54	60	29°23,4	31°35,9	gravelly sand, partly shelly
"	0117-0130	55	54	29°21,3	31°39,0	muddy fine-medium sand

DATE	TIME	STATION	DEPTH(m)	LATITUDE	LONGITUDE	VISUAL DESCRIPTION
31-3-82	0200-0207	56	51	29°19,1	31°41,9	muddy fine-medium sand
"	0225-0235	57	49	29°17,1	31°45,2	muddy fine-medium sand
"	0250-0300	58	51	29°16,0	31°47,1	grey mud w/brown mud veneer
"	0313-0326	59	45	29°14,6	31°49,1	medium-coarse sand
"	0412-0417	60	42	29°09,2	31°47,6	medium-coarse sand
"	0449-0453	61	35	29°06,8	31°45,4	grey mud w/brown mud veneer
"	0543-0545	62	23	29°07,4	31°40,9	brownish mud
"	0617-0621	63	20	29°08,3	31°38,4	mud-clastic (fecal pellets?)
"	0650-0653	64	32	29°10,2	31°38,8	green-grey mud w/brown mud veneer
"	0732-0743	65	45	29°13,1	31°41,3	3 drops (sm. samples) brown mud. NB. possible cont.fr/paint flakes and metal
"	0824-0834	66	48 49)	29°15,95	31°43,0	thick sandy mud
"	0920-0927	67	49) 49 51)	29°18,4	31°39,0	3 drops (sm. samples) - slightly muddy fine sand
"	0957-1007	68	42	29°15,0	31°37,0	3 drops (sm. samples) - soft brown mud
"	1120-1129	70	15	29°13,8	31°32,1	3 drops - clean fine sand
"	1141-1145	71	13	29°14,2	31°30,75	fine sandy mud (traces of brown mud on top)
"	1157-1205	72	17	29°14,9	31°30,1	thick dark black mud w/2cm brown mud top layer
"	1215-1220	73	24	29°16,0	31°30,7	thick very black mud w/thin layer brown mud on top
"	1233-1239	74	24	29°16,2	31°29,7	thick black mud w/thin veneer of brown mud
"	1248-1300	75	19	29°15,5	31°29,3	thick black mud w/thin veneer of brown mud
"	1330-1340	76	40	29°18,3	31°30,6	slightly sandy grey mud
"	1410-1418	77	50	29°20,7	31°31,4	slightly muddy medium sand
"	1443-1450	78	43	29°18,0	31°33,0	black mud w/2cm top layer of brown mud
"	1525-1530	79	48	29°16,3	31°38,6	muddy medium sand
"	1555-1600	80	50	29°16,1	31°41,7	slightly muddy medium sand (mud in clasts)
"	1628-1632	81	44	29°13,9	31°44,5	slightly muddy medium-coarse sand (mud in clasts)
"	1728-1733	82	51	29°17,4	31°50,0	slightly sandy greyish mud
"	1816-1820	83	71	29°21,1	31°52,0	medium-coarse shelly sand, 1 or 2 mud clasts
"	1848-1852	84	69	29°21,0	31°49,6	slightly sand mud w/some shell fragments
"	1923-1928	85	70	29°23,2	31°47,2	stiff mud w/bits of brown mud (presumably on top origin)
"	1953-1959	86	73	29°25,0	31°47,0	2 drops (1)muddy fine-medium sand (2)fine-medium sandy mud - sampled
"	2023-2029	87	72	29°25,8	31°44,2	stiff dark grey mud w/thin veneer brown mud
"	2047-2053	88	74	29°26,7	31°42,4	dark grey mud w/some brown on top
"	2117-2123	89	74	29°27,4	31°40,4	dark grey mud w/some brown on top
"	2144-2150	90	70	29°28,4	31°38,0	coarse muddy sand
"	2240-2246	91	97	29°33,4	31°35,1	fine sandy mud w/slight brown top layer
"	2313-2320	92	103	29°35,7	31°33,0	fine sandy mud
"	2348-2355	93	108	29°35,2	31°34,2	muddy fine-medium sand
1-4-82	0043-0048	94	100	29°32,6	31°38,5	fine sandy mud
"	0105-0112	95	99	29°31,6	31°41,2	slightly sandy mud
"	0136-0145	96	114	29°30,8	31°44,5	slightly sandy mud
"	1752-1758	98	27	29°07,4	31°43,6	fine sand (clean)
"	1826-1830	99	24	29°05,0	31°45,5	very fine clean sand
"	2001-2006	100	51	29°16,1	31°45,8	muddy slightly shelly sand - surficial shelly m-c sand
"	2025-2030	101	49	29°17,5	31°47,8	medium-coarse, slightly muddy sand
"	2122-2127	102	68	29°23,2	31°49,8	coarse shelly clean sand
"	2210-2215	103	66	29°24,3	31°45,0	dark grey mud
"	2254-2302	104	63	29°22,2	31°41,8	shelly sandy grey mud (surficial sand?)
"	2333-2345	105	70	29°25,7	31°40,7	slightly shelly grey mud

APPENDIX B.

TABLE B-1 : INSTRUMENTAL CONDITIONS FOR MAJOR AND TRACE ELEMENT ANALYSIS BY XRF SPECTROMETRY IN THE DEPARTMENT OF GEOCHEMISTRY, U.C.T. (COLL.: F-Fine, C-Coarse- DETECTOR: F-Flow, S-Scintillation, (v)-vacuum; SAMPLE TYPE: F-Fusion Disc, B-Briquette).

ELEMENT	INSTRUMENT	LINE	TUBE	KV	MA	CRYSTAL	COLL.	DETECTOR	TIME PK.	TIME BKG	SAMPLE TYPE
MAC	SRS-1	Ka	Mo	60	50	LiF(220)	F	S			B
	PW1220	Ka	Mo	70	28	LiF(220)	F	S			B
Si	SRS-1	Ka	Cr	50	60	PE	C	F (v)	100		F
Ti	SRS-1	Ka	Cr	50	60	LiF(200)	F	F (v)	20		F
Al	SRS-1	Ka	Cr	50	60	PE	C	F (v)	100		F
Fe	SRS-1	Ka	W	60	50	LiF(220)	F	F (v)	20		F
Mn	SRS-1	Ka	W	60	50	LiF(220)	F	F (v)	40		F
Mg	SRS-1	Ka	Cr	50	60	TLAP	F	F (v)	200		F
Ca	SRS-1	Ka	Cr	50	60	LiF(200)	F	F (v)	20		F
Na	SRS-1	Ka	Cr	50	60	TLAP	C	F (v)	200	200	B
K	SRS-1	Ka	Cr	50	60	LiF(200)	C	F (v)	20		F
P	SRS-1	Ka	Cr	50	60	Ge	C	F (v)	100		F
S	PW1400	Ka	Cr	50	55	Ge	C	F (v)	80	80	B
Rb	PW1400	Ka	Mo	50	55	LiF(200)	F	S (v)	80	80	B
Sr	SRS-1	Ka	W	60	50	LiF(220)	F	S	100	80	B
	PW1400	Ka	W	50	55	LiF(200)	F	S (v)	80	80	B
Y	SRS-1	Ka	W	60	50	LiF(220)	F	S	100	80	B
	PW1400	Ka	W	50	55	LiF(200)	F	S (v)	80	80	B
Zr	SRS-1	Ka	W	60	50	LiF(220)	F	S	100	80	B
	PW1400	Ka	W	50	55	LiF(200)	F	S (v)	80	80	B
Nb	SRS-1	Ka	W	60	50	LiF(220)	F	S	100	80	B
	PW1400	Ka	W	50	55	LiF(200)	F	S (v)	80	80	B
U	PW1400	La	Mo	50	55	LiF(200)	F	S (v)	80	80	B
Th	PW1400	La	Mo	50	55	LiF(200)	F	S (v)	80	80	B
Pb	PW1400	Lb	Mo	50	55	LiF(200)	F	S (v)	80	80	B
Zn	PW1400	Ka	Au	60	45	LiF(220)	F	FS (v)	80	80	B
Cu	PW1400	Ka	Au	60	45	LiF(220)	F	FS (v)	80	80	B
Ni	PW1400	Ka	Au	60	45	LiF(220)	F	FS (v)	80	80	B
Co	PW1400	Ka	W	50	55	LiF(220)	F	F (v)	80	80	B
Cr	PW1400	Ka	W	50	55	LiF(220)	F	F (v)	80	80	B
V	PW1400	Ka	W	50	55	LiF(220)	F	F (v)	80	80	B
Ba	PW1400	La	Cr	50	55	LiF(200)	F	F (v)	80	80	B
Sc	PW1400	Ka	Cr	50	55	LiF(200)	F	F (v)	80	80	B
Br	PW1400	Ka	Mo	50	55	LiF(200)	F	S (v)	80	80	B
Ga	PW1400	Ka	Mo	50	55	LiF(200)	F	FS (v)	80	80	B
La	PW1400	La	W	50	55	LiF(220)	F	F (v)	80	80	B
Ce	PW1400	Lb	W	50	55	LiF(220)	F	F (v)	80	80	B
Nd	PW1400	La	W	50	55	LiF(220)	F	F (v)	80	80	B
As	PW1400	Ka	Mo	50	55	LiF(200)	F	FS (v)	80	80	B

APPENDIX B.

TABLE B-2 : LOWER LIMITS OF DETECTION AND ABSOLUTE ERRORS (STANDARD DEVIATION) FOR ALL OXIDES AND ELEMENTS ANALYZED BY XRFS. (NOTE: Values given are averages of all samples; variations in the values occur due to differing mass absorption coefficients of the samples).

OXIDE	LLD (%)	ABSOLUTE ERROR (1 STD.DEV.)
SiO_2	0.03	0.25
TiO_2	0.005	0.01
Al_2O_3	0.03	0.08
Fe_2O_3	0.03	0.13
MnO	0.03	0.01
MgO	0.11	0.12
CaO	0.01	0.06
Na_2O	0.08	0.09
K_2O	0.002	0.03
P_2O_5	0.01	0.01
ELEMENT	(ppm)	
S	5.0	4.2
Rb	0.8	0.3
Sr	1.3	0.6
Y	1.5	0.5
Zr	1.4	0.6
Nb	1.4	0.5
U	1.5	0.5
Th	2.0	0.7
Pb	2.2	0.8
Zn	0.8	0.3
Cu	1.1	0.4
Ni	1.2	0.4
Co	1.9	0.7
Cr	1.6	0.8
V	1.9	0.9
Ba	2.6	1.7
Sc	1.1	0.4
Br	1.1	0.4
Ga	0.8	0.3
La	3.3	1.2
Ce	5.8	2.1
Nd	3.4	1.2
As	0.8	0.3

APPENDIX C.

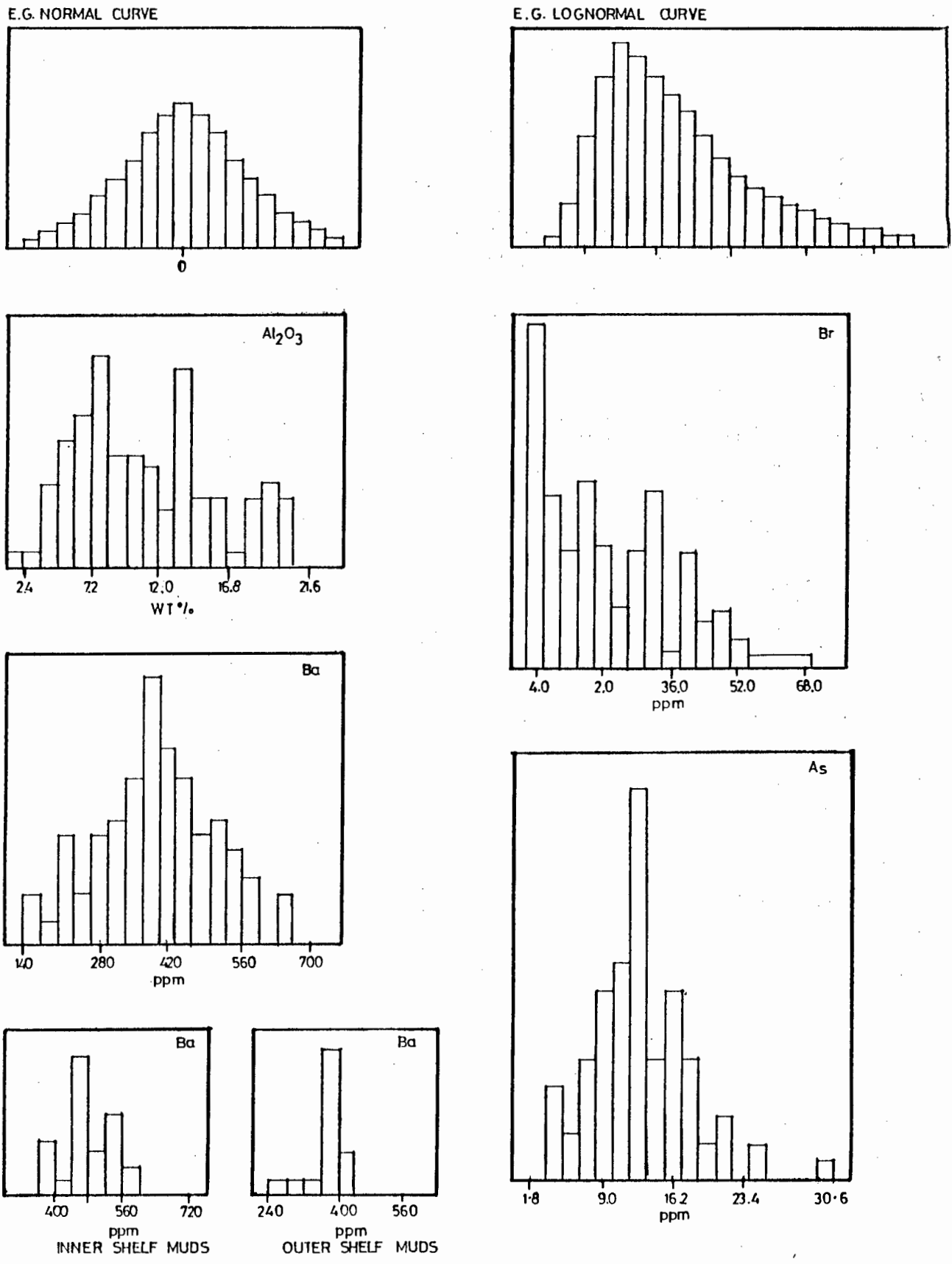

Figure C-1. Sample histograms showing frequency distributions of some elements analysed. (Note: all vertical axes are scales of relative frequency. The log-normal 'curve' represents a distribution that would plot to a normal 'curve' if the log of the X-axis values were used.)